UNIVERZITA KARLOVA / CHARLES UNIVERSITY

Přírodovědecká fakulta

Katedra aplikované geoinformatiky a kartografie
Studijní program: Kartografie, geoinformatika a dálkový průzkum Země

Faculty of Science
Department of Applied Geoinformatics and Cartography
Study programme: Cartography, Geoinformatics and Remote Sensing

VYUŽITÍ LABORATORNÍ/TERÉNNÍ SPEKTROSKOPIE A OBRAZOVÝCH DAT DÁLKOVÉHO PRŮZKUMU ZEMĚ PRO STUDIUM VEGETACE

Disertační práce

Laboratory/Field Spectroscopy and Remote Sensing Image Data for Vegetation Studies

Doctoral thesis

Mgr. Lucie Červená

Vedoucí dizertační práce / Thesis Supervisor: RNDr. Lucie Kupková, Ph.D.

Konzultantka dizertační práce / Thesis Co-Supervisor: prof. RNDr. Jana Albrechtová, Ph.D.

Srpen 2018 / August 2018

Prohlášení

Prohlašuji, že jsem tuto práci zpracovala samostatně s využitím informačních zdrojů a literatury, na které odkazuji. Tato práce ani její podstatná část nebyla předložena k získání stejného nebo jiného akademického titulu.

Publikace tvořící dizertační práci byly zpracovávané ve vědeckých týmech, avšak můj podíl byl významný na všech částech zpracování publikací od návrhu metodiky, přes sběr a zpracování dat až po interpretaci a sepsání výsledků. Konkrétní procentuální podíly autorů na jednotlivých publikacích jsou uvedeny v textu práce.

V Praze dne 27. srpna 2018

Lucie Červená

Acknowledgements

There had been hardly any doctoral thesis finished without the support and assistance of dozens of people.

Firstly, I would like to express my sincere gratitude to my supervisor Lucie Kupková for her guidance and patience, fruitful discussions, constructive feedback, continuous support and encouregements. I am also very thankful to my co-supervisor Jana Albrechtová for a great support, opportunities to study abroad, useful ideas and expertise advices related to plant physiology. I would like to thank also to all my co-authors for a valuable cooperation, discussion and inspiring ideas, Markéta Potůčková and Zuzana Lhotáková in particular.

My thanks are addressed to all members of the Department of Applied Geoinformatics and Cartography, who created pleased environment in which I have worked for many years. My thanks go also to the research team of the Department of Experimental Plant Biology for organizing the Norway spruce needle sampling and laboratory analysis of the collected samples. My research would have been impossible also without the help of Jakub Lysák and many other colleagues and students in the field in the Krkonoše Mountains as well as at the office.

A very special gratitude goes out to The Krkonoše Mountains National Park Administration for allowing the research in the beautiful area of relict arctic-alpine tundra and to the national park's botanist Stanislav Březina for introducing the tundra species to us and a continuous collaboration.

I would like to thank to the Grant Agency of Charles University (Project GAUK 938214) and the Ministry of Education, Youth and Sports of the Czech Republic (Project LH 12097) for supporting this project financially.

Last but not least, my deepest thanks go to my family for the support over the years and to my friends for providing distractions outside university. I would like to thank especially to Jakub Benda and Kateřina Novotná for being here for me during my entire doctoral studies and to Jakub also for great scientific discussions.

Abstract

Dominant vegetation species of two structurally and functionally different montane ecosystems were studied by means of laboratory and field spectroscopy and remote sensing image data: (1) a homogeneous human-influenced evergreen coniferous forest represented by a Norway spruce forest in the Krušné hory Mountains and (2) a heterogeneous natural ecosystem of a relict arctic-alpine tundra in the Krkonoše Mountains with predominance of grasses.

The first part dealing with the Norway spruce forest is especially focused on the methods of laboratory spectroscopy. The assessment of Norway spruce stands on a regional and a global scales requires detailed knowledge of their spectral properties at the level of needles and shoots in the beginning, but ground research is very time-demanding. Open spectral libraries could help to get more ground-truth data for subsequent analysis of tree species in forests ecosystems. However, the problem may arise with the comparability of spectra taken by different devices. The present thesis focuses on a comparability of spectra measured by a field spectroradiometer coupled with plant contact probe and/or two integrating spheres (Paper 3) and proves the significant differences in spruce needle spectra measured by the contact probe and integrating sphere, spectra of broadleaved plants (tobacco) also differ but the mean values of indices calculated using these spectra are in the range of the corresponding standard deviations, while spectra of homogeneous materials (colored papers, Spectralon) are comparable. Furthermore, data on different scales (laboratory retrieval of photosynthetic pigments and water content, the spectra of the needles measured by the contact probe, the spectra of crowns derived from airborne hyperspectral image acquired by an APEX sensor) are evaluated for the purpose of the detection of the differences in the physiological status of the Norway spruce stands among various factors - needle age class, position in the tree crown, stands or areas (Paper 2). Two areas in Krušné hory Mountains which were affected by various intensities of air pollution during the 1970's showed only slight differences in 2013 based on the laboratory biochemical data and no differences based on the spectroscopic data. Some heterogeneity was proven among eleven studied stands in these two areas based on all three datasets. Based on the laboratory data (biochemical and also spectral), the differences among the needle age classes and positions in the tree crown were proven. The differences among the positions in the tree crown were elaborated in the next part of the thesis, where the empirical models for chlorophyll, carotenoids and water content estimations are modeled based on the spectra measured by the contact probe for three positions in the Norway spruce crown (the sunlit productive upper and lower parts, the shaded basal part) - Paper 4. The results are more accurate for the shaded basal part of the tree crown than for the sunlit upper part, which can be the consequence of the architecture of the shoots. The paper also confirms better results of the correlations when using partial least square regression (PLSR) over that of simple regressions and vegetation indices. Besides the methodological findings, the thesis has an ecological contribution (Paper 1 a 2) in the evidence of the Norway spruce homogeneous stands' regeneration after the air pollution elimination (especially in the central part of the Krušné hory Mountains) – although the stands are still not

completely undamaged, the difference between the two areas located in the central and western parts of the Krušné hory Mountains are not so significant already (especially in the central part of the Krušné hory Mountains).

The traits of the stands are one of the most important for correct function of homogeneous ecosystems, while the species composition of plant community plays an important role and also needs to be studied in the heterogeneous ecosystems. The species composition is the main focus of the thesis part dealing with the montane relict arctic-alpine tundra ecosystem (Papers 5 a 6). The accuracies of the classifications for several types of remote sensing image data with various spectral and spatial resolutions (Landsat, Sentinel-2, WorldView-2, orthoimages and airborne hyperspectral image data acquired by APEX and AISA sensors) were compared. For these data classifications, two differently detailed legends were used. The legends were design in accordance with the spatial resolution of the image data and the categories were specified to have a contribution to the monitoring and protection of the area with an emphasis being placed on the distinction among the expansively strong species (grasses *Calamagrostis villosa, Molinia caerulea* and *Pinus mugo* shrubs) and the original grass species *Nardus stricta*. The best classification results (an overall accuracy higher than 80%) were reached based on the aerial hyperspectral image data AISA with a high spatial resolution. In order to increase the accuracy of the classification of the heterogeneous ecosystems, such as the tundra in the Krkonoše Mountains, spatial resolution appears to be the most important based on our results. This was demonstrated by good accuracies of the orthoimages with a spatial resolution of 12.5 cm and only 4 spectral bands classifications (an overall accuracy 71.96% in the case of a detailed legend and 80% in the case of a simplified one). In the tundra ecosystem of Krkonoše Mountains, the traits of the vegetation cover (height, plant covet and fAPAR) were investigated using field spectroscopy along the elevation and nutrient gradient stretching from the Luční bouda hut to the Luční hora Mountain in two periods during the 2015 season (Paper 7). Different vegetation indices were tested for empirical modeling. The best results were achieved for the plant cover, while the worst were for fAPAR. The study of the vegetation traits in the tundra has so far yielded the first results and will continue intensively (the analysis of the chlorophyll content, the green percent vegetation cover (PVC) determined from the ratio of the green and dry biomass, LAI, etc.).

Keywords: Laboratory spectroscopy, Field Spectroscopy, Remote Sensing, Norway Spruce, Montane Ecosystems, Relict Arctic-Alpine Tundra, The Krušné hory Mountains, The Krkonoše Mountains, Leaf Optical Properties, Reflectance, Grass sp., Foliage Traits.

Abstrakt

Dominantní druhy vegetace dvou strukturálně a funkčně odlišných horských ekosystémů byly studovány pomocí laboratorní a terénní spektroskopie a obrazových dat dálkového průzkumu Země: (1) člověkem ovlivněný homogenní stálezelený jehličnatý les reprezentovaný porostem smrku ztepilého v Krušných horách a (2) přirozený heterogenní ekosystém reliktní arkto-alpínské tundry v Krkonoších s převahou travin.

První část týkající se smrku ztepilého je zaměřena především na laboratorní spektroskopii. K hodnocení smrkových porostů na regionální a globální úrovni je potřeba podrobných znalostí o jejich spektrálních vlastnostech na úrovni jehlic a výhonů, avšak pozemní průzkum je velmi časově náročný. K získání většího množství pozemních dat pro analýzy porostů by mohly pomoci otevřené spektrální knihovny. Problém však může nastat s porovnatelností spekter pořízených různými přístroji. Tato práce se zaměřila na srovnatelnost spekter naměřených spektroradiometrem v kombinaci s kontaktní sondou a dvěma integračními sférami (Paper 3) a prokázala, že spektra naměřená kontaktní sondou a integrační sférou pro smrkové jehlice jsou signifikantně odlišná, pro listnaté druhy s dorziventrálním typem listu (reprezentované tabákem) jsou též odlišná, ale průměrné hodnoty vegetačních indexů z nich odvozených se již pohybují v rámci příslušných směrodatných odchylek, zatímco pro homogenní materiály, jako jsou barevné papíry nebo Spektralon, jsou spektra naměřená různými přístroji srovnatelná. Dále bylo v práci hodnoceno, zda data na různé měřítkové úrovni (v laboratoři určené obsahy pigmentů a vody v jehlicích, laboratorní spektra jehlic naměřená kontaktní sondou a spektrální data na úrovni porostu odvozená z obrazových leteckých hyperspektrálních dat APEX) dávají stejné výsledky v hodnocení rozdílů mezi skupinami měření ovlivněných různými faktory, jako jsou ročníky jehlic, pozice v koruně, stanoviště či lokalita výskytu (Paper 2). Dvě lokality v Krušnohoří ovlivněné různou intenzitou atmosférického znečištění v 70. letech vykazovaly mírné rozdíly v roce 2013 pouze na základě laboratorních biochemických dat, nikoli na základě dat spektrálních. Určitá heterogenita byla prokázána však mezi jednolivými jedenácti zkoumanými stanovišti na těchto dvou lokalitách na základě všech tří typů dat. Na základě podrobných laboratorních dat (biochemických i spektrálních) byly prokázány signifikantní rozdíly mezi jednotlivými ročníky jehlic i pozicí v koruně stromu. Pozicí v koruně stromu se pak práce zabývá i v další části, kde jsou porovnávány empirické modely pro odhad chlorofylu, karotenoidů a vody spočítané na základě odrazivosti naměřené kontaktní sondou pro tři různé úrovně koruny (bazální zastíněnou a produkční svrchní a spodní) – Paper 4. Výsledky dokazují, že modely pro zastíněnou bazální část koruny jsou přesnější než pro produkční část, což může být ovlivněno architekturou výhonů. Práce též potvrzuje lepší výsledky korelací s využitím metody PLSR než jednoduchých regresí a vegetačních indexů. Kromě metodických poznatků má práce i přínos po ekologické stránce (Paper 1 a 2), protože bylo prokázáno, že po eliminaci atmosférického znečištění smrkové monokulturní lesy v Krušných horách (zejména v jejich střední části) regenerují, i když nejsou zcela nepoškozené, a již nejsou pozorovatelné tak

významné rozdíly ve stavu porostů mezi jednotlivými lokalitami středního a západního Krušnohoří.

Zatímco pro správné fungování homogenních ekosystémů jsou důležité především vlastnosti porostu, v heterogenních ekosystémech hraje významnou roli navíc i jejich druhová skladba rostlinného společenstva, které je třeba věnovat také patřičnou pozornost. Především druhovou skladbou se zabývá část věnovaná reliktní arkto-alpínské tundře (Paper 5 a 6). Porovnávány jsou dosažené přesnosti klasifikací pro několik typů obrazových dat dálkového průzkumu Země různého spektrálního i prostorového rozlišení (Landsat, Sentinel-2, WorldView-2, ortofota a letecká hyperspektrální data ze senzorů APEX a AISA). Pro klasifikace těchto dat byly využity různě podrobné legendy. Legendy byly stanoveny s ohledem na prostorové rozlišení obrazových dat a kategorie byly specifikovány tak, aby měly přínos pro monitoring a ochranu oblasti, přičemž důraz byl kladen na rozlišení expanzivně silných druhů (trávy třtina chloupkatá, bezkolenec modrý a klečové porosty) a původního druhu trávy smilky tuhé. Nejlepších výsledků klasifikace (celková přesnost více než 80 %) bylo dosaženo na základě leteckých hyperspektrálních dat AISA s vysokým prostorovým rozlišením. Pro zvýšení přesnosti klasifikace heterogenních ekosystémů, jako je krkonošská tundra, se jako klíčové na základě našich výsledků jeví prostorové rozlišení dat. To dokazují dobré výsledky objektové klasifikace s prostorovým rozlišením 12,5 cm, ale pouze čtyřmi spektrálními pásmy (celková přesnost 71,96 % v případě podrobné legendy a přes 80 % v případě zjednodušené). V krkonošské tundře byly dále zkoumány vlastnosti porostů (výška, pokryvnost a fAPAR), a to s využitím terénní spektroskopie podél výškového a výživového gradientu táhnoucího se od Luční boudy na Luční horu ve dvou termínech v sezóně 2015 (Paper 7). Byly hledány především vhodné vegetační indexy pro tvorbu empirických modelů. Nejlepších výsledků bylo dosaženo pro pokryvnost, zatímco nejhorších pro fAPAR. Studium vlastností porostů v krkonošské tundře přineslo zatím základní výsledky a bude dále intenzívně pokračovat (například analýzy obsahu chlorofylu, podílu živé a uschlé biomasy, LAI apod.).

Klíčová slova: Laboratorní spektroskopie, terénní spektroskopie, dálkový průzkum Země, smrk ztepilý, horské ekosystémy, reliktní arkto-alpínská tundra, Krušné hory, Krkonoše, optické vlastnosti listu, odrazivost, trávy, vlastnosti listoví.

Table of Contents

List of Figures

Figures, where the source is not stated, are the work of the author of the thesis.

List of Tables

List of Abbreviations

$ANMB_{650-725}$	Area under curve normalized to Maximal Band depth between 650-725nm
ANN	Artificial Neural Networks
ANOVA	Analysis of variance
APEX	Airborne Prism Experiment (airborne hyperspectral sensor)
ARTMO	Automated Radiative Transfer Models Operator Graphic User Interface
ASD	Analytical Spectral Devices
CCC	Total canopy chlorophyll content
CP	Contact probe
CR	Continuum removal
CRI_{700}	Carotenoid reflectance index
DN	Digital numbers
fAPAR	Fraction of photosynthetically active radiation absorbed by the vegetation canopy
GER	Geophysical Environmental Research, now Spectra Vista Corporation
GF	Gap fraction
GfAPAR	Fraction of photosynthetically active radiation absorbed only by its photosynthesizing components
IS	Integrating sphere
KRNAP	Krkonoše Mountains National Park
LiDAR	Light Detection and Ranging
LOO	Leaf-one-out
LUT	Look-Up-Tables
MLC	Maximum Likelihood Classifier
MODIS	Moderate Resolution Imaging Spectroradiometer
MSR	Multiple stepwise regression
NDI	Normalized Differential Index
NDVI	Normalized difference vegetation index
NED	Noise Equivalent Radiance
NEΔL	Noise Equivalent Delta Radiance
NOAA AVHRR	National Oceanic and Atmospheric Administration Advanced Very High Resolution Radiometer
OA	Overall accuracy

OBIA	Object based image analysis
PA	Producer's accuracy
PCA	Principal component analysis
PLSR	Partial Least Square Regression
PVC	Green percent vegetation cover
RAMI	Radiation transfer model intercomparison initiative
RMSEP	Root Mean Squared Error of Prediction
RTM	Radiative transfer model
S/N	Signal to Noise Ratio
SVM	Support Vector Machine
SWIR	Shortwave infrared
TCARI/OSAVI	Ratio of transformed chlorophyll absorption in reflectance index and optimized soil adjusted vegetation index
UA	User's accuracy
UAV	Unmanned Aerial Vehicle
VNIR	Visible and near infrared

1 Introduction

Natural ecosystems have evolved while experiencing abiotic and biotic disturbances such as drought, winds or insect outbreaks. However, nowadays they must cope, in addition, with human-related (anthropogenic) stressors, which can be either direct as logging and clearing (especially in the case of forests) or indirect in the form of climate change factors, air pollution or invasive species spreading (Trumbore, Brando, and Hartmann 2015). These stressors have an impact on the ecosystem's functioning, composition (e.g., Morin et al. 2018) and extent. It is necessary to understand the ecosystem processes and its functioning to protect the ecosystems in an effective way. That is why the monitoring of ecosystems on different scale levels is essential, and methods of laboratory/field spectroscopy and remote sensing can be very helpful in proper management measures. The usefulness of spectroscopy and remote sensing methods has already been proven in many studies dealing with: land cover and forest changes on global, regional or local scales (e.g., Global Land Cover Facility research center: http://glcf.umd.edu/; Huang et al. 2009; Townshend et al. 2012; Song et al. 2014; Feng et al. 2016), forest health assessment (Angela Lausch et al. 2016, 2017; Pause et al. 2016; Senf, Seidl, and Hostert 2017), species composition (Fassnacht et al. 2016; Raczko and Zagajewski 2018), changing biodiversity analyses (Turner et al. 2003; A. Lausch et al. 2016; Vihervaara et al. 2017), carbon cycling (Patenaude, Milne, and Dawson 2005; Nestola et al. 2018) and ecosystem functioning, processes and services (Pettorelli et al. 2018). Although vegetation studies are one of the most common in remote sensing research, there is still a lot of unresolved issues because of the diversity and complexity of vegetation ecosystems.

This thesis contributes to scientific issues in the use of laboratory/field spectroscopy and remote sensing in two significantly different montane ecosystems: (1) a homogeneous human-influenced evergreen coniferous forest represented by a Norway spruce forest in the Krušné hory Mountains and (2) heterogeneous natural ecosystem of the relict arctic-alpine tundra in the Krkonoše Mountains with predominance of grasses. The Norway spruce forest was selected as a representative of a homogeneous man-managed forest ecosystem for its prevailing abundance in Czechia – 50.5 % of the forest land in 2016 (Ministerstvo zemědělství 2017). Due to the major area covered by the Norway spruce forest and its great ecological and economic importance, it is important to monitor its condition to prevent any large degradation since reforestation is a long-term process. On the contrary, the relict arctic-alpine tundra is a unique heterogeneous natural ecosystem covering just a very small area in the higher altitudes of the Krkonoše Mountains. The tundra ecosystem is very sensitive to the ongoing local and global environmental changes (Chapin et al. 1995; Elmendorf et al. 2012), therefore, its research and protection is necessary.

1.1 Structure of the thesis

The thesis is based on ten contributions, which I co-authored. These are three peer-reviewed book chapters, five peer-reviewed papers and two shorter peer-reviewed conference papers. Firstly, in the overview section (Chapter 2), a brief theory of laboratory spectroscopy measurements and vegetation trait modeling are presented (subchapters 2.1 and 2.2). These two subchapters summarize and slightly adapt all three peer-reviewed book chapters. The overview also adds information about studies using laboratory/field spectroscopy and remote sensing data for selected ecosystems (Norway spruce forest and relict arctic-alpine tundra) monitoring and the challenges associated with it (subchapter 2.3). The aims and research questions of this thesis are presented in Chapter 3. Secondly, the original research articles which I co-authored are included: Chapter 4 consists of four publications providing new insights in laboratory spectroscopy for a Norway spruce ecosystem (Papers 1 – 4). Three publications (Papers 5 – 7) focused on remote sensing data for relict arctic-alpine tundra ecosystem evaluation are presented in Chapter 5. The papers represent answers to the research questions presented in Chapter 3. The results are synthesized and discussed in Chapter 6 and Chapter 7 presents the most important conclusions and possibilities of future research.

The original research articles deal specifically with:

Norway spruce forest ecosystem

Paper 1 "TEMPORAL CHANGES IN NORWAY SPRUCE PHYSIOLOGICAL STATUS USING HYPERSPECTRAL DATA: A CASE STUDY OF MOUNTAINOUS FORESTS AFFECTED BY LONG-TERM ACIDIC DEPOSITIONS" presents the first results of the state of Norway spruce forests assessment in the Krušné hory Mountains. It compares the biochemical and biophysical needle parameters from the trees sampled in the Krušné hory Mountains between 1998 and 2013, the geochemical conditions of study stands in the western and central part of the Krušné hory Mountains in 2012 and constructs prediction models for photosynthetic pigments and water content based on laboratory spectroscopy.

Paper 2 "STATISTICAL COMPARISON OF SPECTRAL AND BIOCHEMICAL MEASUREMENTS ON AN EXAMPLE OF NORWAY SPRUCE STANDS IN THE ORE MOUNTAINS, CZECH REPUBLIC" deals with the statistical comparison and ascertainment of the relationships among various factors (areas, stands, needle age classes or positions in the tree crown) based on different datasets – biochemical and biophysical (photosynthetic pigment and water content), laboratory spectroscopic (the spectral reflectance measured by ASD FieldSpec 4 wide-res and plant contact probe) and image spectroscopic (airborne hyperspectral image acquired by APEX sensor).

Paper 3 "COMPARISON OF REFLECTANCE MEASUREMENTS ACQUIRED WITH A CONTACT PROBE AND AN INTEGRATION SPHERE: IMPLICATIONS FOR THE SPECTRAL PROPERTIES OF VEGETATION AT A LEAF LEVEL" focuses on the comparison of the reflectance spectra acquired by different laboratory devices (two integrating spheres and a plant contact probe). Besides the Norway spruce samples, tobacco leaves and artificial samples with stable optical properties were measured and the variability among the devices were evaluated.

Paper 4 "MODELS FOR ESTIMATING LEAF PIGMENTS AND RELATIVE WATER CONTENT IN THREE VERTICAL CANOPY LEVELS OF NORWAY SPRUCE BASED ON LABORATORY SPECTROSCOPY" addresses the differences of the Norway spruce needles' optical and biochemical/biophysical properties in the tree crown and presents the empirical models for three different canopy levels.

Relict arctic-alpine tundra ecosystem

Papers 5 and 6 evaluate different remote sensing image data for tundra species classifications, Paper 5 "CLASSIFICATION OF VEGETATION ABOVE THE TREE LINE IN THE KRKONOŠE MTS. NATIONAL PARK USING REMOTE SENSING MULTISPECTRAL DATA" is focused on multispectral data with different spatial resolutions, Paper 6 "CLASSIFICATION OF TUNDRA VEGETATION IN THE KRKONOŠE MTS. NATIONAL PARK USING APEX, AISA DUAL AND SENTINEL-2A DATA" is focused on hyperspectral data and Sentinel-2A data.

Paper 7 "FIELD SPECTROSCOPY FOR VEGETATION EVALUATION ALONG THE NUTRIENT AND ELEVATION GRADIENT ABOVE THE TREE LINE IN THE KRKONOŠE MOUNTAINS NATIONAL PARK" is similarly focused, as Paper 4, on empirical modeling, but for tundra vegetation and its height, plant cover and fAPAR. It also compares the models for two datasets acquired in different vegetation phenology phases.

2 Overview of the studied topic

As this thesis is primarily focused on laboratory/field spectroscopy, the main principles of measuring the vegetation optical properties by spectroradiometers are described. Moreover, the basic principles of the empirical (statistical) and radiative transfer modeling of the vegetation traits are explained. These two parts are based on three peer-reviewed chapters (Červená, Potůčková, et al. 2017a, 2017b; Červená, Mišurec, et al. 2017) of the book Albrechtová, Kupková, and Campbell (2017) which I co-authored. Chapter 2 is terminated by the summarization of the challenges in the research of the selected ecosystems by the laboratory/field spectroscopy and remote sensing methods.

2.1 Laboratory spectroscopy [1]

2.1.1 Field spectroradiometers – theory of measurement

A spectroradiometer is composed from entrance slits, diffraction gratings/prisms and detector arrays. Together, these components form a spectrograph or optical bench. The spectroradiometer comes into existence by adding the fore-optics, optical paths and calibration and control systems. (Mac Arthur 2013)

Diffraction grating is an optical device dispersing polychromatic (white) light into its constituent wavelengths (monochromatic light). It is constructed as finely spaced grooves on a surface (with a typical groove size of < 1μm). When a collimated light is reflected from a diffraction grating, it is captured by detector arrays. The detectors are constructed from different materials, a specific material for a limited range of wavelengths. Just like the detectors, the diffraction gratings are also restricted by the spectral range. Hence, the spectroradiometer measuring visible, near infrared and shortwave infrared light consists of several spectrographs, Figure 1. (Mac Arthur 2013)

[1] This chapter is translated from an original (Červená, Potůčková, et al. 2017a) published in the peer-reviewed book Albrechtová, Kupková, and Campbell (2017).

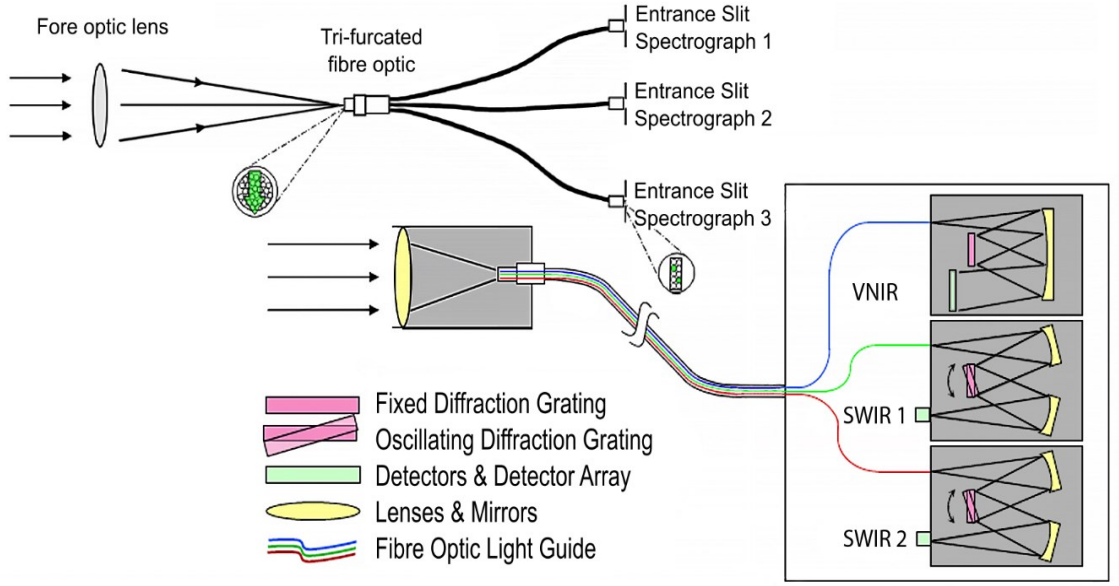

Figure 1: Spectroradiometer construction
(Source: adapted after Mac Arthur (2013)

Numerous manufactures of spectroradiometers exist, some well-known ones are GER (Geophysical Environmental Research, now Spectra Vista Corporation), ASD (Analytical Spectral Devices) and the newer Spectral Evolution. In this study, an ASD FieldSpec 4 Wide-Res was used and, therefore, is described more in the next subchapter.

2.1.1.1 ASD FieldSpec 4 Wide-Res

The spectroradiometer ASD FieldSpec 4 Wide-Res has a full spectral range (350–2500 nm), which is measured by three detectors: A silicon detector for the visible and near infrared portion of the electromagnetic spectrum (VNIR: 350–1000 nm) and two indium gallium arsenide (InGaAs) detectors covering the shortwave infrared (SWIR1: 1000–1800 nm and SWIR2: 1800–2500 nm). (ASD Inc. 2016)

The spectral resolution of the spectroradiometer is 3 nm in VNIR and 30 nm in the SWIRs, while the sampling interval is about 1.4 nm in the VNIR and 2 nm in the SWIRs. The difference between the spectral resolution and sampling interval is visualized in Figure 2. However, the measured values are automatically interpolated using a cubic spline, so the resulting data acquired by the ASD FieldSpec 4 Wide-Res spectroradiometer has 2151 bands 1 nm wide. (ASD Inc. 1999, 2016)

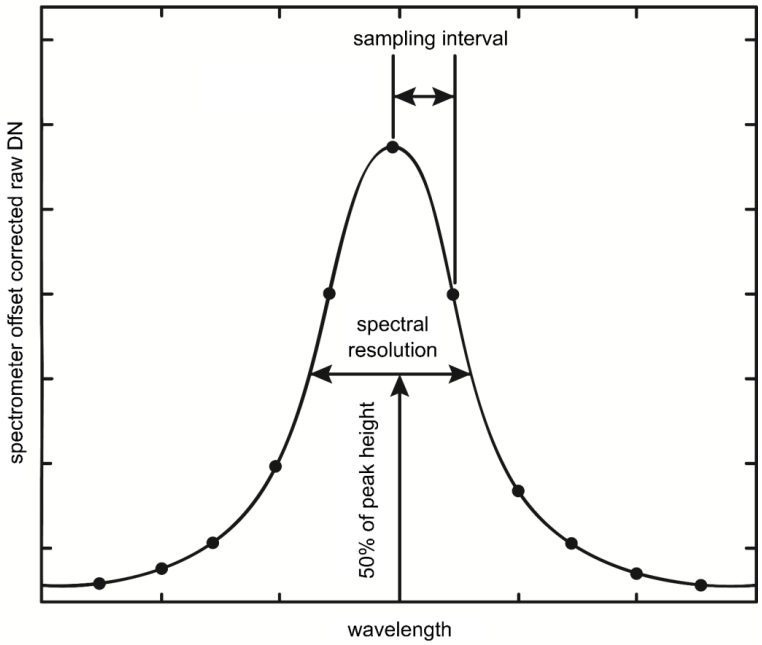

Figure 2: Spectral resolution and sampling interval
(Source: adapted after ASD Inc. (1999)

The next important specifications of spectroradiometers are the Signal to Noise Ratio (S/N) and other characteristics evaluating the "purity" of the measured radiance – the Noise Equivalent Radiance (NED) representing the value of radiance which is S/N = 1 or the Noise Equivalent Delta Radiance (NEΔL) representing the ratio of the reference radiance to the required S/N ratio (Gibbons and Richard 1979; Green 1992; Mac Arthur 2013). The specifications for the ASD FieldSpec 4 Wide-Res instrument are the following: NEΔL: $1.0*10^{-9}$ W/cm^2/nm/sr for a wavelength of 700 nm (VNIR), $1.2*10^{-9}$ W/cm^2/nm/sr for 1400 nm (SWIR 1) and $1.9*10^{-9}$ W/cm^2/nm/sr for 2100 nm (SWIR 2) (ASD Inc. 2016). Nevertheless, these values can slightly change for every device (ASD Inc. 1999).

Reflectance measurements by a field spectroradiometer can be undertaken in the field using the spectroradiometer's optical cable only or in combination with a so-called pistol grip (see Figure 3), which has a built-in bulls-eye level for added precision. This kind of reflectance measurements are usually used for larger areas of reflectance measurements and for surfaces that are difficult to measure in laboratory conditions – e.g., canopy reflectance of heterogeneous grasslands or large anthropogenic surfaces. This type of measurement was used for the arctic-alpine tundra reflectance measurements in this thesis (Paper 7). However, field spectroradiometer can also be used in the laboratory – coupled with a contact probe or integrating sphere. The optical properties of the vegetation at the leaf or shoot level, soil samples, etc. are usually measured this way. These types of measurements were used for the Norway spruce optical properties measurements in this thesis (Papers 1-4) and will be described in detail in next subchapter (2.1.3).

Figure 3: Spectroradiometer ASD FieldSpec 4 Wide-Res with pistol grip and measuring the white reference (99% Spectralon)

The contact probe (Figure 4) is designed for the contact measurement of solid materials. It has its own light source, whose intensity differs between the models determined for inanimate materials and the models for vegetation reflectance measurements. In the case of the vegetation measurement, the intensity of the illumination is lower to avoid overheating and the degradation of the samples (a plant contact probe). Construction of the contact probe is proposed to minimize measurement errors associated with stray light and light scattering. The contact probe is designed to measure just the reflectance, not the transmittance of the sample. (ASD Inc. 2016)

Figure 4: Spectroradiometer ASD FieldSpec 4 Wide-Res with a plant contact probe

The integrating sphere (Figure 5a) collects the reflected (or transmitted) light from the samples over a full hemisphere. The sphere, by nature of its internal diffuse reflection and integration of the energy, is insensitive to the directional reflectance features coming from the sample, and, therefore, gives a very repeatable "averaged" response to the reflectance of the sample placed in the beam at the sphere port. The inside of the sphere is covered by a highly diffuse polymer material called Zenith®. Zenith® is highly reflective (> 95 %) and a Lambertian reflector over the wide spectral range of 350-2500 nm. The light source is a bulb resembling, by its properties, the sunlight and produces a collimated beam. The sphere contains six entrance ports (Figure 5b) equipped with a sample holder, a light source holder, a light trap, white plugs, etc. The settings of the individual ports differ according to type of measurement – i.e., reflectance or transmittance of sample, instrument calibration using the white reference and stray light measurement. (ASD Inc. 2016)

The spectroscopic measurements are saved as dimensionless integer values called DNs (digital numbers). Their relationship to the spectral radiance L [$W*m^{-2}sr^{-1}\mu m^{-1}$] is given by the instrument's calibration curve (Liang 2004).

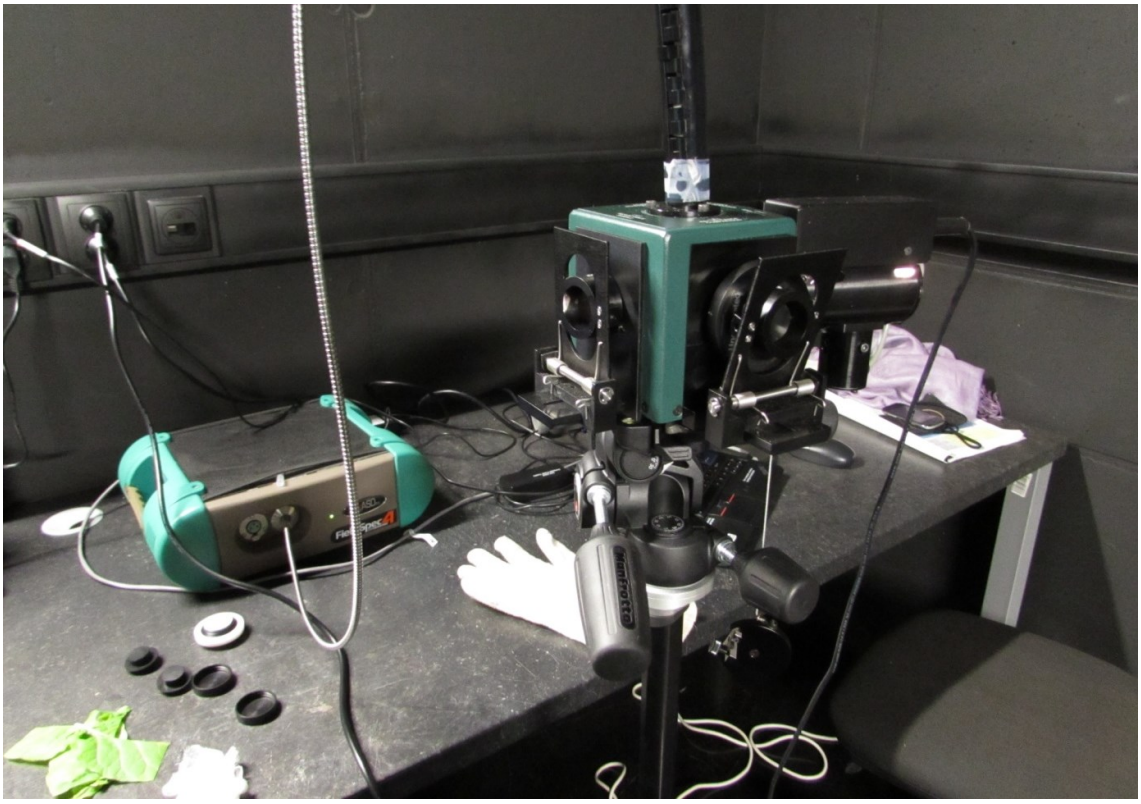

Figure 5: Integrating sphere – a) overall view when the vegetation sample optical properties are measured b) view from above with the ports description.

2.1.2 ASD contact probe measurements of Norway spruce shoots

In the case of herbs or deciduous trees, planar leaf reflectance measurements, it is recommended to measure several parts of the leaf (avoiding the veins) placed on a black surface with minimum reflectance. Concerning conifers, it is impossible to measure just one needle, thus, the whole shoots of the same age are measured. The shoots are placed side by side close together in one direction in two or three layers on a black-painted plate ensuring minimal reflection of the background. The contact probe's field of view (a diameter of 10 mm) must always be fully adjacent to the sample to be sure that no ambient light is getting into the measurement process. A dark chamber for measurements is the optimal choice. The recorded radiance at the interval of the wavelengths 350 – 2500 nm coming from sample is normalized to the radiance of the white reference (99% Spectralon) – Equation 1 – to get the relative reflectance. As for the planar leaves, it is advisable to measure the Norway spruce sample in more parts and calculate the median or average from all the measurements for one sample (Figure 6). The single measurement (at one contact probe position) is also the average of more measurements. The number of scans to the average can be changed for each measurement at the spectroradiometer's settings – a value greater than 25 is recommended in the manual to maximize the signal to noise ratio (ASD Inc. 2012).

$$[1] \qquad R_{sample} = \frac{DN_{sample}}{DN_{WR}}$$

R_{sample} ... relative reflectance of the sample, DN_{sample} ... measured reflected radiation from the sample (in DN values), DN_{WR} ... measured reflected radiation of the white reference (99% Spectralon)

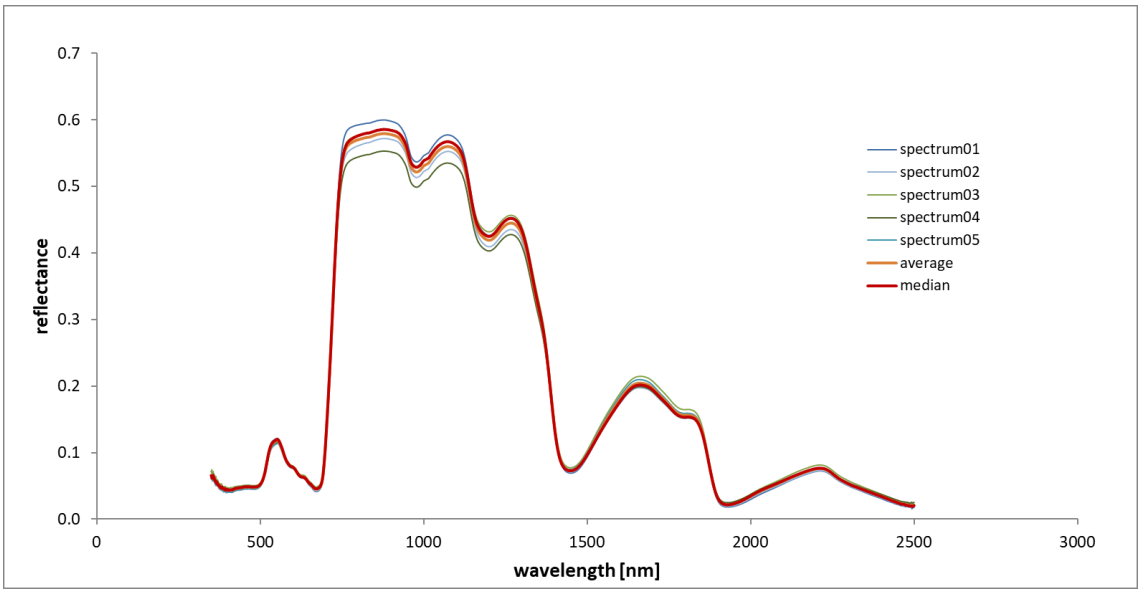

Figure 6: Five reflectance spectral curves measured for one sample and their median and average

2.1.3 ASD integrating sphere measurements of Norway spruce needles

The optical properties measurements using the integrating sphere should be repeatable and accurate, but it is necessary to understand what participates in the measured signal (Equation 2; ASD Inc. 1999):

[2] *Measured signal = true signal + dark current + stray light + random noise*

The dark current is an internal noise of the instrument and is recorded every time when the white reference is measured, thus, it can be easily subtracted so it is a negligible contributor. The stray light is usually quite stable, for the ASD FieldSpec 4 Wide-Res, it reaches around 1 % of reflectance in the SWIR and 2 % of reflectance in the VNIR. Because of its stability, it can be measured just at the beginning and at the end of all the measurements. It can be also ignored for not so precise measurements. The random noise is the integral part of every measuring device and it is not possible to correct it. Nevertheless, it is negligible in most cases.

The basic principles of getting the reflectance or transmittance curves are the same as for the contact probe measurements. The radiance coming from the sample is normalized to the radiance coming from the white reference. There are two principles of measuring the optical properties in the integrating sphere. The first one corrects the data for the so-called substitution

error and the second one does not. The approach correcting the substitution error tries to keep the overall radiance in the sphere constant during all the measurements (the samples and the white reference also). Otherwise, in the case of measuring the vegetation sample reflectance, the overall radiance is lower because of its relatively high transmittance in comparison to almost zero transmittance of the Spectralon. Configuration of the ports is summed up in Table 1. When averaging the scans, it is necessary to set it to the higher value for the integrating sphere than for the contact probe, because there is a higher signal to noise ratio (for the Norway spruce needles, 100 scans are usually averaged).

Table 1: Configuration of the ASD RTS-3ZC integrating sphere for the reflectance and transmittance measurements
(adapter after Yanez-Rausell, Malenovsky, et al. 2014; ASD Inc. 2008)

	Method	Measured Quantity	Sphere Ports Configuration				
			Port A	Port B	Port C	Port D	Port E
Reflectance measurement	Does not correct for the substitution error	stray light	L	W (uncal)	LT	P	P
		white reference	L	W (uncal)	W (cal)	P	P
		sample	L	W (uncal)+SH	S+SH	P	P
	Corrects for the substitution error	stray light	L	W (cal)+SH	LT	P	P
		white reference	L	S+SH	W (cal)+SH	P	P
		sample	L	W (uncal)+SH	S+SH	P	P
Transmittance measurement	Does not correct for the substitution error	stray light	P	LT	W (uncal)	L	P
		white reference	P	W (cal)	LT	L	P
		sample	P	W (cal)	LT	L+S+SH	P
	Corrects for the substitution error	stray light	P	LT	W (uncal)	L	P
		white reference	P	W (cal)+SH	S+SH	L	P
		sample	P	W (cal)	LT	L+S+SH	P

L – Lamp; W – White reference: uncal … uncalibrated Zenith standard, cal … calibrated Zenith standard; S – Sample, SH – Sample Holder, LT – Light Trap, P – white Plug

The needles' measurements in the integrating sphere are more difficult than the planar leaves' measurements. The first design on how to measure conifers in an integrating sphere was proposed by Daughtry, Biehl, and Ranson (1989). Mesarch et al. (1999) edited the process and Yanez-Rausell, Schaepman, et al. (2014) and Yanez-Rausell, Malenovsky, et al. (2014) made it more accurate and summarized it. The process of measuring the needles in the integrating sphere proposed by these authors can be summarized as follows:

1) Placing the needles into the sample holders: It is necessary to keep the gaps among the needles as small as possible, but the needles cannot touch each other or even overlap.
2) Measuring the reflectance and transmittance of the sample in the sphere by spectroradiometer (as summed up in Table 1)
3) Black-white scan of needles in the sample holder: The scanner having both bottom and top illuminations must be used to avoid any shadows in the scanned picture (Figure 7a)
4) Automatic calculation of the gap fraction and needle surface based on number of black and white pixels in the image.
5) Calculation of the resulting reflectance and transmittance based on all the measurements (the spectra acquired by the spectroradiometer and the gap fraction calculated from the scanned images) using the Equations 3 and 4.

$$[3] \qquad R_{needle} = \frac{\frac{\left(DN_{sample} - DN_{stray\ light}\right) \cdot R_W}{DN_{WR} - DN_{stray\ light}}}{1 - GF}$$

R_{needle} ... reflectance of the needles, DN_{sample} ... measured radiance from the sample, i.e., the needles and the gaps among them (in DN values), $DN_{stray\ light}$ ... measured stray light (in DN values), DN_{WR} ... measured radiance from the white reference (99% Spectralon), R_W ... reflectance of the integrating sphere walls (close to 100 %), GF ... Gap fraction

$$[4] \qquad T_{needle} = \frac{\frac{DN_{sample}}{DN_{WR}} - GF}{1 - GF}$$

T_{needle} ... transmittance of the needles, DN_{sample} ... measured radiance from the sample, i.e., the needles and the gaps among them (in DN values), DN_{WR} ... measured radiance from the white reference (99% Spectralon), GF ... Gap fiction

The biochemical estimation of the pigments and water content is usually undertaken together with the optical properties measurements. To be able to do this, it is necessary to expand the above steps. Before placing the needles into the sample holder, it is necessary to estimate how many of them will be needed and weigh them (fresh sample weight). When not all the needles are placed into the sample holder, it is crucial to keep them with the sample and after the optical properties measurements and sample holder scan (Figure 7a) take the needles out from the sample holder and scan them all together with the remaining needles (all the weighed needles; Figure 7b). Subsequently, these needles are put into a tube, dried and weighed again (dry sample weight). Biochemical analyses are then performed. The scanned images of needles serve as the basis for recalculating the contents of the biochemical compounds contents from the mg of compound/g dry matter to the mg of compound/cm^2. These units are essential, for example, for the radiative transfer models (subchapter 2.2.3).

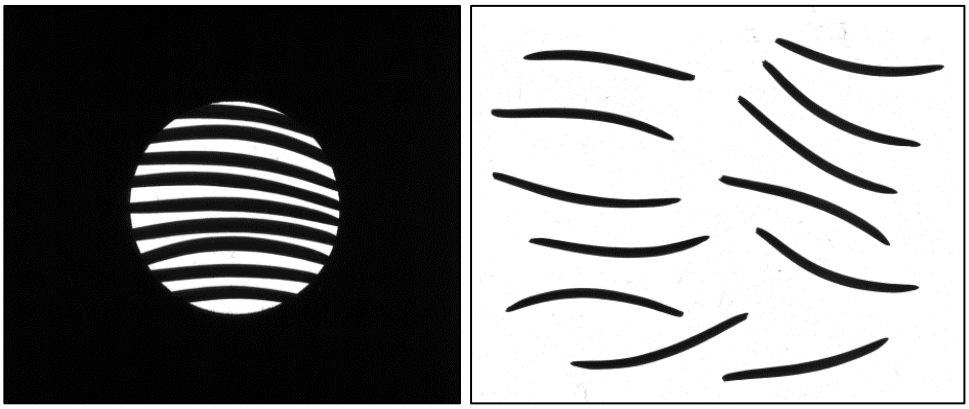

Figure 7: a) Scan of needles placed into sample holder, b) scan of all weighed needles (needles taken out from the sample holder + remaining needles for the sample)

2.2 Spectra preprocessing and vegetation traits modeling [2]

The spectra acquired by the laboratory/field spectroscopy offer many possibilities how to process them. The spectra can be compared among each other or with the spectral libraries (typical, for example, for geological applications) to classify them into some categories. However, in vegetation studies, spectra are usually used for vegetation traits modeling. The traits can be biochemical (pigments like chlorophyll or carotenoids contents), biophysical (water content) or structural (leaf area index etc.). All the models in optical remote sensing can be grouped into two major categories 1) empirical, using statistical methods and 2) physical, using physical principles, i.e., radiative transfer models. Alternatively, a combination of them (hybrid models) also exists (Liang 2004). This thesis is focused on empirical modeling, so the principles of it are discussed in detail, however, basic principles of RTM are also summed up for comparison. The spectra can also be transformed differently before entering the models, the most frequent methods of spectra transformation are derivatives (e.g., Thulin et al. 2012), continuum removal (e.g., Kokaly and Clark 1999a) or band ratios called vegetation indices (e.g., Main et al. 2011), these methods are also shortly described.

2.2.1 Spectra transformations

Algebraic transformations of the original spectral reflectance curves are used for the minimization of noise and other factors influencing the spectral information. Derivations and Continuum removal are two of the often-used methods for transforming the whole spectral curves. On the contrary, vegetation indices transform spectra by just rationing selected bands.

[2] This chapter is compiled based on two chapters (translated and slightly modified; Červená, Potůčková, et al. 2017b; Červená, Mišurec, et al. 2017) published in the peer-reviewed book Albrechtová, Kupková, and Campbell (2017).

2.2.1.1 Derivatives

The first derivative of the reflectance spectral curve (Figure 8) expresses a slope, i.e., the rate of change in the reflectance values between the neighboring wavelengths. In the case of discrete data, the first difference is used instead of the first derivative and is calculated according to Equation 5 (T. P. Dawson and Curran 1998):

$$[5] \qquad D_{\lambda(i)} = \frac{R_{\lambda(j+1)} - R_{\lambda(j)}}{\Delta\lambda}$$

$D_{\lambda(i)}$ ... the first difference of the reflectance at wavelength i which is located in the middle of wavelengths j and j+1; $R_{\lambda(j)}$, $R_{\lambda(j+1)}$ ... the reflectance values at wavelengths j resp. j+1; $\Delta\lambda$ ... the difference between wavelengths j a j+1

Similarly, higher order derivatives can be computed. In comparison to the original reflectance spectral curves, the second order and higher derivatives should be relatively insensitive to variations in the illumination intensity caused by changes in the sun's angle, cloud cover and topography. (Tsai and Philpot 1998)

However, derivatives are notoriously sensitive to noise. Thus, smoothing or otherwise minimizing noise is a major issue (Tsai and Philpot 1998). Among the various methods for smoothing spectral data, algorithms based on the least-square fits are most commonly used – perhaps the most common is the Savitzky and Golay method (Savitzky and Golay 1964), which provides a simplified least square procedure for simultaneously smoothing and differentiating the data (Tsai and Philpot 1998).

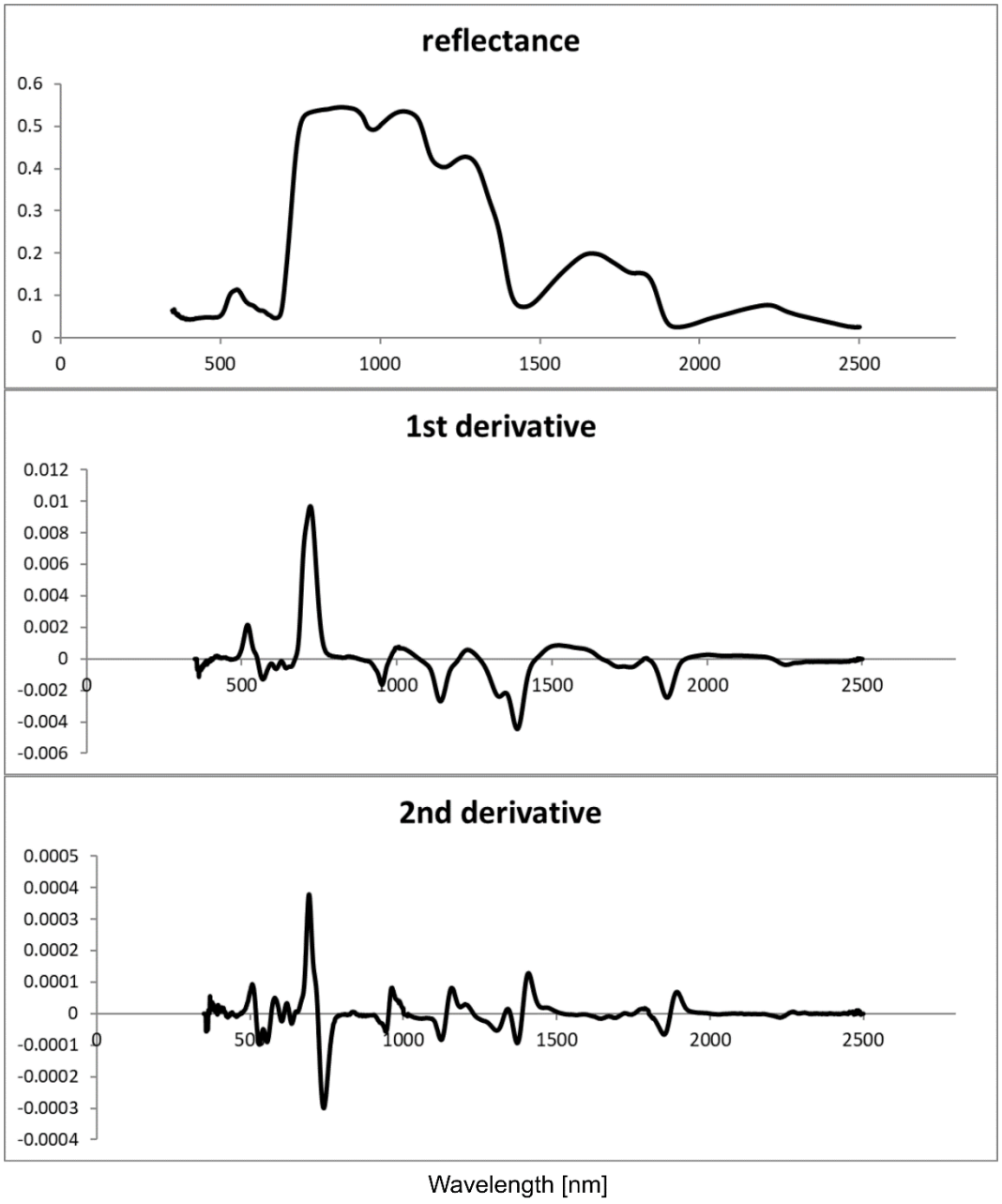

Figure 8: Reflectance spectral curve of the Norway spruce (up) and its first and second derivatives (lower)

2.2.1.2 Continuum Removal

The main objective of the method called Continuum removal (CR) is to enhance and normalize the shape of the spectral curve (Kokaly and Clark 1999). Continuum removal is usually performed on a selected interval of the wavelengths characterizing the studied phenomena, typically around the absorption maximum. The starting and ending points of the selected wavelengths interval determine the Continuum line and their new value equals one. Other transformed reflectance values inside the interval reach new values from zero to one by Equation 6.

$$[6] \qquad R'_\lambda = \frac{R_\lambda}{R_{C(\lambda)}}$$

R'_λ ... the reflectance value after CR transformation at wavelength λ, R_λ ... the original reflectance value at the same wavelength (λ), $R_{C(\lambda)}$ ... the continuum value (i.e., the value at wavelength λ given by the line connecting the end points of the spectral curve's selected interval) (Kokaly and Clark 1999)

Continuum removal at the delimited part of the spectral curve (Figure 9) allows one to compute the absorption band depth or its area. This is used in the vegetation index called the Area under curve Normalized to the Maximal Band depth between 650 and 725 nm, $ANMB_{650-725}$. (Z. Malenovský et al. 2006)

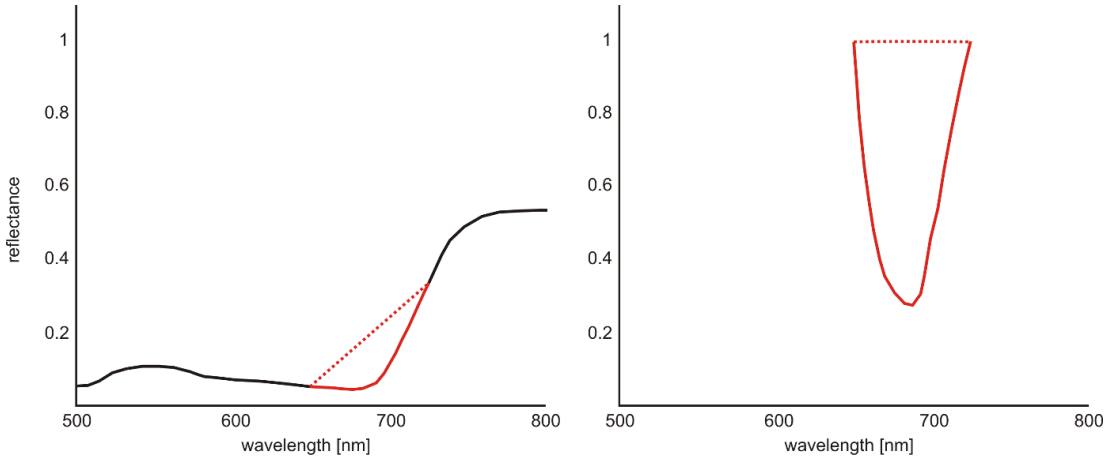

Figure 9: Continuum Removal principle – example for the wavelengths interval of $ANMB_{650-725}$ index

2.2.1.3 Vegetation indices

The main purpose of vegetation indices is a reduction of the data spectral range from hundreds or even thousands of values to just one value which will represent the studied vegetation trait. The biochemical compounds (or biophysical) have their typical absorption features (minima and maxima) and vegetation indices try to use them.

The overview of commonly used indices is possible to find in a book Hyperspectral Remote sensing of vegetation (Thenkabail, Lyon, and Huete 2012) or in Czech book Letecký dálkový průzkum Země (Zemek 2014b) resp. its English version (Zemek 2014a). A comprehensive list of the indices suitable for chlorophyll content estimations are offered in the publications of Main et al. (2011) and le Maire, François, and Dufrêne (2004); and for carotenoids contents, the publications of Hernández-Clemente, Navarro-Cerrillo, and Zarco-Tejada (2012) and Yi et al. (2014).

Zemek (2014b, 2014a) separates indices for chlorophyll content estimations to seven categories:

1) Simple ratio indices of reflectance or first derivative at two wavelengths
2) Normalized difference indices (e. g. NDVI)
3) Indices using three spectral bands
4) Combined indices – also possibly including some coefficients (e.g. TCARI/OSAVI)
5) Indices based on spectral continuum, integral indices
6) Red edge inflection point
7) Other

Other possible division is considering the scale level for which the indices were designed: 1) leaf level (i.e., spectral curves measured by a spectroradiometer and contact probe or integrating sphere), 2) ground level (i.e., spectroradiometric measurements in the field), 3) crown or canopy level – aerial or satellite remote sensing data. Also, a division into broad-band (multispectral data) and narrow-band (hyperspectral data) indices exists.

2.2.2 Empirical models

The empirical (or statistical) models are based on finding the relationship between the quantitative parameter of the vegetation derived in the laboratory or in the field (dependent variable) and the vegetation optical properties, usually reflectance (independent variable). Different kinds of regressions are used for these purposes, e.g., simple linear regression, multiple stepwise regression (MSR) or partial least square regression, PLSR (Main et al. 2011; Thulin et al. 2012; Yi et al. 2014). These methods will be described in following subchapters.

An advantage of the empirical models is their computational simplicity and speed. They work well locally, but it is not possible to transfer them to another locality, time period, ecosystem or other remote sensing data (Liang 2004).

2.2.2.1 Simple regression

The simplest type of regression (as the name implies) is simple linear regression, where the dependency between two quantitative characteristics is expressed by a straight line defined by Equation 7:

$$[7]\ y = a + bx + \varepsilon$$

y ... dependent variable, x ... independent variable, a and b ... regression coefficients, i.e., values which are estimated by the least squares using the sample data, ε ... random variability ("error").

However, simple regression does not have to always be linear, the sample data can also be approximated by a polynomial curve (usually 2nd order polynomial – parabola, i.e., quadratic regression). In practice, the data is usually transformed firstly by the selected function and then

approximated again by the straight line. Dependencies approximated by the exponential or power function can also be transformed to a linear problem.

The coefficient of determination (R^2) describes the proportion of the variance in the dependent variable that is predictable from the independent variable. It is a statistical measure of how well the regression predictions approximate real data points. It reaches values in the interval <0, 1>, higher values close to one mean more successful regression (an R^2 of 1 indicates that the regression predictions perfectly fit the data). This coefficient is also used for the evaluation of other types of regression.

For more information about the mathematical background of simple and multiple stepwise regression, see the statistical books, e. g. Zvára (2003) or Zvára (2008). How to compute these methods in the free available statistical software R (https://www.r-project.org/) is summarized by Pekár and Brabec (2009) or Crawley (2013).

2.2.2.2 Multiple stepwise regression

Multiple stepwise regression is a method which tries to find the optimal model by adding or subtracting the independent variables step by step. The objective is to maximize the prediction power with the least number of independent variables (wavelengths) which are statistically relevant for the prediction of the dependent variable values (vegetation trait values). This method is also used as an explorative one.

Two basic approaches how to compute multiple stepwise regression exist – forward and backward selection. Forward selection creates a model progressively from a constant by adding more independent variables (wavelengths) based on the simple correlation coefficient. Firstly, the statistically significant independent variable which describes the dependent variable best is added. Then, a similar procedure is applied with the exception that the newly added independent variable cannot be correlated with any other independent variable added to the model earlier. Backward selection computes the resulting model reversely, i.e., it adds all the possible independent variables to the model and then eliminates those, which are not statistically significant, step by step. This method is not used in spectroscopy very often because of the huge number of independent variables (wavelengths).

The result of both methods is based on the limitation of the maximum number of wavelengths that can be used is equal to the number of samples. The wavelengths are sorted according to their influence on the studied vegetation trait (biochemical or biophysical compounds or structural parameter). However, due to the requirement to maintain the relationship between the spectral reflectance and vegetation trait as simply as possible, it is not appropriate to use a larger number of wavelengths for the resulting equation than about 10 % of the number of input samples. The resulting model can look like this (for the spectral reflectance ρ), Equation 8.

$$[8]\ \text{vegetation\_trait} = a_0 + a_1 * \rho(\lambda_1) + a_2 * \rho(\lambda_2) + \ldots + a_n * \rho(\lambda_n)$$

a0, a1, a2, ..., an ... regression function coefficients, $\rho(\lambda i)$ ... reflectance at wavelength λi

The power of the resulting model is, for simple regression, given by the coefficient of determination (R^2).

2.2.2.3 Partial least square regression

In comparison to the two previously described methods, partial least square regression uses all the input spectral reflectance values. It uses the principles of the Principal component analysis (PCA) and multiple linear regression. It is used often in spectroscopy, because it allows one to predict the dependent variables, also from the huge number of independent ones. Compared to PCA, which constructs new components only on the basis of the highest variability in the input data (which may not explain the studied variable at all), the PLSR constructs new components on the basis of the highest variability which also explains the dependent variable (they are correlated).

The key question for creating the models using PLSR is: How many components is it optimal to use for the model? A redundant number of components can describe the calibration data better, but simultaneously it also describes its random errors, so the general prediction power is lost. This is called over-fitting. On contrary, under-fitting means not using all the relevant information available in the data. For the optimal number of component estimation and, thus, reaching the maximal prediction power of the model, the method of cross-validation is used. Cross-validation randomly splits the data into *k* disjoint subsets of approximately the same size. In an extreme scenario (method Leaf-one-out, LOO), the number of disjoint subsets equals the number of samples. Then, the prediction model is computed based on *k*-1 subsets. The values of the dependent variable are predicted based on this model for the skipped subset of data. This is repeated until every sample has just one prediction of the studied dependent variable. These predictions are then compared to the reference (measured) values using, for example, the Root Mean Squared Error of Prediction (RMSEP). The RMSEP value can be plotted as a function of the number of components. For a good PLSR model the satisfactory number of components is where the first significant local minimum of the RMSEP is situated (usually, it corresponds to units up to ten components). Similarly, the coefficient of determination can be used for the number of the component estimate (its first local maximum). The coefficient of determination is also used for the complete prediction model power evaluation.

For computing the PLSR method, the free available statistical software R (https://www.r-project.org/) with a package 'pls' can be used (Mevik and Wehrens 2007).

2.2.3 Radiative transfer models

Radiative transfer models (RTMs) are based on algorithms simulating radiation propagation in the environment and its interactions with objects. RTMs successfully simulate the radiative

transfer interactions of light scattering and absorption through the atmosphere. These models are typically used for the atmospheric correction of airborne/satellite data and allow for the retrieval of atmospheric composition, e.g., 6S – the Second Simulation of the Satellite Signal in the Solar Spectrum (Vermote et al. 1997). However, RTMs also simulate the radiative transfer interaction of light and vegetation – on the leaf level with biochemical and biophysical properties and at canopy level with structural properties (ARTMO 2018). Compared to the empirical models, the main advantage of RTMs is that they are transferable from the areas where they were trained to other locations with the same vegetation cover. It is also possible to use RTMs for vegetation monitoring over time. On the other hand, the development and training of RTMs is very complicated and time-demanding. It is necessary to have it in mind, as well that every model generalizes the reality in some way and when using the inappropriate model, the results can be distorted (Liang 2004). Although radiative transfer modeling is not the object of the presented thesis, it is shortly described in the following text as it is often used as alternative to empirical modeling. Another reason to mention RTMs here is that the spectra acquired by laboratory spectroscopy on which one part of the thesis is focused are essential inputs for radiative transfer modeling and any inaccuracies in the spectra measurements can cause inaccuracies in the resulting models.

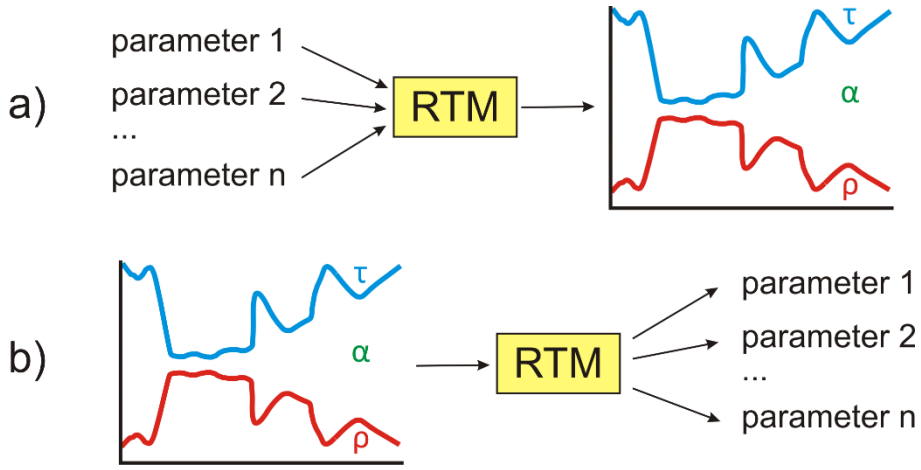

Figure 10: Forward (a) and inverse (b) radiative transfer modeling
τ ... transmittance, plotted as 1 – τ; α ... absorbance; ρ ... reflectance; RTM ... radiative transfer model

Radiative transfer models work in two modes – forward and inverse (see Figure 10). In the forward modeling (Figure 10a), the output is a spectral reflectance or transmittance curve based on the specific combination of biochemical, biophysical and structural properties of the vegetation leaf/crown/canopy and sensor's configuration. The comparison of the modeled spectral curves with the spectral curves measured in the laboratory or field gives the prediction power of the model. It also identifies the intervals of the wavelength where the model is in good agreement and where the shortcomings are. This helps in improving the model, and allows for

the selection of the spectral features to be used in the model application (Schlerf and Atzberger 2006). However, for remote sensing, inverse modeling (Figure 10b) plays an important role. The inversions of RTMs are successfully used on a leaf level, but they are problematic at the canopy level because of these models' complexity. A successful inversion of an RTM requires three factors: a good model, an appropriate inversion procedure, and a set of calibrated spectral curves (S Jacquemoud 2000). Outside the number of different models, there are more inversion strategies which were summed up by Schlerf and Atzberger (2006) followingly:

1) Look-Up-Tables (LUT) – a database created by forward modeling. It contains many possible combinations of studied vegetation parameters and spectra modeled. To estimate the vegetation parameters using the LUT approach, a measured reflectance spectrum is compared to all spectra stored in the LUT. The estimated solution corresponds to the parameter combination giving the highest agreement between measured and simulated canopy reflectance (i.e., the smallest value of the merit function). The main disadvantage of this approach is the fact that LUT tends to be rather large if the parameter space is to be sampled with a high density and/or if many parameters are to be estimated. This may lead to a time-consuming search as each pixel has to be scanned individually.
2) Predictive equations – also rely on a large database of simulated spectral curves. However, it is only used to establish the regression equations between the optical and vegetation properties. In this way, this approach is very similar to the empirical modeling, but the field work is not necessary as the spectral curves are simulated by the model. An advantage of this procedure is its speed and an application to real imagery is straightforward. On the contrary, for every parameter, a separate regression equation must be specified; the form of the relationship must also be specified explicitly by the researcher.
3) Artificial Neural Networks (ANN) – algorithm uses a connected layer composed of neurons to train the non-linear relationship between the inputs (simulated spectra) and outputs (vegetation properties). The relationships are given by weights and are straightly applied to real imagery to determine the vegetation parameters. The algorithm is fast and the relationships can be nonlinear, but the training phase is very time-demanding and an algorithm can behave unpredictably in the case of imperfections in the training data.
4) Numerical optimization techniques using iterations – traditional inversion trying to estimate the model parameters by minimizing a merit function. These techniques have several drawbacks: achieving globally optimal and stable results is difficult as well as retrieving two or more parameters simultaneously. And generally, these methods are computationally ineffective because of the iterations.

As mentioned above, radiative transfer models were developed on two levels – leaf and canopy. Leaf level RTMs simulate optical properties of the individual leaves or needles based

on their biochemical, biophysical and structural properties. Canopy level RTMs simulate interactions of solar radiation in the whole vegetation cover and leaf optical properties are just one input of these models. Other necessary inputs are typically vegetation height, density, shape of the crowns and other parameters describing the vegetation cover structure. All approaches to modeling the radiation in a canopy can be summarized into four categories after Goel (1988): (1) Turbid medium models; (2) Geometrical models; (3) Computer simulation models and (4) Hybrid models. Also, models connecting both leaf and canopy levels exist – e.g., PROSAIL (Stéphane Jacquemoud et al. 2009, http://teledetection.ipgp.jussieu.fr/prosail/), which is often used because of its simplicity. This model combines leaf level model PROSPECT (S. Jacquemoud and Baret 1990) and canopy level model SAIL (W. Verhoef 1984). A summary and comparison of all standardly used RTMs on the canopy level is provided at the official website (http://rami-benchmark.jrc.ec.europa.eu/HTML/) of the radiation transfer model intercomparison (RAMI) initiative.

Using RTM is quite complicated for the broader remote sensing community because every model was developed in a different programming language and the codes are often difficult to access. However, nowadays the Automated Radiative Transfer Models Operator (ARTMO) Graphic User Interface (GUI) (http://ipl.uv.es/artmo/) implemented in MATLAB exists (ARTMO 2018). It is a software package that provides essential tools for running and inverting a suite of plant RTMs, both on the leaf and on the canopy level (Verrelst, Romijn, and Kooistra 2012). Version 3.23 contains the following models on the leaf level: PROSPECT 4 (S. Jacquemoud and Baret 1990; S. Jacquemoud et al. 1996; Fourty et al. 1996), PROSPECT 5 (Feret et al. 2008) and PROSPECT-D (Féret et al. 2017), LIBERTY (Terence P. Dawson, Curran, and Plummer 1998), DLM (Stuckens et al. 2009) and Fluspect-B, also simulating leaf chlorophyll fluorescence spectra (Vilfan et al. 2016); and on the canopy level: 4SAIL (Wout Verhoef and Bach 2003), FLIGHT (North 1996; M. I. Disney, Lewis, and North 2000) and INFORM (Atzberger 2000; Schlerf and Atzberger 2006); and a combined model SCOPE linking the top of the canopy observations of radiance with land surface processes (e.g., photosynthesis) (van der Tol et al. 2009; van der Tol et al. 2014).

2.3 Challenges in laboratory/field spectroscopy and remote sensing for selected ecosystems

2.3.1 Norway spruce forest ecosystem (Krušné hory Mountains)

Norway spruce forests have great ecological and economic importance (Rautiainen et al. 2018), however, being a tree monoculture, they are very vulnerable to different biotic (e.g., forest insect disturbances) and abiotic (e.g., wind, fire, atmospheric pollution, higher soil acidity) stress factors (Manion 1991; Albrechtová, Kupková, and Campbell 2017). That is why monitoring the pysiological status of monocultural forest is necessary and, as many studies in

the last decades proved, satellite and airborne remote sensing is a perfect tool for it. Multispectral sensors (mainly Landsat data) are the most common source of remote sensing data for monitoring the forest decline, e.g., for Norway spruce forest disturbances caused by Bark beetle monitoring (Senf, Seidl, and Hostert 2017) and their predictions (Hais et al. 2016) or for Norway spruce forest damage caused by air pollution (Lambert et al. 1995) and for monitoring Norway spruce stand recovery also (Mišurec et al. 2016). However, the applicability of multispectral data for vegetation studies is limited – their spectral and spatial resolutions allow one to distinguish only basic forest damage classes (e.g., Lambert et al. 1995). Therefore, airborne hyperspectral imagery started to be used for monitoring forests. Hyperspectral remote sensing allows one to detect the initial stages of Norway spruce forest decline (Campbell et al. 2004; Brovkina et al. 2017) and to estimate the quantity of various vegetation traits related mostly to the physiology and biochemistry (Homolová, Malenovský, et al. 2013). Plant pigments are the most studied traits (Homolová, Malenovský, et al. 2013) and among them chlorophylls *a* and *b* (*Cab*) have received the most attention (for Norway spruce, e.g., Schlerf et al. 2010; Zbyněk Malenovský et al. 2013). Carotenoids (e.g., Hernández-Clemente, Navarro-Cerrillo, and Zarco-Tejada 2012) and anthocyanins (Gitelson, Keydan, and Merzlyak 2006 - just the deciduous species) are the other studied pigments, but studies specifically focused on these pigments in Norway spruce are rare. Besides the pigments, lignin and cellulose, polyphenols, leaf water content, leaf mass per area and elements such as nitrogen, phosphorus, potassium, magnesium or calcium can be potentially retrieved from spectral data too (Homolová, Malenovský, et al. 2013). Forest biophysical variables (e.g., LAI, crown volume) can be accurately estimated by imaging spectrometry data also (e.g., Schlerf, Atzberger, and Hill 2005).

However, there are still many challenges in the quantitative remote sensing of Norway spruce forest traits. The canopy structure is the first challenge, which affects canopy reflectance (M. Disney, Lewis, and Saich 2006; Rautiainen et al. 2004) and, thus, the accuracy of biochemical traits retrieval (Homolová, Malenovský, et al. 2013). The second challenge is associated with obtaining reliable information on the optical properties of Norway spruce needles in the laboratory. This information is needed for the parameterization of RTMs, the interpretation of remotely sensed hyperspectral data and for the successful calibration and validation of remote sensing methods. These two issues concerning the canopy structure and the laboratory spectroscopy measurements of the needles are described more in the next text as articles engaged with this doctoral thesis contribute to their solution. Another challenges, as reported in a review by Rautiainen et al. (2018), are the multiple scattering of photons occurring in coniferous canopies due to the needles' arrangement in whorls or shoots and the significant contribution by the understory layer or the forest floor to the remotely sensed reflectance of the coniferous forests.

The position in the canopy is especially important for conifers. As was proven by Lukeš et al. (2013), the spectra of Norway spruce needles were more dependent on the canopy's position than the spectra of birch leaves. Different levels of irradiation in the Norway spruce canopy

actually have an influence on the shape of the needles, the shaded ones are usually flatter compared to the sun exposed needles with a more circular or rhomboidal cross-section (Cescatti and Zorer 2003). This can cause an uncertainty in the field measurements of the Norway spruce's leaf area and, thus, the biochemical properties, which are often expressed on a leaf area basis. The total leaf area is straightforward to estimate for broadleaved, dorsiventral leaves (twice the projected leaf area measured, for example, by desktop scanners) but models taking the three-dimensional shape of coniferous needles into account and its variations caused by different irradiation are necessary for the Norway spruce (Homolová, Lukeš, et al. 2013). Some studies also use LiDAR (Light Detection and Ranging) technology to model the canopy structure of coniferous forests (van Leeuwen and Nieuwenhuis 2010). The 3D tree architecture (including information about the stem, main branches and spatial distribution and density of the foliage) derived from ground-based or aerial LiDAR scanning is then used as one of the detailed inputs for radiative transfer modeling (Yáñez et al. 2008; Homolová et al. 2017). This thesis contributes to the research of the Norway spruce canopy structure by the comparison of prediction empirical models for photosynthetic pigments and water content estimations based on laboratory spectroscopy for the three vertical canopy levels.

All the field spectroscopy devices (IS, CP, leaf clip) were designed to measure the optical properties of dorsiventral leaves, not coniferous needles. Methodologies for Norway spruce needle measurements in an integrating sphere were already proposed by Daughtry, Biehl, and Ranson (1989) and improved by Mesarch et al. (1999); Yanez-Rausell, Schaepman, et al. (2014) and Yanez-Rausell, Malenovsky, et al. (2014) as described in subchapter 2.1.3. Nevertheless, the measurements are very time-demanding and provide many opportunities for measurement uncertainty, e.g., the resulting reflectance and transmittance spectra, despite being corrected, still depend on the gap fraction of the sample (Mesarch et al. 1999). Measurements of the shoots by a plant contact probe are described, for example, in Lhotáková et al. (2013), but this type of measurement can be affected by the multiple scattering of photons. Measurements of the coniferous needles using a plant contact probe and fore optics lens are described and compared by Einzmann et al. (2014), who recommended measurements with a plant contact probe because of its accuracy, speed, flexibility and ability to collect spectra from smaller size samples also. However, it is still unclear, which method of reflectance spectra collection is more applicable for needles. The present thesis aims on answering this question by comparing the spectra collected with a contact probe and an integrating sphere. Besides the comparison of the spectra acquired by different laboratory devices for different types of material (Spectralon, colored papers, tobacco leaves and Norway spruce needles), the thesis also evaluates different data on different scales (biochemical/biophysical retrievals of pigments and water content, laboratory and airborne image spectroscopy measurements) for the detection of the differences in the physiological status of Norway spruce stands.

The planting of Norway spruce in the Czech Republic has significantly exceeded its natural areal extension and, nowadays, it also grows in less suitable areas for this species (Albrechtová, Kupková, and Campbell 2017). Because of the wide extension of Norway spruce (50.5 % of the

forest land in the Czech Republic in 2016, Ministerstvo zemědělství 2017) it is often studied by Czech researchers. This thesis contributes to the assessment of the Norway spruce physiological status in the forests of the Krušné hory Mountains, which used to be a part of the so-called "Black Triangle" – the border area of Czechia, Germany and Poland with the biggest concentration of atmospheric pollution producers (coal burning power plants and heavy industry) (Valášek 1998). The main imission pollutants with an acidifying influence were sulfur dioxide SO2 and oxides of nitrogen NOx, which reached a maximal content in the atmosphere at the beginning of the 1980's as a result of the peak of brown coal mining and combustion in the region (Šrámek et al. 2015; Albrechtová, Kupková, and Campbell 2017). The high level of air pollution led to the large-scale dieback of the Norway spruce forests between 1970 and 2000 in the Krušné hory Mountains. However, due to the prevailing eastward direction of the wind, trees in the western part of the mountains were significantly less damaged than in the eastern part. The desulphurization of power plants in northern Bohemia began in 1993 and, nowadays, the one major negative factor affecting tree physiological status in Norway spruce forests is just the persistent acidification of the soils, which is less favorable in the western part of the Krušné hory Mountains as a result of the geologic bedrock (Šrámek et al. 2015). The Norway spruce forest damage in this area was studied by Lambert et al. (1995) and Ardö et al. (1997) using Landsat data and by Campbell et al. (2004) using hyperspectral data. The papers presented in this thesis, together with the study of Mišurec et al. (2016), are part of the follow up project.

2.3.2 Relict arctic-alpine tundra ecosystem (Krkonoše Mountains)

Generally, tundra represents a natural ecosystem dominated by grasses and dwarf pine, sensitive to the climate change, the latter being more pronounced in arctic areas (Hassol 2004). Virtanen and Ek (2014) therefore stressed the urgent need for realistic and accurate land cover classification of arctic ecosystems. However, the coarse resolution data (Landsat, MODIS, NOAA AVHRR), which cannot reveal actual vegetation pattern in such fragmented landscape as tundra (Virtanen and Ek 2014), are usually used for vegetation and land cover change evaluation in Arctic (e. g Stow et al. 2004; Johansen, Karlsen, and Tømmervik 2012). But recently, field spectroscopy is starting to be used for detailed mapping also in Arctic regions – it was employed by Bratsch et al. (2016) and by Davidson et al. (2016) together with WorldView-2 data for mapping Arctic tundra vegetation communities in Alaska.

The constraints such as frequent cloud cover, a short vegetation season, a hilly relief, a fragmented landscape and often poor accessibility of tundra regions, are the reason that not many quantitative studies based on remote sensing or field spectroscopy data have been published for this ecosystem. The estimates of the biomass based on field spectroscopy were published by Hope, Kimball, and Stow (1993) and Bratsch et al. (2017) for Arctic tundra. Field spectroscopy was also used for the estimation of the green percent vegetation cover (PVC) for a study site in the Canadian High Arctic by Liu, Budkewitsch, and Treitz (2017). More studies were conducted for alpine meadows, e.g., the relationships between the biomass and field

spectroscopy data were studied by Halabuk et al. (2013); Sakowska, Juszczak, and Gianelle (2016) evaluated the seasonal changes in the grassland total canopy chlorophyll content (CCC), the fraction of photosynthetically active radiation absorbed by the vegetation canopy (fAPAR) and the fraction of photosynthetically active radiation absorbed by its photosynthesizing components (GfAPAR) only based on continuous field spectroscopic measurements and simulated Sentinel-2 data. Biophysical parameters of mountain meadows in the Krkonoše Mountains were studied by field spectroscopy and APEX hyperspectral data by Anna Jarocińska and her colleagues (Jarocinska et al. 2014; Jarocińska 2014; Jarocińska et al. 2016). The natural heterogeneous grassland's biophysical parameters were studied also by Darvishzadeh (Darvishzadeh, Skidmore, Schlerf, Atzberger, et al. 2008; Darvishzadeh, Skidmore, Schlerf, and Atzberger 2008). This thesis presents the first research of the biophysical parameters (vegetation height, cover and fAPAR) of relict arctic-alpine tundra in the Krkonoše Mountains based on field spectral measurements.

The relict arctic-alpine tundra located in the Krkonoše Mountains National Park (KRNAP; Figure 11) is a unique ecosystem combining arctic, alpine and middle European flora and fauna. Three main types of tundra are present here – cryo-eolian / lichen tundra (mosses, lichens and alpine heathlands) on the tops of the highest mountains, vegetated-cryogenic / grassy tundra (*Pinus mugo* scrub, peat bogs and closed alpine grasslands dominated with *Nardus stricta* and subalpine tall grasslands) on the plateaus of the Luční bouda and Labská bouda and niveo-glacigenic / flower-rich tundra in the glacier cards. This strictly protected area lies above the tree line and although it covers only 47 km^2 (7.4 % of the total Krkonoše Mountains area), several endemic species can be found here. (Soukupová et al. 1995; Kociánová, Štursa, and Vaněk 2015)

Currently, changes in vegetation composition in the relict arctic-alpine tundra in the Krkonoše Mountains are being recorded. Closed alpine grassland dominated with *Nardus stricta* are threatened by the spread of competitive grasses *Calamagrostis villosa* (Hejcman et al. 2009) and *Molinia caerulea* (Hejcman, Češková, and Pavlů 2010). Also, the expansion of *Pinus mugo* scrub (Štursa and Wild 2014) and of Norway spruce (Treml, Ponocná, and Büntgen 2012) were observed. Further changes in the vegetation composition are caused by direct human influence, e.g., by tourism (Vítek, Vítková, and Müllerová 2012). Therefore, a detailed mapping and monitoring the changes is necessary. Remote sensing can be very helpful for this task (e.g., Stow et al. 2004; Davidson et al. 2016; Marcinkowska-Ochtyra et al. 2018) although there are many mentioned constraints above (such as frequent cloud cover and a short vegetation season) which make its using more difficult. The first mapping and assessment of the changes in the tundra vegetation of the Krkonoše Mountains plateau was performed by Müllerová (2005) using multispectral aerial imagery from 1986, 1989 and 1997. She separated six, respectively nine, classes, however, not the particular species of the competitive grasses. Other research in the area of the Krkonoše Mountains tundra mapping has been made by Polish scientists (Marcinkowska et al. 2014; Marcinkowska-Ochtyra et al. 2017, 2018). They were using APEX hyperspectral data for classifications of up to twenty-four classes. Classifications of relict arctic-alpine tundra

in the Krkonoše Mountains in this thesis are focused on the differentiation of the above-mentioned species (original *Nardus stricta* and expanding grass species, *Pinus mugo* and other categories specific for the area) and on the evaluation of different remote sensing data and methods for the purposes of regular monitoring of this unique area.

Figure 11: The relict arctic-alpine tundra located in the Krkonoše Mountains – the area around Lučnídouda hut

3 Objectives and research questions

The main objective of this doctoral thesis was to explore the possibilities of laboratory spectroscopy and remote sensing hyperspectral and multispectral data utilization for the evaluation of two structurally and functionally different montane ecosystems – Norway spruce forest and relict arctic-alpine tundra. Each chapter then contributes to the specific issues associated with the selected ecosystems studies as described in subchapters 2.3.1 and 2.3.2.

In the case of the Norway spruce montane forest ecosystem, the contributions of this thesis are in comparison of the spectra acquired by different laboratory devices and in evaluation of the differences between the spectral and biochemical/biophysical information on different scale levels and in a tree crown. All the studies are conducted based on the datasets gained in the Krušné hory Mountains, where the forests were heavily damaged by acid deposits (mainly SO_2) during the 1970's, therefore, the thesis also includes an applied ecological asset in evaluating the actual status of the Norway spruce forests located in the area. The specific research questions for the chapter dealing with the Norway spruce forest are following:

Q1. Do the differences in the physiological status of the Norway spruce stands recorded during the 1990's between two differently polluted areas located in the western (Přebuz) and central (Kovářská) Krušné hory Mountains still exist? Is it possible to detect these differences based on the biochemical/biophysical retrievals of the pigments and water content, as well as from the laboratory and airborne image spectroscopic measurements? A different scale is also considered, i.e., the differences at the level of the areas, stands, position in the crown and the needle age classes.

Q2. Are there differences between the spectra collected with a plant contact probe and an integrating sphere? Are the retrieved leaf biochemical properties obtained from the spectral measurements performed with a CP and an IS yielding comparable results? To what extent does the leaf morphological type (dorsiventral leaves vs. coniferous needles) affect the differences between the spectral leaf properties obtained with a CP and an IS?

Q3. Are the prediction empirical models for the photosynthetic pigments and water content estimations based on laboratory spectroscopy on the leaf level of the Norway spruce comparable for the three vertical canopy levels?

In case of relict arctic-alpine tundra ecosystem, the contributions of this thesis are especially in the observation of a very unique ecosystem. As mentioned in Chapter 2.3.2 the detailed mapping and biophysical properties monitoring of tundra ecosystems are needed worldwide and even in Arctic tundra regions field spectroscopy and aerial hyperspectral data are used rarely. The specific research aims for chapter dealing with relict arctic-alpine tundra are the following:

A1. To compare the selected multispectral and hyperspectral data with the various spatial and spectral resolutions for the tundra vegetation classification using two differently detailed legends and different classifiers including an object-based image analysis and a per-pixel approach.

A2. To construct the prediction empirical models for the tundra vegetation height, cover and fAPAR based on the field spectral measurements and to compare how the models differ if the datasets are acquired in a different phenology phase (July 2015 and August 2015).

4 Norway spruce forest ecosystem

This chapter consists of four publications (three peer-reviewed papers and one shorter peer-reviewed conference paper) providing new insights in laboratory spectroscopy for Norway spruce montane forest ecosystem and evaluating the actual physiological status of Norway spruce forests located in the Krušné hory Mountains:

Paper 1: **Červená, Lucie**, Zuzana Lhotáková, Veronika Kopačková, Lucie Kupková, Jan Mišurec, Markéta Potůčková, Pavel Cudlín, Petya Entcheva-Campbell, a Jana Albrechtová. 2014. „Temporal changes in Norway spruce physiological status using hyperspectral data: A case study of mountainous forests affected by long-term acidic depositions". *EARSeL eProceedings*. http://dx.doi.org/10.12760/02-2014-1-13.

Paper 2: Potůčková, Markéta, **Lucie Červená**, Lucie Kupková, Zuzana Lhotáková, a Jana Albrechtová. 2016. „Statistical comparison of spectral and biochemical measurements on an example of Norway spruce stands in the Ore Mountains, Czech Republic". *Geoinformatics FCE CTU* 15 (1): 69–83. https://doi.org/10.14311/gi.15.1.6.

Paper 3: Potůčková, Markéta, **Lucie Červená**, Lucie Kupková, Zuzana Lhotáková, Petr Lukeš, Jan Hanuš, Jan Novotný, a Jana Albrechtová. 2016. „Comparison of Reflectance Measurements Acquired with a Contact Probe and an Integration Sphere: Implications for the Spectral Properties of Vegetation at a Leaf Level". *Sensors* 16 (12): 1801. https://doi.org/10.3390/s16111801.

Paper 4: **Červená, Lucie,** Zuzana Lhotáková, Lucie Kupková, Monika Kovářová, a Jana Albrechtová. 2014. „Models for estimating leaf pigments and relative water content in three vertical canopy levels of Norway spruce based on laboratory spectroscopy". In *EARSeL 34th Symposium Proceedings*, editoval Bogdan Zagajewski, Marlena Kycko, a Rainer Reuter, 6.1-6.8. Warsaw, Poland: EARSeL and University of Warsaw. https://doi.org/0.12760/03-2014-11.

Paper 1: "TEMPORAL CHANGES IN NORWAY SPRUCE PHYSIOLOGICAL STATUS USING HYPERSPECTRAL DATA: A CASE STUDY OF MOUNTAINOUS FORESTS AFFECTED BY LONG-TERM ACIDIC DEPOSITIONS"

Červená, Lucie, Zuzana Lhotáková, Veronika Kopačková, Lucie Kupková, Jan Mišurec, Markéta Potůčková, Pavel Cudlín, Petya Entcheva-Campbell, a Jana Albrechtová. 2014. „Temporal changes in Norway spruce physiological status using hyperspectral data: A case study of mountainous forests affected by long-term acidic depositions". *EARSeL eProceedings*. http://dx.doi.org/10.12760/02-2014-1-13.

Author Contributions:

LČ – 27%, ZL – 25%, VK – 19%, LK – 7%, JM – 6%, MP – 2%, PC – 2%, PE-C – 2%, JA – 10%

EARSeL eProceedings, Special Issue: 34th EARSeL Symposium, 2014 71

TEMPORAL CHANGES IN NORWAY SPRUCE PHYSIOLOGICAL STATUS USING HYPERSPECTRAL DATA: A CASE STUDY OF MOUNTAINOUS FORESTS AFFECTED BY LONG-TERM ACIDIC DEPOSITIONS

Lucie Červená[1], Zuzana Lhotáková[2], Veronika Kopačková[3], Lucie Kupková[1], Jan Mišurec[3], Markéta Potůčková[1], Pavel Cudlín[4], Petya Entcheva-Campbell[5], and Jana Albrechtová[2]

1. Charles University in Prague, Faculty of Science, Department of Applied Geoinformatics and Cartography, Prague, Czech Republic; {lucie.cervena / marketa.potuckova }(at)natur.cuni.cz, lucie.kupkova(at)gmail.com
2. Charles University in Prague, Faculty of Science, Department of Experimental Plant Biology, Prague, Czech Republic; {zuzana.lhotakova / jana.albrechtova}(at)natur.cuni.cz
3. Czech Geological Survey, Prague, Czech Republic; veronika.kopackova(at)seznam.cz, jan.misurec(at)geology.cz
4. CzechGlobe, Academy of Sciences of the Czech Republic, České Budějovice, Czech Republic; cudlin.p(at)czechglobe.cz
5. Joint Center for Earth Systems Technology, University of Maryland Baltimore County and NASA Goddard Space Flight Center, Greenbelt, Maryland, USA; petya.k.campbell(at)nasa.gov

ABSTRACT

A decline in the Norway spruce forests of the Krušné Hory Mts., Czech Republic, has been reported since the early 1950's. It was attributed to the combination of severe atmospheric pollution and climatic conditions. The physiological status of the Norway spruce forests has been assessed using ground-truth data (biochemical and spectroscopic data) as well as two hyperspectral data sets acquired in 1998 (ASAS sensor, NASA Goddard Space Flight Center) and in 2013 (APEX sensor, developed by a Swiss-Belgian consortium on behalf of ESA, currently operated by VITO). The very first results coming from the analysis of the foliar chemistry indicate that the stands exhibit different physiological statuses corresponding to the pollution gradients in 1998 and 2013. Slight improvement of the Norway spruce physiological status was recorded in the eastern part of the mountains (e.g. total carotenoids to chlorophyll ratio), while the status of the western-located stands slightly worsened. These findings may correspond to a tremendous decrease in the atmospheric pollution which was most severe in the east. However, remains of the pollution can be still seen in the adverse soils conditions. Further linkages among foliar chemistry and reflectance and soil chemistry are currently under investigation.

INTRODUCTION

The physiological status of trees within forest ecosystems determines their proper functioning (1,2). The contents of foliar biochemical compounds, such as photosynthetic pigments, phenolic compounds or lignin, can be used as non-specific indicators of the physiological status and early pre-visual indicators of tree damage (1). Variations in leaf biochemical composition affect foliar optical properties and can be retrieved from continuous spectral data (3,4). There are two modelling approaches to link content of biochemical compounds or biophysical parameters of vegetation to spectra: empirical models (different regressions, e.g. (2)) and physical models (radiative transfer, e.g. (5)).

Due to coal burning power plants in the close vicinity of the Krušné Hory Mts. a strong gradient of acidic deposition leading from heavy (the eastern part) to light (the western part) developed during the 1970's and 1980's. Although the load of SO_2 has significantly decreased since 1991, the full recovery of forests damaged by previous acid deposition is a long term process. Thus, the main goal of the INMON project is to assess the temporal changes in the physiological status of Norway

DOI: 10.12760/02-2014-1-13

spruce in Krušné Hory Mts. using two hyperspectral data sets acquired in 1998 (ASAS sensor) and in 2013 (APEX sensor). In this paper, we will focus on three specific objectives:

i. to compare biochemical and biophysical needle parameters from trees sampled at the western part (Přebuz) and the eastern part (Kovářská) of the Krušné Hory Mts. between 1998 and 2013
ii. to construct the prediction models for photosynthetic pigments and water content based on laboratory spectroscopy
iii. to compare the geochemical conditions of study stands at the western part (Přebuz) and the eastern part (Kovářská) of the Krušné hory Mts. in 2012.

METHODS

The study sites were selected at two different localities in the Krušné Hory Mts. about 50 km apart. Přebuz located in the western part of the mountains was considered as healthy or slightly damaged in contrast to Kovářská located in the eastern part, which suffered from the heavy acidic load and the trees exhibited visible damage symptoms (2). Even-aged forest stands older than 60 years (15 sites at Kovářská and 22 sites at Přebuz in 1998) and older than 80 years (five sites at Kovářská and six sites at Přebuz in 2013) were selected. In 2013, the sites studied in 1998 were revisited if possible. In 2013, the sampled trees did not show any visible damage symptoms. The hyperspectral image data was acquired on 6th September 2013 using the APEX airborne imaging spectrometer. Simultaneously, a supportive calibration and validation ground campaign was organized to support the processing of the hyperspectral data.

Needle sampling for biochemical analyses was accomplished for five representative trees per site within the periods 15-28 August 1998 and 22-25 August 2013. In both years, the first three needle age classes were used for photosynthetic pigments (total chlorophylls, total carotenoids) determination using dimethylformamide extractions according to Porra (6), followed by spectrophotometric detection and calculations according to Welburn (7). The pigment concentrations were then expressed as mass of pigment per gram of needle dry mass (mg/g). The relative water content (*RWC*) was determined as the percentage of water in the fresh needles.

Simultaneously with the needle sampling in 2013 the spectral reflectance of spruce foliage was measured in the range between 350 and 2,500 nm using an ASD FieldSpec 4 Wide-Res spectrometer in combination with the fibre optic contact probe (similar to (4)). Branchlets consisting of only one age class were arranged in the same direction to create a consistent layer to fill in the field of view (spot size 10 mm) of the contact probe. Five independent spectra were taken on different parts of one sample and afterwards the median spectrum was calculated (altogether 165 median spectra: 11 sites $\times$ 5 trees $\times$ 3 needle age classes). Due to the noise in the spectra in the 350-450 nm regions, this interval was excluded from further analyses. Selected spectral indices were calculated from the spectra: Modified Chlorophyll Absorption in Reflectance Index *MCARI* (8), Transformed Chlorophyll Absorption Ratio Index / Optimized Soil Adjusted Vegetation Index *TCARI/OSAVI* (9), Triangular Vegetation Index *TVI* (10) for correlations with total chlorophyll and Water Index *WI* (11) and Normalized Difference Water Index *NDWI* (12) for correlations with *RWC*. Often used indices for carotenoids were calculated, but the regression model results were not significant. Also partial least square regressions (*PLSR*) using all reflectance values in the range of 450 - 2,500 nm for estimation of *RWC* and pigments were performed. The regression models were trained on four fifths of the dataset; data from one tree per site were used for model validation. All calculations were performed in R software with pls package or in Microsoft Excel 2007.

In each forest stand, representative sampling pits were chosen to collect soil samples. Material was collected from organic and mineral soil horizons. Exchangeable cations and selected trace elements were determined together with soil pH, TEA and total contents of C and N.

RESULTS

Total contents of photosynthetic pigments did not significantly differ between 1998 and 2013 either at Kovářská (eastern locality) or at Přebuz (western locality). However, the ratio between total carotenoids and total chlorophylls (Car/Cab) significantly decreased at Kovářská in contrast to a significant increase in Přebuz. This change in Car/Cab documents the different progress of tree physiological status between 1998 and 2013: Improvement at the eastern and worsening at the western part of the Krušné Hory Mts (Table 1). Relative water content (*RWC*) also significantly decreased, indicating much drier canopy conditions in 2013 (Table 1). Since *RWC* can vary strongly in relationship to temperature and humidity, we will further compare the meteorological conditions at both sites at the time of data collection.

Table 1: Differences in the foliar chemistry at two studied localities between 1998 and 2013 (Mann-Whitney test., Means and standard deviations (S.D.) are shown for each year and locality studied. Significant difference at α = 0.05, n.s. = not significant; d.m. needle dry mass.*

	Přebuz (Western part)			**Kovářská (Eastern part)**		
	1998	2013		1998	2013	
Needle parameter	Mean (S.D.)	Mean (S.D.)	*p*-value	Mean (S.D.)	Mean (S.D.)	*p*-value
Total chlorophyll (mg/g d.m.)	3.42 (0.815)	3.26 (0.666)	0.141812 n.s.	3.29 (0.837)	3.58 (0.589)	0.277424 n.s.
Carotenoids (mg/g d.m.)	0.43 (0.106)	0.42 (0.077)	0.517501 n.s.	0.45 (0.121)	0.451 (0.070)	0.893544 n.s.
Car/Cab	0.13 (0.011)	0.13 (0.009)	0.000578 *	0.14 (0.011)	0.13 (0.006)	0.000084 *
RWC (%)	60.80 (3.500)	57.50 (2.750)	0.000000 *	60.00 (4.920)	58.30 (2.730)	0.003330 *

Prediction models for photosynthetic pigments and water content based on different methods (indices and PLSR) calculated from laboratory spectra did not produce very strong correlation results (Table 2) in comparison with, for example, (2,3,9). The best results were achieved using the *TCARI/OSAVI* index (for photosynthetic pigments), *WI* (for water content) and *PLSR* (in accordance with (3)).

Table 2: Regression models between the spectra and biochemical and biophysical parameters (R2 – coefficient of determination, RMSE – root mean square error, comp. – number of components considered in the model)

	Total chlorophyll (mg/g d.m.)			**Carotenoids (mg/g d.m.)**			***RWC* (%)**	
Method	R^2 *	***RMSE***	**method**	R^2 *	***RMSE***	**method**	R^2 *	***RMSE***
MCARI	0.522	0.462	x	x	x	*WI*	0.501	1.746
TCARI/OSAVI	0.648	0.375	x	x	x	*NDWI*	0.482	1.976
TVI	0.494	0.489	x	x	x	x	x	x
PLSR	0.776 (6 comp.)	0.332	*PLSR*	0.774 (6 comp.)	0.038	*PLSR*	0.783 (8 comp.)	1.456

** P-values for all the models were lower than $2.2 \cdot 10^{-16}$.*

Both study sites exhibited differences in soil geochemical conditions. Comparing Kovářská to Přebuz, the latter was characterized by lower base cation contents and the top organic horizon (O) had a very low pH (pH<3) (Figure 1). In general, soil environment at the Přebuz site represents less favourable conditions, in which selected trace elements (Hg, Pb) could be present at a mobile form.

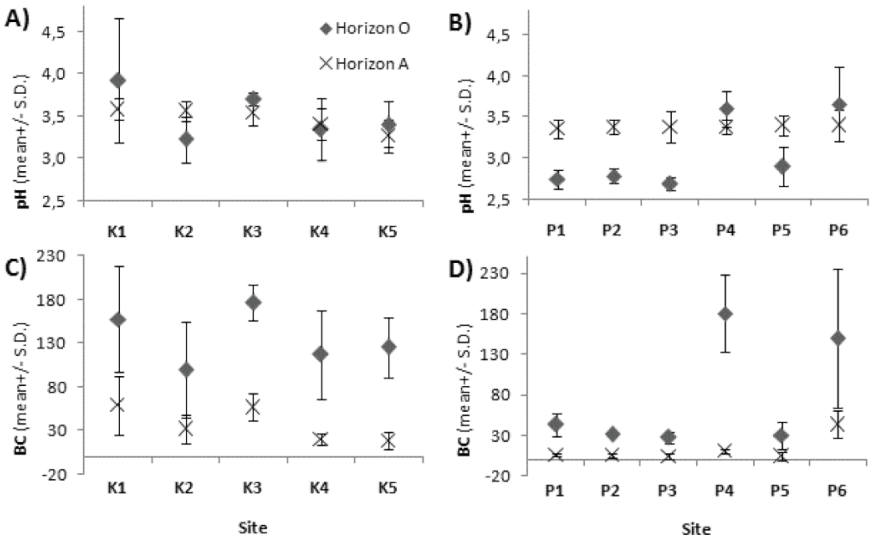

Figure 1: pH (A: Kovářská, B: Přebuz) and base cation (BC) content in (mmol·kg^{-1}) (C: Kovářská, D: Přebuz) and (SD: Standard Deviation).

CONCLUSIONS

The photosynthetic pigment content alone does not always clearly indicate changes in tree physiological status and a combination of several stress indicators is required (3). The carotenoids in needles protect the pigment-protein complexes from photodamage (13) and thus the increase in *Car*/*Cab* ratio indicates higher levels of tree stress at Přebuz, the western locality. The results of soil analyses also indicate less favourable conditions for trees at Přebuz. It appears that after removal of main acidic deposition sources in the 1990's, the soil acidification is now the main driving factor of the Norway spruce physiological status in Krušné Hory Mts. The improvement of forest soils damaged by previous acidic deposition is a long-term process and only slight recovery was observed after a decade in other mountainous regions of the Czech Republic (14).

In this paper, only preliminary results from foliar chemistry ground truth are presented. However, we will draw more complex conclusions about the temporal change in Norway spruce physiological status after processing the hyperspectral data providing the information on a larger spatial scale. We also plan to employ additional needle biochemical stress indicators (e.g. soluble phenolics, lignin) in our future work to better understand the Norway spruce physiological status and its response to soil conditions.

The next step of the project is to improve the predictive models for pigments and other biochemical stress indicators based on the spectral measurements using an integrating sphere. After that, upscaling from the foliar to the canopy level and classification of already acquired hyperspectral data (by APEX in 2013 and by ASAS in 1998) will be performed. The methodology for hyperspectral data processing to compare the health status of Norway spruce stands in the Krusne Hory Mts. in the end of the 1990's and at present will be adjusted. Also linking foliage chemical composition and spectral properties with soil chemical properties (basic cations, heavy metals, pH, C/N, DOC, DON, etc.) will continue.

ACKNOWLEDGEMENTS

The support by the Ministry of Education of the Czech Republic is acknowledged: LH12097. We are grateful to Drahomíra Bartáková and Monika Kovářová for laboratory analyses and to students who helped with needle sampling and spectral measurements.

REFERENCES

1 Soukupova J, M Cvikrova, J Albrechtova, B N Rock & J Eder, 2000. Histochemical and biochemical approaches to the study of phenolic compounds and per-oxidases in needles of Norway spruce (Picea abies). New Phytologist,146(3): 403-414

2 Entcheva-Campbell P K, B N Rock, M E Martin, C D Neefus, J R Irons, E M Middleton & J Albrechtova, 2004. Detection of initial damage in Norway spruce canopies using hyperspectral airborne data. International Journal of Remote Sensing, 25: 5557-5583

3 Misurec J, V Kopackova, Z Lhotakova, J Hanus, J Weyermann, P Entcheva-Campbell & J Albrechtova, 2012. Utilization of hyperspectral image optical indices to assess the Norway spruce forest health status. Journal of Applied Remote Sensing, 6: 063545-1-063545-25

4 Lhotakova Z, L Brodsky, L Kupkova, V Kopackova, M Potuckova, J Misurec, A Klement, M Kovarova, & J Albrechtova, 2013. Detection of multiple stresses in Scots pine growing at post-mining sites using visible to near-infrared spectroscopy. Environmental Science-Processes & Impacts, 15: 2004-2015

5 Malenovsky Z, J Albrechtova, Z Lhotakova, R Zurita-Milla, J Clevers, M E Schaepman, and P Cudlin, 2006. Applicability of the PROSPECT model for Norway spruce needles. International Journal of Remote Sensing, 27: 5315-5340

6 Porra R J, W A Thompson & P E Kriedemann, 1989. Determination of accurate extinction coefficients and simultaneous equations for assaying Chlorophyll-a and Chlorophyll-b extracted with 4 different solvents – verification of the concentration of chlorophyll standards by atomic-absorption spectroscopy. Biochimica et Biophysica Acta, 975: 384-394

7 Wellburn A R, 1994. The spectral determination of Chlorophyll-a and Chlorophyll-b, as well as total Carotenoids, using various solvents with spectrophotometers of different resolution. Journal of Plant Physiology, 144: 307-313

8 Daughtry C S T, C L Walthall, M S Kim, E Brown De Colstoun & J E McMurtreyll, 2000. Estimating corn leaf chlorophyll concentration from leaf and canopy reflectance. Remote Sensing of Environment, 74: 229-239

9 Haboudane D, 2002. Integrated narrow-band vegetation indices for prediction of crop Chlorophyll content for application to precision agriculture. Remote Sensing of Environment, 81: 416-426

10 Broge N & E Leblanc, 2000. Comparing prediction power and stability of broadband and hyperspectral vegetation indices for estimation of green leaf area index and canopy chlorophyll density. Remote Sensing of Environment, 76: 156-172

11 Penuelas J, J Pinol, R Ogaya, and I Filella, 1997. Estimation of plant water concentration by the reflectance water index WI (R900/R970). International Journal of Remote Sensing, 18: 2869-2875

12 Gao B C, 1996. NDWI - A normalized difference water index for remote sensing of vegetation liquid water from space. Remote Sensing of Environment, 58: 257-266

13 Demmig-Adams B, 1998. Survey of thermal energy dissipation and pigment composition in sun and shade leaves. Plant and Cell Physiology, 39: 474-482

14 Boruvka L, V Podrazsky, L Mladkova, I Kunes & O Drabek, 2005. Some approaches to the research of forest soils affected by acidification in the Czech Republic. Soil Science and Plant Nutrition, 51: 745-749

Paper 2: "STATISTICAL COMPARISON OF SPECTRAL AND BIOCHEMICAL MEASUREMENTS ON AN EXAMPLE OF NORWAY SPRUCE STANDS IN THE ORE MOUNTAINS, CZECH REPUBLIC"

Potůčková, Markéta, Lucie Červená, Lucie Kupková, Zuzana Lhotáková, a Jana Albrechtová. 2016. „Statistical comparison of spectral and biochemical measurements on an example of Norway spruce stands in the Ore Mountains, Czech Republic". *Geoinformatics FCE CTU* 15 (1): 69–83. https://doi.org/10.14311/gi.15.1.6.

Author Contributions:

MP – 38%, **LČ – 34%**, LK – 10%, ZL – 9%, JA – 9%

Statistical comparison of foliage spectral and biochemical measurements on an example of Norway spruce stands in the Ore Mountains, Czech Republic

Markéta Potůčková[a], Lucie Červená[a], Lucie Kupková[a], Zuzana Lhotáková[b] and Jana Albrechtová[b]

Charles University in Prague, Faculty of Science
[a]Department of Applied Geoinformatics and Cartography
[b]Department of Experimental Plant Biology
{marketa.potuckova, jana.albrechtova}@natur.cuni.cz,
{LucieCervena, zuza.lhotak}@seznam.cz, Lucie.kupkova@gmail.com

Abstract

The physiological status of vegetation and changes can be monitored by means of biochemical analysis of collected samples as well as by means of spectroscopic measurements either on the leaf level, using field (or laboratory) spectroradiometers or on the canopy level, applying hyperspectral airborne or spaceborne image data. The present study focuses on the statistical comparison and ascertainment of relations between three datasets collected from selected Norway spruce forest stands in the Ore Mountains, Czech Republic. The data sets comprised i) biochemically retrieved photosynthetic pigments (chlorophylls, carotenoids) and water content of 495 samples collected from 55 trees from three different vertical levels of a tree crown and the first three needle age classes, ii) the spectral reflectance of the same shoot samples measured with an ASD Field Spec 4 Wide-Res spectroradiometer equipped with a plant contact probe, iii) an airborne hyperspecral image acquired with an Apex sensor. The datasets cover two areas (western and central) in the Ore Mountains that were affected differently by acid deposits in the 1970's and 1980's. A one-way analysis of variance (ANOVA), Tukey's honest significance test, hot spot analysis and linear regression were applied either on the original measurements (the content of leaf compounds and reflectance spectra) or derived values, i.e. selected spectral indices. The results revealed a generally low correlation between the photosynthetic pigments, water content and spectral measurement. The results of the ANOVA showed significant differences between model areas only in the case of the leaf compound dataset. Differences between the stands on various levels of significance existed in all three datasets and are discussed. The study also proved that the vertical gradient of the biochemical and biophysical parameters in a tree crown play a role when the optical properties of the forest stands are modelled. It is possible to conclude that the differences in the physiological conditions of stands observed in high extent in 1998 still were slightly detectable in 2013, though the physiological conditions levelled up. From the point of view of optical properties, the differences between the areas are not significant on laboratory or image reflectance spectra.

Keywords: Laboratory spectroscopy, hyperspectral imagery, Ore Mountains, Norway spruce, Chlorophyll, Carotenoids, RWC.

Introduction

Laboratory and image-based spectral measurements have been used in numerous biological, ecological and environmental studies to evaluate the physiological status of the vegetation [4], [16]. Variations in plant condition are indicated e.g. by changes in the content of specific leaf compounds such as photosynthetic pigments (chlorophylls, carotenoids) and water that can be determined by biochemical analyses of the collected leaf samples. The optical properties of the leaves follow these changes (e.g. [6], [25]). It has been documented that a worsening of the physiological status of vegetation can be detected either from the biochemical or biophysical parameters, because the metabolic changes occur much earlier than macroscopic changes such as needle yellowing or needle loss. Similarly, those initial damage phases of leaves can be detected from their spectra prior to observation from macroscopic indicators. For example, Campbell et al. [5] detected the initial stages of foliage damage in Norway spruce (*Picea abies* L. Karst.) using ASAS hyperspectral airborne data and vegetation indices derived from red edge. The relation between the optical properties of vegetation and its biochemical or biophysical parameters can be described using empirical models (e.g. [7], [15]) or radiative transfer models (e.g. [8], [9], [14], [20]).

The Norway spruce forests in the Ore Mountains (Western Bohemia) were strongly affected by acid deposits (mainly SO_2) causing heavy damage between 1970 and 2000, especially in the central part of the mountain range. The principal sources of SO_2 pollution were industry and coal burning power plants located in the south-eastern foothills of the Ore Mountains. Due to the prevailing eastward direction of the wind, the disturbance of the western part of the mountains was considerably less than that in the central and eastern parts [1]. The study conducted by Campbell et al. [5] in 1998 evaluated the level of forest damage in two areas selected in the central and western areas of the mountains using, among other things such as macroscopic damage indicators, image spectroscopy and biochemically determined content of leaf photosynthetic pigments and water in the collected needle samples. The tree damage followed the west-east gradient in air SO_2 pollution with heavier damage of the Norway spruce stands in the central Ore Mountains in comparison with the stands in the western Ore Mountains. In 2012, a follow up project aiming at evaluating the physiological status of the Norway spruce stands at the same two areas and several identical study stands started. This study again combined biochemical determination of leaf compounds and spectroscopic measurements of the optical properties of canopy on both the needle (laboratory spectroscopic measurements) and the crown (hyperspectral images) levels. The presented study is a part of this project.

The main objectives of the presented study were to find out if i) the differences in the physiological status of the Norway spruce stands still exist between the selected model areas (located in the western and central Ore Mountains); ii) the same differences can be detected from biochemical analysis, laboratory and airborne image spectroscopic measurements; iii) the recognised differences will change depending on the 'scale', i.e. when the areas, stands, position in the crown and the age of the shoots are considered.

Material

The study areas were situated in the Ore Mountains in the areas that were either heavily damaged in 1998 (the central part in the neighbourhood of the Kovářská village) or in the

initial damage stage without severe visual symptoms (the western part in the neighbourhood of the town of Přebuz) due to acid deposits in the 1970's and 1980's. Within the homogeneous Norway spruce mature forest (50 years and older), five even-aged representative trees were selected at each of eleven study stands (five for the Kovářská and six for the Přebuz areas, see Figure 1). During the field campaign, 22 - 25 August 2013, the samples from three vertical crown levels (the sunlit productive upper and lower parts and the shaded basal part of the tree crown) and the first three needle age classes were collected. Laboratory spectral measurements using an ASD Field Spec 4 Wide-Res spectroradiometer and assessment of photosynthetic pigments and water content were carried out on these 495 samples. The airborne image hyperspectral data were acquired with the APEX sensor on 6 September 2013; a supporting field calibration and validation campaign was conducted on the same date.

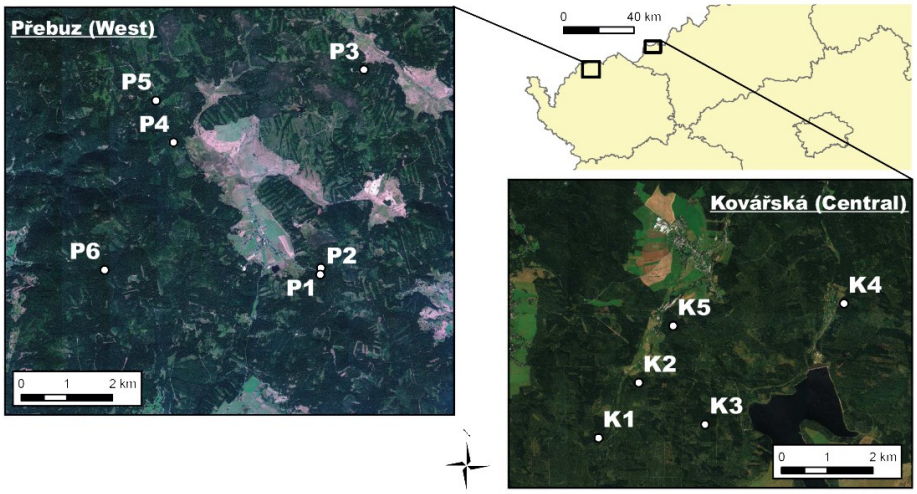

Figure 1: The location of the study areas Kovářská and Přebuz with Norway spruce stands. Each stand was represented by five selected trees.

Biochemical and biophysical parameters

Needle samples collected in the field were cooled and transported to the laboratory where they were stored and frozen to -20°C until processing. The extraction of photosynthetic pigments (chlorophyll a and b and total carotenoids) was performed according to [23] and [27]. The relative water content (RWC) corresponded to the percentage of water in the fresh needles. Table 1 summarises the content of analysed leaf compounds related to the areas (A) and position of the sample in the tree crown (B). In the following text, the results connected to the content of the biochemical and biophysical parameters will be referred to as BioC/P.

Laboratory spectral measurements

The laboratory spectral measurements were performed with an ASD Field Spec 4 Wide-Res spectroradiometer equipped with a plant contact probe (CP). The spectroradiometer collects radiance in the spectral interval from 350 nm to 2,500 nm using three detectors

Table 1: Descriptive statistics of the leaf photosynthetic pigments and relative water content in needles of Norway spruce. A: for the study areas of Kovářská (central) and Přebuz (western). B: for the position in the crown. st.d. – standard deviation, d.m. – dry mass.

A: Area	Přebuz (western)		Kovářská (central)	
Descriptive statistics	mean	st.d.	mean	st.d.
Total chlorophyll (mg/g d.m.)	2.97	0.66	3.19	0.67
Total carotenoids (mg/g d.m.)	0.40	0.08	0.42	0.08
Relative water content (%)	56.27	3.11	56.91	3.22

B: Position in the crown	Shaded basal		Productive lower		Productive upper		All data	
Descriptive statistics	mean	st.d.	mean	st.d.	mean	st.d.	mean	st.d.
Total chlorophyll (mg/g d.m.)	3.44	0.62	3.10	0.66	2.76	0.55	3.09	0.66
Total carotenoids (mg/g d.m.)	0.44	0.07	0.41	0.08	0.37	0.07	0.41	0.08
Relative water content (%)	57.91	2.76	56.26	3.13	55.46	3.12	56.53	3.17

(VNIR: 350 – 1,000 nm, SWIR1: 1,000 – 1,800 nm and SWIR2: 1,800 – 2,500 nm). The original spectral resolution is 3 nm in VNIR and 10 nm in SWIR bands and sampling interval of 1.4 nm. The output data are resampled to 1 nm interval using cubic spline interpolation [3], [2]. Due to the noise in the collected measurements, the applied spectral interval was reduced to wavelengths between 400 and 2,400 nm in the presented study.

A layer of Norway spruce shoots of the same age class arranged in the same direction and with minimal gaps were placed on a black surface (98% absorption) to minimize background spectral noise. In order to improve the spectral-to-noise ratio, 50 measurements at one position of the CP were averaged. Moreover, each sample was measured at five positions of the CP and their median was used further as the final ASD CP observation of one sample. The relative reflectance of the Norway spruce samples was calculated from the recorded spectral radiance values by normalizing them with the measured radiance of a 99% reflective spectralon according to the formula:

$$R_{sample} = \frac{DN_{sample}}{DN_{WR}} \tag{1}$$

where R_{sample} is the calculated relative reflectance, DN_{sample} and DN_{WR} are the recorded digital numbers of the sample and the spectralon (so-called 'white reference'). The needles for biochemical analysis were sampled from the same branch as were the shoots for spectral measurements. For the purpose of comparison with the APEX hyperspectral image data, the ASD CP measurements were resampled to the bands with the central wavelengths and full width at half maximum value (FWHM) corresponding approximately to the APEX data (based on metadata FWM ranges from 3 to 13 nm, dependent on the wavelength).

Hyperspectral image data

Airborne hyperspectral images were acquired with the APEX (Airborne Prism Experiment) sensor working in the spectral rage from 400 nm to 2,500 nm. The images contained 286 spectral bands with an average bandwidth of 7 nm. The ground resolution was 2 metres. The image acquisition, pre-processing, radiometric calibration, geometric and atmospheric corrections were performed by the Belgian company VITO (more details can be found in [21],

[24]). The position of each tree was determined by GNSS. As the average crown diameter was about 5 m, the four nearest pixels to the measured tree location were selected. The spectra corresponding to these four pixels were manually checked and after removing possible outliers due to e.g. shadows, a mean of spectra was calculated and used for further processing as the spectrum representing the given tree (see Figure 2).

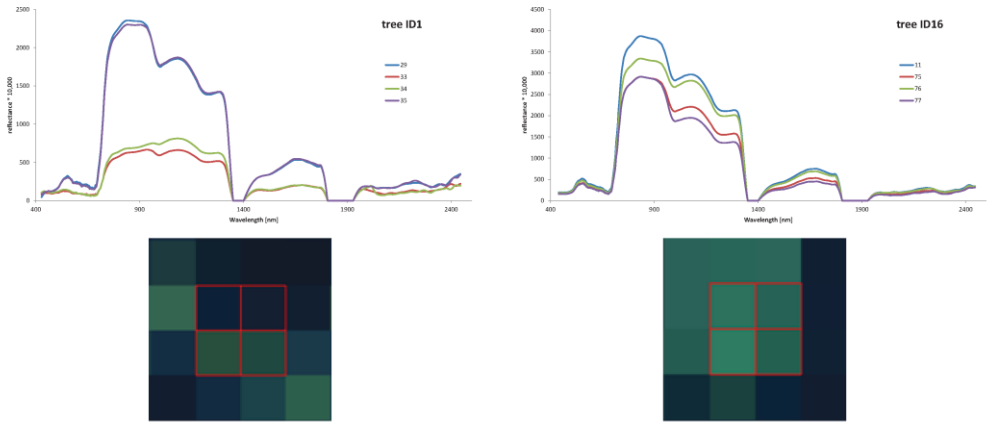

Figure 2: Averaging the APEX spectra. The tree crown is represented by four neighbouring pixels. In the event that the spectral reflectance of some pixels significantly differed from the others and from the expected 'vegetation' spectrum, it was not included in the calculation of the mean (left – spectra 33 and 34 will be excluded due to shadows; right – the mean of all spectra will be calculated).

Methods for spectra comparison

To evaluate the differences in the measured values of BioC/P and optical properties of the needles between various factors (area, stand, needle age class and position in the crown), a two-step procedure was adopted. First, **one-way analysis of variance** (ANOVA) was used to test whether any differences between the groups of the examined factor exist. The tested null hypothesis was that the means of all the groups were equal. When the null hypothesis was rejected at the confidence level of 95% ($\alpha = 0.05$), the alternative hypothesis was valid, i.e. at least one group was significantly different. To find out which group means were the most distinct from the others, the multiple comparison **Tukey's honest significance test** was performed afterwards. Both statistical analyses were carried out in the R software package using the *aov* and *TukeyHSD* functions. Interactions between the factors (and therefore the multiple factor ANOVA) were not applied in order to keep the interpretation of the results simple and to be able to find the differences between the specific groups of the given factor.

A **hot spot analysis** based on the evaluation of the spatial association of a variable within a specified distance of a single point [10] was run in ArcGIS software in order to validate the above-mentioned methods on the tree level and to visualize the space distribution of the sought differences of the evaluated parameters, e.g. the contents of photosynthetic pigments and water. This method identifies statistically significant hot spots (high values) and cold spots (low values) within the context of the neighbouring features. A feature with a high/low

value is considered to be a statistically significant hot/cold spot just in the event that it is surrounded by other features with high/low values as well.

Further, **spectral indices**, which showed the highest correlation with the chlorophyll, carotenoids and water contents in Norway spruce needles in our previous studies (e.g. [7]) were calculated in order to compare the results of BioC/P and spectral measurements when evaluating the differences between groups on all possible levels of detail. R_x refers to spectral reflectance on the wavelength x nm in the formulas 2 to 6.

Ratio of Transformed Chlorophyll Absorption Ratio Index and Optimized Soil Adjusted Vegetation Index TCARI/OSAVI [12]; higher values of this index indicate less chlorophyll content:

$$TCARI/OSAVI = \frac{3 \times \left[(R_{700} - R_{670}) - 0.2 \times (R_{700} - R_{550}) \times \left(\frac{R_{700}}{R_{670}} \right) \right]}{\frac{1.16 \times (R_{800} - R_{670})}{R_{800} + R_{670} + 0.16}} \tag{2}$$

Modified Red Edge Normalized Difference Vegetation Index mND_{705} or MRENDVI in ENVI 5.3 [25] corrects for leaf specular reflection:

$$MRENDVI = \frac{R_{750} - R_{705}}{R_{750} + R_{705} - 2 \times R_{445}} \tag{3}$$

Carotenoids' concentration index CRI700 [11]:

$$CRI700 = \frac{1}{R_{515}} - \frac{1}{R_{700}} \tag{4}$$

Water Index WI [22]:

$$WI = \frac{R_{900}}{R_{970}} \tag{5}$$

Moisture stress index MSI (formula 6) indicates the water stress of the plants, i.e. the higher values of the index indicate a lower water content [13].

$$MSI = \frac{R_{1600}}{R_{820}} \tag{6}$$

The empirical relation between the BioC/P parameters and the indices derived from laboratory and image spectra was estimated using linear regression and its strength was expressed by the coefficient of determination R^2.

Results

Several tests based on one-way analysis of variance (ANOVA) were carried out for BioC/P, laboratory and image spectroscopic data in order to indicate whether significant differences in the measured values are dependent on the location (area and stand). Moreover, the BioC/P and ASD CP data allowed comparison between positions in the tree crown and needle age classes.

In the first test, the differences in the measured laboratory spectra between the two areas were evaluated. The relative spectral reflectance values collected for all the samples on the

two study areas (western Kovářská – 225 samples and central Přebuz – 270 samples) on each wavelength in the interval from 400 to 2,400 nm were used as inputs to ANOVA. The results showed that there were no significant differences where the areas were considered ($p>0.05$). On the other hand, the spectra differed significantly ($p \ll 0.05$) if the stands are used as the factor in ANOVA with the only exception of the narrow interval around 1,900 nm (the water absorption band). The same test carried out on the image spectra revealed no significant dependence on the area or on the stand with the exception of the wavelengths around 660 nm, i.e. the chlorophyll absorption band (Figure 3).

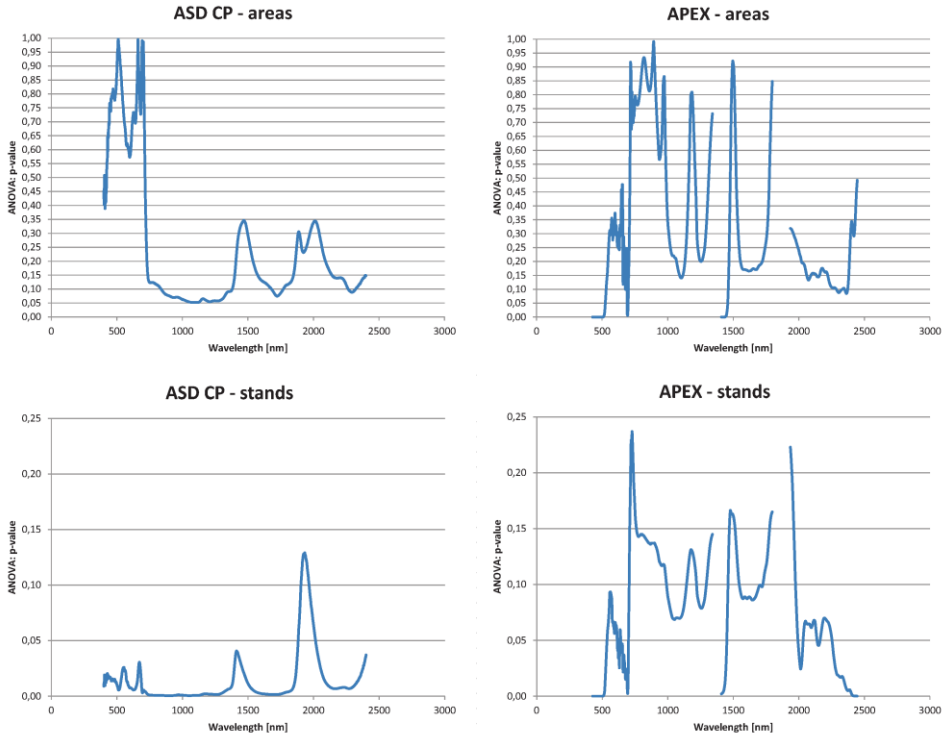

Figure 3: p-values of ANOVA (α=0.05) showed the significance of differences in the collected Norway spruce laboratory (ASD CP) and image spectra (Apex) dependent on the single factors of area and stand. $p>0.05$ indicates that the areas and stands do not differ significantly.

In the second test, the TCARI/OSAVI, CRI700 and WI indices were derived from both laboratory and airborne image spectra. The ANOVA was carried out again in order to find out if there are differences in the content of leaf pigments (chlorophyll and carotenoids) and water dependent on the following single factors (where relevant) – area, stand, position in the crown and age of the shoots. The BioC/P measurements of the Norway spruce samples were also included in order to be able to perform a comparison of all three methods. In the case of BioC/P and ASD CP measurements, 495 samples were used and in the case of the APEX data, it was 55 samples corresponding to single trees. In addition, a reduction of observations was performed for BioC/P and ASD CP measurements by averaging the leaf

compounds and spectral indices' values for each tree. Thus, the number of measurements also decreased to 55 and they were comparable to the image data. Table 2A shows that the BioC/P measurements of pigments and water content revealed dependence on all studied factors. Regarding pigments, ASD CP derived indices are in correspondence with the BioC/P measurements with the exception of the area factor. On the other hand, the results of ANOVA based on the TCARI/OSAVI and CRI700 indices corresponded to the results carried out on spectral measurements (ASD CP: 495 samples, Apex: 55 samples; also compare Figure 3). Stronger dependence of relative water content was observed only on the detailed structure levels of trees, i.e. when the position in the crown or age of the shoots were considered as factors for the analysis. As expected, reducing the number of observations by averaging brought a higher similarity between all three types of measurements and it caused smaller differences between observations (Table 2B).

Table 2: Results of single factor ANOVA for BioC/P measurements and indices derived from laboratory and image spectral measurements on Norway spruce – A: 495 samples, B: 55 samples. Location parameters on different levels of detail were used as factors in the analysis. Significance codes: $0 \leq p \leq 0.001$: $\star\star\star$ (very significant), $0.001 < p \leq 0.01$: $\star\star$, $0.01 < p \leq 0.05$: $\star$, $0.05 < p \leq 0.1$: $\circ$ and $0.1 < p \leq 1$: n.s. (not significant).

A: 495 samples	Chlorophyll		Carotenoids		Relative water content	
	BioC/P	ASD CP: TCARI/OSAVI	BioC/P	ASD CP: CRI700	BioC/P	ASD CP: WI
Area	$\star\star\star$	n.s.	$\star\star$	n.s.	$\star$	n.s.
Stand	$\star\star\star$	$\star\star\star$	$\star\star\star$	$\star\star\star$	$\circ$	n.s.
Position in the crown	$\star\star\star$	$\star$	$\star\star\star$	$\star\star$	$\star\star\star$	n.s.
Age of the shoots	$\star\star\star$	$\star\star\star$	$\star\star\star$	$\star\star\star$	$\star\star\star$	$\star\star\star$

B: 55 samples	Chlorophyll			Carotenoids			Relative water content		
	BioC/P	TCARI/OSAVI		BioC/P	CRI700		BioC/P	Wi	
		ASD CP	Apex		ASD CP	Apex		ASD CP	Apex
Area	$\star$	n.s.	$\star$	$\circ$	n.s.	n.s.	$\circ$	n.s.	n.s.
Stand	$\star$	$\circ$	$\star$	n.s.	$\star$	$\star$	n.s.	n.s.	n.s.

The Tukey's HSD test performed on the BioC/P and ASD CP data revealed that there were stands significantly different from others and it also confirmed results published earlier about differences of the pigment and water contents in the tree vertical profile [26] and between younger and older tree shoots (e.g. [19]). The outcomes of the Tukey's HSD test are summarised in Table 3.

The spatial distribution of the differences among stands with respect to the contents of the leaf pigments and water was also calculated using Hot Spot Analysis (Getis-Ord Gi*) in the ArcGIS software and further visualised (see Appendix p. 83). The spectra resampled to the Apex resolution were applied for calculation of the indices in the case of the ASD CP data. In the case of BioC/P measurements, the hot spot analysis detected significantly higher chlorophyll and water contents at stands K5 and K2, respectively, and lower carotenoid content at stand P4, which confirmed the results of Tukey's HSD test. The results of both analyses were also in agreement in the case of the ASD CP data (compare Table 3B and Table 4).

Table 3: Results of Tukey's HSD test showing the extremes in factors used in ANOVA. A: summary of extreme differences in three factors. The cases in which the ANOVA did not reveal significant results are marked in red (compare Tab. 2.A). B: ID of stands with significantly highest/lowest values of the leaf pigment and water content. C: same as B but with regard to the position in the crown and age of the shoots.

A: Max. differences	Chlorophyll		Carotenoids		Relative water content	
	BioC/P	ASD CP: TCARI/OSAVI	BioC/P	ASD CP: CRI700	BioC/P	ASD CP: WI
Stand	K5, P2	P4, K2, K5	K5, P4	K3, K2	K2, K4	P4, P1
Position in the crown	H-D	H-D, S-H	H-D	H-D	H-D, S-D	S-D
Age of the shoots	1-2, 1-3	1-2, 1-3	1-3	1-3	1-2, 1-3	1-3

B: Stand	Chlorophyll		Carotenoids		Relative water content	
	BioC/P	ASD CP: TCARI/OSAVI	BioC/P	ASD CP: CRI700	BioC/P	ASD CP: WI
Lowest values	P2, P4	K5	P4	K2	--	--
Highest values	K5	P4, K2	K5	K3	K2, K4, K5	P4, P1, K2

C: Position in the crown Age of the shoots	Maximum		Minimum	
	Shoots	Position	Shoots	Position
Chlorophyll	3	Shaded basal	1	Productive upper
Carotenoids	3	Shaded basal	1	Productive upper
Relative water content	1	Shaded basal	3	Productive upper

Table 3B and Table 4 also showed that both performed tests did not mark the same stands as significantly different when the various measurement methods (BioC/P, ASD CP and Apex) were compared. These discrepancies could be explained mainly by the fact that, though correlated, each of the methods worked with samples of a different hierarchical scale (level of detail). The 'cross' position of stands P4 and K5 in the BioC/P and ASD CP columns is correct, as the low value of chlorophyll content is expressed with a high value of the presented TCARI/OSAVI index and vice versa. A weak relation between the BioC/P, ASD CP and Apex measurements is demonstrated in Figure 4 showing the correlation between the leaf pigment and water content and vegetation indices derived from the ASD CP and Apex spectral reflectance values. No higher correlation was achieved by using other spectral indices sensitive to chlorophyll or water contents, e.g. the coefficient of determination R^2 of the linear regres-

Table 4: Stand IDs with significantly highest/lowest values of leaf pigment and water content according to hot spot analysis.

Stand	Chlorophyll			Carotenoids			Relative water content		
	BioC/P	TCARI/OSAVI		BioC/P	CRI700		BioC/P	WI	
		ASD CP	Apex		ASD CP	Apex		ASD CP	Apex
Lowest values	P4, P2	K5	P1, P5	P4	K2	P5	--	K5	--
Highest values	K5	P4, K2	K1	--	K3	P3	K2	K2	P6

sion between ASD CP and Apex MRENDVI and MSI equalled 0.039 and 0.002, respectively.

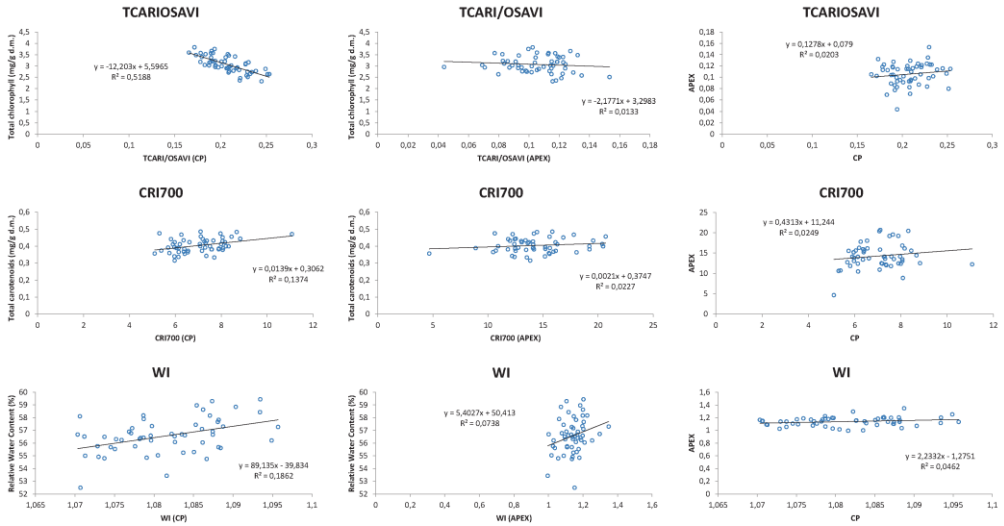

Figure 4: Relation between biochemically derived leaf compounds and indices calculated from laboratory (ASD CP) and image (APEX) spectral reflectance values expressed by means of linear regression and the coefficient of determination R^2.

The resampling of ASD CP data to the Apex spectral resolution did not improve the correlation between the indices and BioC/P. Nevertheless, Figure 5 demonstrates well a higher homogeneity of laboratory derived indices in comparison with indices derived from airborne images. A systematic shift between corresponding indices can also be observed.

Discussion

From Table 1 it is obvious that the mean values of the BioC/P parameters were slightly lower in the Přebuz area. The comparison based on the BioC/P parameters revealed significant differences for all factors tested by one-way ANOVA (Table 2A). The question remains why significant differences were also observed for the area factor. Mišurec et al. [21] came to the conclusion that the significant differences in pigment and water needle contents did not exist in this case what can be explained by the different subset of shoots included in the tests: the values of BioC/P for only one of the tree vertical crown levels were used in that study [21]. Considering the vertical position of needles within the tree crown as a very significant factor mediated by irradiance gradient and influencing pigment and water contents as well as spectral indices (Table 2), it was not surprising that by selecting only one vertical position, the results could shift. Table 2A also shows that there was a good agreement between the results using photosynthetic pigments and TCARI/OSAVI and CRI700 indices as variables in ANOVA on the stand, position in the crown and the needle level and the observed differences are significant in all these cases. A low significance is obtained as soon as the measurements are averaged on the position and stand levels in the cases of relative water content and WI. The results of the Tukey's HSD test are in correspondence with results found in literature—the

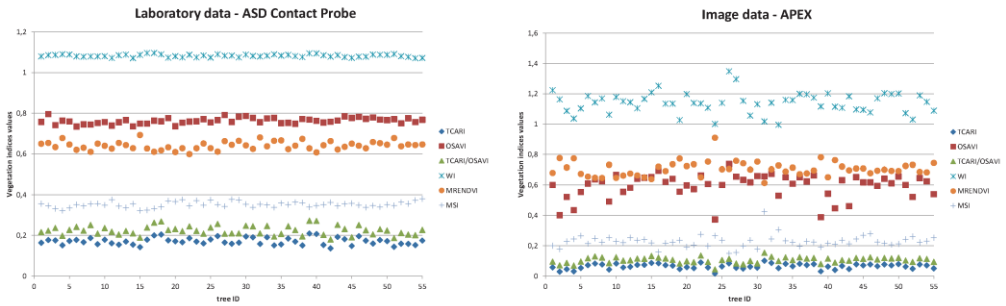

Figure 5: Spectral indices derived from APEX data and ASD CP spectra resampled to Apex spectral resolution. Each stand consists of five trees: stand P1: trees ID 1–5, . . . , P6: 26–30, K1: 31–35, . . . , K5: 51–55. CRI700 is not included due to its higher absolute values in comparison with other indices.

content of photosynthetic pigments (expressed on needle dry mass) increases from the upper to lower parts of the tree crown and with the age of the shoots, while the water content shows an opposite trend [7], [26]. Averaging the BioC/P and ASD CP observations per tree brought better agreement with the optical hyperspectral data. However, it diminished the variability and the number of observations in the dataset and, thus, lowered the significance levels of differences between the observed factors. For future studies, the weighing of observation dependent on the position in the crown shall be considered, as the lower crown parts do not have to have the same influence on the radiation collected by the airborne sensor, especially in the case of the denser forest stands.

The performed hot-spot analysis clearly showed the spatial distribution of stands with significantly different (low or high) values of the observed BioC/P parameters or indices. This was its main advantage in the comparison with the Tukey's HSD test. Both types of results can be used in further analysis concerning the relation to other environmental parameters such as soil composition and properties or macroscopic evaluation of physiological status of forest stands.

The correlation between the BioC/P parameters and indices calculated from the ACD CP and APEX spectra proved to be very low in comparison with other studies on conifers (e.g. [17], [18]) which can be explained by the generally low variability in the observed parameters. As expected, due to the origin of the samples, the relatively highest correlation was obtained for the BioC/P and ASD CP measurements. Empirical models based on the same dataset using more spectral indices and partial least square regression are further elaborated in [7].

Conclusion

The presented study focused on revealing connections between the foliar chemistry compounds, laboratory and airborne image spectroscopic measurements. While the first two can be used for an evaluation of the physiological condition of vegetation on different hierarchical levels within a stand, the airborne hyperspectral data provide large scale evaluation on a canopy level. It was shown that similar results could be obtained when the detailed data

were averaged on a tree level (and optionally resampled to the spectral resolution of the image data). The results support the findings that the vertical gradient of the BioC/P parameters in the canopy play a role when the optical properties of forest stands are modelled. Regarding the physiological status of Norway spruce in the model areas, based on the BioC/P parameters, it is possible to conclude that the differences in the physiological conditions of stands observed in high extent in 1998 [5] still existed in 2013, though they were rather mild considering the absolute values of the derived compounds. From the point of view of optical properties, the differences between the areas are not significant on laboratory or image reflectance spectra.

Acknowledgements

The study was supported by the Ministry of Education, Youth and Sports of the Czech Republic under Grant No LH 12097 (PI J. Albrechtová) and NPUI LO1417.

References

[1] Jonas Ardö et al. "Satellite Based Estimations of Coniferous Forest Cover Changes: Krusne Hory, Czech Republic". In: *Ambio* 26.3 (1997), pp. 158–166.

[2] ASD Inc. *Analytical Spectral Devices*. 2013. URL: http://www.asdi.com/products-and-services (visited on 06/03/2016).

[3] ASD Inc. *Analytical spectral devices*. Ed. by David C Hatchell. Technical Guide 3rd. Ed. 1999. URL: http://www.geo-informatie.nl/courses/grs60312/fieldwork/New%20Folder%20%282%29/Fieldspec%20fieldguide%20TG_Rev4_web.pdf (visited on 06/03/2016).

[4] Richard J. Aspinall, W. Andrew Marcus, and Joseph W. Boardman. "Considerations in collecting, processing, and analysing high spatial resolution hyperspectral data for environmental investigations". In: *Journal of Geographical Systems* 4.1 (2002), pp. 15–29. DOI: 10.1007/s101090100071.

[5] P. K. Entcheva Campbell et al. "Detection of initial damage in Norway spruce canopies using hyperspectral airborne data". In: *International Journal of Remote Sensing* 25.24 (2004), pp. 5557–5584. DOI: 10.1080/01431160410001726058.

[6] Gregory A Carter and Alan K Knapp. "Leaf optical properties in higher plants: linking spectral characteristics to stress and chlorophyll concentration". In: *American Journal of Botany* 88.4 (2001), pp. 677–684. DOI: 10.2307/2657068.

[7] Lucie Červená et al. "Models for estimating leaf pigments and relative water content in three vertical canopy levels of norway spruce based on laboratory spectroscopy". In: *EARSeL 34th Symposium Proceedings*. Ed. by B. Zagajewski, M. Kycko, and R. Reuter. EARSeL and University of Warsaw, 16–20 June 2014. DOI: 10.12760/03-2014-11. URL: http://www.earsel.org/symposia/2014-symposium-Warsaw/pdf_proceedings/EARSeL-Symposium-2014_6_1_cervena.pdf (visited on 06/03/2016).

[8] Roshanak Darvishzadeh et al. "Mapping grassland leaf area index with airborne hyperspectral imagery: A comparison study of statistical approaches and inversion of radiative transfer models". In: *ISPRS Journal of Photogrammetry and Remote Sensing* 66.6 (2011), pp. 894–906. DOI: 10.1016/j.isprsjprs.2011.09.013.

[9] Jean-Baptiste Feret et al. "PROSPECT-4 and 5: Advances in the leaf optical properties model separating photosynthetic pigments". In: *Remote Sensing of Environment* 112.6 (2008), pp. 3030–3043. DOI: 10.1016/j.rse.2008.02.012.

[10] Arthur Getis and J Keith Ord. "The analysis of spatial association by use of distance statistics". In: *Geographical analysis* 24.3 (1992), pp. 189–206. DOI: 10.1111/j.1538-4632.1992.tb00261.x.

[11] Anatoly A Gitelson et al. "Assessing carotenoid content in plant leaves with reflectance spectroscopy". In: *Photochemistry and Photobiology* 75.3 (2002), pp. 272–281. DOI: 10.1562/0031-8655(2002)0750272accipl2.0.co2.

[12] Driss Haboudane et al. "Integrated narrow-band vegetation indices for prediction of crop chlorophyll content for application to precision agriculture". In: *Remote sensing of environment* 81.2 (2002), pp. 416–426. DOI: 10.1016/s0034-4257(02)00018-4.

[13] E Raymond Hunt and Barrett N Rock. "Detection of changes in leaf water content using near-and middle-infrared reflectances". In: *Remote sensing of environment* 30.1 (1989), pp. 43–54. DOI: 10.1016/0034-4257(89)90046-1.

[14] Stéphane Jacquemoud et al. "PROSPECT+ SAIL models: A review of use for vegetation characterization". In: *Remote Sensing of Environment* 113 (2009), S56–S66. DOI: 10.1016/j.rse.2008.01.026.

[15] Raymond F Kokaly and Roger N Clark. "Spectroscopic determination of leaf biochemistry using band-depth analysis of absorption features and stepwise multiple linear regression". In: *Remote sensing of environment* 67.3 (1999), pp. 267–287. DOI: 10.1016/s0034-4257(98)00084-4.

[16] Raymond F Kokaly et al. "Characterizing canopy biochemistry from imaging spectroscopy and its application to ecosystem studies". In: *Remote Sensing of Environment* 113 (2009), S78–S91. DOI: 10.1016/j.rse.2008.10.018.

[17] Lucie Kupková et al. "Chlorophyll determination in silver birch and scots pine foliage from heavy metal polluted regions using spectral reflectance data". In: *EARSeL e-Proceedings*. Vol. 11. 1. 2012, pp. 64–73. URL: http://eproceedings.org/static/vol11_1/11_1_kupkova1.pdf (visited on 06/03/2016).

[18] Zuzana Lhotáková et al. "Detection of multiple stresses in Scots pine growing at post-mining sites using visible to near-infrared spectroscopy". In: *Environmental Science: Processes & Impacts* 15.11 (2013), pp. 2004–2015. DOI: 10.1039/c3em00388d.

[19] Zuzana Lhotáková et al. "Does the azimuth orientation of Norway spruce (Picea abies/L. /Karst.) branches within sunlit crown part influence the heterogeneity of biochemical, structural and spectral characteristics of needles?" In: *Environmental and experimental botany* 59.3 (2007), pp. 283–292. DOI: 10.1016/j.envexpbot.2006.02.003.

[20] Z Malenovský et al. "Applicability of the PROSPECT model for Norway spruce needles". In: *International Journal of Remote Sensing* 27.24 (2006), pp. 5315–5340. DOI: 10.1080/01431160600762990.

[21] Jan Mišurec et al. "Detection of Spatio-Temporal Changes of Norway Spruce Forest Stands in Ore Mountains Using Landsat Time Series and Airborne Hyperspectral Imagery". In: *Remote Sensing* 8.2 (2016), p. 92. DOI: 10.3390/rs8020092.

[22] J Peñuelas et al. "Estimation of plant water concentration by the reflectance water index WI (R900/R970)". In: *International Journal of Remote Sensing* 18.13 (1997), pp. 2869–2875. DOI: 10.1080/014311697217396.

[23] RJ Porra, WA Thompson, and PE Kriedemann. "Determination of accurate extinction coefficients and simultaneous equations for assaying chlorophylls a and b extracted with four different solvents: verification of the concentration of chlorophyll standards by atomic absorption spectroscopy". In: *Biochimica et Biophysica Acta (BBA)-Bioenergetics* 975.3 (1989), pp. 384–394. DOI: 0.1016/s0005-2728(89)80347-0.

[24] Michael E Schaepman et al. "Advanced radiometry measurements and Earth science applications with the Airborne Prism Experiment (APEX)". In: *Remote Sensing of Environment* 158 (2015), pp. 207–219. DOI: 10.1016/j.rse.2014.11.014.

[25] Daniel A Sims and John A Gamon. "Relationships between leaf pigment content and spectral reflectance across a wide range of species, leaf structures and developmental stages". In: *Remote sensing of environment* 81.2 (2002), pp. 337–354. DOI: 10.1016/s0034-4257(02)00010-x.

[26] Quan Wang and Pingheng Li. "Canopy vertical heterogeneity plays a critical role in reflectance simulation". In: *Agricultural and forest meteorology* 169 (2013), pp. 111–121. DOI: 10.1016/j.agrformet.2012.10.004.

[27] Alan R Wellburn. "The spectral determination of chlorophylls a and b, as well as total carotenoids, using various solvents with spectrophotometers of different resolution". In: *Journal of plant physiology* 144.3 (1994), pp. 307–313. DOI: 10.1016/s0176-1617(11)81192-2.

Appendix: The spatial distribution of the differences among stands with respect to the content of the leaf pigments and water calculated using Hot Spot Analysis (Getis-Ord Gi*) in the ArcGIS software.

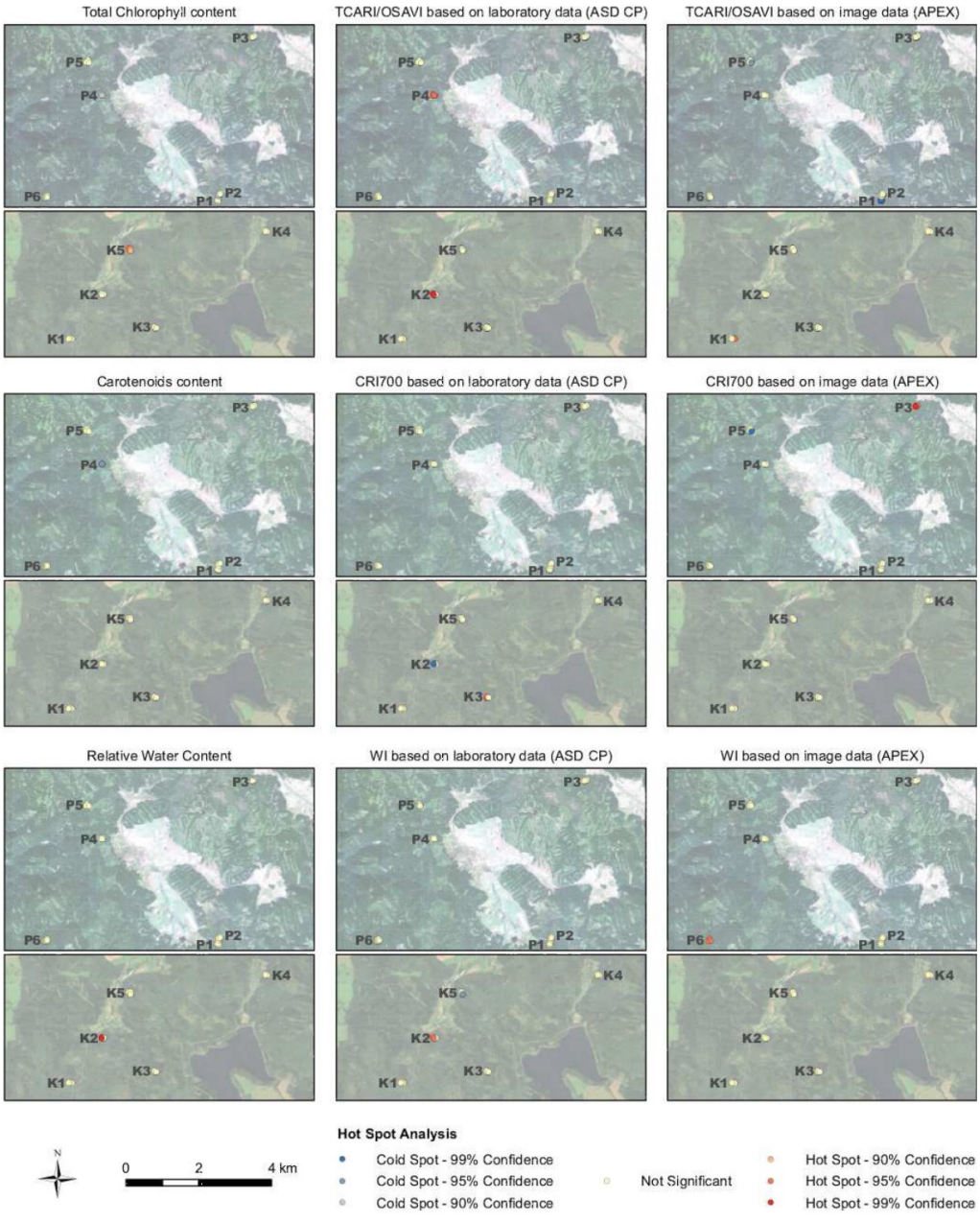

Paper 3*:* "COMPARISON OF REFLECTANCE MEASUREMENTS ACQUIRED WITH A CONTACT PROBE AND AN INTEGRATION SPHERE: IMPLICATIONS FOR THE SPECTRAL PROPERTIES OF VEGETATION AT A LEAF LEVEL"

Potůčková, Markéta, Lucie Červená, Lucie Kupková, Zuzana Lhotáková, Petr Lukeš, Jan Hanuš, Jan Novotný, a Jana Albrechtová. 2016. „Comparison of Reflectance Measurements Acquired with a Contact Probe and an Integration Sphere: Implications for the Spectral Properties of Vegetation at a Leaf Level". *Sensors* 16 (12): 1801. https://doi.org/10.3390/s16111801.

Author Contributions:

MP – 30%, **LČ – 28%**, LK – 11%, ZL – 8%, PL – 8%, JH – 4%, JN – 4%, JA – 7%

sensors

MDPI

Article

Comparison of Reflectance Measurements Acquired with a Contact Probe and an Integration Sphere: Implications for the Spectral Properties of Vegetation at a Leaf Level

Markéta Potůčková [1,*], Lucie Červená [1], Lucie Kupková [1], Zuzana Lhotáková [2], Petr Lukeš [3], Jan Hanuš [3], Jan Novotný [3] and Jana Albrechtová [2]

1 Department of Applied Geoinformatics and Cartography, Faculty of Science, Charles University in Prague, Albertov 6, 128 43 Prague 2, Czech Republic; lucie.cervena@natur.cuni.cz (L.Č.); lucie.kupkova@natur.cuni.cz (L.K.)

2 Department of Experimental Plant Biology, Faculty of Science, Charles University in Prague, Viničná 5, 128 44 Prague 2, Czech Republic; zuzana.lhotakova@natur.cuni.cz (Z.L.); jana.albrechtova@natur.cuni.cz (J.A.)

3 Global Change Research Institute, Academy of Sciences of the Czech Republic, v.v.i., Bělidla 986/4a, 603 00 Brno, Czech Republic; lukes.p@czechglobe.cz (P.L.); hanus.j@czechglobe.cz (J.H.); novotny.j@czechglobe.cz (J.N.)

* Correspondence: marketa.potuckova@natur.cuni.cz; Tel.: +420-221-951-406

Academic Editor: Assefa M. Melesse
Received: 9 August 2016; Accepted: 15 October 2016; Published: 28 October 2016

Abstract: Laboratory spectroscopy in visible and infrared regions is an important tool for studies dealing with plant ecophysiology and early recognition of plant stress due to changing environmental conditions. Leaf optical properties are typically acquired with a spectroradiometer coupled with an integration sphere (IS) in a laboratory or with a contact probe (CP), which has the advantage of operating flexibility and the provision of repetitive in-situ reflectance measurements. Experiments comparing reflectance spectra measured with different devices and device settings are rarely reported in literature. Thus, in our study we focused on a comparison of spectra collected with two ISs on identical samples ranging from a Spectralon and coloured papers as reference standards to vegetation samples with broadleaved (*Nicotiana Rustica* L.) and coniferous (*Picea abies* L. Karst.) leaf types. First, statistical measures such as mean absolute difference, median of differences, standard deviation and paired-sample t-test were applied in order to evaluate differences between collected reflectance values. The possibility of linear transformation between spectra was also tested. Moreover, correlation between normalised differential indexes (NDI) derived for each device and all combinations of wavelengths between 450 nm and 1800 nm were assessed. Finally, relationships between laboratory measured leaf compounds (total chlorophyll, carotenoids and water content), NDI and selected spectral indices often used in remote sensing were studied. The results showed differences between spectra acquired with different devices. While differences were negligible in the case of the Spectralon and they were possible to be modelled with a linear transformation in the case of coloured papers, the spectra collected with the CP and the ISs differed significantly in the case of vegetation samples. Regarding the spectral indices calculated from the reflectance data collected with the three devices, their mean values were in the range of the corresponding standard deviations in the case of broadleaved leaf type. Larger differences in optical leaf properties of spruce needles collected with the CP and ISs are implicated from the different measurement procedure due to needle-like leaf where shoots with spatially oriented needles were measured with the CP and individual needles with the IS. The study shows that a direct comparison between the spectra collected with two devices is not advisable as spectrally dependent offsets may likely exist. We propose that the future studies shall focus on standardisation of measurement procedures so that open access spectral libraries could serve as a reliable input for modelling of optical properties on a leaf level.

Keywords: broadleaved leaf; broadleaved plants; conifers; contact probe; integration sphere; needle; spectroradiometer; spectroscopy

1. Introduction

As many recent studies have proved, laboratory measurements of leaf optical properties in the visible and infrared regions are a valuable technique for understanding different plant physiological processes and stress detection [1–5], as well as photosynthesis efficiency evaluation, energy balance calculation, global terrestrial net primary productivity modelling [6–9] or vegetation stress detection [10–14]. Despite its wide applications, significant measurement uncertainties and knowledge gaps exist. These are related mainly to non-flat leaves, such as coniferous needles exhibiting a long and thin leaf type spatially oriented around a shoot [5,15–18].

Measurements of optical properties at the leaf level are typically acquired with a laboratory spectroradiometer coupled with an integrating sphere (IS). Within a sphere, light reflected or transmitted from a sample is integrated over a full hemisphere to yield measurements insensitive to sample anisotropic directional reflectance (transmittance) behaviour. This allows for repeatable measurements of vegetation samples.

Another mean of leaf optical properties' acquisition includes contact measurements with a reflectance (contact) probe. A contact probe (CP) is a device mainly designed for contact measurements of solid raw materials such as minerals and grains, but also used for vegetation samples. Like an IS, a probe has its own light source (typically krypton halogen bulb) integrated within its body. A CP is retrofitted with a black, slip-on circular spacer that maintains a constant distance from the probe lens to the sample. In contrast to hemispherical measurements in an IS, a CP does not allow transmittance measurements. Also, some additional measurement ambiguities caused by multiple and multi-directional reflectance or possible damages of vegetation samples due to heat transferred from light source must be considered. However, use of a CP has some advantages like avoiding problems with stray light, operating flexibility and speed. Also, by its design, it allows for repetitive and non-destructive in-situ measurements of samples.

Though designed mainly for solid materials, CP measurements have also been successfully used for assessing metal stress in *Arabidopsis thaliana* plants [12], for estimating chlorophyll content in field crops [19] or detecting water stress in poplar at both the leaf and canopy levels [20]. Our research team used CP measurements within a framework of two projects. The first project focused on the assessment of mining-related impacts on selected tree species—Scots pine (*Pinus sylvestris* L.) and silver birch *(Betula pendula* Roth). We proved that measurements based on a CP (in our case an Analytical Spectral Devices, ASD Inc., Boulder, CO, USA contact probe) may provide valuable inputs for statistical modelling of vegetation parameters [4,21]. Laboratory spectroscopic data for the second project focused on the development and improvement of methods for monitoring of Norway spruce (*Picea abies* L. Karst.) health status in the Krušné hory Mts., Czech Republic [22,23]. Here, both an ASD CP and ASD IS were used.

In order to be able to cross-compare leaf optical properties measured by either contact probes or integrating spheres, one should be aware of the constancy among the measurements. A literature review revealed studies comparing reflectance values measured with different spectroradiometers [24–26], with a CP and a fore optic lens [27]; however, up to now no study on mutual comparison of a CP and an IS has been published. Particularly in the case of coniferous needles spatially arranged on a shoot, the methodology of measurement matters remarkably, possibly affecting the values obtained by different devices. There is a gap in experiments that would compare spectra measured on identical samples (standard samples or vegetation specimens or other materials e.g., soils, rocks) using a CP and an IS or experiments comparing measurements acquired by two or more different types of ISs. Confirmation of comparability of reflectance measured by a CP and an IS

could bring simplification of field/laboratory vegetation optical properties measurements and their interpretation in some cases.

To address the above mentioned scientific issues, we designed an empirical laboratory experiment to compare spectra measured with different devices. Our main research questions were: (1) Are there differences between spectra collected with a CP and an IS? (2) Are the retrieved leaf biochemical properties obtained from spectral measurements performed with a CP and an IS yielding comparable results? (3) To what extent does the leaf type (broadleaved leaf and coniferous needles with their spatial arrangement on a shoot) affects spectral leaf properties obtained with a CP and an IS? We measured both reference standards (a Spectralon, coloured papers) and vegetation samples of both leaf types (broadleaved leaves of *N. rustica* and *P. abies* needles) using an ASD CP and two integrating spheres: An ASD IS (RTS-3ZCr2) and a Labsphere IS (RTC-060-SF) and we proposed a methodology for comparison of measurements obtained with different devices at three levels: Using raw spectra, derived vegetation indices and the quantitative retrieval of leaf-level biochemical parameters.

2. Materials and Methods

2.1. Materials

2.1.1. Reference Materials

Although our methodology is focused on vegetation spectra, we also measured two types of artificial samples with stable optical properties—A Spectralon and a set of coloured papers. These represented stable reference materials, which do not change during the measurement process (e.g., due to a loss of water as in the case of some vegetation samples).

Reflectance was measured for a calibrated Zenith Lite® Diffuse Reflectance Target (nominal reflectance of 95%, SphereOptics GmbH, Herrsching, Germany). The supplied calibration protocol was used as a reference. Next, reflectance spectra of nine different coloured papers were measured; the used paper-weight was 80 g/m^2 for five colours: white, black, blue, light green and red, and 160 g/m^2 for white, green, red and yellow colour. The impact of a substitution error (see Section 2.2) on measurements acquired with an IS was examined on the coloured paper samples.

2.1.2. Vegetation Samples

In our experiments, two types of plant samples were measured: tobacco leaves (*Nicotiana Rustica* Roth) as a representative of a 'broadleaved' leaf type, i.e., dorsiventral leaf, and Norway spruce (*Picea abies* L. Karst.) needles as a representative of a 'coniferous' leaf type:

Tobacco leaves: Tobacco plants (36 individuals) were grown in pots in a greenhouse for two months during early summer. Three leaves were measured per each plant. First, a mature leaf located in the lower part of the plant was divided into thirds and measured simultaneously using both the CP and the two ISs. Further, two younger leaves of subsequent insertion were cut; one was measured using the CP and the other one was divided in halves and measured simultaneously in the two IS. Finally, two leaf samples were used for the biochemical determination of photosynthetic pigments and water content. The design of the experiment is shown in Figure 1.

Norway spruce needles: The needles were collected in 2013 from mature even-aged forest stands in the Krušné hory mountains, Czech Republic [28]. In total, 55 trees were sampled—Reflectance spectra of the first two needle age classes from three vertical crown levels were measured. Next, the chlorophyll, carotenoids and water contents were biochemically estimated. After excluding outliers, 96 samples were used for the analysis. A detailed description of the dataset and evaluation of relations between biochemical and spectral measurements for Norway spruce needles can be found in [22,23].

Examples of spectra of coloured papers, tobacco leaves and spruce needles collected with different devices are shown in Figure 2.

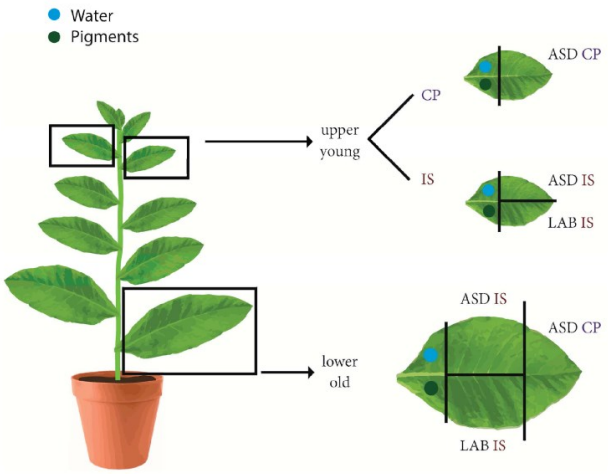

Figure 1. Design of the sampling and measurements in the tobacco experiment. CP—Contact probe, IS—Integrating sphere. ASD, LAB—Producers of the devices.

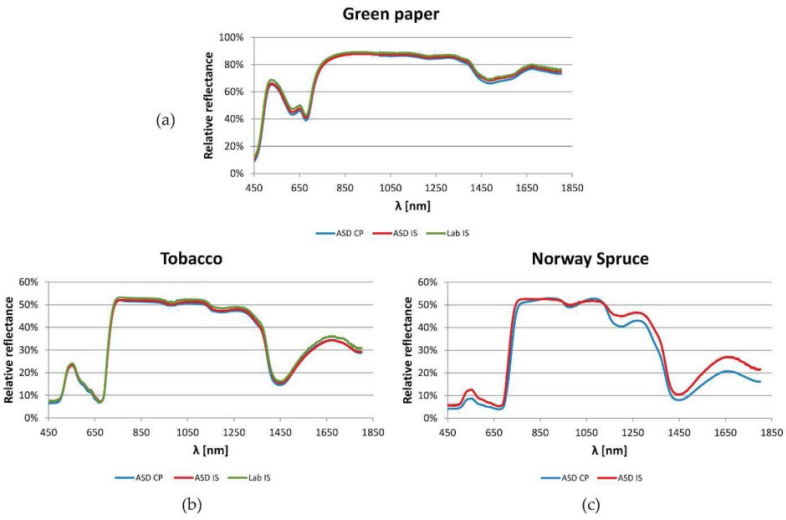

Figure 2. Examples of reflectance spectra of (**a**) coloured (green) paper and vegetation samples—(**b**) tobacco; (**c**) Norway spruce. CP—Contact probe, IS—Integrating sphere. ASD, LAB—Producers of the devices.

2.1.3. Biochemical Measurements

Photosynthetic pigments were extracted using dimethylformamide according to [29] and determined specrophotometrically. Pigment contents were calculated applying equations published in [30] and expressed on dry weight basis ($\mu g/cm^2$). Norway spruce needles were scanned before the pigment extraction. The ratio between the needle dry mass and needle projection area was calculated and used for conversion of amount of pigments to $\mu g/cm^2$, the standard unit in vegetation spectroscopy and remote sensing [16]. In case of tobacco, the samples of constant area were cut from the leaf and amount of pigments was directly related to a leaf unit area (cm^2).

The relative water content (RWC) was determined as the percentage of water in the fresh needles or leaves (the fraction of biomass weight decrease after drying). Fresh needles or leaves were weighed immediately after sampling, oven dried at 80 °C for 48 h and then weighed again.

2.2. Instruments

Spectral reflectance was measured in the range between 350 and 2500 nm using a FieldSpec 4 Wide-Res spectroradiometer (ASD Inc., Boulder, CO, USA). The ASD CP light source is a halogen bulb with colour temperature of approximately 2900 K whereas the ASD IS is supplied with a collimated tungsten light source [31]. According to the manufacturer's protocol, subsequent reflectance and transmittance measurements of a sample requires changing the lamp position between two ports of the IS. It requires some time and it may introduce additional uncertainty due to the shift in light source position and intensity. Thus, in the next step we also tested the Labsphere integrating sphere (Lab IS, North Sutton, NH, USA), light source (KI-120 Koehler Illuminator with 120 W, 3200 K tungsten halogen lamp, Lab IS, North Sutton, NH, USA) of which is fixed during the measurements and only the sample is exchanged between the ports. However, due to the noise in data collected with the Lab IS, all calculations were performed only in the spectral interval from 450 to 1800 nm. Thus, Table 1 also characterises the ASD FieldSpec 4 Wide-Res spectroradiometer's detectors just for this part of spectra: 512 elements silicon array for the visible and near infrared parts of the spectrum (350–1000 nm) and Graded Index InGaAs Photodiodes for the shortwave infrared part of the spectrum (SWIR1: 1000–1800 nm). Their wavelength accuracy is 0.05 nm and the final spectral curve is composed of bands 1 nm wide.

Table 1. ASD FieldSpec 4 Wide-Res spectroradiometer specification [32].

Parameter	VNIR (350–1000 nm)	SWIR1 (1001–1800 nm)
Material of the detector	Silicone	InGaAs, TE Cooled
Spectral resolution	3 nm (at 700 nm)	30 nm (at 1400 nm)
Noise Equivalent Radiance (NEdL, $W/cm^2/nm/sr$)	1.0×10^{-9} (at 700 nm)	1.5×10^{-9} (at 1400 nm)
Stray light	0.02%	0.01%
Maximum radiance	2× Solar	10× Solar

2.2.1. CP Measurements

Samples were placed on a plate coated with black paint (albedo < 0.05) to minimize the reflection of radiation transmitted through the sample (see also [4,22]). The relative reflectance spectrum for each measurement was calculated as a ratio of the measured radiance of the sample to the radiance of 99% spectralon panel (white reference), according to Equation (1):

$$R_{\text{sample\_rel}} = \frac{DN_{\text{sample}}}{DN_{\text{WR}}} \quad (1)$$

where $R_{\text{sample\_rel}}$ is the relative reflectance of the sample, DN_{sample} is the measured reflected radiation from the sample (in DN values), DN_{WR} is the measured reflected radiation of the non-calibrated 99% Spectralon (white reference; the calibration protocol was not available for this Spectralon panel).

Five measurements were taken on different parts of a sample. The sample-specific value was calculated as a median of these five individual measurements. In case of tobacco, single leaf was selected for the measurements, whereas for Norway spruce, needles of the same age class (same shoot) were arranged in a stack still keeping spatial orientation on a shoot (upper part of the needles oriented upwards), see also [27]. Different scan averaging was applied for CP and IS measurements to avoid overheating of samples measured by the CP (Table 2).

2.2.2. IS Measurements

All samples were measured according to the manufacturer's protocol [31]. Because only reflectance measurements could be compared between the IS and CP, transmittance was not in focus in our study and is not discussed in the present paper. The scan averaging for all measurements was set up to 100 (Table 2) to improve the signal to noise ratio.

Table 2. The measured material and methods. IS—Integration sphere, CP—Contact probe, ASD, Lab—Device manufacturers.

Material	Number of Samples	Instrument	Scan Averaging	Methods of Measurement	
Spectralon	1	ASD CP	20	Absolute reflectance (comparison with the calibration data)	
		ASD IS	100 (20)	Absolute reflectance (comparison with the calibration data)	
Colour papers	9	ASD CP	20	Five measurements—Median spectrum	Relative reflectance
		ASD IS	100	Substitution error vs. no substitution error	
		Lab IS	100	Substitution error vs. no substitution error	
Tobacco leaves	72	ASD CP	20	Five measurements—Median spectrum	
		ASD IS	100	No substitution error	
		Lab IS	100	No substitution error	
Norway spruce needles	96	ASD CP	50	Five measurements—Median spectrum	
		ASD IS	100	Substitution error	

For narrow leaf samples (i.e., spruce needles) so called gap-fraction correction was further applied (see e.g., [5,15,18]). To assess the impact of the substitution error (SE, the error caused by the difference in the total energy collected with the optical cable when the reference and sample are placed in the port) samples were measured in two configurations (see Table 3); Figure 3 shows the scheme of the ports of the ASD IS.

Table 3. Configurations of ASD integrating sphere. SE—Substitution error, see the text.

Method	Measured Quantity	Sphere Ports Configuration				
		Port A	Port B	Port C	Port D	Port E
1—Does not correct for SE	R_{WR}	L	W (uncal)	W (cal)	P	P
	R_{sample}	L	W (uncal)	S	P	P
2—Corrects for SE	R_{WR}	L	S*	W (cal)*	P	P
	R_{sample}	L	W (uncal)*	S*	P	P

SE—Substitution error, see the text, R_{WR}—Reflectance of the white reference, R_{sample}—Reflectance of the sample, L—Integrating sphere external light source; W—White reference (uncal—Uncalibrated Zenith standard, cal—Calibrated Zenith standard), S—Sample, P—White plug, *—For Norway Spruce needles measurements the sample holder was added [18].

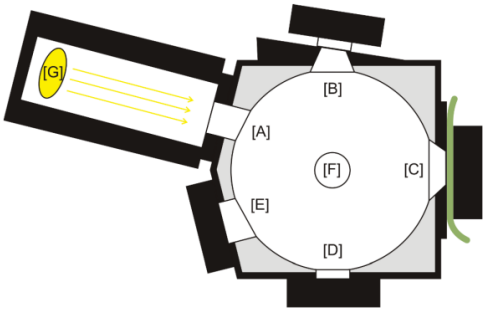

Figure 3. Schema of the ASD integration sphere and its ports: [A] Reflectance input; [B] Reflectance comparison; [C] Reflectance sample; [D] Transmission input; [E] Specular Exclusion Light Trap; [F] Fiber Adapter Port; [G] Collimated Light Source Assembly. The picture shows the setup of sample's reflectance measurement. For the white reference measurement content of the ports [B] and [C] are changed as described in the Table 3.

The relative reflectance spectra of the colour papers and tobacco leaves were computed based on the abovementioned standard Equation (1) described in the manufacturer's manual [31]. The stray

light correction was not taken into account as the errors are negligible (it yields maximum of 0.01% of measured sample reflectance). In the case of the Spectralon, the absolute reflectance values were calculated as:

$$R_{\text{sample\_abs}} = \frac{DN_{\text{sample}}}{DN_{\text{WR}}} \times R_{\text{WR}} = R_{\text{sample\_rel}} R_{\text{WR}} \quad (2)$$

where $R_{\text{sample\_abs}}$ is the absolute reflectance of the sample, DN_{sample} is the measured reflected radiation from the sample (in *DN* values), DN_{WR} is the measured reflected radiation from the 99% Spectralon (white reference) and R_{WR} is the calibrated reflectance value of the 99% Spectralon.

Due to their size, measurements of Norway spruce needles require more complex approach, which includes the gap-fraction correction of samples placed in a special sample-holder [33], revised by [15], summarized and extended in [5,18]. The gap-fraction is typically retrieved from the scans of sample-holders. The relative reflectance spectra of the needles are then derived from the measured radiance and the gap-fraction according to the Equation (3) [5,15]:

$$R_{\text{needle}} = \frac{\frac{\left(DN_{\text{sample}} - DN_{\text{straylight}}\right)}{DN_{\text{WR}} - DN_{\text{straylight}}}}{1 - GF} \quad (3)$$

where R_{needle} is the reflectance of individual needles, DN_{sample} is the measured reflected radiation from the sample, i.e., needles + gaps in *DN* values, $DN_{\text{straylight}}$ is the measured stray light radiation in *DN* values, DN_{WR} is the measured reflected radiation from the calibrated 99% Spectralon (white reference) in *DN* values, *GF* is the gap-fraction.

Measurements with all devices were carried out in a spectroscopic laboratory. In the case of the Spectralon, colour papers and spruce needles measurements, the ASD IS and ASD CP were subsequently connected to one ASD FieldSpec 4 Wide-Res spectroradiometer; another spectroradiometer of the same type was used for the Lab IS measurements. Tobacco samples were simultaneously measured with all three devices connected to three ASD FieldSpec 4 Wide-Res spectroradiometers.

2.3. Methodology of Spectra Comparison

The most reliable spectra comparison would be based on the absolute reflectance values calculated according to Equation (2). This approach was used in the case of the first test with the calibrated the 95% Zenith Lite® Diffuse Reflectance Target, further called the 95% Zenith Lite® Sepectralon calibrated reference. CP measurements were carried out with a non-calibrated 99% Spectralon. Equation (1) was then used for calculating reflectance values, which were relative to the 99% Spectralon. This approach widely applied in the field campaigns was utilized in the case of colour papers as well as vegetation experiments mostly for practical reasons—The diameter of an internal ASD IS 99% Calibrated Reference Standard just covers the ASD CP field of view and is therefore a potential source of errors. Using the 95% Zenith Lite® Spectralon as a white reference is complicated in the ASD IS measurements because the spectralon is relatively big and difficult to be held in the port. Moreover, it does not fit to the above mentioned internal 99% standard coating the inside of the IS.

The rationale for spectra comparison is based on the following idea. If we assume a theoretical case of equal absolute reflectance values derived from a CP and an IS, their difference can be expressed as:

$$R_{\text{CP\_abs}} - R_{\text{IS\_abs}} = R_{\text{CP\_rel}} R_{\text{WR\_CP}} - R_{\text{IS\_rel}} R_{\text{WR\_IS}} = 0 \quad (4)$$

where R_{rel} and R_{abs} are the absolute and relative reflectance values calculated according the Equations (1) and (2), respectively, and R_{WR} is the calibrated reflectance of the Spectralons used for the CP and IS measurements.

Thus, the relation between the relative measurements can be modelled with a linear function, multiplicative term of which corresponds to the unknown ratio C_{WR} between the reflectance values of the used Spectralons:

$$R_{CP\_rel} = R_{IS\_rel}\frac{R_{WR\_IS}}{R_{WR\_CP}} = R_{IS\_rel}C_{WR} \quad (5)$$

The test based on the calibrated Spectralon revealed an offset $C_{Oabs} = R_{CP\_abs} - R_{IS\_abs}$ between the reflectance values derived from CP and IS measurements. Equation (5) was therefore extended to a full linear model described with Equation (6):

$$R_{CP\_rel} = R_{IS\_rel}\frac{R_{WR\_IS}}{R_{WR\_CP}} + \frac{C_{O\_abs}}{R_{WR\_CP}}C_{Oabs} = R_{IS\_rel}C_{WR} + C_O \quad (6)$$

where C_O is the unknown offset of absolute values C_{Oabs} divided by R_{WR_CP}. The coefficients C_{WR} and C_O are spectrally dependent.

The measurements of colour papers, tobacco leaves and Norway spruce needles collected with different devices were first compared using selected statistical quantities. The mean absolute difference was applied as a measure of a mean magnitude of differences in reflectance. The median of differences quantifies a systematic shift between the compared spectra. The standard deviation was added to describe the variability of the differences around the mean value. First, the standard deviation was calculated from all samples of the same type of material acquired by one device for each wavelength between 450 and 1800 nm. To quantify the differences among spectra using a single quantity, a mean of standard deviations was then computed. Since the measurements were carried on the same samples with all devices, the similarity between the spectra was also evaluated on each wavelength and all combinations of devices by means of the paired-sample t-test with the level of significance $\alpha = 0.05$. Furthermore, it was possible to estimate the coefficients of linear relation between the R_{CP_rel} and R_{IS_rel} values for each studied wavelength according to Equation (6). The similarity between the transformed spectral curves obtained from different devices was again evaluated based on the mean absolute difference, the mean standard deviation and the paired-sample t-test.

Normalized differential indexes (NDI) are commonly used when the relation between the spectral response of vegetation and its biochemical parameters are sought. Equation (7) represents a general expression of the normalised differential vegetation index calculated for reflectance values R on the wavelengths λ_1 and λ_2:

$$NDI_{\lambda_{12}} = \frac{R_{\lambda_2} - R_{\lambda_1}}{R_{\lambda_2} + R_{\lambda_1}} \quad (7)$$

The NDI has a value from the interval <−1; 1>. It slightly differs if the relative or absolute reflectance is used for calculation. Due to the lack of calibrated spectralon for the ASD CP, the NDI were calculated from the relative reflectance values in our experiments. Based on the NDI values of samples measured either by the CP and the IS, the differences and correlation in NDI values were evaluated for colour papers and plant samples. In addition, the correlation of NDI with selected leaf compounds (total chlorophyll, carotenoids and water content) obtained from all three devices was calculated to demonstrate its applicability for quantitative remote sensing of vegetation.

Finally, we assessed the relationship between spectral indices often used in quantitative remote sensing of vegetation and leaf compounds. A linear regression and a calculation of a coefficient of determination R^2 for all used devices and about fifty indices, summarized for chlorophyll in [34,35], for carotenoids in [36,37] and for water in [38] (pp. 232–233), were performed. Based on the results, four indices listed in Table 4 are presented further in this study.

Table 4. Evaluated spectral indices. R is reflectance on a given wavelength.

Index Name	Formula	Reference
Optimized Soil-adjusted Vegetation Index 2	$OSAVI2 = (1 + 0.16) * (R_{750} - R_{705})/(R_{750} + R_{705} + 0.16)$	[39]
Carotenoid Vegetation Index ($R_{NIR} * CRI_{550}$)	$R_{NIR}CRI_{550} = ((1/R_{510} - 1/R_{550}) * R_{770})$	[40,41]
Moisture Stress Index	$MSI = R_{1600}/R_{820}$	[42]
Transformed Chlorophyll Absorption Ratio Index	$TCARI = 3 * [(R_{700} - R_{670}) - 0.2 * (R_{700} - R_{550}) * R_{700}/R_{670})]$	[43]
Carotenoid Vegetation Index	$CRI_{700} = 1/R_{515} - 1/R_{700}$	[40]
Normalise Differential Water Index	$NDWI = (R_{857} - R_{1241})/(R_{857} + R_{1241})$	[44]

Sensors **2016**, *16*, 1801

3. Results and Discussion

First, spectral measurements collected with three device settings, ASD CP, ASD IS and Lab IS were directly compared and evaluated. Then the relationship between spectral measurements and leaf compounds was assessed. The reflectance values are presented as a reflectance factor (i.e., %). To avoid further confusion, a reader should note that the differences and standard deviations of reflectance are also given in %; however they describe absolute, between-sample differences and not relative values.

3.1. Spectra Comparison

3.1.1. Calibrated Reference

First, reflectance of the 95% Zenith Lite® calibrated reference was measured with the ASD IS and ASD CP. It was used both as a white reference and the sample, i.e., the ratio between the collected spectra—Relative reflectance, see Equation (1), should be close to 1 and possible deviations reflect the noise in the signal. Two measurements were carried out with both device settings.

In the case of the ASD IS, 20 and 100 of scans per measurement were used. The absolute reflectance measurements, according to the Equation (2), from the ASD IS showed a high correspondence to the calibrated reflectance values of the 95% Zenith Lite® calibrated reference regardless the number of averaged scans. The 99% quantile of absolute differences between the collected and reference reflectance values in the spectral interval from 450 nm to 1800 nm equalled to 0.3% and 0.4% for 20 and 100 scans, respectively. The higher number of scans yields better SNR [45] what was also confirmed in our study (Figure 4). Based on this result, averaging of 100 scans was used for further measurements.

As shown in Figure 4, the shape of the reflectance curves acquired with the ASD CP was also similar to the calibrated standard, nevertheless one of them (called as ASD CP1 in Figure 4) revealed a systematic shift of 1.3%. Both measurements were performed under the same conditions and close in time. A closer look at raw data revealed that the CP optics had not been in a full contact with the Spectralon when measuring the white reference. The recorded R_{WR} values were therefore lower what caused a higher R_{abs}. The second measurement (ASD CP2) fits the 95% Zenith Lite® calibrated reference. The 99% quantile of absolute differences in reflectance equals to 0.3% what is comparable to the ASD IS.

Relative differences (Figure 4) emphasized discrepancies between both devices, especially in the spectral interval between 450 and 1000 nm, where the CP slightly overestimated while the IS slightly underestimated the calibrated reflectance values. Also, a spectral shift between two detectors at VNIR and SWIR1 at 1000 nm was present in the data. The paired-sample t-test revealed significant differences between the spectra at $\alpha = 0.05$.

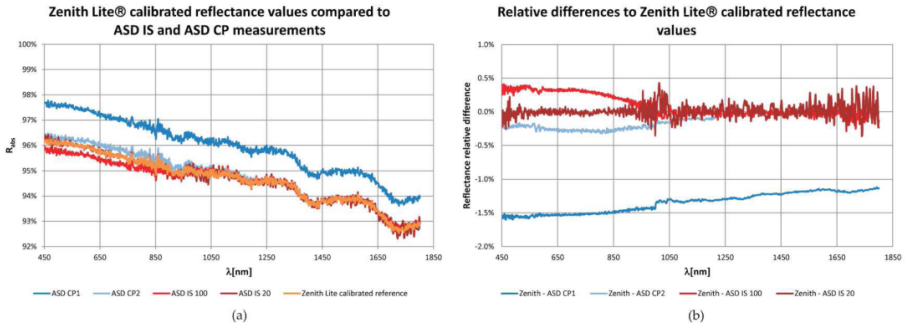

Figure 4. Comparison of the 95% Zenith Lite® Spectralon calibrated reflectance values (R_{ZL}) with reflectance determined by means of ASD IS and ASD CP measurements. (**a**) Original reflectance curves; (**b**) The relative differences calculated as $(R_{\text{ZL}} - R_{\text{ASD IS/CP}})/R_{\text{ZL}}$.

3.1.2. Coloured Papers

Due to the lack of a calibrated Spectralon for the CP measurements, only relative spectra of papers measured with the ASD CP, ASD IS and Lab IS were compared. The influence of the substitution error (SE) correction on spectra measured with the IS was also studied.

First, differences between original spectra were evaluated. As Table 5 shows, the best agreement between the relative reflectance values was achieved between ASD IS and Lab IS when the correction for the SE was applied. The reflectance values of the Lab IS were about 1.3% higher and the standard deviation was 0.5%. When comparing the IS and CP measurements, the correction of the SE changed the offset of the spectra while it had almost no influence on the standard deviation. Due to the offset between the spectra, the paired-sample t-test revealed significant differences between compared devices for all wavelengths with the only exception of ASD CP and ASD IS spectra without a SE correction. After including the mean difference between devices calculated for each wavelength, all combinations of spectra passed the paired-sample t-test on all wavelengths, i.e., no significant differences were observed.

Table 5. Comparison of differences in coloured papers relative reflectance [%] measurements by three devices before (Mean absolute difference, Median of differences, Mean standard deviation, Root Mean Square Error—RMSE) and after linear regression (Lin. reg. mean absolute residual, Lin. reg. mean st. d.—Linear regression mean standard deviation). Measurements that were not corrected for the substitution error are in parenthesis. CP—Contact probe, IS—Integration sphere, ASD, Lab—Producers of the measurement devices.

Differences in Relative Reflectance [%]	Mean Absolute Difference	Median of Differences	Standard Deviation	RMSE	Lin. reg. Mean Absolute Residual	Lin. Reg. Mean st. d.
ASD CP–ASD IS	2.4 (1.3)	−2.2 (0.4)	1.5 (1.7)	2.7 (1.8)	1.0 (1.1)	1.2 (1.4)
ASD CP–Lab IS	3.6 (1.8)	−3.6 (−1.5)	1.4 (1.2)	3.9 (2.0)	0.9 (0.7)	1.1 (0.9)
ASD IS–Lab IS	1.4 (2.3)	−1.3 (−2.3)	0.5 (0.7)	1.5 (2.4)	0.3 (0.6)	0.4 (0.7)

In the next step, linear regression parameters according to Equation (6) between reflectance values of colour papers were calculated for each combination of devices and wavelengths. After applying the linear model, the offset between the spectra was eliminated, the absolute difference decreased in most cases and the standard deviation was practically preserved (see Table 5). It is worth mentioning that after the regression, the mean absolute residual between the measurements in the IS—when the SE was corrected—was on the level of results when ASD IS reflectance was compared to the 95% Zenith Lite® calibrated reference. The linear regression lowered differences in a comparison of CP and IS with and without the SE correction; the mean absolute residuals of 0.9% and standard deviation of 1.1% were achieved.

An example demonstrating the spectral dependence of three selected statistical measures evaluating relative reflectance values derived for the same samples using the ASD CP and ASD IS is shown in Figure 5. In contrast to measured leaves, the differences are more spectrally invariant in the case of colour papers what could be caused by a lower variability in colour paper reflectance especially in the NIR part of the spectrum.

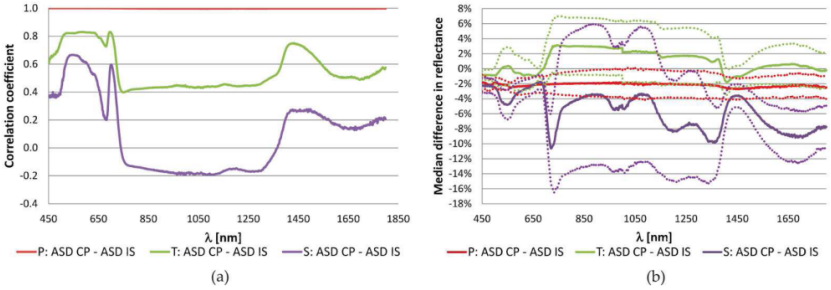

Figure 5. Spectral dependence of (**a**) the correlation coefficient and (**b**) the mean difference in reflectance obtained from the comparison of available samples measured with the ASD contact probe (CP) and ASD integration sphere (IS) for each wavelength in the spectral interval from 450 nm to 1800 nm. P—Coloured papers (9 samples), T—Tobacco leaves (72 samples), S—Norway spruce (96 samples). The dot lines around the median difference in reflectance show the interval of ± standard deviation.

3.1.3. Vegetation Samples

The spectra comparison of tobacco leaves and Norway spruce samples was carried out in the same way as in the case of the colour papers. The application of the SE correction on measurements of tobacco samples brought changes in the offset of the spectra and did not significantly alter the other statistical values (see Table 6). As the correction is fully supported from the theoretical point of view, only measurements with applied correction for SE were used in all the following experiments.

Table 6. Comparison of differences in tobacco leaves (T) and Norway spruce (S) relative reflectance [%] measurements before (Mean absolute difference, Median of differences, Mean standard deviation, Root Mean Square Error - RMSE) and after linear regression (Lin. reg. mean absolute residual, Lin. reg. mean standard deviation—st. d.). Measurements that were not corrected for the substitution error are in parenthesis. CP—Contact probe, IS—Integration sphere, ASD, Lab—Producers of the measurement devices.

Differences in Relative Reflectance [%]	Mean Absolute Difference	Median of Differences	Standard Deviation	RMSE	Lin. Reg. Mean Absolute Residual	Lin. Reg. Mean st. d.
T: ASD CP–ASD IS	2.5 (5.0)	0.7 (4.6)	2.9 (2.9)	3.1 (5.4)	1.5	2.0
T: ASD CP–Lab IS	2.4 (2.5)	−1.3 (0.6)	2.7 (2.8)	3.4 (3.1)	1.5	1.9
T: ASD IS SE–Lab IS	2.5 (4.2)	−2.0 (−4.1)	1.8 (1.8)	3.0 (4.5)	1.3	1.7
S: ASD CP–ASD IS	6.8	-5.2	5.0	7.9	2.8	3.4

The comparison of the original tobacco spectra revealed similar results for all three devices; the smallest offset was observed between the ASD CP and ASD IS measurements (see Table 6). The paired-sample t-test proved significant differences between all measured spectra. Subtracting the offset between the spectra calculated for each wavelength from one of the compared measurements was sufficient to pass the paired-sample t-test for all combinations of devices with *p*-values close to 1.

Table 6 also shows that the application of the linear regression decreased the absolute differences in spectral values with a factor of 1.5 to 2 and in the case of comparison of the CP and ISs it also lowered the standard deviation. In comparison to the coloured papers, the higher values of statistical measures were mainly caused by a higher variability of optical properties of the samples and their slightly different insertion on a plant as it was demonstrated in Figure 1. The correlation coefficient between spectral measurements of 72 samples in each wavelength was lower (r_{T_mean} = 0.558) than in the case of coloured papers (r_{P_mean} = 0.998), see Figure 5.

Castro-Esau et al. [24] compared reflectance spectra of three leaf plants (*Cafea Arabica*, *Lantana camara*, *Eriobotrya japonica*) collected with three different spectroradiometers by means of D metric that corresponds to Root Mean Square Error (RMSE). Using the same IS but different spectrometers they received the D value about 0.5%. Using different spectrometers and different

devices for data collection (optical cable, pistol grip), the D values increased to 2%–6% which is the range of RMSE in Table 6.

Norway spruce samples were measured with the ASD CP and ASD IS (including the SE correction). The statistical values describing differences between the two devices were in most cases doubled in comparison to the tobacco samples (Table 6). The correlation coefficient between the two measurements was low (ranging from −0.2 to 0.2) in the large spectral interval from 750 nm to 1400 nm as shown in Figure 5a. The variability among the samples was the highest of all tested materials as indicated by the standard deviation values both in Figure 5 and Table 6. The t-test applied on the original data proved significant differences between the spectra on all used wavelengths. Significant differences did not exist anymore after the linear transformation of CP spectra. The larger discrepancies in comparison to other tested materials were mainly influenced by a different measurement procedure. While only a single layer of needles was measured in the IS, a compact layer of needles on shoots causing multiple, multidirectional reflectance between the layers (needles) but also a loss of signal caused a difference in radiances recorded with the CP. The median of differences was negative what implicated the higher reflectance values measured with the ASD IS. This result was in correspondence with [46] dealing with an upscaling model from needle to shoot spectra. The application of such model would require estimation of a shoot structural parameter which was not performed in the scope of this study. The results are therefore biased by omitting this correction step.

3.1.4. Normalized Differential Index

In the next step, the normalised differential index was calculated for all measured samples, devices, device settings and combinations of wavelengths in the interval between 450 nm and 1800 nm. The summary statistics of differences in NDI between the devices is shown in Table 7. The differences in NDI were at the level of 0.01 in the case of the coloured papers. Due to a higher variability and a higher number of samples, the differences in the plant material were higher, with a factor of 2–3 in the case of tobacco and with the factor of 6 and 3 for the mean absolute difference and standard deviation, respectively, in the case of Norway spruce. The linear transformation of spectra brought improvements for most measurements.

Table 7. Mean absolute difference (MAD) and mean of standard deviations (MStD) in normalized differential index (NDI) differences calculated for all available samples and all combinations of wavelengths in the interval 450 nm–1800 nm. CP—Contact probe, IS—Integration sphere, ASD, Lab—Producers of the measurement devices.

NDI Differences: Coloured Papers				
		ASD IS–Lab IS	**ASD CP–ASD IS**	**ASD CP–Lab IS**
Original data	MAD	0.005	0.009	0.011
	MStD	0.007	0.009	0.010
After lin. regression	MAD	0.003	0.004	0.005
	MStD	0.004	0.006	0.007

NDI Differences: Tobacco				
		ASD CP–ASD IS	**ASD CP–Lab IS**	**ASD IS–Lab IS**
Original data	MAD	0.027	0.026	0.017
	MStD	0.026	0.028	0.019
After lin. regression	MAD	0.012	0.015	0.014
	MStD	0.016	0.021	0.019

NDI Differences: Norway Spruce		
		ASD CP–ASD IS
Original data	MAD	0.062
	MStD	0.029
After lin. regression	MAD	0.019
	MStD	0.024

The spectral dependency of differences in the NDI is demonstrated in Figure 6. It shows examples of the correlation coefficient between the NDI values calculated for different materials from all samples and all combinations of wavelengths for the ASD CP and ASD IS. It generally confirms the increasing discrepancy between the spectra obtained by different instruments and device settings when moving from relatively homogeneous materials (i.e., coloured papers and tobacco leaves) to more complicated measurements of Norway spruce needles. The graphical results are, thus, in correspondence with statistics summarized in Table 7. Figure 6 also follows the results shown in Figure 5a. The high

correlation in original spectra emanates high correlation in NDI and vice versa. The drop of correlation values around 1000 nm is caused by the spectral shift between the spectroradiometer's sensors.

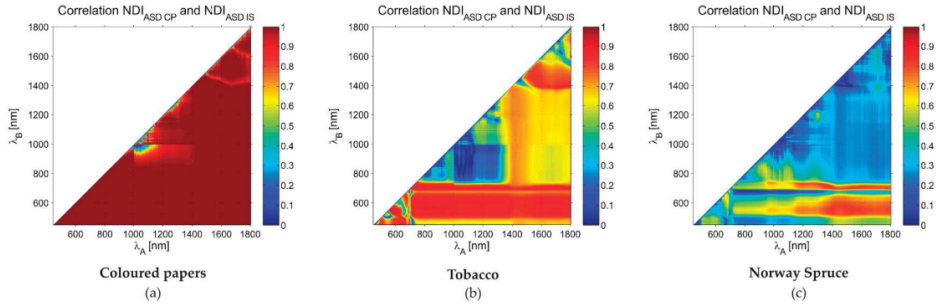

Figure 6. Spectral dependence of correlation coefficient (its absolute value) between normalized differential index (NDI) values derived from relative reflectance measured with the ASD CP and ASD IS for (**a**) coloured papers; (**b**) tobacco leaves; (**c**) Norway spruce needles. CP—Contact probe, IS—Integration sphere, ASD, Lab—Producers of the measurement devices.

3.2. Retrieval of Leaf Biochemical Properties

The NDI values were also correlated with the content of photosynthetic pigments and water content determined with the laboratory analyses as described in Section 2.2. The summary of the mean contents of chlorophyll, carotenoids and water is given in Table 8.

Table 8. Content of the biochemical parameters in the collected samples—Chlorophyll a/b (Cab), Carotenoids (Car) and relative water content (RWC). The samples for ASD CP measurements were taken from slightly different parts of the leaves than samples for the ASD IS and Lab IS (for a detailed explanation see Figure 1). CP—Contact probe, IS—Integration sphere, ASD, Lab—Producers of the measurement devices.

Parameter	Tobacco Leaves ASD CP		Tobacco Leaves ASD/Lab IS		Norway Spruce Needles	
	Mean	StD	Mean	StD	Mean	StD
Cab [μg/cm^2]	21.3	5.0	20.5	4.8	38.9	11.0
Car [μg/cm^2]	2.4	0.5	2.3	0.6	5.1	1.3
RWC [%]	84.7	5.9	85.3	5.8	57.9	2.5

The correlation coefficients between all three leaf compounds and NDI derived for tobacco and Norway spruce samples from all available reflectance measurement were calculated. Figure 7 depicts examples of correlation between chlorophyll and NDI, RWC and NDI (the relations of NDI to carotenoids are not presented; contents of carotenoids and chlorophyll are highly correlated and the diagrams show almost identical patterns). In spite of differences in the correlation coefficient values, the diagrams show similar trends for all three devices in the case of tobacco. The NDI derived from the ASD IS measurements of Norway spruce needles have stronger correlation to chlorophyll in the combination of spectral ranges 700–1400 nm and 550–750 nm in comparison to the NDI derived from ASD CP. The correlation to water content is in general low for both types of vegetation samples with a narrow peak region at 1500–1800 nm and around 1400 nm (water absorption band). A detailed study of local maxima in Figure 7 could provide a base for proposing spectral indices sensitive to leaf compounds. Our study did not aim at such analysis; higher variability in samples would be necessary for derivation and validation of such indices.

Finally, the relationship between the leaf compounds and corresponding spectral indices derived from different devices was evaluated. Table 9 gives an overview of indices that revealed the highest values of the coefficient of determination (R^2). With the exception of the chlorophyll

Sensors **2016**, *16*, 1801

content, the R^2 were too small to prove a significant relationship between the leaf compounds and corresponding indices.

Table 9. The coefficient of determination R^2 showing the strength of the linear dependence between selected spectral indices derived from measured spectra and results of biochemical analyses for tobacco and Norway spruce samples. Only indices with the highest R^2 value are presented. In parenthesis, mean value and standard deviation of spectral indices are given. Cab—Total chlorophyll, Car—Total carotenoids, RWC—Relative water content; for explanation of spectral indices see Table 4.

Tobacco				
Parameter	**Spectral Index**	**R^2 (Mean ± Stand Deviation)**		
		ASD CP	**ASD IS**	**Lab IS**
Cab [µg/cm^2]	OSAVI 2	0.63 (0.272 ± 0.069)	0.64 (0.281 ± 0.041)	0.65 (0.288 ± 0.052)
Car [µg/cm^2]	$R_{NIR}CRI_{550}$	0.15 (1.87 ± 0.53)	0.21 (1.66 ± 0.20)	0.16 (1.64 ± 0.32)
RWC [%]	MSI	0.03 (0.602 ± 0.029)	0.15 (0.636 ± 0.026)	0.06 (0.631 ± 0.029)
Norway Spruce				
Parameter	**Spectral Index**	**ASD CP**	**ASD IS SE**	
Cab [µg/cm^2]	TCARI	0.48 (0.171 ± 0.038)	0.46 (0.261 ± 0.061)	
Car [µg/cm^2]	CRI700	0.20 (6.52 ± 1.69)	0.10 (3.99 ± 0.81)	
RWC [%]	NDWI	0.43 (0.120 ± 0.021)	0.07 (0.066 ± 0.011)	

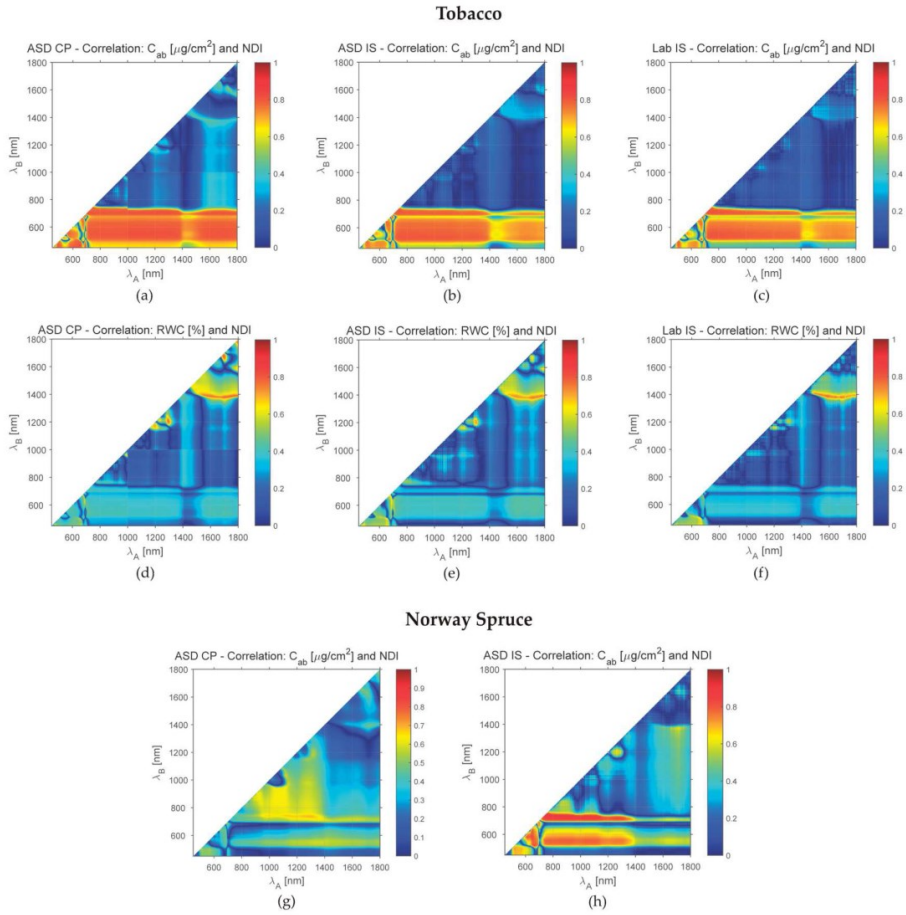

Figure 7. *Cont.*

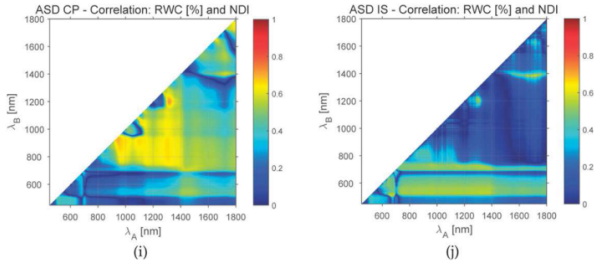

Figure 7. Absolute values of the correlation coefficient between leaf compounds (total chlorophyll—Cab and relative water content—RWC) and NDI (normalised differential index) derived for (**a**–**f**) tobacco samples and (**g**–**j**) Norway spruce and the used devices. CP—Contact probe, IS—Integration sphere, ASD, Lab—Producers of the measurement devices.

The main reason is a low variability in carotenoids and water content in the dataset (see Table 8) despite our efforts to introduce differences in physiological status of sampled plants (e.g., different regimes in watering and using both mature and young leaves in the case of tobacco). This was probably caused by the fact that tobacco plants are not well structurally adapted to a water loss, e.g., by thick cuticle or presence of hairs. However, tobacco is a standard model plant species, reliably and fast growing in greenhouse conditions.

The performed t-tests showed that majority of the fifty calculated indices differed significantly between the tested devices. Among indices presented in Table 9, the null hypothesis about the non-significant differences between the indices derived from tobacco samples was confirmed only for following combinations of devices: OSAVI 2—ASD IS & Lab IS; $R_{NIR}CRI_{550}$—ASD CP & ASD IS, ASD CP & LAB IS.

As Table 9 also shows, the mean values of indices among devices differed within the standard deviation in the case of tobacco. Looking at coniferous samples, the mean values of indices obtained with the ASD IS and the ASD CP differed with a factor of 1.5 to 2. The reason for this is obviously in the measurement procedure connected with leaf type as described in Section 3.1.3.

4. Conclusions

The objective of our study was to test whether the spectral measurements collected with a CP and an IS yield comparable results. The main motivation of this study arose from our practical experience with the CP measurements being both convenient for field work and also less time consuming than the IS measurements. The comparison of spectra collected with two ISs was another objective as the data exchange between research groups is frequent and comparability and quality are then important issues. It must be stressed out that the present conclusions are based on the datasets where the relative reflectance values were used due to a lack of a calibrated Spectralon used for the CP measurements. It is assumed that using of absolute reflectance values could result in further improvement.

The calibrated reflectance values of the 95% Zenith Lite® calibrated reference and absolute reflectance measured with the ASD IS and ASD CP differed less than 0.5% (in relative units) in the best cases, which is on the level of the instrument performance [47]. In order to achieve such a result, attention has to be paid to both the measurement itself in order to avoid possible measurement errors (such as a loose contact between the contact probe and the sample) and rigorous data post-processing (e.g., excluding outliers from the measurements). The effect of the stray light correction was small (less than 0.01%) and, thus, not significant for our experiments.

The experiment with the coloured papers revealed higher discrepancies between spectral reflectance values obtained from different devices and device settings in comparison to the Spectralon. It showed that differences exist even when two ISs of a different manufacturer are compared. The main conclusions are that (i) the best agreement was achieved between measurements from ASD IS and

Lab IS when the correction for substitution error was applied; (ii) if the samples measured with the same devices exist, they can be used for derivation of parameters of a linear transformation (at each wavelength) that can bring the compared spectra to a better agreement. Based on following tests with two different leaf types—tobacco and Norway spruce—this transformation gave better results for broadleaved than for coniferous vegetation.

The last objective of the study was to show to what extent does the leaf type (broadleaved leaf and coniferous needles with their spatial arrangement on a shoot) affect spectral leaf properties obtained by a CP and an IS. The study revealed that in the case of broadleaved leaf type, the differences in using the IS and CP are smaller than in the case of coniferous needles. Coniferous needles have a thick cuticle and rhomboid shape on cross section. In addition, needles are attached to a shoot under different angles and this spatial architecture, which causes multidirectional reflectance, may affect measurements with a CP since needles are kept on a shoot during these measurements. In contrast to measurements with an IS where single, detached needles are laid parallel on a tray of a sample holder and, thus, shoot architecture does not interfere with measurements. In future studies, models for shoot spectral properties based on needle spectral measurements shall be applied and evaluated. As a broadleaved plant species in our case we used tobacco with a leaf type without a specific anatomic adaptation of epidermis. It may happen that broadleaved leaf types with pronounced epidermal structure corresponding to more xeropmorphic leaf adaptations could exhibit more differences, though.

The relation between NDI derived from spectra collected by different devices followed the observation that in spite of our effort to have an identical sample per one set of measurements, some individual variability had been present (increasing from papers, through tobacco to spruce needles). It caused higher differences in corresponding spectra and subsequently also higher differences in the derived NDI. The data collected with the ASD FieldSpec 4 Wide-Res spectroradiometer were sampled with the interval of 1 nm. The noise in data could influence the calculated NDI. Therefore smoothing original spectra with a suitable filter, e.g., a Savitzky–Golay filter [48,49] could improve the results. The conclusions about NDI are valid also for specific vegetation indices used in quantitative remote sensing for modelling of relation between spectral observations and the content of biochemical or biophysical compounds in vegetation.

The present study contributes to an effort in using a more coherent approach of leaf optical property acquisition, which is essential for using such data in standardization when upscaling to a canopy level. Leaf optical properties measured at leaf level can directly enter to radiative transfer models at canopy level and contribute significantly to their parametrization and further to simulation of imaging spectrometer data [50]. The study shows that a direct comparison between the spectra collected with two devices is not advisable as spectrally dependent offsets may likely exist as we demonstrated for the compared devices and device settings. They are caused by the construction of the devices, light sources used, measurement procedures and properties of the measured material, e.g., leaf type and structure. As an implication of our results for remote sensing vegetation studies we can recommend to be very careful with comparisons of laboratory spectral measurements conducted with different devices and under different conditions. The experiments should be documented in detail in order to be repeatable and reproducible, and the same devices should be used in the case of mutual comparison. When using two or more devices a definition of a linear model transforming a spectrum of one device to another one is a solution that decreases the differences. In order to find parameters of such a model, a subset of the samples has to be measured with both devices which in principle corresponds to the approach of introducing an internal standard suggested for soil spectral measurements [26]. Elaboration on procedures that enable to work with spectra on a leaf level acquired with different devices would open a possibility of using various open access spectral databases and spectral libraries as a robust data source for spectroscopy modelling on a leaf level.

Acknowledgments: The study was supported by the Ministry of Education, Youth and Sports of the Czech Republic under projects No. LH 12097 and No. NPUI LO1417. We thank to Drahomíra Bartáková for technical help with biochemical analyses, Miroslav Barták for preparation of the graphics in Figure 1.

Author Contributions: Markéta Potůčková did the core writing of Sections 2.3, 3 and 4, participated at measurements of tobacco optical properties, and contributed to processing, analysis and interpretation of all measurements. Lucie Červená performed all experiments with ASD IS and CP, data processing and analysis, wrote sections concerning materials and instruments. Lucie Kupková did literature review, wrote the introduction and participated at measurements of optical properties of plant materials. Jan Hanuš and Jan Novotný performed all measurements with Lab IS and pre-processed the data. Petr Lukeš considerably contributed to methodology and interpretation of the results. Zuzana Lhotáková contributed to acquirement of the biochemical results and contributed to the interpretation of the results. Jana Albrechtová contributed mainly to the design of the study regarding selection and preparation of plant material, also interpretation of the results and final manuscript editing. All authors contributed to writing and editing of the paper and approved the final manuscript.

Conflicts of Interest: The authors declare no conflict of interest.

References

1. Soukupova, J.; Rock, B.N.; Albrechtova, J. Spectral characteristics of lignin and soluble phenolics in the near infrared—A comparative study. *Int. J. Remote Sens.* **2002**, *23*, 3039–3055. [CrossRef]
2. Malenovský, Z.; Albrechtová, J.; Lhotáková, Z.; Zurita-Milla, R.; Clevers, J.G.P.W.; Schaepman, M.E.; Cudlín, P. Applicability of the PROSPECT model for Norway spruce needles. *Int. J. Remote Sens.* **2006**, *27*, 5315–5340. [CrossRef]
3. Kokaly, R.F.; Asner, G.P.; Ollinger, S.V.; Martin, M.E.; Wessman, C.A. Characterizing canopy biochemistry from imaging spectroscopy and its application to ecosystem studies. *Remote Sens. Environ.* **2009**, *113*, S78–S91. [CrossRef]
4. Lhotáková, Z.; Brodský, L.; Kupková, L.; Kopačková, V.; Potůčková, M.; Mišurec, J.; Klement, A.; Kovářová, M.; Albrechtová, J. Detection of multiple stresses in Scots pine growing at post-mining sites using visible to near-infrared spectroscopy. *Environ. Sci. Process. Impacts* **2013**, *15*, 2004.
5. Yanez-Rausell, L.; Schaepman, M.E.; Clevers, J.G.P.W.; Malenovsky, Z. Minimizing measurement uncertainties of coniferous needle-leaf optical properties, Part I: Methodological review. *IEEE J. Sel. Top. Appl. Earth Obs. Remote Sens.* **2014**, *7*, 399–405. [CrossRef]
6. Medlyn, B.E. Physiological basis of the light use efficiency model. *Tree Physiol.* **1998**, *18*, 167–176. [CrossRef] [PubMed]
7. Cheng, Y.-B.; Middleton, E.M.; Hilker, T.; Coops, N.C.; Black, T.A.; Krishnan, P. Dynamics of spectral bio-indicators and their correlations with light use efficiency using directional observations at a Douglas-fir forest. *Meas. Sci. Technol.* **2009**, *20*, 95107. [CrossRef]
8. Zhang, Y.; Guanter, L.; Berry, J.A.; Joiner, J.; van der Tol, C.; Huete, A.; Gitelson, A.; Voigt, M.; Köhler, P. Estimation of vegetation photosynthetic capacity from space-based measurements of chlorophyll fluorescence for terrestrial biosphere models. *Glob. Change Biol.* **2014**, *20*, 3727–3742. [CrossRef] [PubMed]
9. Xin, Q.; Gong, P.; Li, W. Modeling photosynthesis of discontinuous plant canopies by linking the Geometric Optical Radiative Transfer model with biochemical processes. *Biogeosciences* **2015**, *12*, 3447–3467. [CrossRef]
10. Zhao, F.; Guo, Y.; Huang, Y.; Reddy, K.N.; Lee, M.A.; Fletcher, R.S.; Thomson, S.J. Early detection of crop injury from herbicide glyphosate by leaf biochemical parameter inversion. *Int. J. Appl. Earth Obs. Geoinform.* **2014**, *31*, 78–85. [CrossRef]
11. Malenovský, Z.; Turnbull, J.D.; Lucieer, A.; Robinson, S.A. Antarctic moss stress assessment based on chlorophyll content and leaf density retrieved from imaging spectroscopy data. *New Phytol.* **2015**, *208*, 608–624. [CrossRef] [PubMed]
12. Martinez, N.E.; Sharp, J.L.; Kuhne, W.W.; Johnson, T.E.; Stafford, C.T.; Duff, M.C. Assessing the use of reflectance spectroscopy in determining CsCl stress in the model species *Arabidopsis thaliana*. *Int. J. Remote Sens.* **2015**, *36*, 5887–5915. [CrossRef]
13. Shi, T.; Liu, H.; Wang, J.; Chen, Y.; Fei, T.; Wu, G. Monitoring arsenic contamination in agricultural soils with reflectance spectroscopy of rice plants. *Environ. Sci. Technol.* **2014**, *48*, 6264–6272. [CrossRef] [PubMed]
14. Shi, T.; Liu, H.; Chen, Y.; Wang, J.; Wu, G. Estimation of arsenic in agricultural soils using hyperspectral vegetation indices of rice. *J. Hazard. Mater.* **2016**, *308*, 243–252. [CrossRef] [PubMed]
15. Mesarch, M.A.; Walter-Shea, E.A.; Asner, G.P.; Middleton, E.M.; Chan, S.S. A revised measurement methodology for conifer needles spectral optical properties. *Remote Sens. Environ.* **1999**, *68*, 177–192. [CrossRef]

16. Homolová, L.; Lukeš, P.; Malenovský, Z.; Lhotáková, Z.; Kaplan, V.; Hanuš, J. Measurement methods and variability assessment of the Norway spruce total leaf area: Implications for remote sensing. *Trees* **2013**, *27*, 111–121. [CrossRef]
17. Lukeš, P.; Stenberg, P.; Rautiainen, M.; Mõttus, M.; Vanhatalo, K.M. Optical properties of leaves and needles for boreal tree species in Europe. *Remote Sens. Lett.* **2013**, *4*, 667–676. [CrossRef]
18. Yanez-Rausell, L.; Malenovsky, Z.; Clevers, J.G.P.W.; Schaepman, M.E. Minimizing measurement uncertainties of coniferous needle-leaf optical properties. Part II: Experimental setup and error analysis. *IEEE J. Sel. Top. Appl. Earth Obs. Remote Sens.* **2014**, *7*, 406–420. [CrossRef]
19. Casa, R.; Castaldi, F.; Pascucci, S.; Pignatti, S. Chlorophyll estimation in field crops: An assessment of handheld leaf meters and spectral reflectance measurements. *J. Agric. Sci.* **2015**, *153*, 876–890. [CrossRef]
20. Eitel, J.U.H.; Gessler, P.E.; Smith, A.M.S.; Robberecht, R. Suitability of existing and novel spectral indices to remotely detect water stress in Populus spp. *For. Ecol. Manag.* **2006**, *229*, 170–182. [CrossRef]
21. Kupková, L.; Potůčková, M.; Lhotáková, Z.; Kopačková, V.; Zachová, K.; Albrechtová, J. Chlorophyll Determination in silver birch and scots pine foliage from heavy metal polluted regions using spectral reflectance data. *EARSeL E-Proc.* **2012**, *11*, 64–73.
22. Červená, L.; Lhotáková, Z.; Kupková, L.; Kovářová, M.; Albrechtová, J. Models for estimating leaf pigments and relative water content in three vertical canopy levels of Norway spruce based on laboratory spectroscopy. In *EARSeL 34th Symposium Proceedings*, Proceedings of the 34th EARSeL Symposium 2014, Warsaw, Poland, 16–20 June 2014; Zagajewski, B., Kycko, M., Reuter, R., Eds.; EARSeL and University of Warsaw: Warsaw, Poland, 2014; pp. 6.1–6.8.
23. Potůčková, M.; Červená, L.; Kupková, L.; Lhotáková, Z.; Albrechtová, J. Statistical comparison of spectral and biochemical measurements on an example of Norway spruce stands in the Ore Mountains, Czech Republic. *Geoinform. FCE CTU* **2016**, *15*, 69–83. [CrossRef]
24. Castro-Esau, K.; Sanchez-Azofeifa, G.; Rivard, B. Comparison of spectral indices obtained using multiple spectroradiometers. *Remote Sens. Environ.* **2006**, *103*, 276–288. [CrossRef]
25. Jung, A.; Götze, C.; Cornelia, G. A comparison of four spectrometers and their effect on the similarity of spectral libraries. In Proceedings of the 6th EARSeL Imaging Spectroscopy SIG Workshop, Tel Aviv, Israel, 16–19 March 2009.
26. Kopačková, V.; Ben-Dor, E. Normalizing reflectance from different spectrometers and protocols with an internal soil standard. *Int. J. Remote Sens.* **2016**, *37*, 1276–1290. [CrossRef]
27. Einzmann, K.; Ng, W.-T.; Immitzer, M.; Pinnel, N.; Atzberger, C. Method analysis for collecting and processing in-situ hyperspectral needle reflectance data for monitoring Norway Spruce. *Photogramm. Fernerkund. Geoinform.* **2014**, *2014*, 423–434. [CrossRef]
28. Mišurec, J.; Kopačková, V.; Lhotáková, Z.; Campbell, P.; Albrechtová, J. Detection of spatio-temporal changes of norway spruce forest stands in ore mountains using landsat time series and airborne hyperspectral imagery. *Remote Sens.* **2016**, *8*, 92. [CrossRef]
29. Porra, R.J.; Thompson, W.A.; Kriedemann, P.E. Determination of accurate extinction coefficients and simultaneous equations for assaying chlorophylls a and b extracted with four different solvents: Verification of the concentration of chlorophyll standards by atomic absorption spectroscopy. *Biochim. Biophys. Acta BBA Bioenerg.* **1989**, *975*, 384–394. [CrossRef]
30. Wellburn, A.R. The spectral determination of chlorophylls a and b, as well as total carotenoids, using various solvents with spectrophotometers of different resolution. *J. Plant Physiol.* **1994**, *144*, 307–313. [CrossRef]
31. ASD Inc. *Integrating Sphere User Manual*; Analytical Spectral Devices, Inc.: Boulder, CO, USA, 2008.
32. FieldSpec 4 Wide-Res Field Spectroradiometer. Available online: http://www.asdi.com/products-and-services/fieldspec-spectroradiometers/fieldspec-4-wide-res (accessed 18 October 2016).
33. Daughtry, C.S.T.; Biehl, L.L.; Ranson, K.J. A new technique to measure the spectral properties of conifer needles. *Remote Sens. Environ.* **1989**, *27*, 81–91. [CrossRef]
34. Main, R.; Cho, M.A.; Mathieu, R.; O'Kennedy, M.M.; Ramoelo, A.; Koch, S. An investigation into robust spectral indices for leaf chlorophyll estimation. *ISPRS J. Photogramm. Remote Sens.* **2011**, *66*, 751–761. [CrossRef]
35. Le Maire, G.; François, C.; Dufrêne, E. Towards universal broad leaf chlorophyll indices using PROSPECT simulated database and hyperspectral reflectance measurements. *Remote Sens. Environ.* **2004**, *89*, 1–28. [CrossRef]

36. Hernández-Clemente, R.; Navarro-Cerrillo, R.M.; Zarco-Tejada, P.J. Carotenoid content estimation in a heterogeneous conifer forest using narrow-band indices and PROSPECT+DART simulations. *Remote Sens. Environ.* **2012**, *127*, 298–315. [CrossRef]
37. Yi, Q.; Jiapaer, G.; Chen, J.; Bao, A.; Wang, F. Different units of measurement of carotenoids estimation in cotton using hyperspectral indices and partial least square regression. *ISPRS J. Photogramm. Remote Sens.* **2014**, *91*, 72–84. [CrossRef]
38. *Hyperspectral Remote Sensing of Vegetation*; Thenkabail, P.S.; Lyon, J.G.; Huete, A., Eds.; CRC Press: Boca Raton, FL, USA, 2012.
39. Wu, C.; Niu, Z.; Tang, Q.; Huang, W. Estimating chlorophyll content from hyperspectral vegetation indices: Modeling and validation. *Agric. For. Meteorol.* **2008**, *148*, 1230–1241. [CrossRef]
40. Gitelson, A.A.; Zur, Y.; Chivkunova, O.B.; Merzlyak, M.N. Assessing carotenoid content in plant leaves with reflectance spectroscopy. *Photochem. Photobiol.* **2002**, *75*, 272–281. [CrossRef]
41. Gitelson, A.A.; Keydan, G.P.; Merzlyak, M.N. Three-band model for noninvasive estimation of chlorophyll, carotenoids, and anthocyanin contents in higher plant leaves. *Geophys. Res. Lett.* **2006**, *33*, L11402. [CrossRef]
42. Hunt, E.; Rock, B. Detection of changes in leaf water content using Near- and Middle-Infrared reflectances. *Remote Sens. Environ.* **1989**, *30*, 43–54.
43. Haboudane, D.; Miller, J.R.; Pattey, E.; Zarco-Tejada, P.J.; Strachan, I.B. Hyperspectral vegetation indices and novel algorithms for predicting green LAI of crop canopies: Modeling and validation in the context of precision agriculture. *Remote Sens. Environ.* **2004**, *90*, 337–352. [CrossRef]
44. Gao, B. NDWI—A normalized difference water index for remote sensing of vegetation liquid water from space. *Remote Sens. Environ.* **1996**, *58*, 257–266. [CrossRef]
45. ASD Inc. *Technical Guide*, 3rd ed.; Analytical Spectral Devices, Inc.: Boulder, CO, USA, 1999.
46. Rautiainen, M.; Mõttus, M.; Yáñez-Rausell, L.; Homolová, L.; Malenovský, Z.; Schaepman, M.E. A note on upscaling coniferous needle spectra to shoot spectral albedo. *Remote Sens. Environ.* **2012**, *117*, 469–474. [CrossRef]
47. Kindel, B.C.; Qu, Z.; Goetz, A.F.H. Direct solar spectral irradiance and transmittance measurements from 350 to 2500 nm. *Appl. Opt.* **2001**, *40*, 3483. [CrossRef] [PubMed]
48. Savitzky, A.; Golay, M.J.E. Smoothing and differentiation of data by simplified least squares procedures. *Anal. Chem.* **1964**, *36*, 1627–1639. [CrossRef]
49. Steinier, J.; Termonia, Y.; Deltour, J. Smoothing and differentiation of data by simplified least square procedure. *Anal. Chem.* **1972**, *44*, 1906–1909. [CrossRef] [PubMed]
50. Schneider, F.D.; Leiterer, R.; Morsdorf, F.; Gastellu-Etchegorry, J.-P.; Lauret, N.; Pfeifer, N.; Schaepman, M.E. Simulating imaging spectrometer data: 3D forest modeling based on LiDAR and in situ data. *Remote Sens. Environ.* **2014**, *152*, 235–250. [CrossRef]

Paper 4: "MODELS FOR ESTIMATING LEAF PIGMENTS AND RELATIVE WATER CONTENT IN THREE VERTICAL CANOPY LEVELS OF NORWAY SPRUCE BASED ON LABORATORY SPECTROSCOPY"

Červená, Lucie, Zuzana Lhotáková, Lucie Kupková, Monika Kovářová, a Jana Albrechtová. 2014. „Models for estimating leaf pigments and relative water content in three vertical canopy levels of Norway spruce based on laboratory spectroscopy". In *EARSeL 34th Symposium Proceedings*, editoval Bogdan Zagajewski, Marlena Kycko, a Rainer Reuter, 6.1-6.8. Warsaw, Poland: EARSeL and University of Warsaw. https://doi.org/0.12760/03-2014-11.

Author Contributions:

LČ – 40%, ZL – 24%, LK – 13%, MK – 5%, JA – 18%

EARSeL 34th Symposium Proceedings, 16-20 June 2014 6.1

Models for estimating leaf pigments and relative water content in three vertical canopy levels of norway spruce based on laboratory spectroscopy

Lucie Cervena[1], Zuzana Lhotakova[2], Lucie Kupkova[1], Monika Kovarova[2] and Jana Albrechtova[2]

[1] Charles University in Prague, Faculty of Science, Department of Applied Geoinformatics and Cartography, Prague, Czech Republic; lucie.cervena@natur.cuni.cz, lucie.kupkova@gmail.com
[2] Charles University in Prague, Faculty of Science, Department of Experimental Plant Biology, Prague, Czech Republic; zuzana.lhotakova@natur.cuni.cz, monika.kovarova@natur.cuni.cz, jana.albrechtova@natur.cuni.cz

Abstract. Unique set of data was obtained during the field campaign in the Krušné hory Mts. (the western part of the Czech Republic) in August 2013. From fifty five representative 80-year-old trees of Norway Spruce (Picea abies L. Karst.) equally distributed on eleven study sites, branches were taken in three vertical canopy levels (sunlit productive upper and lower parts of a tree crown, shaded saturated part of a tree crown) and first three needle age classes were analysed. Spectral reflectance of these spruce foliage samples was measured in the range between 350 and 2,500 nm using an ASD FieldSpec 4 Wide-Res spectrometer in combination with the fibre optic contact probe. Some samples were also measured in the integrating sphere. Photosynthetic pigment (total chlorophylls, total carotenoids) contents and relative water content were determined in laboratory for all samples. The results of analysis of variance (ANOVA) show that the contents of pigments and relative water content are significantly different not only between the needle age classes (what is widely known) but also in the vertical canopy levels. There are only few studies dealing with vertical heterogeneity in Norway spruce canopy. Thus, the main goal of this study is to build and compare the statistically based prediction models for photosynthetic pigments and water content estimation for three vertical canopy levels of Norway Spruce. These results in classifications of biochemical and biophysical properties of Norway Spruce stands using hyperspectral remote sensing data.

Keywords. Norway Spruce, laboratory spectroscopy, Krusne hory Mts., RWC, Chlorophyll, Carotenoids.

1. Introduction

Remotely sensed leaf biochemical and biophysical properties can be used for large-scale spatial and temporal monitoring of vegetation physiological status or ecosystem functioning. For airborne hyperspectral data interpretation or modelling of reflectance at canopy level several foliar properties play minor role (e.g. internal leaf structure). However, leaf clumping, proportion of woody constituents or vertical gradients in biochemical and biophysical leaf traits may influence radiative transfer modelling at the canopy level.

Leaf biochemical composition affects foliar optical properties and can be retrieved from continuous spectral data [1], [2]. There are two modelling approaches to link content of biochemical compounds or biophysical parameters of vegetation to spectra – empirical (different regressions, e.g. [1]) and physical (radiative transfer models, e.g [3]). The main advantage of the empirical

 ISBN 978-83-63245-65-8, DOI: 10.12760/03-2014-11, Zagajewski B., Kycko M., Reuter R. (eds.)

models is their simplicity. The physical models are more precise but need more complex input information – e.g. PROSPECT needs at least four input parameters: leaf mesophyll structure parameter N, chlorophyll concentration C_{ab}, water depth C_w, and the dry matter concentration C_m [4], LIBERTY needs nine parameters (Average Cell Diameter, Intercellular Air Space, Baseline Absorption, Albino Absorption, Needle Thickness and concentrations of Chlorophyll, Water, Lignin/Cellulose and Nitrogen [5].They usually require also a long computation time.

In mature tree canopies the vertical gradient of irradiance is the key factor, which determines leaf structure, biochemical composition and rate of physiological processes such as light harvesting and photosynthesis [6]. In terms of light-dependent leaf traits several studies were conducted with focus on leaf physiological functions or morphology (e.g. [7], [8]), but only few dealt with leaf optical properties along the vertical profile of the canopy (e.g. [9]). Wang and Li [9] showed that vertical variations in leaf biophysical and biochemical traits such as chlorophyll, water or dry mass content, significantly influence optical properties at the canopy level. Thus considering several vertical canopy layers consisting of leaves with different optical properties could be crucial for reflectance simulations and modelling at canopy level. Effect of vertical heterogeneity [9] and leaf clumping [10] on canopy optical properties and their modelling was studied as far for broadleaved trees and the information about conifer foliage is lacking.

Thus, the objectives of this study are: 1) to construct the prediction empirical models for photosynthetic pigments and water content based on laboratory spectroscopy for the three vertical canopy levels of Norway Spruce on the leaf level; 2) to compare the models for the individual canopy levels among them and with the model based on data from all levels.

2. Methods

2.1. Study area

The study area is located in the Western part of the Czech Republic in the Krušné hory Mts. Two localities situated about 50 km apart with different impact of the acidic deposition during 1970's and 1980's were selected. While trees in Přebuz (western part of the mountains) were healthy or just slightly damaged, trees in Kovářská (eastern part of the mountains) were heavily affected and still exhibited visible damage symptoms in 1990's [11]. In 2013 the sampled trees on both localities already did not show any visible damage symptoms.

2.2. Field campaign

The field campaigne was conducted within the period 22-25 August 201. On each locality six (Přebuz) resp. five (Kovářská) sites of even-aged forest stands older than 80 years were selected for further evaluation. From five representative trees per site branches were taken in three vertical canopy levels (sunlit productive upper and lower parts of a tree crown, shaded saturated part of a tree crown) and first three needle age classes were analysed (Figure 1). The content of photosynthetic pigments (total chlorophylls, total carotenoids) was determined using dimethylformamide extractions according to Porra [12], followed by spectrophotometric detection and calculations according to Welburn [13]. The pigment concentrations were expressed as weight of pigment per gram of needle dry mass (mg/g). The relative water content (RWC) was determined as the percentage of water in the fresh needles.

Simultaneously with the needle sampling the spectral reflectance of spruce foliage was measured in the range between 350 and 2,500 nm using an ASD FieldSpec 4 Wide-Res spectrometer in combination with the fibre optic contact probe. The radiance spectra were normalized against a 99% Spectralon white reference to produce relative reflectance spectra for each measurement. Shoots consisting of only one age class were arranged in the same direction to create a consistent layer to fill in the field of view (spot size 10 mm) of the contact probe. Shoots were placed on a

 ISBN 978-83-63245-65-8, DOI: 10.12760/03-2014-11,
Zagajewski B., Kycko M., Reuter R. (eds.)

spectrally black surface to minimize the background spectral noise or radiation transmitted through the needles. The scan average on the spectroradiometer was set to 50 to improve the signal to noise ratio. Five independent spectra were taken on different parts of one sample and afterwards median spectrum was calculated (together 495 median spectra: 11 sites x 5 trees x 3 vertical canopy levels x 3 needle age classes). Due to the noise in the spectra in the 350 - 450 nm regions, this interval was excluded from further analyses.

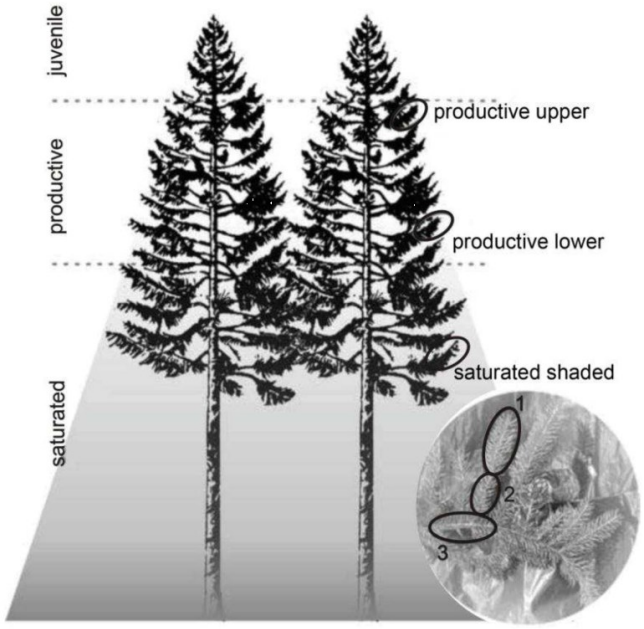

Figure 1: Sampling scheme (adapted after Kopackova 2014 [14]).

2.3. Data processing

Firstly, hierarchical analysis of variance was performed. The aim of this method was to find out if there are significant differences in pigments (chlorophylls and carotenoids) contents and relative water contents between the studied localities, vertical canopy levels and needle age classes. Significant differences were proven between all the mentioned factors. Differences in pigments and relative water content between the localities were expected due to the different impact of pollution in these areas in the past, differences between the needle age classes are widely known [15], [16]. The differences in studied needle parameters between the vertical canopy levels reflected the light availability within the canopy and their relationships with needle optical properties will be further evaluated in this study. Obvious differences can be also seen in the averaged spectra, particularly in the NIR spectral region (Figure 2).

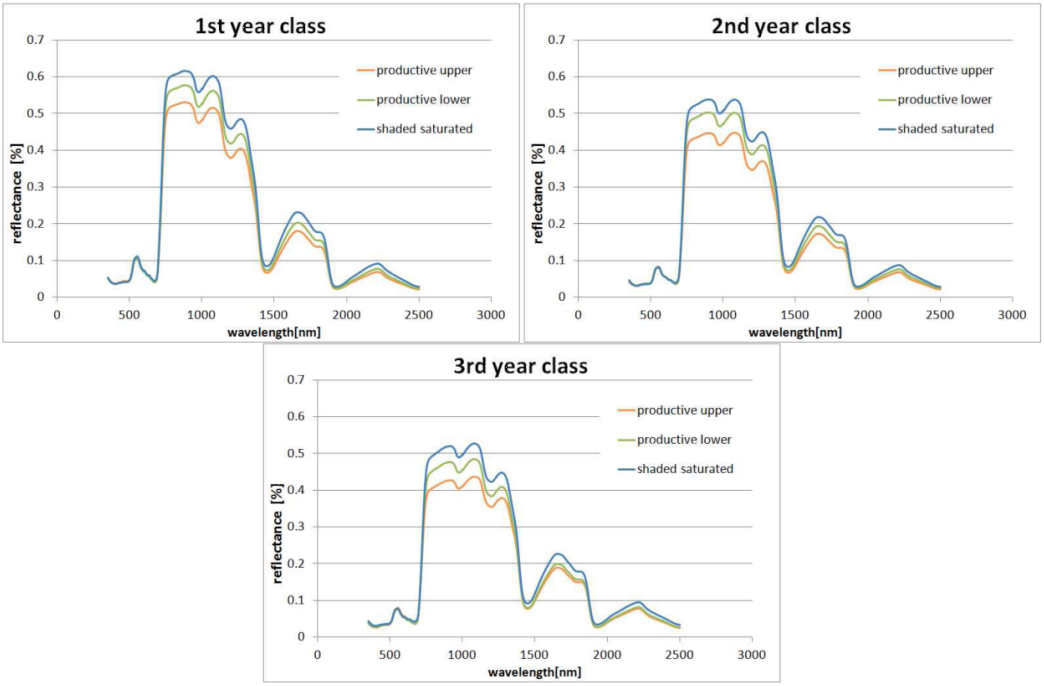

Figure 2: Averaged reflectance spectra for needle age classes (1st, 2nd and 3rd) and three vertical canopy levels (productive upper, productive lower and shaded saturated); n = 55 for each group.

Secondly, selected spectral indices were calculated from the measured spectra: $NDVI_{705}$ [17], $mNDVI_{705}$ [18], MCARI [19], TCARI/OSAVI [20], TVI [21] and $ANMB_{650-725}$ [22] for correlations with total chlorophyll contents; CRI550, CRI700, RNIR*CRI550, RNIR*CRI700 [23], [24] for correlations with total carotenoids contents and water index (WI) [25] and normalize difference water index (NDWI) [26] for correlations with RWC. Also partial least square regressions (PLSR) using all the reflectance values and continuum removed (CR) values in range 450 – 2500 nm for estimation of RWC and pigments were performed. The regression models were built not only for all the data together but also for separate datasets containing data from only one canopy vertical level. The models were always trained on 4/5th of the dataset; data from one tree per site were used for the models validations. The models were evaluated using Coefficients of Determination (R^2) and Root Mean Square Errors (RMSE). All the calculations were performed in R software with pls package with help of Microsoft Excel 2007.

3. Results

Table 1 presents averages and standard deviations for the pigments and relative water contents in the different vertical levels of the tree crown. It can be seen that the averaged contents of pigments and water are slightly lowering with the higher position in the tree crown.

© EARSeL and University of Warsaw, 2014, ISBN 978-83-63245-65-8, DOI: 10.12760/03-2014-11, Zagajewski B., Kycko M., Reuter R. (eds.)

Table 1. Descriptive statistics for the datasets for leaf biochemical and biophysical properties

Part of the crown	shaded saturated		productive lower		productive upper		all data	
descriptive statistics	average	st.d.	average	st.d.	average	st.d.	average	st.d.
Total Chlorophyll (mg/g d.m.)	3.44	0.62	3.10	0.66	2.76	0.55	3.09	0.66
Total Carotenoids (mg/g d.m.)	0.44	0.07	0.41	0.08	0.37	0.07	0.41	0.08
Relative Water Content (%)	57.91	2.76	56.26	3.13	55.46	3.12	56.53	3.17

Results of all the computed statistical models are presented in Table 2. The best results were generally achieved by the PLSR method with coefficient of determination at least 0.61 (number of components used is presented in the brackets for each PLSR model in Table 2). By the simple regressions with the indices, the best results were obtained for estimations of total chlorophyll content using TCARI, for total carotenoids content CRI_{700} and for relative water content WI. On the other hand, the poorest results were achieved using indices $NDVI_{705}$, $mNDVI_{705}$, $ANMB_{650-725}$ (total chlorophyll) and $RNIR*CRI_{550}$, $RNIR*CRI_{700}$ (total carotenoids).

Looking at the position of studied needles in the tree crown, generally the most accurate models were achieved for the shaded saturated part and the worst for sunlit productive upper part. The accuracies of the models constructed based on all data were mostly similar (based on R^2) to the models based on the data from productive lower part of the tree crown. However, for the RWC estimations by linear regressions with the indices the models based on all data were the poorest ones and the best results were achieved for the data from productive upper part of the tree crown.

Table 2. Results of all the regression models between the spectra and biochemical and biophysical parameters (R^2 – coefficient of determination, number in the brackets – number of components considered in the PLSR model, RMSE – root mean square error; p-values for all the models were lower than 0.01.)

Part of the crown	shaded saturated		productive lower		productive upper		all data	
Total Chlorophyll (mg/g)								
statistical model	R^2	RMSE	R^2	RMSE	R^2	RMSE	R^2	RMSE
MCARI	0.6197	0.46	0.4956	0.41	0.269	0.45	0.4692	0.49
TCARI	0.7107	0.38	0.5792	0.33	0.3237	0.42	0.5585	0.42
TCARI/OSAVI	0.7228	0.38	0.5588	0.31	0.294	0.42	0.5482	0.41
TVI	0.5553	0.48	0.5516	0.46	0.2541	0.44	0.4673	0.51
PLSR (450-2,500 nm)	(6) 0.7763	0.33	(6) 0.6811	0.31	(6) 0.6477	0.35	(5) 0.7157	0.33
PLSR (450-2,500) - CR	(5) 0.7758	0.33	(4) 0.6402	0.34	(4) 0.6159	0.34	(4) 0.6952	0.35
Total Carotenoids (mg/g)								
statistical model	R^2	RMSE	R^2	RMSE	R^2	RMSE	R^2	RMSE
CRI550	0.1211	0.07	0.1538	0.07	0.1209	0.06	0.1267	0.07

© EARSeL and University of Warsaw, 2014, ISBN 978-83-63245-65-8, DOI: 10.12760/03-2014-11, Zagajewski B., Kycko M., Reuter R. (eds.)

CRI700	0.2014	0.06	0.2724	0.06	0.2080	0.05	0.2367	0.06
PLSR (450-2,500 nm)	(6) 0.7737	0.04	(7) 0.7170	0.04	(5) 0.6917	0.04	(7) 0.7198	0.04
PLSR (450-2,500) - CR	(5) 0.7790	0.04	(5) 0.6928	0.04	(5) 0.689	0.04	(5) 0.7024	0.04
Relative Water Content (%)								
statistical model	R^2	RMSE	R^2	RMSE	R^2	RMSE	R^2	RMSE
WI	0.5014	1.72	0.5934	2.17	0.6223	2.05	0.491	2.23
NDWI	0.4817	1.95	0.5701	2.24	0.6126	2.13	0.4759	2.36
PLSR (450-2,500 nm)	(8) 0.7831	1.46	(8) 0.8027	1.95	(8) 0.7790	1.88	(8) 0.7667	1.58
PLSR (450-2,500) - CR	(7) 0.7610	1.70	(8) 0.8248	2.13	(6) 0.7344	1.80	(8) 0.7705	1.60

4. Conclusions

The best prediction models for estimating the contents of leaf pigments and relative water content were achieved by the PLSR method (as in e.g. [27]). The simple linear regressions with the indices did not work very well, although they are often used [17] – [26]. The R^2 values for simple regressions with chlorophyll content reached in this study for shaded canopy part were comparable with values presented by Croft et al. 2014 [28] (R^2 = 0.61- 0.59) on needles of *Picea mariana* using wide range of different indices. Poor CRI550 and CRI700 performance for prediction of carotenoids content is rather surprising as these indices have already been successfully applied on conifers (*Pinus sylvestris*, R^2 = 0.72 and 0.73 respectively) [29]. The best models using the indices were achieved for the datasets coming from the shaded saturated part of the tree crown. In contrary; the worst results were achieved for the sunlit productive upper part of the tree crown. This could be caused by the more complex shoot architecture occupying larger spatial fraction in this part of the crown. The needles from this part of the tree crown were often very short and/or very tough, perpendicular to the shoot, which may affect resulting spectra by additional scattering. Whether this is the main reason for less accurate models for the sunlit upper part of the Norway spruce crown could be tested in the future by another method of measurements – e.g. acquiring the spectra in the integrating sphere.

Croft et al. 2014 [28] also discussed that generally poorer performance of chlorophyll indices on conifers in comparison to broadleaved species is based on higher complexity of a coniferous shoots and in technical difficulties of reflectance measurements on needles even if an integration sphere is used. The highest R^2 values for regressions of indices with water content (0.57 and above) are similar with results achieved by Stimson et al. 2005 [30] on *Pinus edulis*. However, the different influence of the vertical canopy level on the performance of pigment- and water-related vegetation indices should be taken into account if dealing with multiple layer canopy data.

The PLSR showed the best model performance for all studied biochemical and biophysical needle parameters and also the variability in RMSE between three vertical canopy levels was lower than RMSE achieved with vegetation indices. We conclude that simple regressions using vegetation indices for prediction of needle biochemical and biophysical properties are more prone to be species- or structure-dependent and may cause bias if dealing with spectral data from multiple vertical levels within a coniferous canopy. We suggest that the light-driven vertical heterogeneity in biochemical and biophysical foliage properties should be taken in account when dealing with using field ground truth data for interpretation of airborne spectral data.

 ISBN 978-83-63245-65-8, DOI: 10.12760/03-2014-11, Zagajewski B., Kycko M., Reuter R. (eds.)

Acknowledgements

The support of the Ministry of Education of the Czech Republic is acknowledged: LH12097. Thanks belong to Drahomira Bartakov and Monika Kovarova for laboratory analyses and students who helped with needle sampling and spectral measurements. Thanks to Dr. Karel Zvara for consulting statistical analysis.

References

[1] Soukupova J, M Cvikrova, J Albrechtova, B N Rock & J Eder, 2000. *Histochemical and biochemical approaches to the study of phenolic compounds and per-oxidases in needles of Norway spruce (Picea abies).* New Phytologist, 146 (3): 403-414.

[2] Misurec J, V Kopackova, Z Lhotakova, J Hanus, J Weyermann, P Entcheva-Campbell & J Albrechtova, 2012. *Utilization of hyperspectral image optical indices to assess the Norway spruce forest health status*. Journal of Applied Remote Sensing, 6: 063545-1 - 063545-25.

[3] Malenovsky Z, J Albrechtova, Z Lhotakova, R Zurita-Milla, J Clevers, M E Schaepman, & P Cudlin, 2006. *Applicability of the PROSPECT model for Norway spruce needles.* International Journal of Remote Sensing, 27: 5315-5340.

[4] Jacquemoud S & F Baret, 1990. *PROSPECT – A Model of Leaf Optical Properties Spectra*. Remote Sensing of Environment, 34 (2): 75 – 91.

[5] Dawson T P, P J Curran & S E Plummer, 1998. *LIBERTY–Modeling the effects of leaf biochemical concentration on reflectance spectra.* Remote Sensing of Environment, 65(1): 50–60.

[6] Niinemets Ü, 2010. *A review of light interception in plant stands from leaf to canopy in different plant functional types and in species with varying shade tolerance*. Ecological Research, 25: 693–714.

[7] Niinemets Ü, A Lukjanova, M H Turnbull & A D Sparrow, 2007. *Plasticity in mesophyll volume fraction modulates light-acclimation in needle photosynthesis in two pines.* Tree Physiology, 27: 1137–1151.

[8] Homolova L, P Lukes, Z Malenovsky, Z Lhotakova, V Kaplan & J Hanus, 2013. *Measurement methods and variability assessment of the Norway spruce total leaf area: implications for remote sensing*. Trees-Structure and Function, 27 (1): 111-121.

[9] Wang Q & P Li, 2013. *Canopy vertical heterogeneity plays a critical role in reflectance simulation*. Agricultural and Forest Meteorology, 169: 111– 121.

[10] Widlowski J-L, J-F Côté & M Béland, 2014. *Abstract tree crowns in 3D radiative transfer models: Impact on simulated open-canopy reflectances.* Remote Sensing of Environment 142: 155–175.

[11] Entcheva-Campbell P K, B N Rock, M E Martin, C D Neefus, J R Irons, E M Middleton & J Albrechtova, 2004. *Detection of initial damage in Norway spruce canopies using hyperspectral airborne data*. International Journal of Remote Sensing, 25: 5557-5583.

[12] Porra R J, W A Thompson & P E Kriedemann, 1989. *Determination of Accurate Extinction Coefficients and Simultaneous Equations for Assaying Chlorophyll-A and Chlorophyll-B Extracted with 4 Different Solvents – Verification of the Concentration of Chlorophyll Standards by Atomic-Absorption Spectroscopy*. Biochimica et Biophysica Acta, 975: 384-394.

[13] Wellburn A R, 1994. *The spectral determination of Chlorophyll-A and Chlorophyll-B, as well as total Carotenoids, using various solvents with spectrophotometers of different resolution*. Journal of Plant Physiology, 144: 307-313.

[14] Kopackova V, J Misurec, Z Lhotakova, F Oulehle & J Albrechtova, 2014. *Using multi-date high spectral resolution data to assess the physiological status of macroscopically undamaged foliage on a regional scale*. International Journal of Applied Earth Observation and Geoinformation, 27: 169–186.

 ISBN 978-83-63245-65-8, DOI: 10.12760/03-2014-11, Zagajewski B., Kycko M., Reuter R. (eds.)

[15] Soukupová J, B N Rock & J Albrechtová, 2001. *Comparative study of two spruce spieces in a polluted mountainous region*. New Phytologist, 150: 133–45.
[16] Lhotakova Z, J Albrechtova, Z Malenovsky, B N Rock, T Polak & P Cudlin, 2007. *Does the azimuth orientation of Norway spruce (Picea abies/L./Karst.) branches within sunlit crown part influence the heterogeneity of biochemical, structural and spectral characteristics of needles?* Environmental and Experimental Botany, 59: 283-292.
[17] Datt B, 1999. *A New Reflectance Index for Remote Sensing of Chlorophyll Content in Higher Plants: Test Using Eucalyptus Leaves.* Journal of Plant Physiology, 154: 30 - 36.
[18] Sims D A & J A Gamon, 2002. *Relationships between leaf pigment content and spectral reflectance across a wide range of species, leaf structures and developmental stages*. Remote Sensing of Environment, 81: 337-354
[19] Daughtry C S T, C L Walthall, M S Kim, E Brown De Colstoun & J E McMurtreyll, 2000. *Estimating corn leaf chlorophyll concentration from leaf and canopy reflectance*. Remote Sensing of Environment, 74: 229-239.
[20] Haboudane D, 2002. *Integrated narrow-band vegetation indices for prediction of crop Chlorophyll content for application to precision agriculture*. Remote Sensing of Environment, 81: 416-426.
[21] Broge N & E Leblanc, 2000. *Comparing prediction power and stability of broadband and hyperspectral vegetation indices for estimation of green leaf area index and canopy chlorophyll density*. Remote sensing of Environment, 76: 156-172.
[22] Malenovský Z, C Ufer, Z Lhotakova, J G P W Clevers, M E Schaepman, J Albrechtova & P Cudlin, 2006. *A new hyperspectral index for chlorophyll estimation of forrest canopy: Area under curve normalized to maximal band dept between 650-725 nm*. EARSeL Symposium Proceedings, 2006, 161-172.
[23] Gitelson A A, U Gritz & M N Merzlyak, 2003. *Relationships between leaf chlorophyll content and spectral reflectance and algorithms for nondestructive chlorophyll assessment in higher plant leaves*. Journal of Plant Physiology, 160: 271–282.
[24] Gitelson A A, G P Keydan & M N Merzlyak, 2006. *Three-band model for noninvasive estimation of chlorophyll, carotenoids and anthocyanin content in higher plant leaves*. Geophysical Research Letters, 33: L11402.
[25] Penuelas J, J Pinol, R Ogaya, & I Filella, 1997. *Estimation of plant water concentration by the reflectance water index WI (R900/R970)*. International Journal of Remote Sensing, 18: 2869-2875.
[26] Gao B C, 1996. *NDWI - A normalized difference water index for remote sensing of vegetation liquid water from space*. Remote Sensing of Environment, 58: 257-266.
[27] Atzbergera C, M Guérifb, F Baretb & W Wernerc, 2010. *Comparative analysis of three chemometric techniques for the spectroradiometric assessment of canopy chlorophyll content in winter wheat*. Computers and Electronics in Agriculture, 73: 165-173.
[28] Croft H, J M Chen & Y Zhang, 2014. *The applicability of empirical vegetation indices for determining leaf chlorophyll content over different leaf and canopy structures*. Ecological Complexity, 17: 119-130.
[29] Hernández-Clemente R, R M Navarro-Cerrillo, L Suárez, F Morales & P J Zarco-Tejada, 2011. *Assessing structural effects on PRI for stress detection in conifer forests*. Remote Sensing of Environment 115: 2360–2375.
[30] Stimson H C, D D Breshears, S L Ustin & S C Kefauver, 2005. *Spectral sensing of foliar water conditions in two co-occurring conifer species: Pinus edulis and Juniperus monosperma*. Remote Sensing of Environment 96: 108-118.

 ISBN 978-83-63245-65-8, DOI: 10.12760/03-2014-11, Zagajewski B., Kycko M., Reuter R. (eds.)

5 Relict arctic-alpine tundra ecosystem

This chapter consists of three publications (two peer-reviewed papers and one shorter peer-reviewed conference paper) focused on remote sensing image data and field spectroscopy for the unique area of relict arctic-alpine tundra ecosystem evaluation.

Paper 5: Suchá, Renáta, Lucie Jakešová, Lucie Kupková, a **Lucie Červená**. 2016. „Classification of Vegetation above the Tree Line in the Krkonoše Mts. National Park Using Remote Sensing Multispectral Data". *AUC GEOGRAPHICA* 51 (1): 113–29. https://doi.org/10.14712/23361980.2016.10.

Paper 6: Kupková, Lucie, **Lucie Červená**, Renáta Suchá, Lucie Jakešová, Bogdan Zagajewski, Stanislav Březina, a Jana Albrechtová. 2017. „Classification of Tundra Vegetation in the Krkonoše Mts. National Park Using APEX, AISA Dual and Sentinel-2A Data". *European Journal of Remote Sensing* 50 (1): 29–46. https://doi.org/10.1080/22797254.2017.1274573.

Paper 7: **Červená, Lucie**, Lucie Kupková, a Renáta Suchá. 2016. „Field Spectroscopy for Vegetation Evaluation along the Nutrient and Elevation Gradient above the Tree Line in the Krkonoše Mountains National Park." *ISPRS - International Archives of the Photogrammetry, Remote Sensing and Spatial Information Sciences* XLI-B6 (červen): 211–14. https://doi.org/10.5194/isprs-archives-XLI-B6-211-2016.

Paper 5: "CLASSIFICATION OF VEGETATION ABOVE THE TREE LINE IN THE KRKONOŠE MTS. NATIONAL PARK USING REMOTE SENSING MULTISPECTRAL DATA"

Suchá, Renáta, Lucie Jakešová, Lucie Kupková, a Lucie Červená. 2016. „Classification of Vegetation above the Tree Line in the Krkonoše Mts. National Park Using Remote Sensing Multispectral Data". *AUC GEOGRAPHICA* 51 (1): 113–29. https://doi.org/10.14712/23361980.2016.10.

Author Contributions:

RS – 30%, LJ – 12%, LK – 29%, **LČ – 29%**

AUC Geographica 113

CLASSIFICATION OF VEGETATION ABOVE THE TREE LINE IN THE KRKONOŠE MTS. NATIONAL PARK USING REMOTE SENSING MULTISPECTRAL DATA

RENÁTA SUCHÁ, LUCIE JAKEŠOVÁ, LUCIE KUPKOVÁ, LUCIE ČERVENÁ

Charles University, Faculty of Science, Department of Applied Geoinformatics and Cartography, Prague, Czech Republic

ABSTRACT

This paper compares suitability of multispectral data with different spatial and spectral resolutions for classifications of vegetation above the tree line in the Krkonoše Mts. National Park. Two legends were proposed: the detailed one with twelve classes, and simplified legend with eight classes. Aerial orthorectified images (orthoimages) with very high spatial resolution (12.5 cm) and four spectral bands have been examined using the object based classification. Satellite data WorldView-2 (WV-2) with high spatial resolution (2 metres) and eight spectral bands have been examined using object based classification and per-pixel classification. Per-pixel classification has been applied also to the freely available Landsat 8 data (spatial resolution 30 metres, seven spectral bands). Of the algorithms for per-pixel classification, the following classifiers were compared: maximum likelihood classification (MLC), support vector machine (SVM), and neural net (NN). The object based classification utilized the example-based approach and SVM algorithm (all available in ENVI 5.2). Both legends (simplified and detailed ones) show best results in the case of orthoimages (overall accuracy 83.56% and 71.96% respectively, Kappa coefficient 0.8 and 0.65 respectively). The WV-2 classification brought best results using the object based approach and simplified legend (68.4%); in the case of per-pixel classification it was the SVM method (RBF) and detailed legend (60.82%). Landsat data were best classified using the MLC (78.31%). Our research confirmed that Landsat data are sufficient to get a general overview of basic land cover classes above the tree line in the Krkonoše Mts. National Park. Based on the comparison of the data with different spectral and spatial resolution we can however conclude that very high spatial resolution is the decisive feature that is essential to reach high overall classification accuracy in the detailed level.

Keywords: vegetation above the tree line, Krkonoše Mountains, object based classification, per-pixel classification, multispectral data

Received 12 October 2015; Accepted 25 November 2015

1. Introduction

The Krkonoše Mountains is a mountain range with a fragmented alpine zone that occupies a narrow span of elevations and has developed into two separated areas. The highest parts of the Krkonoše Mts. National Park (KRNAP) rise above the tree line and are covered by relict tundra. These areas are included in the international tundra monitoring program (INTERACT: International Network for Terrestrial Research and Monitoring in the Arctic) (Soukupová et al. 1995; Jeník and Štursa 2003).

For vegetation mapping and related analyses in large, isolated areas that often receive legal protection, such as tundra, remote sensing methods are commonly used. Data with various spatial and spectral resolutions are analysed using different methods of per-pixel and object based classification.

Regarding the vegetation classification above the tree line, Král (2009) classified the orthoimages with infrared band with spatial resolution 0.9 metres using the maximum likelihood algorithm in Jeseníky Mountains. Král (2009) especially focused on transitional zones between subalpine forests and alpine tundra. In this way, he defined seven land cover classes: anthropogenic areas, pastures and barren land, *Pinus mugo* scrub, deciduous trees, spruce cultures, dry spruce stands, and rocks. The overall accuracy equalled 78%.

Orthoimages were also examined by Müllerová (2005) who studied the tundra vegetation in the Krkonoše Mts. National Park. Having used multispectral aerial data and the maximum likelihood method, she defined seven classes: *Pinus mugo* scrub, *Nardus stricta* stands, subalpine tall grasslands and tall-herb vegetation, vegetation along roads, roads, water areas, and wetlands. The overall accuracy equalled 79%. The use of unsupervised classification (ISODATA method) brought overall accuracy of 63% and six classes were identified.

Zagajewski et al. (2005) conducted mapping in the eastern part of the Tatra National Park, Poland. They focused on the mountain vegetation of subalpine, alpine, and sub-nival zones utilizing hyperspectral data and maximum likelihood and neural net methods. Hyperspectral aerial images were acquired by DAIS 7915 and by ROSIS sensors. Based on unsupervised classification and visual interpretation of the images, seven classes for supervised classification were defined: *Pinus mugo* scrub, forests, meadows, rocks, lakes, shadows, and roads. Overall accuracy reached 71–85%. Hyperspectral data were used also by Marcinkowska et al. (2014). They classified vegetation communities in the Krkonoše Mts. National Park using APEX data and Support Vector Machines classifier.

http://dx.doi.org/10.14712/23361980.2016.10
Suchá, R. – Jakešová, L. – Kupková, L. – Červená, L. (2016):
Classification of vegetation above the tree line in the Krkonoše Mts. National Park using remote sensing multispectral data
AUC Geographica, 51, No. 1, pp. 113–129

Object based classification was used by Laliberte et al. (2007) in order to distinguish between green and aging vegetation in New Mexico. The study area was located about 1,200 metres a. s. l. They combined the methods of decision tree and nearest neighbour. The classification accuracy equalled 92%. Object based classifications of orthoimages was also used by Lantz et al. (2010) in order to examine changes in vegetation characteristics (cover and patch size) across a latitudinal gradient in the Mackenzie Delta Uplands. Four classes were identified: shrub tundra, dwarf shrub tundra, water, and bare ground, with overall accuracy 78.1% (Kappa coefficient 0.66).

All of the above-mentioned studies used data with very high spatial resolution. Data collected by Landsat sensors (one pixel equals to 30 × 30 metres) are commonly used to produce land cover classifications in large areas (see Dixon, Candade 2008) or to examine forest cover (Wolter et al. 1995, etc.). Landsat data, however, are only rarely used for examination of grassland vegetation, except in the case of vast regions in the northern tundra (Johansen et al. 2012; Pattison et al. 2015).

Several authors compared a number of pixel classification algorithms (Zagajewski 2005) or per-pixel and object based classification – see Yu et al. (2006), Cleve et al. (2008), or Myint et al. (2011). So far, no study has been carried out that would compare the potential of different multispectral data and different types of classification algorithms, including comparison of object based and per-pixel approach for classification of alpine vegetation. Thus, our study aims at evaluation and comparison of selected multispectral data with various spatial and spectral resolutions for land cover classification above the tree line (focus is put on different vegetation classes), using different classifiers including object based image analysis (OBIA) and per-pixel approach. Orthoimages can serve as an example of very high resolution data in this study. Data collected by WorldView-2 satellite show high spatial and spectral resolutions; the freely available data collected by Landsat 8 (moderate resolution) are also examined.

As different vegetation types cover only small patches of land, it is expected that spatial resolution of the data may be crucial for the classification. On the other hand, different vegetation types are clearly confined and usually do not overlap. Thus, we presume that the object based approach applied to high resolution data should bring more accurate results than the per-pixel approach.

2. Study Area

Arctic-alpine tundra occurs in the highest parts of the Krkonoše Mountains above the tree line (from 1,300 m a. s. l. up). It covers a limited area of 47 km^2 (32 km^2 on the Czech territory, 15 km^2 on the Polish territory), i. e. just 7.4% of the total Krkonoše area. The Scandinavian Ice Sheet repeatedly expanded as far as to the northern foothills of the Krkonoše Mountains and during the Holocene, tundra was a permanent phenomenon here (Treml et al. 2008; Margold et al. 2011). As a result of this palaeogeographical history, the Krkonoše Mountains represent a "biodiversity crossroads" where Nordic and alpine flora and fauna coexist (Jeník and Štursa 2003).

The area covered by natural arctic-alpine tundra was expanding due to deforestation and grazing from Early Middle Ages (9th–11th century, Speranza et al. 2000; Novák et al. 2010) until the beginning of the 19th century when mountain agriculture (grazing and grass mowing) peaked (Lokvenc 1995). Direct human impacts then gradually diminished until the 1940s. Almost no direct human intervention in the tundra zone has occurred since then as these areas became strictly protected as nature reserves. The alpine vegetation is being occasionally disturbed mainly by periodical avalanches and debris flows. Closed alpine grasslands, subalpine tall grasslands, *Pinus mugo* scrub, alpine and subalpine scrub currently form the prevailing vegetation types; in the highest altitudes also mosses, lichens, and alpine heathlands are common (Chytrý et al. 2001).

Two spatially separated parts make up the study area: Western Tundra and Eastern Tundra (Figure 1). The western part is situated near Labská bouda and covers about 1,284 hectares. The Eastern part is located around Luční bouda covering 2,284 hectares.

Both parts of tundra on the Czech territory were examined in full using the Landsat data. Classifications of the other data sources have been executed only in selected parts of the study area (565 hectares in the western part, 839 hectares in the eastern part) – Figure 1. Classifications using the detailed legend were applied only in the western area.

3. Data and Methods

3.1 Data

Three sensors of different spectral and spatial resolution represent multispectral data in this study. First, there are orthoimages acquired by aerial sensor on June 18, 2012. Second and third are two satellite sensors: WordView-2 and freely available Landsat 8. The WordView-2 images were acquired on July 22, 2014 (western part) and on August 10, 2014 (eastern part). The Landsat 8 cloud-free image acquired on July 27, 2013 (ID: LC81910252013208LGN00) was chosen from the Landsat archive.

Table 1 shows basic information on the data. No atmospheric corrections were made as classifications were carried out separately for all images; consequently, such adjustments were not necessary (Song et al 2001). Spatial accuracy was secured by geometric corrections and orthorectification (orthoimages, WV-2) using digital surface model created from aerial laser data (cloud of points, 5 points/m^2) and L1T product in the case of Landsat

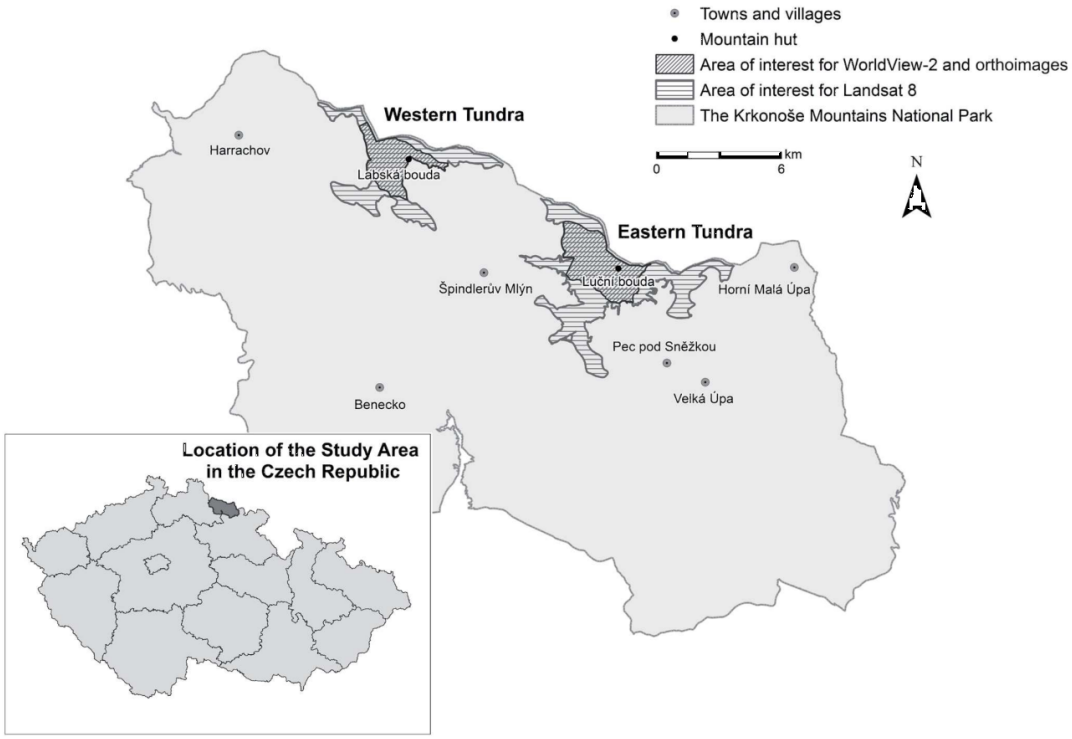

Fig. 1 Study area. Source: Authors

Tab. 1 Data parameters.

Data	Spatial resolution (metres)	Number of bands used for classifications	Radiometric resolution	Date
Orthoimages	0.125	4 (blue, green, red, NIR)	8 bit	June 18th, 2012
WV-2	2	8 (coastal, blue, green, yellow, red, red edge, NIR, NIR2)	11 bit	July 22th, 2014; August 10th, 2014
Landsat 8	30	7 (coastal, blue, green, red, NIR, SWIR1, SWIR2)	12 bit	July 27th, 2013

data (the latter utilizes corrections of digital surface model and surface points GLS2000).

Fifty nine polygons corresponding to vegetation classes as defined in the legend were identified in the field. Data were collected in the period June 23 – June 25, 2014. Polygons were located by GPS (Trimble Geoexplorer 3000 Geo XT, accuracy 10 centimetres) and classified on the botanical basis according to the legend (see Chapter 3.2). Polygons corresponding to classes *Pinus mugo* scrub, *Picea abies* stands, water and block fields, and anthropogenic areas were added later using manual vectorization based on visual interpretation of orthoimages.

3.2 Classification Legend

Definition of the legend constitutes the crucial part of the research. Classifications were made using two types of legends: the detailed legend (12 classes, respectively 13 for OBIA – Figure 3) for orthoimages and WV-2 data, and simplified one (8 classes, respectively 9 classed for OBIA – Figure 3) for all three types of data.

The detailed legend was created in cooperation with national park botanists and includes the most important classes of grassland vegetation as well as other vegetation classes, and also classes without any vegetation cover (Figure 2).

The detailed legend was used for orthoimages and WV-2 in the Western Tundra only. As many vegetation classes cover small patches of land less than 900 m^2 (equal to 1 pixel of Landsat 8), it became necessary to create a simplified legend suitable also for Landsat data classification. This simplified legend includes eight classes and was used for classification of all data types for the sake of comparison.

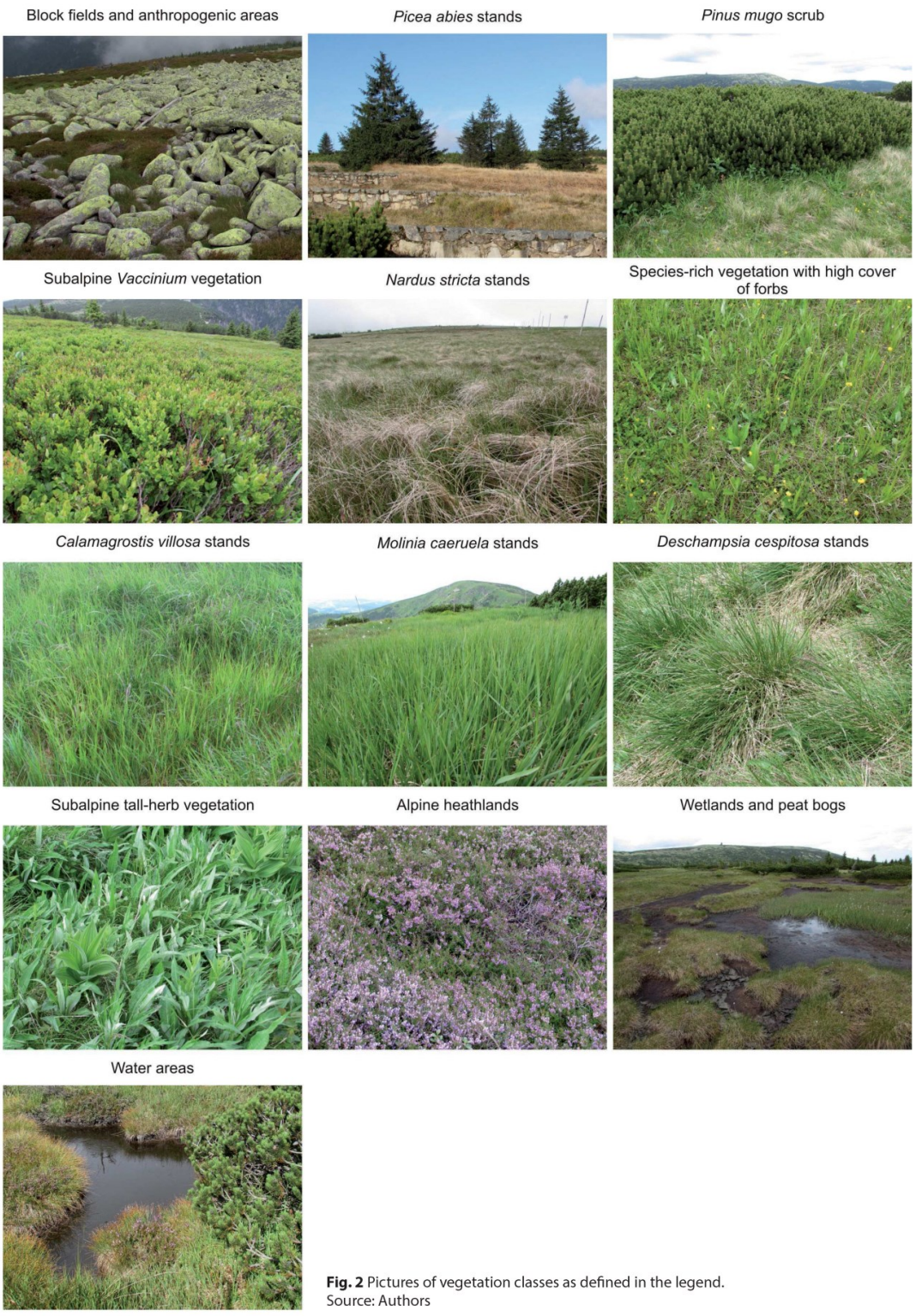

Fig. 2 Pictures of vegetation classes as defined in the legend.
Source: Authors

Detailed legend
1. Block fields and anthropogenic areas
2. *Picea abies* stands
3. *Pinus mugo* scrub
4. Subalpine *Vaccinium* vegetation
5. Closed alpine grasslands
5a. *Nardus stricta* stands
5b. Species-rich vegetation with high cover of forbs
6. Subalpine tall grasslands
6a. *Calamagrostis villosa* stands
6b. *Molinia caeruela* stands
6c. *Deschampsia cespitosa* stands
7. Subalpine tall-herb vegetation
8. Alpine heathlands
9. Wetlands and peat bogs
10. Water areas (only for OBIA)

Simplified legend
1. Block fields and anthropogenic areas
2. *Picea abies* stands
3a. *Pinus mugo* scrub dense (more than 80% of total cover)
3b. *Pinus mugo* scrub sparse (30–80% of total cover)
4. Closed alpine grasslands dominated by *Nardus stricta*
5. Grasses (except *Nardus stricta*) and subalpine *Vaccinium* vegetation
6. Alpine heathlands
7. Wetlands and peat bogs
8. Water areas (only for OBIA)

3.3 Training and Validation Data

The dataset collected in the field and completed with polygons added on the basis of orthoimages visual interpretation (see Chapter 3.1) was divided into training and validation parts.

Training dataset for per-pixel and object based classification of WV-2 and orthoimages using detailed classification legend contains 33 training polygons divided into 13 classes. The total area of training dataset is about 6,700 m^2.

Thirty seven polygons (area of 11,800 m^2) were used for validation. The training dataset for simplified legend was created by visual interpretation of orthoimages (WV-2 data, orthoimages). The total area of training data covered 17,396 m^2 (western part) and 31,800 m^2 (eastern part), respectively. For validation, combined validation and training datasets for the detailed legend (see above) re-classified into the simplified legend were utilized.

Training dataset for the simplified legend, based on visual interpretation of orthoimages, was also created in the case of Landsat 8 data. The rather big size of Landsat pixels, however, necessitated the use of larger areas. Altogether 1,133 pixels were trained (total area 1,019,700 m^2). The validation was again based on the dataset collected in the field (see Chapter 3.1). This dataset, however, had to be radically altered using visual interpretation of orthoimages and Landsat 8 images. The polygons identified in the field were always smaller than one Landsat 8 pixel. Thus, in cases when also the surrounding area was identified as the same class of the simplified legend, the respective pixels were taken into consideration in the accuracy assessment. On the contrary, pixels that clearly included a different land cover were deleted. Following the above mentioned adjustments, the Landsat validation dataset included 332 pixels covering the area of 298,000 m^2.

3.4 Mask

Clouds, shadows, and snow had to be masked from the imagery. The mask for WV-2 images was created by unsupervised classification ISODATA. Altogether 40 classes were identified and further aggregated into four groups: shadows and water areas in Western Tundra, plus clouds and snow in Eastern Tundra. The mask consisting of mentioned four classes had been applied to the imagery before the classification process started.

The mask applied to orthoimages (snow, shadows of vegetation and terrain) was created by object based classification using ENVI software and the rule-based approach. For the rules and attributes see Table 2. All four spectral bands and two parameters (Scale Level 40, Merge Level 80) were employed to carry out the segmentation.

For Landsat data, the mask of clouds and their shadows (located at NW part of the study area) was created using ISODATA classification.

Tab. 2 Rules and attributes used for orthoimages mask creation

Class	Attribute	Rule
shadows	Spectral Mean	1 < NIR < 65
snow	Spectral Mean	NIR > 255

3.5 Classification

The classification methods correspond to data types. Big differences among spatial resolutions of different data types justify the use of per-pixel and object based classification. Blaschke (2010) argues that the per-pixel approach brings better results when data with low spatial resolution are used; on the contrary, if data with high spatial resolution were available, object based classification is more appropriate. In our research, only object based classification is used for orthoimages, and only per-pixel classification for Landsat data. The WorldView-2 data were analysed using both object based and per-pixel approach enabling the comparison of results brought by these two methods. For schematic workflow see Figure 3.

3.6 Classification per-pixel

Three different per-pixel supervised classification algorithms were employed in this study: maximum likelihood

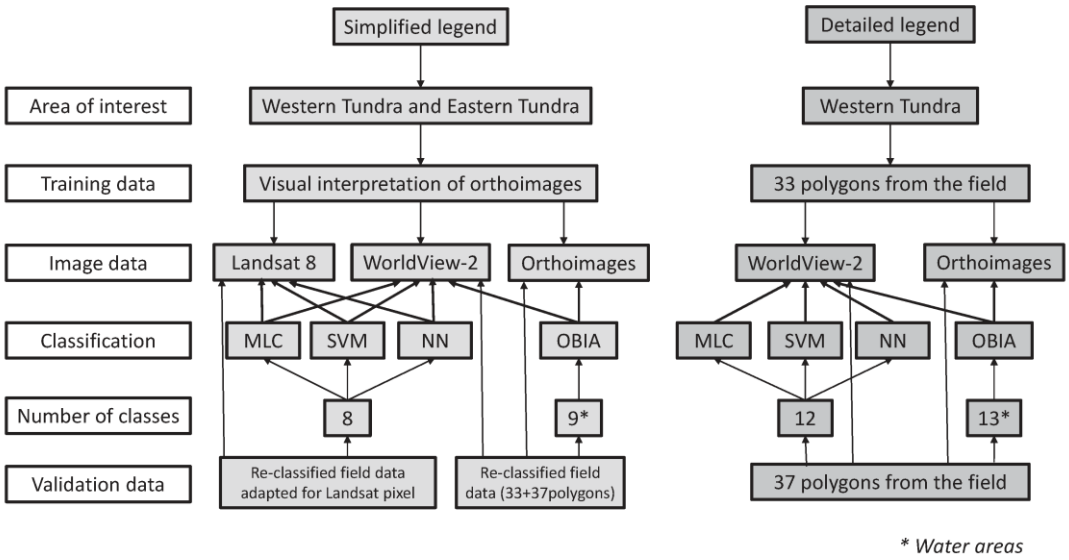

Fig. 3 Workflow.

classification (MLC), support vector machine (SVM), and neural net algorithms (NN).

Maximum likelihood classification

There are two conditions for successful application of this widely used algorithm. First, the image data should show normal distribution (Fernandez-Prieto 2006). Second, the training samples' statistical parameters (e.g., mean vector and covariance matrix) should truly represent the corresponding land cover class (Duarte et al. 2005). When ENVI software is used for maximum likelihood algorithm, parameters cannot be changed in any way with the exception of probability threshold parameter. The latter, however, was not used.

Machine learning algorithms

The machine learning classification algorithms, such as support vector machines (SVM) or artificial neural networks (or neural networks; NN), are also pixel-based classifiers (Petropoulos et al. 2012; Camps-Valls et al. 2004). Both methods belong among supervised non-parametric methods, which means that no particular data distribution is required (e.g. normal distribution). This makes a difference compared to other conventional classifiers, such as maximum likelihood classifier (Jones and Vaughan 2010). This fact is a big advantage of NN and SVM as the majority of remotely sensed data show an unknown statistical distribution.

Support vector machines algorithm

The support vector machines algorithm is based on the statistical learning theory and aims to find the best hyperplane in a multidimensional feature space that optimally separates classes. The term "best hyperplane" is used to refer to a decision boundary obtained in a training step and minimizing misclassifications. Training samples used for construction of hyperplane are called support vectors. These lie on the margin of classes to be classified and are extracted automatically by the algorithm (Jones and Vaughan 2010; Petropoulos et al. 2012; Mountrakis et al. 2011; Camps-Valls et al. 2004). Three Kernel types were tested using ENVI software in the case of SVM classification: radial basic functions (RBF), linear, and polynomial. In the case of RBF, Gamma was set to 0.125 for WV-2 and 0.143 for Landsat 8. Kernel Polynomial 2 was chosen in the case of polynomial function.

Neural networks algorithm

The artificial neural networks algorithm is designed to simulate human learning process by establishing linkages between input and output data via one or more hidden layers. The basic unit of each layer is called neuron (node) (Benediktsson et al. 1990). The classic model of a feed-forward multilayer neural network, known as multilayer perception (MLP) has fully-connected neurons between all layers (input, output, and hidden), which means that each neuron of a given layer feeds all the neurons in the next layer (Camps-Valls et al. 2004). This model is used in our processing tool, ENVI 5.2 software.

The neural network algorithm, applied to WV-2 data, was used in two modes. First, the default setting of ENVI software was applied. Second, the setting shown in Table 3 was used. Default setting was also applied to Landsat 8 data as the hidden layers and changes of some other parameters did not bring better results.

Table 3 Parameters of neural network algorithm

Training Threshold Contribution	0.9
Training Rate	0.9
Training Momentum	0.1
Training RMS Exit Criteria	0.05
Iteration	5000

3.7 Object based image classification

The object based image analysis (OBIA) does not examine pixels, but works with homogeneous clusters of pixels called segments. Segments are areas generated by one or more criteria of homogeneity. Thus, compared to single pixels, segments include additional spectral information (e.g. mean values per band, minimum and maximum values, mean ratios, variance etc.) (Blashke 2010). The example-based approach in ENVI software was employed for object based classification using the support vector machine algorithm.

Segmentation

The ENVI software includes only two segmentation algorithms: edge and intensity. The edge algorithm, where images are divided on the bases of Sobel's method of edge detection, was chosen in this study. Segmentation (orthoimages and WV-2) was carried out using all four/eight spectral bands. The parameters applied are shown in Table 4.

The ENVI software processes the segmentation each time it is started; consequently, the software does not allow to use any previously segmented image for further classifications.

Tab. 4 Segmentation parameters

Parameter	Orthoimages	WV-2
scale level	45	50
merge level	80	85
texture kernel size (pixels)	5 × 5	3 × 3

Example based classification

The example based classification sorts segments into pre-defined classes using training areas (segments), selected attributes, and classification algorithm. The following spectral and texture attributes were chosen: spectral mean, spectral max, spectral min, spectral standard deviation, texture mean, and texture variance. The above mentioned attributes were calculated for all spectral bands. The SVM classification algorithm with Kernel type radial basic function was used.

3.8 Accuracy Assessment

The ENVI software was used for accuracy assessment in all cases using validation polygons as defined for different data types (Chapter 3.3 and Figure 3). First, Confusion Matrix was created on the basis of ground true ROIs. The total accuracy was assessed as was the producer's and user's accuracy for different classes. Kappa coefficient for each classification was calculated, too.

4. Results

Table 5 shows the results of classifications (object based and per-pixel) for the detailed legend (applied in the western part of the tundra for orthoimages and WV-2 data). Table 6 shows the results for the simplified legend (applied in both parts of the tundra for all types of data). Figures 4–7 show the best classification map outputs for different types of data.

Tab. 5 Results of different classification methods (detailed legend) in Western Tundra.

Method	Data	Accuracy (%)	Kappa coeficient
OBIA-SVM (RBF)	orthoimages	**71.96**	0.65
	WV-2	**66.50**	0.60
SVM (RBF)	WV-2	60.82	0.54
SVM (polynomial)	WV-2	60.45	0.54
SVM (linear)	WV-2	60.30	0.54
NN	WV-2	60.13	0.54
MLC	WV-2	58.07	0.53
NN (default)	WV-2	54.59	0.49

4.1 Classification results: orthoimages

Orthoimages were classified by the object based approach only. This was applied to the detailed legend (western part) as well as to the simplified legend (western and eastern parts). The best classification results were obtained in the Eastern Tundra for simplified legend; the overall accuracy reached 83.56% (Kappa coefficient = 0.8). When different classes of the legend are compared, the classes "block field and anthropogenic areas", "water areas", and "wetlands and peatbogs" show the best results. The user's and producer's accuracy exceeded 90% in all cases.

On the contrary, the class "closed alpine grasslands dominated by *Nardus stricta*" shows the worst results of all. Though the producer's accuracy equalled 99.7%, the user's accuracy reached only 27%. The most common overlaps were with "*Pinus mugo* scrub sparse" and also with "wetlands and peatbogs".

In the case of detailed legend (Western Tundra), the overall accuracy equals 71.96% and Kappa coefficient 0.65. The best results were again achieved for the classes "water areas", "block fields and anthropogenic areas", and also for "*Pinus mugo* scrub". Producer's and user's accuracy varied in the range 87–100%. The classes "wetlands and peat bogs" and "subalpine *Vaccinium* vegetation" also show very good results with producer's and user's accuracy

Tab. 6 Results of different classification methods (simplified legend) in both parts of Tundra.

Method	Data	Area	Accuracy (%)	Kappa coefficient
OBIA-SVM (RBF)	orthoimages	East	**83.56**	0.8
	orthoimages	West	73.1	0.67
	WV-2	East	**66.37**	0.6
	WV-2	West	**68.4**	0.62
MLC	WV-2	East	57.04	0.48
	WV-2	West	59.96	0.51
	Landsat	West/ East	**78.31**	0.75
SVM (polynomial)	WV-2	East	42.49	0.39
	WV-2	West	56.11	0.46
	Landsat	West/ East	68.37	0.63
SVM (RBF)	WV-2	East	42.82	0.35
	WV-2	West	56	0.46
	Landsat	West/ East	68.67	0.64
SVM (linear)	WV-2	East	41.19	0.32
	WV-2	West	55.28	0.45
	Landsat	West/ East	68.37	0.64
NN (default)	WV-2	East	41.71	0.33
NN (default)	WV-2	West	57.42	0.47
NN	WV-2	East	36.64	0.27
NN	WV-2	West	58.36	0.48
NN (log)	Landsat	West/ East	63.55	0.58

ranging between 70% and 80%. On the contrary, the classes "alpine heathlands", "*Calamagrostis villosa* stands", and "*Deschampsia cespitosa* stands" show poor accuracy (less than 10%). In the case of alpine heathlands, the selected sample did not include enough training areas.

4.2 Classification results: WV-2 data

Per-pixel and object based approaches were used in the case of WV-2 data. Both classifications were applied to detailed legend (Western Tundra) as well as to simplified legend (Western and Eastern Tundra).

Best results were obtained in the case of object based classification applied to simplified legend in the western part (overall accuracy = 68.4%, Kappa coefficient = 0.62). Classes "*Picea abies* stands" and "block fields and anthropogenic areas" were classified with the highest accuracy. Producer's and user's accuracy varied in the range 90–100%. Very good results were also obtained in the case of "grasses (except *Nardus stricta*) and subalpine *Vaccinium* vegetation" with producer's and user's accuracy equalling ca. 80%. "*Pinus mugo* scrub dense" was often confused with "*Pinus mugo* scrub sparse". The class "closed alpine grasslands dominated by *Nardus stricta*" shows the worst results (producer's accuracy = 73.73%, user's accuracy = 35.51%).

The overall accuracy of object based classification in the western part (detailed legend) was almost identical to that in the eastern part (simplified legend) – around 66%, Kappa coefficient = 0.6). Producer's and user's accuracy reached almost 100% in the case of "block fields and anthropogenic areas" class. Also the classes "*Pinus mugo* scrub" and "*Picea abies* stands" showed very good results (producer's and user's accuracy 80–99%). As in the case of orthoimages, the classes "alpine heathlands", "*Calamagrostis villosa* stands", and "*Deschampsia cespitosa* stands" were classified with poor accuracy (producer's and user's accuracy below 5%).

Per-pixel classifications of WV-2 brought worse results than the object based one. Overall accuracy ranged between 50 and 60%. As regards the detailed legend (Western Tundra), the SVM (RBF) classification brought the best results (60.82%, Cappa coefficient = 0.54). The MLC method worked best for the simplified legend (59.96%, Cappa coefficient = 0.51).

Classes "*Pinus mugo* scrub" (producer's accuracy = 85.35%, user's accuracy = 76.49%) and "block fields and anthropogenic areas" show best results within the detailed legend classified by per-pixel approach (SVM RBF method). Also "subalpine *Vaccinium* vegetation" was classified well (producer's accuracy = 70.26%, user's accuracy = 70.14%)

The results of earlier field research suggested that classes "*Calamagrostis villosa* stands" and "*Molinia caeruela* stands" would be confused with each other most often. This assumption was partly confirmed by per-pixel approach; however, also classes "*Nardus stricta* stands" and "*Deschampsia cespitosa* stands" often overlapped. Surprisingly, it was "*Deschampsia cespitosa* stands" that showed the best results of all grassland vegetation – producer's accuracy equalled 70.26%, user's accuracy 40.21% (SVM RBF method).

Regarding the assessment of simplified legend in Western and Eastern Tundra, "*Pinus mugo* scrub" (dense and sparse) again showed the bests results. The producer's accuracy exceeded 90% in both cases; user's accuracy ranged around 60%. However, "*Pinus mugo* scrub dense" was often confused with "*Pinus mugo* scrub sparse". For future WV-2 classification, it may be appropriate to merge these two classes.

In the Western Tundra, "block fields and anthropogenic areas" and "closed alpine grasslands dominated by *Nardus stricta*" showed very good results. Classes "Alpine heathlands" and "block fields and anthropogenic areas" performed best in the East.

4.3 Classification results: per-pixel approach applied to Landsat data

Landsat data were classified only by per-pixel algorithms that were applied to simplified legend, simultaneously in both parts of the tundra. MLC algorithm brought the best results (overall accuracy 78.31%); other algorithms brought worse results by more than 10%.

The classes "*Pinus mugo* srub dense", "Alpine heathlands", "*Picea abies* stands", and "block fields and anthropogenic areas" were classified without major problems – producer's and user' accuracy exceeded 80% and often were close to 100%. In the case of "*Pinus mugo* scrub sparse", producer's accuracy equals 100%, but user's accuracy was rather low (45.9%). It means that "*Pinus mugo* scrub sparse" was overclassified, largely to the detriment of "grasses (except *Nardus stricta*) and subalpine *Vaccinium* vegetation". On the contrary, the class "closed alpine grasslands dominated by *Nardus stricta*" showed a sort of a reverse effect: the producer's accuracy was rather low (44.44%) as the latter was often confused with "grasses (except *Nardus stricta*) and subalpine *Vaccinium* vegetation".

It can be concluded that most problems were posed by grassland vegetation and by classes where grassland vegetation occurs extensively. Other land cover types were classified well also by Landsat data.

4.4 Classification results: map outputs

Classification map outputs can be found in Colour Appendix. Figure 4 shows the best classification results for detailed legend; Figures 5 and 6 show that for simplified legend and object based classification of orthoimages and WordView-2 data in Western and Eastern Tundra. The best results for Landsat 8 data are shown in Figure 7.

When classification outputs are compared, varying spatial resolution of different data types is instantly recognizable. Based on different spatial resolution final mosaics of classified categories differs (areal extent, spatial distribution, shape). While Landsat 8 data are useful rather for general overview, orthoimages provide accurate maps of land cover within the study area for all classes of the detailed legend.

5. Discussion and Conclusions

The major aim of this study was to assess and compare the potential of selected multispectral data with various spatial and spectral resolutions for land cover classification above the tree line. Different types of classifiers were used including per-pixel and object based approach.

Though vegetation types are usually well defined and do not overlap too much in the tundra of Krkonoše, a vast array of species exists there. These species often alternate with each other within a limited area. Consequently, spatial resolution plays a more important role than spectral resolution in the case of object based classification. It was the object based classification of orthoimages (spatial resolution 12.5 cm, four spectral bands) that brought the best results for both legends – overall accuracy equalled 72–84%. Thus, it has been confirmed that application of object based classification is more appropriate than per-pixel approach when data with very high spatial resolution are examined. Orthoimages and object based classification can be recommended to National Park authorities as appropriate tools for landscape monitoring in this area of high nature value. Another advantage is that orthoimages are updated every second year by the state and consequently available for free to the National Park management. On the contrary, object based classification requires a specialized software, the classification itself is rather difficult, and processing time quite long.

The object based classification of WorldView-2 data was less accurate than in the case of orthoimages (68.4% at best) though WV-2 data provide better spectral resolution. The per-pixel approach applied to WV-2 data (detailed legend) was even less accurate; the highest accuracy (60.82%) brought the SVM (RBF) algorithm.

Classification of Landsat data applied to simplified legend (MLC method) brought surprisingly good results – overall accuracy equalled 78%. Construction of the legends may be the reason why per-pixel classifications applied to simplified legend were more accurate in the case of Landsat data rather than for WV-2 data. A special simplified legend optimized for Landsat data was created. The use of training or validation polygons for detailed legend proved to be impossible as in most cases these polygons were smaller than the pixel size (30 × 30 metres); thus, clear pixels for detailed legend could not be defined.

Such a simplified, specially adjusted legend, however, was not fully appropriate for WorldView-2 data. Classes "*Pinus mugo* scrub dense" and "*Pinus mugo* scrub sparse" posed biggest problems in the case of simplified legend and were often confused with each other. Though such a precise definition of *Pinus mugo* (dense vs. sparse) is essential for Landsat data, it is apparently not appropriate for high resolution data as WV-2. Moreover, some training and validation polygons were covered by clouds during research time; consequently, part of WV-2 data could not be used.

This study also compared the suitability of per-pixel and object based classification for different data types. Per-pixel classification proved to be fully appropriate in the case of Landsat data. On the contrary, per-pixel classification of high resolution orthoimages brought unsatisfactory results. Object based classification of Landsat data (spatial resolution 30 metres) does not make much sense either on such a small territory where vegetation classes alternate often. Both types of classification were applied to WorldView-2 data; object based classification brought better results by some 10% than the per-pixel one.

Different algorithms for per-pixel classification were compared, too. The examination of WV-2 data showed that the MLC classifier worked best for simplified legend. In the case of detailed legend, however, the more sophisticated algorithm, SVM (RBF), brought better results.

Earlier field research suggested that classifications would be more accurate in the Eastern Tundra as different vegetation types as specified in the legends seemed to be clearly defined there. As an example, "*Molinia caeruela* stands" and "*Calamagrostis villosa* stands" covered compact areas surrounded by "*Nardus stricta* stands". This presumption was confirmed by orthoimages classification (overall accuracy 83.56%). Classification of WV-2 data, however, brought different results – in part probably due to clouds and shadows on the image.

Classification results may be influenced by varying weather conditions, and also by the season. Vegetation classes tend to be rather compact during spring and autumn, while in summer (July, August) the grassland vegetation advances and different types blend. The blossom may also influence spectral bands in some cases. The above mentioned differences may have played a certain role when orthoimages and WV-2 data were compared. Unfortunately, it is practically impossible to acquire all required multispectral data of different spectral and spatial resolution within one year and one season. That is why it was necessary to examine data acquired in different years. Research results may be partly influenced by this fact.

Regarding classification accuracy of different classes, all types of data brought good results for non-vegetation classes (block fields and anthropogenic areas, water areas). Also the category subalpine *Vaccinium* vegetation shows high accuracy for detailed legend (orthoimages and WV-2 data). As expected, subalpine tall grasslands subcategories with similar spectral signatures (*Calamagrostis villosa* stands and *Deschampsia cespitosa* stands, *Molinia caeruela* stands) show less satisfactory results. The worse-than-expected results in the case of alpine heathlands were probably influenced by the low presence of training polygons. On the contrary, Landsat 8 data covered the whole tundra and therefore also more training polygons – consequently, alpine heathlands were classified with high accuracy (MLC: user's accuracy 95.65%, producer's accuracy 81.48%).

Pinus mugo scrub usually shows good classification results, too. In the case of simplified legend, *Pinus mugo* scrub was further subdivided into dense and spare subcategories; such a subdivision, however, proved to be inappropriate for WV-2 data and orthoimages. As Landsat data consist of rather big pixels, it is difficult to find really uniform categories. *Pinus mugo* scrub sparse is often mixed with grassland vegetation within one pixel. *Pinus mugo* scrub dense does not have this problem and brings better results when classified as a separate class. When it comes to very high resolution data, however, *Pinus mugo* scrub practically does not mix with other categories. Some categories of simplified legend may be too broadly defined for high resolution data. This was proved to a certain extent in the case of closed alpine grasslands dominated by *Nardus stricta* and grasses (except *Nardus stricta*) and subalpine *Vaccinium* vegetation classes.

The results comparing detailed and simplified legends show that in the case of multispectral data with different spatial resolution it is difficult – if not impossible – to find such a compromise that would be appropriate for data of different resolution. One single legend cannot serve a basis for comparison of different data; the level of detail should always be related to data resolution.

It can be concluded that in the case of simplified legend – the overall accuracy of Landsat data (MLC algorithm, 78.31%) and object based classification of orthoimages (83.56%) – our results are similar to those mentioned in earlier scientific sources. As an example, Müllerová (2004) classified multispectral data in Krkonoše in 1986, 1989, and 1997; supervised classification identified nine classes of local vegetation with accuracy 81.1%. Král (2009) classified alpine vegetation on the Czech territory, too. In the latter case, the accuracy of orthoimages equalled 78% (MLC method). However, the rather high spectral variation of different land cover classes and low spectral resolution of orthoimages resulted in mixed character of many classes. Wundram a Loffler (2008) classified alpine vegetation in Norway and achieved similar results. The maximum likelihood method applied to orthoimages (RGB bands) resulted in overall accuracy equalling 51%.

Algorithm MLC used for Landsat data classification brought the accuracy of 78.31% in our research. Knorn et al. (2009) utilized Landsat data for land cover classification in the Carpathians; SVM method brought accuracy up to 98.9% for nine classes. Landsat data were also used by Johansen et al. (2012) for tundra mapping on Svalbard. The final product was a map (scale 1: 500,000) containing eighteen classes. The processing chain contained six stages including unsupervised classification and merging the classes based on ancillary data. Verification of the final product is problematic in such remote areas; the overlap between Landsat data classification and traditional vegetation mapping in Gipsdalen Valley reached 55.36% (eight aggregated classes were tested).

Our research confirms that Landsat data are sufficient to get a general overview of basic land cover classes above the tree line in the Krkonoše Mts. National Park. Alternatively, the recently launched Sentinel-2 satellite could be used – images have comparable spatial resolution and better spectral resolution. Detailed classification, however, requires orthoimages with very high spatial resolution, plus sophisticated algorithms of object based classification should be used. WorldView-2 data brought the least satisfactory results in our research. However, this may have been influenced by clouds, and also by problems with exact definition of the legend as discussed above. Based on the comparison of the data with different spectral and spatial resolution we can conclude that very high spatial

resolution is the decisive feature that is essential to reach high overall classification accuracy in the detailed level. Zagajewski (2005) and other scientists suggest that utilization of hyperspectral data of very high spatial resolution (alternatively combined with LiDAR data – see Dalponte 2012) could bring further improvements of classification accuracy.

Acknowledgements

This research was made possible by the support of The Charles University in Prague Grant Agency: GAUK project No. 938214 – Remote sensing for classification of vegetation above tree-line in the Krkonoše Mts.National Park. Our grateful thanks go also to RNDr. Stanislav Březina, PhD., and Mgr. Jan Šturma who helped to carry out botanical research and to create the legends.

REFERENCES

BENEDIKTSSON, J. A., SWAIN, P. H., ERSOY, O. K. (1990): Neural network approaches versus statistical methods in classification of multisource remote sensing data. IEEE Transactions on geoscience and remote sensing 28(4), 540–551. http://dx.doi.org/10.1109/TGRS.1990.572944

BLASCHKE, T. (2010): Object based image analysis for remote sensing. ISPRS Journal of Photogrammetry and Remote Sensing 65(1), 2–16. http://dx.doi.org/10.1016/j.isprsjprs.2009.06.004

CAMPS-VALLS, G., GÓMEZ-CHOVA, L., CALPE-MARAVILLA, J. (2004): Robust support vector method for hyperspectral data classification and knowledge discovery. IEEE Transactions on geoscience and remote sensing, Valencia, 20, pp. 1–13. http://dx.doi.org/10.1109/tgrs.2004.827262

CLEVE, C., KELLY, M., FAITH, R. K., MORITZ, M. (2008): Classification of the wildland–urban interface: A comparison of pixel and object-based classifications using high-resolution aerial photography. Computers, Environment and Urban Systems 32, 317–326. http://dx.doi.org/10.1016/j.compenvurbsys.2007.10.001

DALPONTE, M., BRUZZONE, L., GIANELLE, D. (2012): Tree species classification in the Southern Alps based on the fusion of very high geometrical resolution multispectral/hyperspectral images and LiDAR data. Remote sensing of Environment 123, 258–270. http://dx.doi.org/10.1016/j.rse.2012.03.013

DIXON, B., CANDADE, N. (2008): Multispectral landuse classification using neural networks and support vector machines: one or the other, or both? International Journal of Remote Sensing 29(4), 1185–1206. http://dx.doi.org/10.1080/01431160701294661

DUARTE, C. M., MIDDELBURG, J. W., CARACO, N. (2005): Major role of marine vegetation on the oceanic carbon cycle. Biogeosciences 2(1), 1726–4170. http://dx.doi.org/10.5194/bg-2-1-2005

FERNANDEZ-PRIETO, D., ARINO, O., BORGES, T., DAVIDSON, N., FINLAYSON, MAX, GRASSL, H., MACKAY, H., PRIGENT, C., PRITCHARD, D., ZALIDIS, G. (2006): The globwetland symposium: summary and way forward. Proc. Glob-Wetland: Looking at Wetlands from Space. ESA Publications Division, Frascati, pp. 19–20.

CHYTRÝ, M., KUČERA, T., KOČÍ, M., GRULICH, V., LUSTYK, P. (2001): Katalog biotopů České republiky. Praha: AOPK ČR.

JENÍK, J., ŠTURSA, J. (2003): Vegetation of the Giant Mountains, Central Europe. In: NAGY, L., GRABHERR, G., KÖRNER, CH., THOMPSON, D. B. A. (eds.), Alpine Biodiversity in Europe (Ecology Studies Vol. 167), New York: Springer, pp. 47–51.

JOHANSEN, B. E., KARLSEN, S. R., TØMMERVIK, H. (2012): Vegetation mapping of Svalbard utilising Landsat TM/ETM+ data. Polar Record 48, 47–63. http://dx.doi.org/10.1017/s0032247411000647

JONES, H. G., VAUGHAN, R. A. (2010): Remote sensing of vegetation: Principles, techniques and applications. Oxford: Oxford University Press.

KNORN, J., RABE, A., RADELOFF, V. C., KUEMMERLE, T., KOZAK, J., HOSTERT, P. (2009): Land cover mapping of large areas using chain classification of neighboring Landsat satellite images. Remote Sensing of Environment 113(5), 957–964. http://dx.doi.org/10.1016/j.rse.2009.01.010

KRÁL, K. (2009): Classification of current vegetation cover and alpine treeline ecotone in the Praděd Reserve (Czech Republic), using remote sensing. Mountain Research and Development 29(2), 177–183. http://dx.doi.org/10.1659/mrd.1077

LALIBERTE, A. S., RANGO, A., HERRICK, J. E., FREDRICKSON, E. L., BURKETT, L. (2007): An object-based image analysis approach for determining fractional cover of senescent and green vegetation with digital plot photography. Journal of Arid Environments 69(1), 1–14. http://dx.doi.org/10.1016/j.jaridenv.2006.08.016

LANTZ, T. C., GERGEL, S. E., KOKELJ, S. V . (2010): Spatial Heterogeneity in the Shrub Tundra Ecotone in the Mackenzie Delta Region, Northwest Territories. Implications for Arctic Environmental Change. Ecosystems, 13/2, pp. 194-204, http://dx.doi.org/10.1007/s10021-009-9310-0

LOKVENC, T. (1995): Analysis of anthropogenic changes of woody plant stands above the alpine timber line in the Krkonoše Mts. Opera Corcontica 32, 99–114.

MARCINKOWSKA, A., ZAGAJEWSKI, B., OCHYTRA, A., JAROCIŃSKA, A., RACZKO, E., KUPKOVÁ L., ŠTYCH, P., MEULEMAN, K. (2014): Mapping vegetation communities of the Karkonosze National Park using APEX hyperspectral data and Support Vector Machines. Miscellanea Geographica 18(2), 23–29. http://dx.doi.org/10.2478/mgrsd-2014-0007

MARGOLD, M., TREML, V., PETR, L., NYPOLOVÁ, P. (2011): Snowpatch hollows and pronival ramparts in the Krkonoše Mountains, Czech Republic: distribution, morphology and chronology of formation. Geografiska Annaler, Ser. A Physical Geography 93, 137–150. http://dx.doi.org/10.1111/j.1468-0459.2011.00422.x

MOUNTRAKIS, G., IM, J., OGOLE, C. (2011): Support vector machines in remote sensing: A review; ISPRS Journal of Photogrammetry and Remote Sensing 66, 247–259. http://dx.doi.org/10.1016/j.isprsjprs.2010.11.001

MÜLLEROVÁ, J. (2005): Use of digital aerial photography for subalpine vegetation mapping: A case study from the Krkonoše Mts., Czech Republic. Plant Ecology 175(2), 259–272. http://dx.doi.org/10.1007/s11258-005-0063-3

MYINT, S. W., GOBER, P., BRAZEL, A., GROSSMAN-CLARKE, S., WENG, Q. (2011): Per-pixel vs. object-based classification of urban land cover extraction using highspatial resolution imagery. Remote Sensing of Environment 115, 1145–1161. http://dx.doi.org/10.1016/j.rse.2010.12.017

NOVÁK, J., PETR, L., TREML, V. (2010): Late-Holocene human-induced changes to the extent of alpine areas in the East

Sudetes, Central Europe. The Holocene 20, 895–905. http://dx.doi.org/10.1177/0959683610365938
PATTISON, R. R., JORGENSON, J. C., RAYNOLDS, M. K., WELKER, J. M. (2015): Trends in NDVI and tundra community composition in the Arctic of NE Alaska between 1988 and 2009. Ecosystems 18, 707–719. http://dx.doi.org/10.1007/s10021-015-9858-9
PETROPOULOS, G. P., ARVANITIS, K., SIGRIMIS, N. (2012): Hyperion hyperspectral imagery analysis combined with machine learning classifiers for land use/cover mapping. Expert Systems with Applications 39, 3800–3809. http://dx.doi.org/10.1016/j.eswa.2011.09.083
RESLER, L. M., FONSTADA, M. A., BUTLERA, D. R. (2004): Mapping the alpine treeline ecotone with digital aerial photography and textural analysis. Geocarto International 19(1), 37–44. http://dx.doi.org/10.1080/10106040408542297
SONG, C., WOODCOCK, C. E., SETO, K. C., PAX LENNEY, M., MACOMBER, S. A. (2001): Classification and change detection using Landsat TM data: When and how to correct atmospheric effects? Remote Sensing of Environment 75(2), 230–244. http://dx.doi.org/10.1016/S0034-4257(00)00169-3
SOUKUPOVÁ, L., KOCIÁNOVÁ M., JENÍK, J., SEKYRA, J. (1995): Arctic alpine tundra in the Krkonoše, the Sudetes. Opera Corcontica 32, 5–88.
SPERANZA, A., HANKE, J., VAN GEEL, B., FANTA, J. (2000): Late-Holocene human impact and peat development in the Černá hora bog, Krkonoše Mountains, Czech Republic. Holocene 10, 575–585. http://dx.doi.org/10.1191/095968300668946885
TREML, V., JANKOVSKÁ, V., PETR, L. (2008): Holocene dynamics of the alpine timberline in the High Sudetes. Biologia 63, 73–80. http://dx.doi.org/10.2478/s11756-008-0021-3
WOLTER, P. T., MLADENOFF D. J., HOST, G. E., CROW, T. R. (1995): Improved Forest classification in the Northern Lake states using multitemporal Landsat imagery. Photogrammetric Engineering and Remote Sensing 61(9), 1129–1143.
WUNDRAM, D., LOFFLER, J. (2008): High-resolution spatial analysis of mountain landscapes using a lowaltitude remote sensing approach. International Journal of Remote Sensing, University of Bonn, 29.4, pp. 961-974. http://dx.doi.org/10.1080/01431160701352113
YU, Q., GONG, P., CLINTON, N., BIGING, G., KELLY, M., SCHIROKAUER, D. (2006): Object-based Detailed Vegetation Classification with Airborne High Spatial Resolution Remote Sensing Imagery. Photogrammetric Engineering and Remote Sensing 72(7), 799–811. http://dx.doi.org/10.14358/PERS.72.7.799
ZAGAJEWSKI, B., KOZLOWSKA, A., KROWCZYNSKA, M., SOBCZAK, M., WRZESIEN, M. (2005): Mapping high mountain vegetation using hyperspectral data. EARSeL eProceedings 4(1), 70–78.

RESUMÉ

Klasifikace vegetace nad horní hranicí lesa v Krkonošském národním parku s využitím multispektrálních dat

Článek hodnotí možnosti multispektrálních dat s rozdílným prostorovým a spektrálním rozlišením pro klasifikaci vegetace nad horní hranicí lesa v Krkonošském národním parku. Letecká ortofota s velmi vysokým prostorovým rozlišením 12,5 cm a čtyřmi spektrálními pásmy byla klasifikována objektovou klasifikací. Družicová data WorldView-2 (WV-2) s vysokým prostorovým rozlišením 2 m a osmi spektrálními pásmy byla klasifikována jak objektově, tak pixelově. Pixelová klasifikace byla provedena i na volně dostupných datech Landsat 8 s prostorovým rozlišením 30 m a sedmi spektrálními pásmy. Z algoritmů pro pixelovou klasifikaci byly porovnávány klasifikátory maximum likelihood classification (MLC), support vector machine (SVM) a neural net (NN). Pro objektovou klasifikaci byl využíván přístup example-based a algoritmus SVM (vše dostupné v ENVI 5.2). Schéma pracovního postupu je na obrázku 3.

Analýza byla provedena v krkonošské tundře. Modelová oblast je situována ve dvou prostorově oddělených částech – východní a západní části tundry (obrázek 1). Pomocí dat Landsat byla hodnocena celá oblast východní (rozloha 1284 ha) i západní (rozloha 2284 ha) tundry v české části KRNAP. Pomocí ostatních datových zdrojů vzhledem k výpočetní náročnosti klasifikací pouze vybrané části území (565 ha na západě v and 839 ha na východě) reprezentativní pro danou oblast.

Klíčovou částí práce byla definice legendy, která byla vytvořena ve spolupráci s botanikem Krkonošského národního parku. Základní podrobná legenda obsahuje celkem 12 tříd (viz níže a viz obrázek 2). Byla využita pro ortofota a WV-2, a to pouze v západní tundře. Vzhledem k tomu, že se dané třídy vyskytují velmi často na menších plochách, než je pixel Landsatu 8 (tj. 900 m^2), bylo nutné vytvořit i zjednodušenou legendu vhodnou pro klasifikaci dat Landsat. Zjednodušená legenda obsahuje 8 tříd a byla použita pro klasifikaci všech zmíněných typů dat za účelem jejich porovnání.

Podrobná legenda
1. kamenná moře a antropogenní plochy
2. smrkové porosty
3. kosodřevina
4. subalpínská brusnicová vegetace
5. alpínské trávníky zapojené
5a. smilka tuhá
5b. druhově bohaté porosty s vysokým zastoupením dvouděložných
6. subalpínské vysokostébelné trávníky
6a. třtina chloupkatá
6b. bezkolenec modrý
6c. metlice trsnatá
7. subalpínské vysokobylinné trávníky
8. alpínská vřesoviště
9. mokřady a rašeliniště
10. vodní plochy (klasifikovány pouze z ortofot)

Zjednodušená legenda
1. kamenná moře a antropogenní plochy
2. smrkové porosty
3a. kosodřevina hustá (> 80% porostu)
3b. kosodřevina řídká (30% - 80% porostu)
4. alpínské trávníky zapojené s vysokým zastoupením smilky tuhé
5. trávy (vyjma smilky tuhé) a subalpínská brusnicová vegetace
6. alpínská vřesoviště
7. mokřady a rašeliniště
8. vodní plochy (klasifikovány pouze z ortofot)

Nejlepší výsledky byly v případě podrobné i zjednodušené legendy dosaženy pro ortofota (celková přesnost klasifikace 83,56, resp. 71,96 %, Kappa koeficient 0,8, resp. 0,65). Klasifikace WV-2 dosáhla nejlepšího výsledku v případě objektového přístupu a zjednodušené legendy (68,4 %), z pixelových klasifikací v případě metody SVM (RBF) a podrobné legendy (60,82 %). Data Landsat byla nejpřesněji klasifikována s využitím MLC (78,31 %). Nejlepší klasifikační výstupy pro jednotlivé typy dat jsou na obrázcích 4–7.

Potvrdil se náš předpoklad, že v případě vegetace v tundře dosáhneme pro data s velmi vysokým prostorovým rozlišením objektovou klasifikací lepších výsledků než klasifikací pixelovou. Ortofota a objektovou klasifikaci lze na základě našich výsledků doporučit managementu národního parku pro monitoring této cenné části Krkonoš. Výhodou je i to, že ortofota jsou pravidelně každé dva roky pořizována ze státních zdrojů a národní parky je mají volně k dispozici. Nevýhodou je naopak nutnost vlastnit SW pro objektovou klasifikaci, poměrně náročný postup klasifikace a delší výpočetní čas.

Pokud se týká přesnosti klasifikace jednotlivých tříd, tak lze říci, že v žádném z typů dat nebyl problém s klasifikací nevegetačních tříd (kamenná moře a antropogenní plochy, vodní plochy). Dobře byla také většinou vyklasifikována kategorie kosodřevina. Pro detailní legendu dosahovala dobré přesnosti také kategorie subalpínská brusnicová vegetace (v případě ortofot i WV-2). Horší klasifikační výsledky jsme podle očekávání zaznamenali v případě podkategorií třídy subalpínské vysokostébelné trávníky, jejichž spektrální signál je podobný (třtina chloupkatá, bezkolenec modrý, metlice trsnatá).

Na základě výsledků klasifikace jednotlivých kategorií s využitím podrobné a zjednodušené legendy lze učinit závěr, že v případě klasifikace multispektrálních dat s řádově různým prostorovým rozlišením je problém najít takovou kompromisní legendu, která by vyhovovala všem prostorovým rozlišením. Srovnání potenciálu těchto dat na základě jedné legendy tedy není zcela možné a při sestavování legendy vždy musíme její podrobnost vztáhnout k rozlišení dat.

Z porovnání dat s rozdílným spektrálním a prostorovým rozlišením vyplynulo, že velmi vysoké prostorové rozlišení dat je zásadním parametrem pro dosažení vysoké celkové přesnosti klasifikace v detailní úrovni.

Renáta Suchá, Lucie Jakešová, Lucie Kupková,
Lucie Červená
Charles University in Prague, Faculty of Science
Department of Applied Geoinformatics and Cartography
Albertov 6, 128 43 Praha 2
Czech Republic
E-mail: renata.sucha@natur.cuni.cz,
jakesova-lucie@seznam.cz
lucie.kupkova@gmail.com
lucie.cervena@natur.cuni.cz

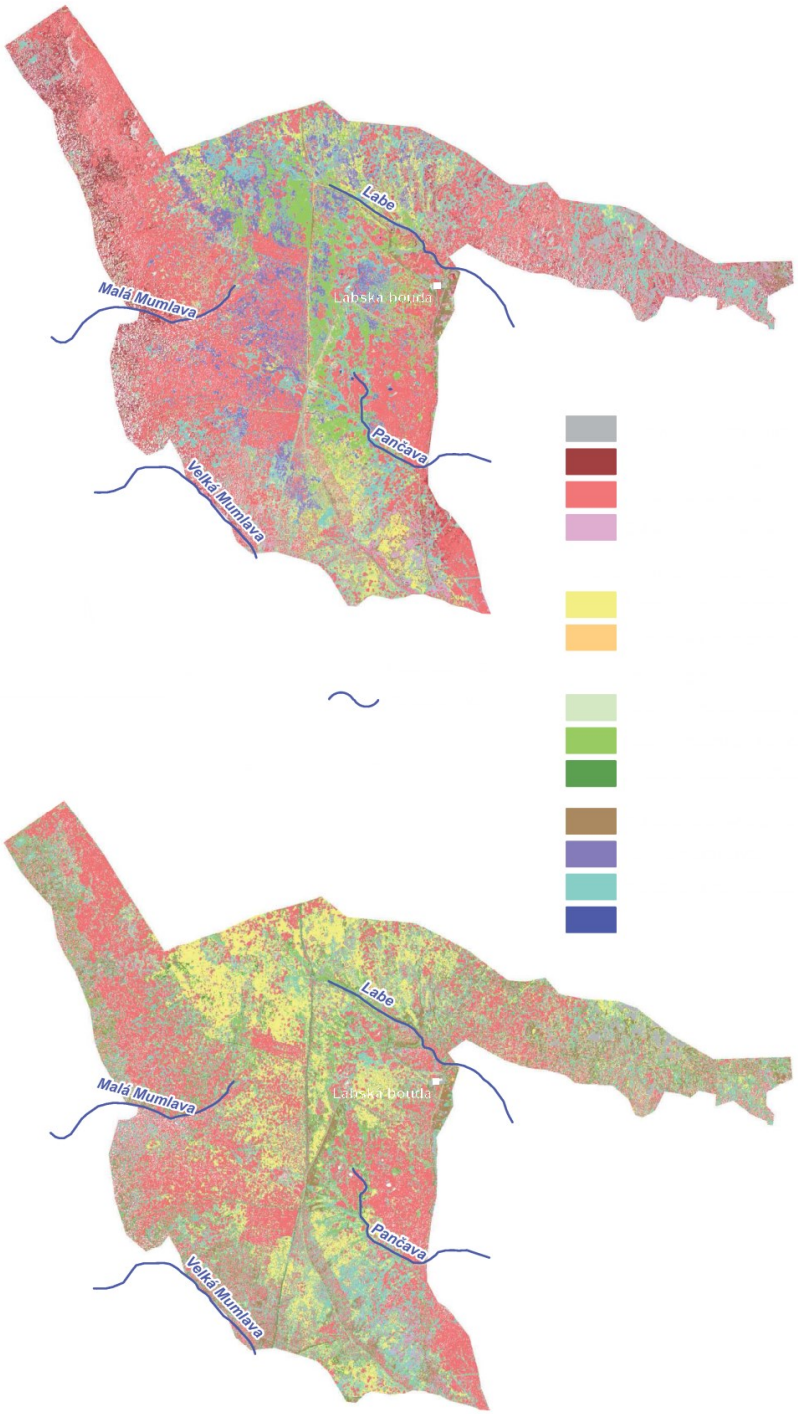

Fig. 4 Classification results for **detailed legend** in **Western** Tundra. Upper figure: **orthoimages – object based** classification SVM (RBF); lower figure: **WordView-2** – **per-pixel** classification SVM (RBF). Source: Authors

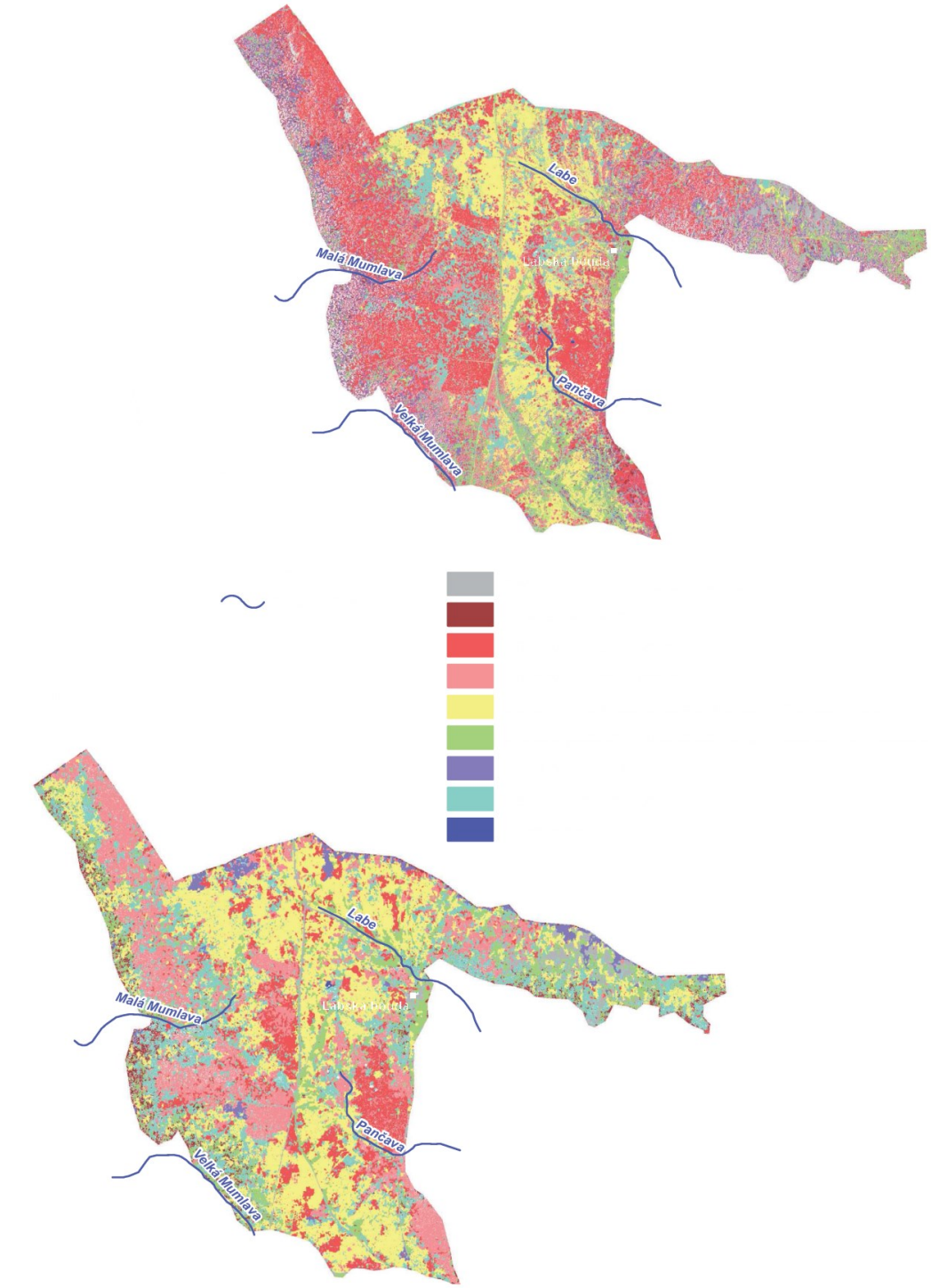

Fig. 5 Results of object based classification SVM (RBF) for **simplified legend** in **Western** Tundra. Upper figure **orthoimages**, lower figure **WordView-2**. Source: Authors

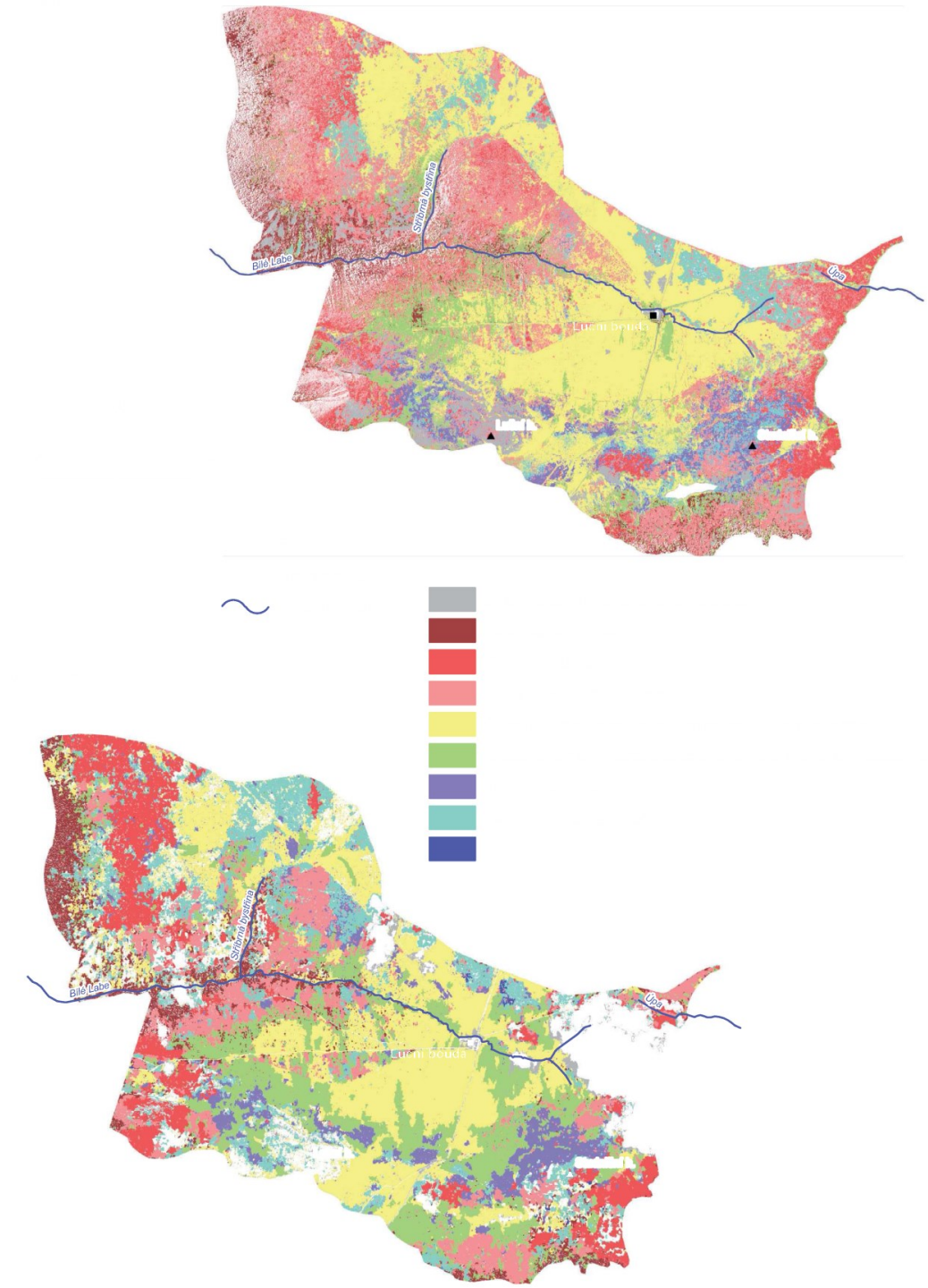

Fig. 6 Results of object based classification SVM (RBF) for **simplified legend** in **Eastern** Tundra. Upper figure **orthoimages**, lower figure **WordView-2**. Source: Authors

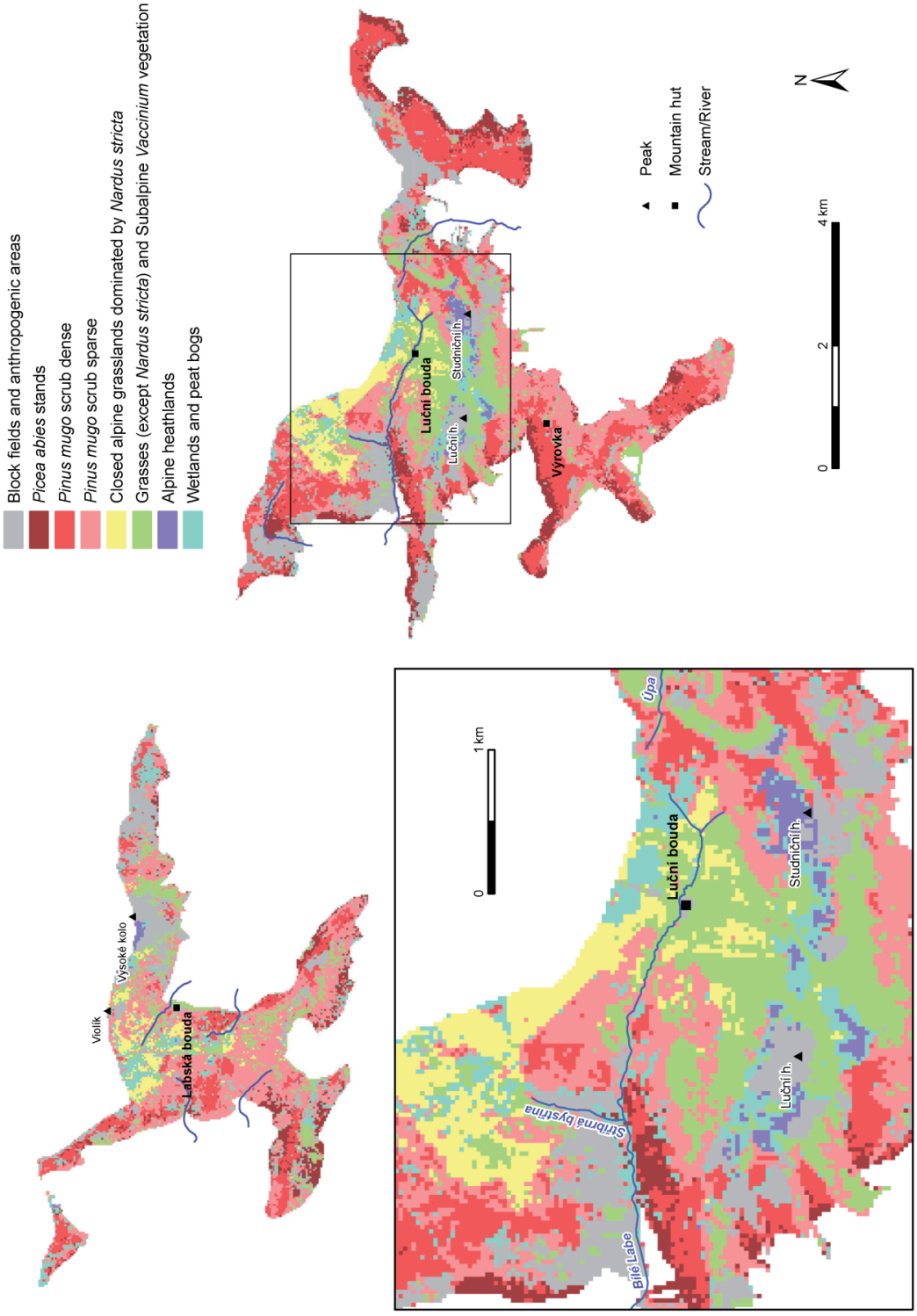

Fig. 7 Classification results for **Landsat 8** – maximum likelihood classifier. Source: Authors

Paper 6: "CLASSIFICATION OF TUNDRA VEGETATION IN THE KRKONOŠE MTS. NATIONAL PARK USING APEX, AISA DUAL AND SENTINEL-2A DATA"

Kupková, Lucie, Lucie Červená, Renáta Suchá, Lucie Jakešová, Bogdan Zagajewski, Stanislav Březina, a Jana Albrechtová. 2017. „Classification of Tundra Vegetation in the Krkonoše Mts. National Park Using APEX, AISA Dual and Sentinel-2A Data". *European Journal of Remote Sensing* 50 (1): 29–46. https://doi.org/10.1080/22797254.2017.1274573.

Author Contributions:

LK – 41%, **LČ – 31%**, RS – 10%, LJ – 9%, BZ – 3%, SB – 3%, JA – 3%

EUROPEAN JOURNAL OF REMOTE SENSING, 2017
VOL. 50, NO. 1, 1274573
http://dx.doi.org/10.1080/22797254.2017.1274573

Taylor & Francis
Taylor & Francis Group

OPEN ACCESS

Classification of Tundra Vegetation in the Krkonoše Mts. National Park Using APEX, AISA Dual and Sentinel-2A Data

Lucie Kupková [a], Lucie Červená [a], Renáta Suchá [a], Lucie Jakešová [a], Bogdan Zagajewski [b], Stanislav Březina [c] and Jana Albrechtová [d]

[a]Faculty of Science, Department of Applied Geoinformatics and Cartography, Charles University in Prague, Albertov 6, Prague 2, Czechia; [b]Faculty of Geography and Regional Studies, Department of Geoinformatics, Cartography and Remote Sensing, University of Warsaw, Krakowskie Przedmieście 30, Warsaw, Poland; [c]The Krkonoše Mountains National Park Administration, Dobrovského 3, Vrchlabí, Czechia; [d]Faculty of Science, Department of Experimental Plant Biology, Charles University in Prague, Viničná 5, Prague 2, Czechia

ABSTRACT

The aim of this study was to evaluate and compare suitability of aerial hyperspectral data (AISA Dual and APEX sensors) and Sentinel-2A data for classification of tundra vegetation cover in the Krkonoše Mts. National Park. We compared classification results (accuracy, maps) of pixel-based (Maximum Likelihood, Suport Vector Machine and Neural Net) and object-based approaches. The best classification results (overall accuracy 84.3%, Kappa coefficient = 0.81) were achieved for AISA Dual data using per-pixel SVM classifier for 40 PCA bands. The best classification results of APEX though were only 1.7 percentage points lower. To get comparable results for Sentinel-2A classification legend had to be simplified. With the simplified legend the accuracy using MLC classifier reached 77.7%.

ARTICLE HISTORY
Revised 22 August 2016
Accepted 28 November 2016

KEYWORDS
Tundra vegetation; The Krkonoše Mountains; Per-pixel classification; Object-based classification; Hyperspectral data; Sentiel-2A

Introduction

Climate change, airborne pollution (e.g. deposition of nitrogen, sulphur, and heavy metals) and habitat loss have been identified as major current threats for biodiversity [Millennium Ecosystem Assessment, 2005; Kłos et al., 2015]. Tundra ecosystems (alpine treeless) belong to the most valuable natural phenomena worldwide. At the same time, biotopes above the treeline are very sensitive to various types of environmental factors. Changes can be very fast in these areas and their dynamics is a good indicator of different types of driving forces. Across the European arctic-alpine tundra areas, changes in vegetation composition and species diversity [Kapfer et al., 2012, 2013], species ranges [Felde et al., 2012], and altitudinal limits of trees and shrubs [Rundqvist et al., 2011; Treml et al., 2012] have been observed over several past decades. Most of these changes have been explained by recent climate changes (warming and reduction of the length of snow cover), or locally by changes of grazing practices or by other human impacts.

Besides botanical studies that are usually limited in space and time, Earth observation has become widely used to trace land cover changes and to identify anthropogenic pressures in protected areas (Nagendra et al. 2015) in the last decades. Recently, new, partly commercial and partly freely available data with very high spatial, good spectral and some of them with also good time resolution, have brought new possibilities for extensive land cover monitoring of rather fragmented extensive tundra biome. Many studies from different areas of the world focusing on tundra ecosystem were published over the last decades. Multispectral data were often used, applying pixel-based, object-oriented, and other special classification methods [Král, 2009; Atkinson and Treitz, 2012; Moody et al., 2014; Reese et al., 2014; Virtanen and Ek, 2014]. Time series of imagery from satellite and aircraft platforms was employed by Lin et al. [2012]. The potential of data fusion – combination of radar data (PolSAR, TerraSAR-X and Radarsat-2) with multispectral Landsat 8 data was tested by Ullman et al. [2014].

While the use of multispectral data (aerial imagery, VHR images like WorldView-2, Ikonos etc.) for vegetation classification has become rather common, utilization of hyperspectral aerial data, especially in the case of tundra, remains scarce. Field spectroscopy intended to distinguish among four arctic tundra plant communities at Ivotuk, Alaska was applied by Bratsch et al. [2016]. A two-step sparse partial least squares and linear discriminant analysis were used for community separation with rather high accuracy (55 – 94%). Halabuk et al. [2013] use field spectroscopy for alpine grasslands with the aim to identify season-dependent relationship between spectral

CONTACT Lucie Kupková lucie.kupkova@natur.cuni.cz Faculty of Science, Department of Applied Geoinformatics and Cartography, Charles University in Prague, Albertov 6, 128 43 Prague 2, Czechia

vegetation indices and aboveground phytomas. Zagajewski [2010] conducted mapping based on aerial hyperspectral data (DAIS 7915 and ROSIS) in the eastern part of the Tatra National Park (Slovakia) with neural net methods.

Remote sensing of vegetation in mountainous areas is rather difficult (great altitudinal difference, steep slopes, cloudy climate etc.) and it is a challenging topic also in the case of tundra in the Krkonoše Mts. This unique southernmost relict area of the arctic-alpine tundra in Europe located in the Czech Republic (50°N, 15°E) is included in the international tundra monitoring program (INTERACT: International Network for Terrestrial Research and Monitoring in the Arctic) [Soukupová et al., 1995; Jeník and Štursa, 2003]. Only few studies using Earth observation for vegetation monitoring in tundra in the Krkonoše Mts. have been published so far. Multispectral orthoimages and maximum likelihood method were used by Müllerová [2005] to detect seven categories: *Pinus mugo* scrub, *Nardus stricta* stands, subalpine tall grasslands and tall-herb vegetation, vegetation along roads, roads, water areas, and wetlands. Hyperspectral data were used by Marcinkowska et al. [2014], who classified tundra and all other types of mountain vegetation in the Szrenica Mount region on the border between Poland and the Czech Republic in the Krkonoše Mts. National Park using APEX data and Support Vector Machines classifier. Jarocińska [2016] carried out an analysis of Krkonoše Mts.' meadows condition. She used APEX images as a base for remote sensing indices, which were verified by field-level acquired data (chlorophyll content, absorption of photosynthetic active radiation, leaf area index, and evapotranspiration).

Our previous study [Suchá et al., 2016] compared suitability of multispectral data with different spatial and spectral resolutions (orthoimages with infrared band, WorldView-2 and Landsat 8) for classifications of vegetation above the tree line in the Krkonoše Mts. National Park. Nevertheless, no study that would use aerial hyperspectral data for the evaluation of tundra vegetation in the Krkonoše Mts. has been published yet. After the Sentinel-2A satellite launch in 2015 there is an additional (freely available) data source with very good spatial, spectral and time resolution that should be examined and compared with other above mentioned available data in tundra vegetation cover classification and research.

The main aim of this study was to evaluate and compare suitability of aerial hyperspectral data (AISA Dual and APEX sensors) and freely available Sentinel-2A data for classification of tundra vegetation cover in the Krkonoše Mts. National Park. Different classification methods (pixel and object-based) were used to find out which classification algorithm for which type of data can bring the most accurate classification results. We expected that the best accuracy will be achieved using hyperspectral data with higher spatial and spectral resolution (AISA Dual). Further assumption was that in the case of Sentinel-2A data with its limited spatial and spectral resolutions some vegetation (especially grassland) categories will not be distinguishable.

Study Area

The highest parts of the Krkonoše Mts. National Park (KRNAP) rise above the treeline (1,300 m a. s. l.) and are covered by relict tundra. It covers an area of 47 km^2 (32 km^2 on the Czech territory, 15 km^2 on the Polish territory), which makes up 7.4% of the total Krkonoše Mts. area. As a result of palaeogeographical history [Treml et al., 2008; Margold et al., 2011], the Krkonoše Mountains represent a "biodiversity crossroads" where Nordic and alpine flora and fauna coexist [Jeník and Štursa, 2003]. Besides the mosses, lichens, and alpine heathlands, the prevailing vegetation types are: closed alpine grasslands dominated by *Nardus stricta*, subalpine tall grasslands, and *Pinus mugo* scrub [Chytrý et al., 2001].

Over the years, the arctic-alpine tundra in the Krkonoše Mts. was affected by human impacts – tundra was expanding due to local agricultural practices that included deforestation and grazing from the 9th century till the beginning of the 19th century [Lokvenc, 1995; Speranza et al., 2000; Novák et al., 2010]. Since early 20th century this human impact has been reduced and the area became strictly protected as a nature reserve. At present, the tundra vegetation is being disturbed by occasional avalanches and debris flows. Fragmented tundra areas are characterized by depauperized species composition under long-term high loads of air-borne nitrogen and sulphur deposition. Observations from the Krkonoše Mts. suggest recent spread of grass *Molinia caerulea* and *Calamagrostis villosa* [Hejcman et al., 2009]. In addition to the shifts in distribution of herb species, expansion of prostrate dwarf pine (*Pinus mugo*) on areas formerly covered by *Nardus stricta*, and expansion of Norway spruce [Harčarik, 2007; Treml et al., 2012] were also recorded.

The Krkonoše tundra has two spatially separated parts: Western and Eastern Tundra. The Western part is situated near Labská bouda and covers about 1,284 hectares. The Eastern part is located around Luční bouda covering 2,284 hectares. Both parts of tundra were examined in full using the Sentinel-2A data (Fig. 1). The computational demands of hyperspectral data processing required creation of a spatial subset in order to facilitate the classifications using AISA and APEX data. This area of interest is located in the Eastern Tundra and covers 656.5 hectares. The boundaries follow the contour lines

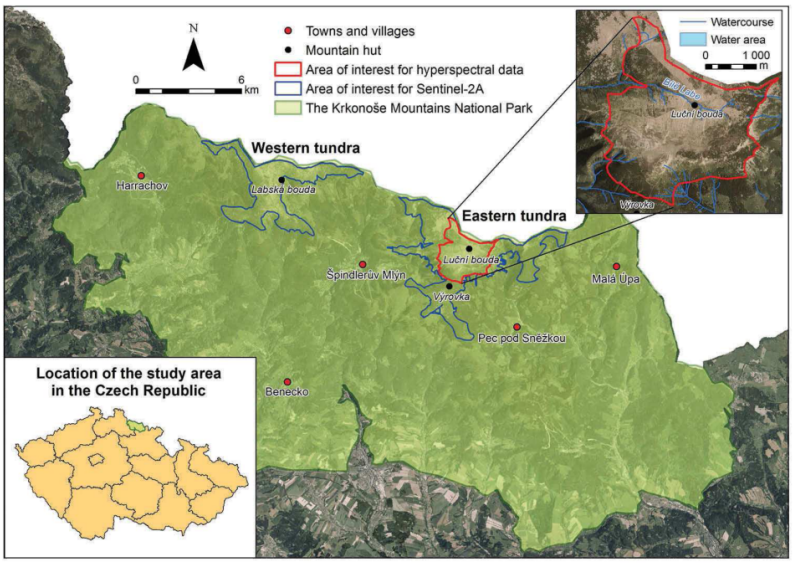

Figure 1. Study areas of Western and Eastern tundra in the Krkonoše Mts.

1,300 m a. s. l. and 1,475 m a. s. l. south of the Luční hora mountain and marked escarpments (Obří důl, deep valleys, etc.) to avoid unwanted shadows – see Figure 1.

Data

Image data

Data from three sensors were used and compared in this study. Aerial hyperspectral image data are represented by two sensors with different spectral resolution and very high spatial resolution. These are APEX (Airborne Prism EXperiment) data acquired on September 10, 2012, and AISA Dual data acquired on June 19, 2013. Besides multispectral data with high spatial resolution, also freely available satellite data from Sentinel-2A sensor were used. The Sentinel-2A cloud-free image acquired on August 30, 2015 was downloaded from Sentinel SciHub as level -1C product. Table 1 shows basic features of all the data used.

Reference data

Reference data were collected during two periods, one in June 23 –25, 2014 and second in July 7–11, 2015. Finally, 123 polygons corresponding to vegetation categories as defined in the detailed legend (for legend definition see chapter Methods) were identified by botanist in the field and recorded using the GNSS system (Trimble Geoexplorer 3000 Geo XT, accuracy 10 centimetres). Polygons corresponding to categories *Pinus mugo* scrub, *Picea abies* stands, water and block fields and anthropogenic areas were added later using manual vectorization based on visual interpretation of orthoimages acquired in June 2012. Samples for all categories were collected in accordance with the categories' spatial distribution and abundance equally in the entire study area.

Table 1. Basic features of the image data used in this study.

Sensor	Number of used bands	Wavelength range	Spatial ground resolution	Acquisition date
APEX	288	400 nm - 2,500 nm	2 to 5 m	09/10/2012
AISA Dual	494	400 nm - 2,500 nm	1 to 3 m	06/19/2013
Sentinel-2A	10	400 nm - 2,300 nm	10 and 20 m	08/30/2015

The dataset collected in the field and completed with polygons added on the basis of orthoimages visual interpretation was divided into training and validation parts. Many studies deal with number of training samples (e.g. Camps-Valls et al. [2004], Pal and Mather [2005], Waske et al. [2010]). They recommend different shares of training and validation data. According to some of them (Pal and Mather [2005]) SVM method works very well with low number of training data (from 20 - 30% of) while this share is not ideal for other classification methods. Based on our experiences (Zagajewski [2010], Suchá et al. [2016]) we used 40% of our data collected in the field for training and 60% for validation in the case of all data types' classifications based on the detailed legend in the Eastern Tundra (Figure 4). Fifty one polygons (11,388 m^2) were used as training dataset and the classification accuracies were assessed by seventy two validation polygons (17,129 m^2), both representing all eleven categories. As a next step, these training and validation datasets were adjusted

to different image data (rasterized to Regions of Interest and edited when needed) – see the chapter Methods.

Regarding the Sentinel-2A data classified according to the simplified legend the training as well as validation data were different (Figure 4). As Sentinel-2A data have significantly bigger pixel than used hyperspectral data the lower number of training pixels could decrease the classification accuracy of Sentinel-2A image. To increase the number of training data polygons based on the visual interpretation of orthoimages were used for training phase. It was possible because the categories of simplified legend were recognizable from the orthoimages. Field dataset from 2014 (available data for the whole tundra area) was used for validation. The final dataset for Sentinel-2A classification based on simplified legend was set from 7,057 pixels in 73 polygons (i.e. 705,700 m^2) for training and 2,106 pixels in 110 polygons (i.e. 210,600 m^2) for validation.

Methods

Classification legend

Detailed classification legend including the most important categories of grassland vegetation as well as other vegetation and non-vegetation categories was created in cooperation with the National Park botanists. The legend contains the following eleven categories:

1. Block fields and anthropogenic areas
2. *Pinus mugo* scrub (Mountain pine)
3. Subalpine *Vaccinium* vegetation (Blueberries, cranberries and bog bilberries)
4. Closed alpine grasslands*
4a. *Nardus stricta* stands (Matgrass)
4b. Species-rich vegetation with high cover of forbs
5. Subalpine tall grasslands*
5a. *Calamagrostis villosa* stands (Hairy reed grass)
5b. *Molinia caeruela* stands (Purple moor grass)
5c. *Deschampsia cespitosa* stands (Tufted hair grass)
6. Alpine heathlands
7. Wetlands and peat bogs
8. Water areas (not for Sentinel-2A)

* Group categories that were not classified

For the pictures of the detailed legend categories see Figure 2. This detailed legend was used for classifications of all the image data (AISA Dual, APEX and Sentinel-2A) in Eastern tundra (see Figure 4). Moreover, the simplified legend with grouped categories specifically created for Landsat 8 classification in Suchá et al. [2016] was used in this study for Sentinel-2A image classification of the whole Krkonoše tundra area (Figure 4). We wanted to check if simplified legend can lead to better classification results than the detailed one in the case of Sentinel-2A data that have lower spatial and spectral resolution in comparison with other used types of data.

The simplified legend contains the following eight categories:

1. Block fields and anthropogenic areas
2. *Picea abies* stands (Norway spruce)
3a. *Pinus mugo* scrub dense (more than 80% of total cover)
3b. *Pinus mugo* scrub sparse (30 – 80% of total cover)
4. Closed alpine grasslands dominated by *Nardus stricta*
5. Grasses (except *Nardus stricta*) and subalpine *Vaccinium* vegetation
6. Alpine heathlands
7. Wetlands and peat bogs

Image data pre-processing

The geometric, radiometric, and atmospheric corrections of hyperspectral image data were conducted by the data providers. In the case of APEX data it was the VITO company (Flemish Institute for Technological Research), the procedure of data pre-processing is described in detail by Schaepman et al. [2015], Sterckx et al. [2016] and Vreys et al. [2016a; 2016b]. In the case of AISA Dual it was Geodis Brno; the pre-processing methods are summed up in the internal technical report [AISA, 2013] and include in-flight calibration data, field spectrometric measurements using ASD FieldSpec 3, and digital elevation model. ENVI/IDL and CaliGeoPro software were used to carry out the corrections. The geometric correction of Sentinel-2A data was ensured by using Level-1C product which includes also orthorectification that makes use of a Digital Elevation Model and transforms the image into cartographic coordinates [European Space Agency, 2015]. Atmospheric correction of Sentinel-2A Top Of Atmosphere reflectance data was not carried out because it is not necessary when all the images are classified separately [Song et al., 2001].

Stacking of AISA Eagle (400 – 1,000 nm, 254 spectral bands) and AISA Hawk (978 – 2,451 nm, 244 spectral bands) data into one file constituted the next step in hyperspectral data processing. In the overlapping part of the spectra for both sensors, the data from AISA Eagle with higher spectral and spatial resolutions have been kept. Consequently, the resulting image consists of 494 bands (out of original 498) and its spatial resolution is 1 m. To cover the study area spatially with the aerial hyperspectral data, a mosaic from four flight lines of AISA Dual data and from two flight lines of APEX data respectively (after exclusion of the zero value bands) was created and

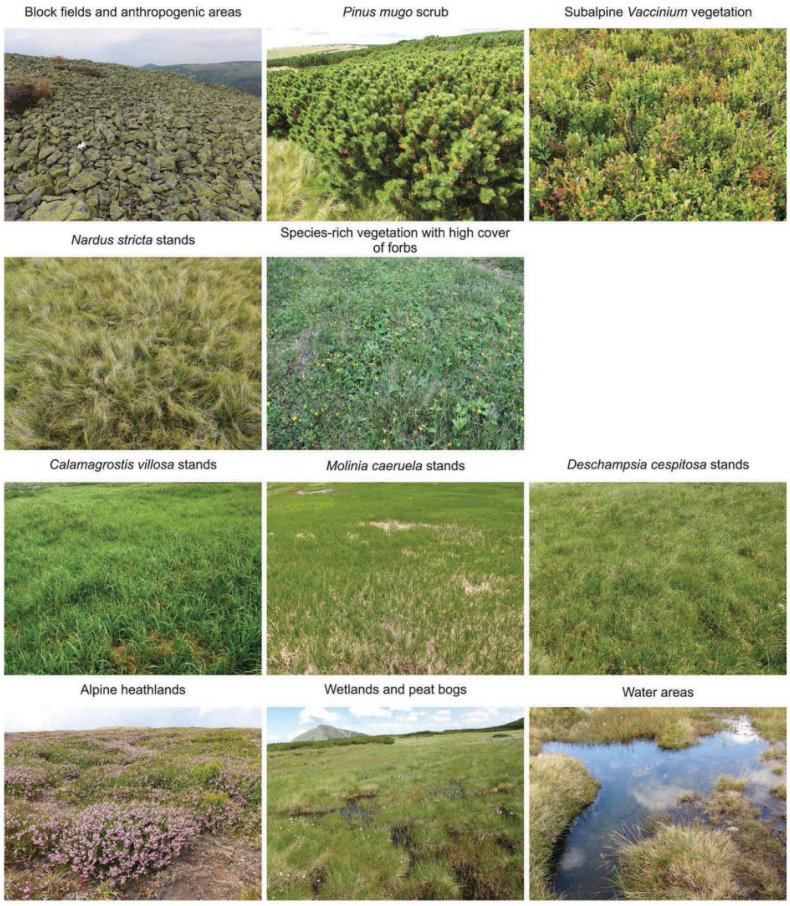

Figure 2. Pictures of vegetation categories as defined in the detailed legend.

colour balancing was performed. The edges of the flight lines with the biggest distortions were not included.

Finally, to reduce data dimensionality and avoid information redundancy, Principal Component Analysis (PCA) procedure was applied. This is a mathematical process that transforms correlated bands into a new image set of uncorrelated principal components. All image bands were transformed into PCA space. For the classification purposes first few components containing almost all the original information (in the case of APEX data 5 PCA components, in the case of AISA data 7 PCA components) were used. Based on results of tests with number of bands entering the classification also 40 PCA transformed bands were used for both data types classification.

Reference data adjustment

In order to improve classification results based on polygons collected in the field, the training polygons were visualized in the feature space for first few principal components and edited. Firstly, the informational categories from the legend were divided into more spectral categories, e.g. the category "block fields and anthropogenic areas" was divided in the case of AISA Dual data to the spectral categories: asphalt road, block fields, and buildings. Also the vegetation categories were divided into more spectral categories in case of marked differences. In total, 21 spectral categories were created for AISA data and 23 for APEX data. Secondly, outliers were erased from the clusters of all spectral categories so that these would consist from similar pixels. Feature spaces for the first two components of AISA and APEX before and after the edits are shown in Figure 3. Finally, the spectral categories were aggregated to form the categories as shown in the legend.

Because big Sentinel-2A pixels don't follow the boundaries of reference polygons identified in the field the field dataset had to be adjusted for Sentinel-2A classification (training and validation

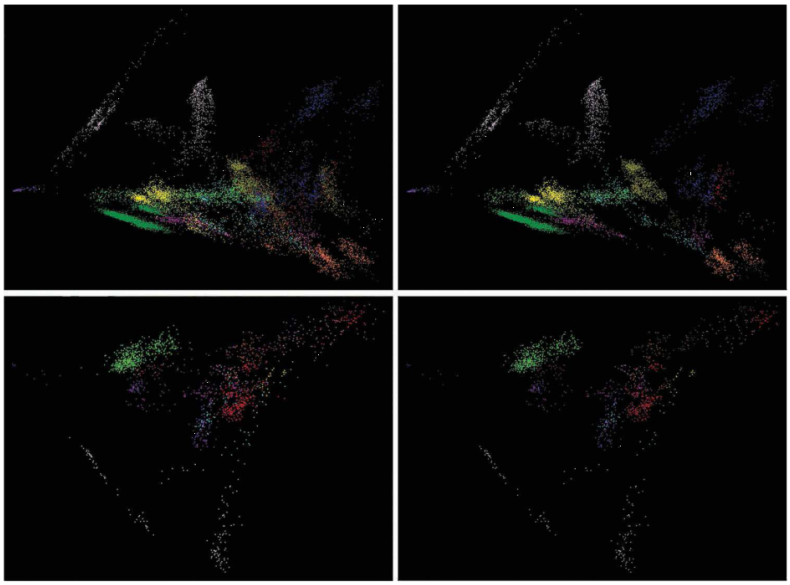

Figure 3. Feature space for training dataset for AISA Dual (top) and APEX (low) data before (left) and after (right) the edits. X axis is the first principal component and Y axis the second one; both combined explain 99.4% of variability in the case of AISA Dual data and almost 100% in the case of APEX data.

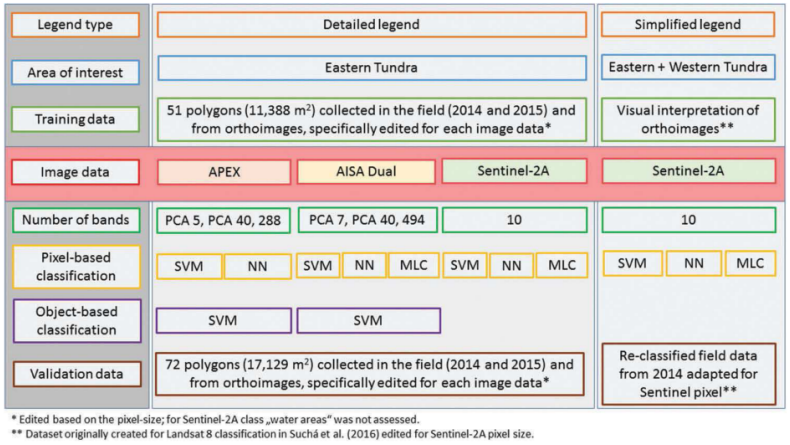

Figure 4. Workflow of data analysis.

data for the detailed legend and validation data for simplified legend) based on visual interpretation of orthoimages. When surrounding area of polygon was identified as the same category as the polygon, the pixel was kept in the training/validation dataset. On the contrary, pixels that contained any different category were not used.

The last adjustment is concerned with water areas. Water areas were not classified from Sentinel-2A image because they are very small. Their extent is usually less or equal to one Sentinel-2A pixel, thus, it was not possible to get enough pixels for training and validating the classifications.

Classification methods and parameters

Two approaches to classifications were tested – per-pixel and object-based ones. As already proved in our previous study [Suchá et al., 2016], the object-based classification can bring very good results for the data with very high spatial resolution (e.g. orthoimages). On the other hand, for larger pixels this approach is

not appropriate as mentioned for example by Blaschke [2010]. In this study, hyperspectral data (APEX, AISA Dual) were classified by object-based approach as well as by pixel-based algorithms (Maximum likelihood, Support Vector Machine, Neural Network). Sentinel-2A data were classified only by per-pixel algorithms. All the algorithms were performed using ENVI 5.3 software and are described in detail in the following text. Parametrization of the classification methods was in general performed in accordance with many analogue studies (Pal and Mather [2005]; Petropoulos et al. [2012], Zhou and Yang [2008]) based on a set of tests. We run all the classification algorithms many times, different number of bands and different settings of parameters were tested (always only one parameter was gradually changing while other parameters stayed the same) and several final sets of parameters' combinations that produced the best (or very good) classification results for each classification method are introduced in the chapter Results (see also Tabs. 2 and 3).

Regarding the original bands as inputs to the classification processes the following bands were used: AISA Dual – all 494 bands, APEX – all bands excluding the zero value bands no. 150–153 and 201–212, Sentinel-2A – all 10m and 20m bands (i.e. 10 bands; 60m bands for atmosphere evaluation were not used). In addition, for hyperspectral data 5 and 40 PCA transformed bands for APEX, resp. 7 and 40 PCA transformed bands for AISA Dual were used for classifications.

Above described phases of the data analysis are schematically shown in Figure 4.

Maximum Likelihood classification (MLC)

To apply successfully this widely used algorithm, two conditions have to be met. First, the image data should show normal distribution [Fernandez-Prieto et al., 2006]. Second, the training samples' statistical parameters (e.g., mean vector and covariance matrix) should truly represent the corresponding land cover category [Duarte et al., 2005].

MLC Classifier was used for Sentinel-2A classification, for APEX and AISA Dual PCA transformed data. ENVI software allows to set just one parameter – probability threshold which was not used.

Table 2. Parameters of neural network algorithm.

Parameter	default	user defined
Number of hidden layers	1	1
Activation function	LOG	LOG
Training Threshold Contribution	0.9	0.9
Training Rate	0.2	0.9
Training Momentum	0.9	0.1
Training RMS Exit Criteria	0.1	0.05
Number of Iterations	1000	5000

Table 3. Segmentation parameters.

AISA Dual	
Scale level	60
Merge level	80
Texture kernel size	3 × 3
APEX	
Scale level	50
Merge level	85
Texture kernel size	3 × 3

Support Vector Machines algorithm (SVM)

The SVM algorithm is a machine learning classification algorithm that belongs among supervised non-parametric methods, which means that no particular data distribution is required (e.g. normal distribution). It is based on the statistical learning theory and aims to find the best hyperplane in a multi-dimensional feature space that optimally separates categories. The term "best hyperplane" is used to refer to a decision boundary obtained in a training step and minimizing misclassifications. Training samples used for construction of hyperplane are called support vectors. These lie on the margin of categories to be classified and are extracted automatically by the algorithm [Camps-Valls et al., 2004; Jones and Vaughan, 2010; Mountrakis et al., 2011; Petropoulos et al., 2012].

All three kernel types (radial basic functions (RBF), linear, polynomial) available in ENVI software were tested. The best results were achieved using the RBF kernel type. Two basic parameters affecting the classifications results are Gamma in kernel function and penalty parameter. The penalty parameter controls the trade-off between allowing training errors and forcing rigid margins. Increasing value of the penalty parameter increases also the cost of misclassifying points and causes ENVI to create a more accurate model that may not generalize well (https://www.harrisgeospatial.com/docs/supportvectormachine.html).
After the series of tests evaluated by classification accuracy results the default parameters were used similarly like in Petropoulos et al. [2012]. It means that gamma kernel was set up as an inverse number of the number of bands in the input image (e.g. for 40 bands of PCA images it was 0.025) and the penalty parameter was 100. Classification probability threshold and pyramid levels were not used.

Neural Network algorithm (NN)

NN algorithm also belongs among machine learning non-parametric methods. It is designed to simulate human learning process by establishing linkages between input and output data via one or more hidden layers. The basic unit of each layer is called neuron (node) [Benediktsson et al., 1990]. The classic model of a feed-forward multilayer neural network, known as multilayer perception (MLP), features fully-connected neurons among all layers (input, output,

and hidden), which means that each neuron of a given layer feeds all neurons in the next layer [Camps-Valls et al., 2004]. This model is used in our processing tool, ENVI 5.3 software.

To ensure maximal classification accuracy different NN architectures and full set of parameters in ENVI during the network training and optimization were tested. The tests were based mainly on our previous experiences [Suchá et al., 2016] and recommended settings from literature (for example Ndehedehe et al., [2013], Zhou and Yang, [2008], Wan-Kadir et al., [2011]). Finally, single layer feed-forward architecture, logistic activation function and parameter configurations shown in Table 2 were used. The first one (ENVI default) best performing for the simplified legend uses the low training rate parameter, which decreases the risk of oscillations or non-convergence of the training result but increases the computation time necessary for the algorithm training phase. ENVI default setting on the other hand uses high value of training momentum which trains larger steps than lower values of momentum rate. It encourages weight changes along the current direction. A setting with opposite values of these two important criteria (training rate and training momentum) provided the best results for classifications based on detailed legend. The parameter training threshold contribution which adjusts the changes to a node's internal weight remains unchanged on quite high level which could result in better classification but worse generalization. (https://www.harrisgeospatial.com/docs/neuralnet.html)

Object-based image classification

The object-based image analysis (OBIA) works with homogeneous clusters of pixels called segments. Segments are areas generated by one or more criteria of homogeneity. Thus, compared to single pixels, segments include additional spectral information (e.g. mean values per band, minimum and maximum values, mean ratios, variance etc.) [Blashke, 2010].

The edge algorithm, where images are divided on the bases of Sobel's method of edge detection, was used for images segmentation. Edge segmentation algorithm is recommended in manual of used software for optical image data (http://www.harrisgeospatial.com/docs/FXRuleBasedTutorial.html). Segmentation parameters had to be set in accordance with spatial resolution and in order to avoid overlap of two different training polygons into one segment. After testing of several combinations *Scale Level* was set on 60 and *Merge Level* on 50 for AISA Dual and on 50, respectively 85 for APEX.

Segmentation was carried out using all bands and also 40 bands from PCA transformation for APEX and 7 PCA bands for AISA Dual data in ENVI software, Feature Extraction extension. The applied parameters are listed in Table 3.

Based on our previous experience [Jakešová et al., 2014] the example-based approach that sorts segments into pre-defined categories using training areas (segments) and selected attributes was employed using the support vector machine algorithm and radial basis function with default setting (RBF). In accordance with Jakešová et al. [2014] example-based approach was able to classify all categories of the detailed legend while detection of some grassland categories (Species-rich vegetation with high cover of forbs, *Calamagrostis villosa* stands, *Deschampsia cespitosa* stands) was not possible using rule-based approach.

Texture is one of the important characteristics in image objects identification [Haralick et al., 1973] and textural parameters may contribute for classification accuracy improvement, especially in the case of low spectral variability between the classified categories. Therefore, beside spectral also textural parameters were extensively tested with the intention to better distinguish spectrally similar grassland categories. We used following spectral and textural attributes for all input bands (same as for segmentation process): Spectral Mean, Spectral Max, Spectral Min, Spectral STD, Texture Range, Texture Mean, Texture Variance, and Texture Entropy.

Results

Results are summarized in the Tables 4 – 9 and error matrices for the best classifications of each data type are in Appendix.

Per-pixel classification - APEX data

The best classification results for the APEX data were obtained by SVM classifier for forty components of PCA (Table 4); the overall accuracy reached 82.59% (Kappa coefficient = 0.79). When different categories of the legend are compared (Table 9), the categories "Block fields and anthropogenic areas", "Water areas" and "*Pinus mugo*" show the best results. The user's and producer's accuracies exceeded 90% in all cases.

Table 4. Results of different classification methods for the APEX data in the Eastern Tundra of the Krkonoše Mts. (detailed legend).

Classification method	Overall accuracy (%)	Kappa coefficient
PCA - 5 bands		
SVM	71.67	0.67
NN (default)	56.81	0.6
NN (user defined)	66.34	0.59
PCA - 40 bands		
SVM	82.59	0.79
NN (default)	26.60	0.002
NN (user defined)	68.78	0.63
all bands		
SVM	77.7	0.74

On the contrary, the category "*Subalpine Vaccinium vegetation*" shows the worst results of all. Though the user's accuracy equalled 100%, the producer's accuracy reached only 8.5%. The most common overlaps were between grassland categories.

Good result was also obtained by SVM classification of all APEX bands. Overall accuracy reached 77.7% (Kappa coefficient = 0.74), while the MLC classifier failed and did not produced any satisfactory results.

Per-pixel classification - AISA Dual data

AISA Dual data with the highest spatial and spectral resolutions in this study gave good results with overall accuracies above 70% for all classification methods (Table 5). The best results were obtained by SVM classifier, especially when 40 components of PCA transformation of original data were used (overall accuracy 84.31%). On the other hand the application of 40 components of PCA, Maximum Likelihood Classifier did not work well – a lot of unclassified places remained in the output. The SVM algorithm was also tested on the original set of 494 bands but the process proved to be quite time consuming and the results were no better than with the transformed data.

As expected, the categories "Block fields and anthropogenic areas", "Water areas" and "*Pinus mugo*" showed the highest classification accuracies (Table 9). On the contrary, grassland categories were often mixed together. Considering all the classifications, the worst results were obtained for "*Subalpine Vaccinium vegetation*" and "Species-rich vegetation with high cover of forbs". The category "*Calamagrostis villosa* stands" showed very low level of producer's accuracy.

Per-pixel classification - Sentinel-2A data

The Sentinel's pixel size (10 and 20 metres) does not wholly meet the requirements for the detailed classification of tundra vegetation in the Krkonoše Mts.

Table 5. Results of different classification methods for the AISA Dual data in the Eastern Tundra of the Krkonoše Mts. (detailed legend).

Classification method	Overall accuracy (%)	Kappa coefficient
PCA - 7 bands		
MLC	76.51	0.72
SVM	77.77	0.73
NN (default)	67.15	0.61
NN (user defined)	72.37	0.67
PCA - 40 bands		
SVM	84.31	0.81
NN (default)	72.68	0.67
NN (user defined)	72.29	0.67
all bands		
SVM	74.24	0.69

Table 6. Results of different classification methods for Sentinel-2A data in the Eastern Tundra of the Krkonoše Mts. (detailed legend).

Classification method	Overall accuracy (%)	Kappa coefficient
all bands 10 a 20 m		
MLC	53.64	0.47
SVM	57.62	0.51
NN (default)	53.86	0.48
NN (user defined)	58.27	0.52

National Park. The overall accuracies reached 50 to 60% (Table 6). Only the categories "Block fields and anthropogenic areas" and "*Pinus mugo*" did not show classification problems (Table 9). Low abundance of the category "Species-rich vegetation with high cover of forbs" in the observed area and its location along the paths in the Eastern Tundra determined the worst results. Looking at the best classification output obtained by NN Classifier, the category "*Molinia caeruela* stands" with the lowest producer's accuracy was often classified as "*Deschampsia cespitosa* stands" and "*Subalpine Vaccinium vegetation*". Also the categories "Alpine heathlands", "*Calamagrostis villosa* stands" and "*Nardus stricta* stands" show low producer's accuracy and not very high user's accuracy.

To get better results from the Sentinel-2A data, the simplified legend, which is more suitable for the pixel size of the data, was tested (Table 7). The categories "*Pinus mugo* scrub dense", "Alpine heathlands", "*Picea abies* stands", and "Block fields and anthropogenic areas" were classified best with user's and producer's accuracies reaching more than 80%. On the contrary, the category "*Pinus mugo* scrub sparse" shows rather low user's accuracy (40%) although the producer's accuracy equalled almost 90%. It means that "*Pinus mugo* scrub sparse" was overclassified, largely instead of "Wetlands and peat bogs", "Grasses (except *Nardus stricta*)" and "Subalpine *Vaccinium* vegetation". It illustrates well the problems brought by larger size of pixels – "*Pinus mugo* scrub", of course, does not respect pixel edges and the surrounding vegetation included in the pixel (mixel) affects the final reflectance.

Object-based approach – APEX and AISA Dual data

Object-based classification was used for APEX and AISA Dual data in Eastern Tundra (detailed legend).

Table 7. Results of different classification methods for the Sentinel-2A data in the Eastern and Western Tundra of the Krkonoše Mts. (simplified legend).

Classification method	Overall accuracy (%)	Kappa coefficient
all bands 10 a 20 m simplified legend		
MLC	77.73	0.74
SVM	70.99	0.67
NN (default)	76.21	0.73

Table 8. Results of object-based classification (SVM RBF) for APEX and AISA Dual data in the Eastern Tundra of the Krkonoše Mts. (detailed legend).

Classification method	Overall accuracy (%)	Kappa coefficient
APEX all bands	62.93	0.56
APEX 40 bands	71.03	0.65
AISA Dual 7 bands	80.66	0.77

Table 8 clearly shows that AISA Dual data for 7 components of PCA brings better results than classifications of the APEX data. The overall accuracy reached 80.66% (Kappa coefficient = 0.77). The best classification results were again achieved for the categories "Block fields and anthropogenic areas", "Water areas" and "*Pinus mugo*" – both the user's and producer's accuracies exceeded 95% in all cases (Table 9). On the contrary, the category "Species-rich vegetation with high cover of forbs" showed the worst results. The most common overlaps were with "*Deschampsia cespitosa* stands". The grassland categories, namely the categories "*Nardus stricta* stands" and "*Calamagrostis villosa* stands" show very good results with producer's and user's accuracies ranging between 73% and 83%.

Results summary

When comparing APEX, AISA Dual, and Sentinel-2A data and methods used for classifications, the best overall accuracy was reached for AISA Dual data using per-pixel SVM classification from 40 PCA bands (overall accuracy 84.3%, Kappa coefficient = 0.81). The difference of the best classification results of APEX compared to AISA Dual was only 1.7 percentage points. Best result of object-based classification (for AISA Dual) brought overall accuracy only about 4 percentage points worse than in the case of per-pixel classification and 10 percentage points better result for AISA Dual than for APEX data. The best result of Sentinel-2A classification for the same detailed legend as for hyperspectral data (NN classifier) reached about 26 percentage points lower accuracy than the best classification result (AISA Dual). On the other hand, with the simplified legend the accuracy using MLC classifier reached 77.7%.

When it comes to the detailed legend categories (Table 9) "Block fields and anthropogenic areas", "Water areas", and "*Pinus mugo*" were classified best with the highest user's and producer's accuracies in the case of both per-pixel and object-based approaches. As for grassland categories generally for the both pixel-based and object-based classifications of all the data types rather bad results were obtained for category "Species-rich vegetation with high cover of forbs". But we have to emphasize that two grassland categories – "*Nardus stricta* stands" and "*Deschampsia cespitosa* stands" – were classified satisfactory from hyperspectral data in the case of both pixel based and also object based methods. OBIA produced the best result in the case of "*Callamagrostis villosa* stands", much better than pixel based classifications. "*Molinia caeruela* stands" were classified best from AISA Dual by pixel based approach. In general, worse results were obtained for grassland categories that often became mixed ("*Calamagrostis villosa* stands", "*Molinia caeruela* stands"). Such results, however, are not surprising from the botanical point of view as these categories represent grasses of similar plant habitus.

As for non-grassland vegetation categories good results for hyperspectral data and all the methods were obtained for category "Alpine heathland" while bad results for "Subalpine *Vaccinium* vegetation". Category "Wetlands and peat bogs" was very satisfactory classified even from Sentinel-2A data.

Map outputs

Figures 5 and 6 show final land cover maps for the best classification results. Figure 5 combines outputs from per-pixel and object-based classifications. Comparison shows that both per-pixel and object-based classification outputs for the same data types are very similar (e.g. both classifications for APEX and both

Table 9. Classification accuracies of specific categories for the best classification results (detailed legend).

	pixel-based classification						OBIA	
Data and classification method	APEX (SVM 40 PCA bands)		AISA (SVM 40 PCA bands)		Sentinel-2A (NN)		AISA (SVM 7 PCA bands)	
Class	PA (%)	UA (%)	PA (%)	UA (%)	PA (%)	UA (%)	PA (%)	UA (%)
1. Block fields and anthropogenic areas	98.60	100.00	99.25	98.58	92.68	95.00	99.93	95.11
2. *Pinus mugo* scrub	99.86	94.78	99.96	98.45	100.00	88.51	100.00	99.36
3. Subalpine *Vaccinium* vegetation	8.54	100.00	63.90	50.19	65.38	45.95	53.15	87.66
4a. *Nardus stricta* stands	73.44	86.01	83.73	71.38	46.02	54.17	79.24	73.27
4b. Species-rich vegetation with high cover of forbs	86.84	44.59	55.32	60.00	50.00	35.29	81.22	33.06
5a. *Calamagrostis villosa* stands	63.95	49.74	55.03	87.29	31.82	43.75	76.20	82.62
5b. *Molinia caeruela* stands	64.54	59.87	66.78	75.22	15.00	60.00	79.15	44.94
5c. *Deschampsia cespitosa* stands	87.31	68.25	85.10	85.81	57.50	26.44	63.49	89.76
6. Alpine heathlands	90.36	82.14	81.60	83.80	37.78	42.50	66.11	73.13
7. Wetlands and peat bogs	58.56	80.30	63.46	86.74	56.76	91.30	40.24	85.07
8. Water areas	100.00	100.00	98.80	100.00	x	x	100.00	100.00

* PA = Producer's accuracy, UA = User's accuracy

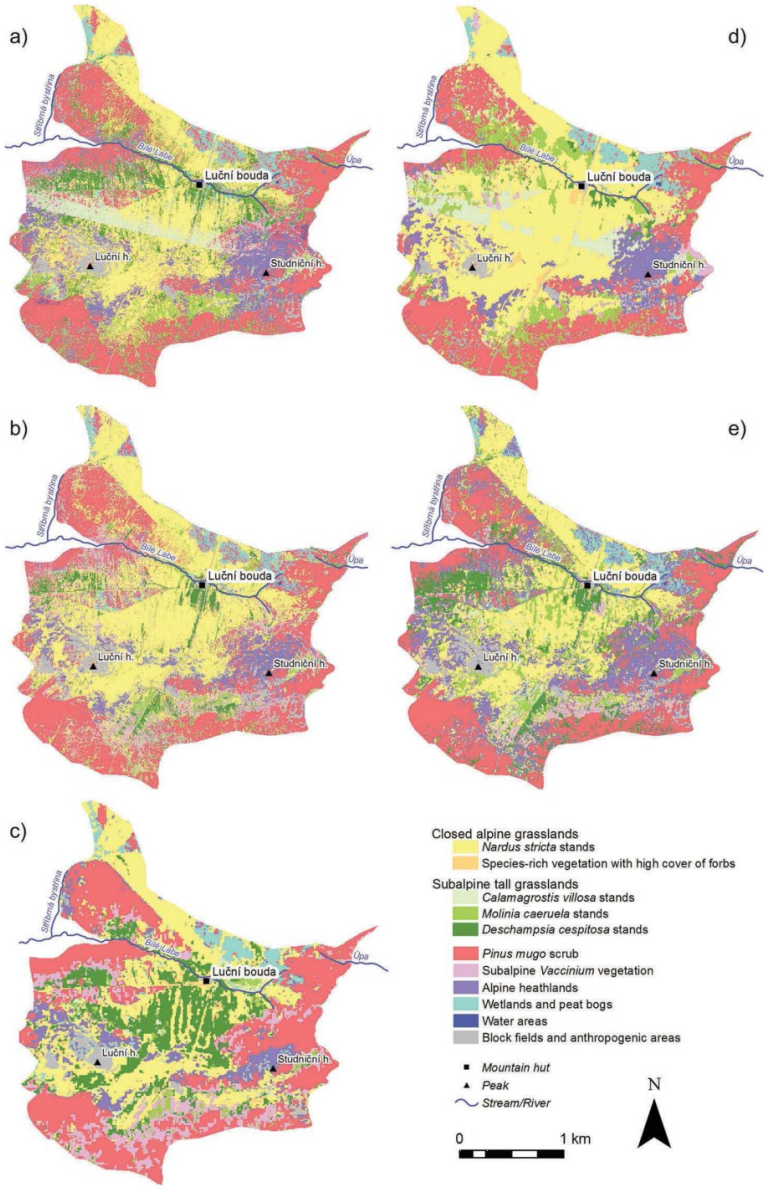

Figure 5. Maps of land cover in the Eastern Tundra of the Krkonoše Mts. for the best classification results of per-pixel and object-based approaches: a) per-pixel classification: APEX data, SVM classifier, 40 PCA bands; b) per-pixel classification: AISA Dual data, SVM classifier, 40 PCA bands; c) per-pixel classification: Sentinel-2A data, NN classifier (user defined); d) object-based classification: APEX data, SVM classifier, 40 PCA bands; e) object-based classification: AISA Dual data, SVM classifier, 7 PCA bands.

classifications for AISA DUAL). Classification output for Sentinel-2A is very similar to the APEX per-pixel map though with recognizable different pixel spatial resolution. Certain differences between APEX and AISA Dual data can be identified. In the case of both per-pixel and object-based classification maps of the APEX category "*Calamagrostis villosa* stands" was classified in the middle of the map (east-west direction) while on the AISA Dual map the same category is absent and different categories were classified instead. This difference may have been partly caused by problematic colour balancing on the borders of two flight lines of APEX data and possibly also by the seasonal abundance of *Calamagrostis villosa* as APEX and AISA data were acquired in different periods of year.

The outputs of Sentinel-2A MLC classification for both Eastern and Western parts of tundra based on simplified legend are shown in Figure 6. It is not possible to compare this output with maps in Figure 5 as the legend is different. However, the comparison of

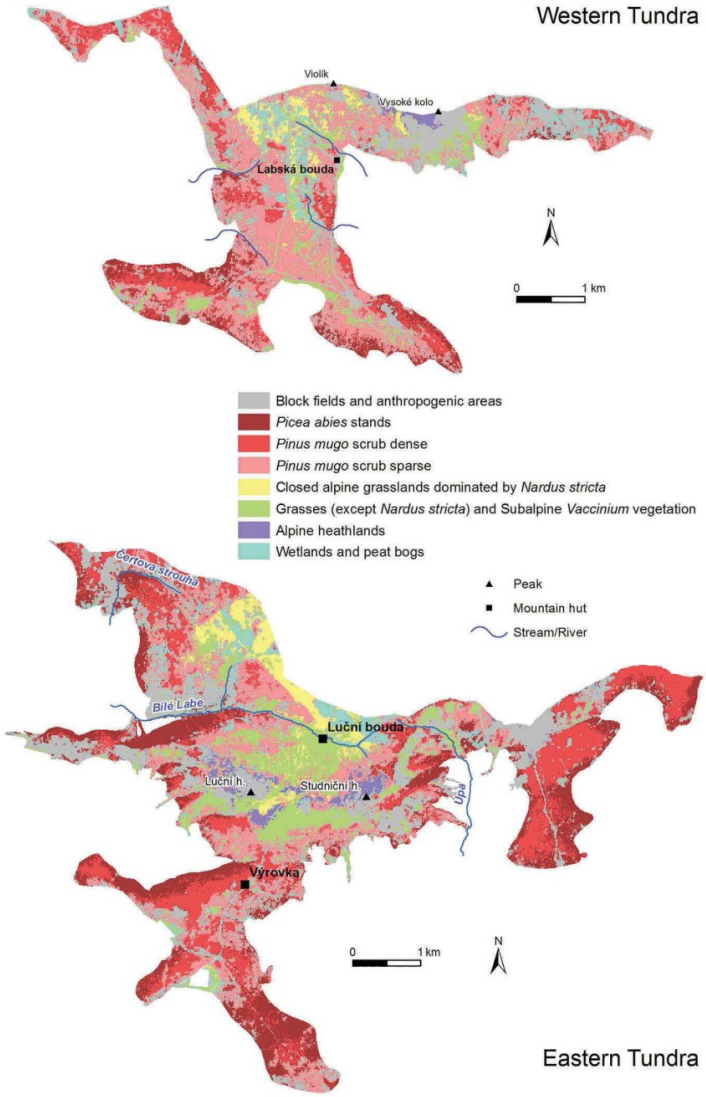

Figure 6. Maps of land cover in the tundra (top: Western Tundra; down: Eastern Tundra) in the Krkonoše Mts. for Sentinel-2A data, MLC classifier.

Sentinel-2A classification map and the Landsat 8 classification map (refer to Suchá et al. [2016]) shows that the spatial distribution of respective categories is almost identical. It is obvious that Sentinel-2A map is more detailed due to higher spatial resolution.

Discussion

Evaluating the different data suitability for tundra vegetation cover classification, besides other factors one has to consider differences in dates of the data acquisition. Consequently, the classification results may have been influenced by varying weather conditions and also by the seasonality in the sense of changing meteorological conditions during one growing season. The ongoing climatic changes may result in dramatic changes of the tundra vegetation patterns; thus, accurate and cost-effective approach of monitoring vegetation types using Earth observation methods are in high demand. Vegetation categories in tundra tend to be rather compact, with short height during spring and autumn, while in summer (July, August) the grassland vegetation advances based on species-specific phenology and different types of grasses are mixed together in one pixel. The onset of flowering may also influence spectral

signature of different species in some cases. For this reason better acquisition dates in tundra on our opinion may be late spring/early summer or late summer/early fall than mid-summer (end of July first half of August). Unfortunately, it is practically impossible to acquire all required data within one year or even within season or months. As we work in our study area for several years we were able to collect rather extensive data series. Though the data are from different years and seasons our results are remarkable because studies using or even comparing aerial hyperspectral data for tundra ecosystems are rare and no study using Sentinel-2A data for tundra has been published yet.

Our results for aerial image hyperspectral data can be compared with other studies that use hyperspectral images for classification of mountain vegetation. Marcinkowska et al. [2014] classified vegetation communities (15 categories) in the Szrenica Mountain region on the border between Poland and the Czech Republic in the Krkonoše Mts. National Park using APEX data and SVM classifier. The overall classification accuracy (79.13%) as well as the Kappa coefficient (0.77) reached slightly lower levels than those in our research. Zagajewski et al. [2010] mapped eastern part of the Tatra National Park, Poland, with aerial hyperspectral data (DAIS 7915 and by ROSIS sensors). They focused on the mountain vegetation of subalpine, alpine, and sub-nival zones utilizing maximum likelihood and neural net methods. The NN classifier allowed to identify 39 vegetation categories with 86% of overall accuracy.

No research comparing hyperspectral and multispectral data classification for tundra ecosystem has been carried out yet. Feilhauer et al. [2014] dealt with Natura 2000 habitat types in a boggy area in Bavaria, Germany, to compare resampled (spectrally and spatially) airborne spectroscopy data (AISA Dual) with the characteristics of two state-of-the-art multispectral sensors (RapidEye and Sentinel-2). The classification models resulted in an overall accuracy in calibration of 64% for the AISA Dual data, 62% for the RapidEye, and 59% for the Sentinel-2 data. Our results for AISA Dual and Sentinel-2A data were better; the legend, however, is not fully comparable.

The results for hyperspectral data from our study can be compared with the results of classifications of multispectral data with very high spatial resolution published by our team in previous study [Suchá et al., 2016]. In Suchá et al. [2016] orthoimages (blue, green, red, NIR bands; spatial resolution 0.125 m) were classified by object-based classifier (SVM algorithm) and WorldView-2 data were classified with per-pixel (SVM, NN, MLC) and object-based (SVM) classifiers. The same detailed legend like in this study was applied, but in the Western Tundra. The best overall classification accuracy for orthoimages was 71.96%, Kappa coefficient equalled 0.65. OBIA achieved for orthoimages (spatial resolution 0.125 m) better results than all used pixel-based classifiers (MLC, NN, SVM), even better than those for APEX data classified by OBIA in our study. In the case of WorldView-2 data, the best results were also brought by object-based approach – overall accuracy was 66.5%, Kappa coefficient 0.6. It is obvious that the use of hyperspectral data brings the best results as regards vegetation cover classification in tundra in the Krkonoše Mts. National Park. The overall accuracy was higher by 12 percentage points for AISA Dual, resp. by 10 percentage points for APEX data compared with orthoimages. For WorldView-2 imagery, the difference makes even almost 18 and 16 percentage points respectively (refer to Suchá et al. [2016]).

References dealing with the same or similar categories we used are scarce therefore the comparison of results is limited. Müllerová [2005] classified "Pine stands" by MLC and ISODATA classifiers with producer's and user's accuracies around 70%, and "Grass communities" with accuracies around 60%. Our results were significantly better for the both categories. Suchá et al. [2016] used different classifiers for multispectral data and orthoimages and the accuracies of "*Pinus mugo* scrub" were comparable to those reached in our analysis while results for the most of vegetation categories were significantly worse than our results. It is interesting that category "Subalpine *Vaccinium* vegetation" was problematic in our case while Suchá et al. [2016] got producer and also user accuracies above 70% for ortophotos and WorldView-2 imagery. Our results can be influenced by above mentioned date of acquisition or by training data. In comparison with ortophotos and multispectral data in Suchá et al. [2016] hyperspectral data revealed significant improvements in classification accuracy of some grassland categories ("*Nardus stricta* stands", "*Deschampsia cespitosa* stands" – per pixel classification and OBIA and "*Callamagrostis villosa* stands" – OBIA).

Conclusions

Three types of data were classified using different classifiers to evaluate and compare the data suitability for tundra vegetation cover classification. In accordance with our expectation the best classification results for tundra vegetation were in our study achieved for the hyperspectral data with the highest spectral and spatial resolution, i.e. AISA Dual data. However, the overall accuracy and also results for most of individual categories in the case of APEX data are comparable and it can be concluded that higher spatial and spectral resolutions of AISA Dual data brought only moderate improvement. Similarly

to many older and recent studies [for example Camps-Valls et al., 2004; Pal and Mather 2005; Petropoulos et al., 2012] the best results for the both types of hyperspectral data were achieved using SVM classification algorithm. As for Sentinel-2A data, especially in the case of simplified legend, NN and MLC methods achieved better results than SVM. For OBIA our results from this study are supportive to our conclusion from Suchá et al. [2016] that one of the main attributes increasing accuracy of this method is spatial resolution.

It has been supposed – and proved – that Sentinel-2A data with 10/20 meters spatial resolution and 10 spectral bands can not get to accuracy of APEX and AISA Dual data for the detailed legend. However, the rather high overall accuracy for the simplified legend is quite promising. The assumption that some grassland categories will not be distinguishable in Sentinel-2A data was confirmed. This supports our conclusion (Suchá et al. [2016]) that it is not appropriate to use the same classification legend for the data with significantly (order of magnitude) different spatial and spectral resolutions.

Our results of Sentinel-2A classification are unique as they are one of the first outputs using real (not simulated) data and therefore they cannot be compared with other studies dealing with Sentinel-2A data. We assume that Sentinel-2A classification accuracy could be increased by using series of images acquired during one season. The detection of *Pinus mugo* could be significantly improved analysing images from spring or autumn (when the surrounding grassland is dry). Series of images could also help to distinguish among the "green" non-forest grass vegetation categories (*Molinia caerulea, Calamagrostis villosa*, and others) that have different seasonal behaviour (growth, flowering, senescence).

All the used data types can be assessed as suitable for the classification of tundra vegetation cover and for the monitoring of the ongoing vegetation changes [Hejcman et al., 2009; Harčarik, 2007; Treml et al., 2012] when appropriate legend and classification method is used. Though rather different detail of information can be achieved based on spatial and spectral resolution and an increase of classification accuracy in case of some grassland categories is desirable. An analysis of time series of the data for the further improvement of the classification accuracy can be applied especially for Sentinel-2A data because of the very good time resolution. But in the case of commercial data it is problematic. For aerial hyperspectral data improvements can be achieved due to experiments with training and validation datasets, using additional classification inputs like DEM and DSM, field spectral signatures, combination of classification methods or new concepts like for example in Waske et al. [2010] or Magiera et al. [2015].

Acknowledgement

We want to thank the European Facility for Airborne Research Transnational Access (EUFAR TA) which funded the APEX data acquisition and to the Administration of the Krkonoše National Park for the AISA Dual data provision and for collaboration during our fieldwork.

Funding

This research was supported by the Charles University in Prague: Project [GAUK 938214], and manuscript finalization was supported by the Ministry of Education, Youth and Sports of the Czech Republic: Project [NPU I LO1417].

ORCID

Lucie Kupková http://orcid.org/0000-0002-0270-0516

References

AISA (2013) - *Hyperspectral scanning, vegetation maps and inventory of forest stands*; KRNAP technical report for year 2013.

Atkinson D., Treitz P. (2012) - *Arctic Ecological Classifications Derived from Vegetation Community and Satellite Spectral Data*. Remote Sensing, 4(12): 3948–3971. DOI: http://dx.doi.org/10.3390/rs4123948.

Benediktsson J.A., Swain P.H., Ersoy O.K. (1990) - *Neural Network Approaches Versus Statistical Methods In Classification Of Multisource Remote Sensing Data*. IEEE Transactions on Geoscience and Remote Sensing, 28(4): 540–552. DOI: http://dx.doi.org/10.1109/TGRS.1990.572944.

Blaschke T. (2010) - *Object based image analysis for remote sensing*. ISPRS Journal of Photogrammetry and Remote Sensing, 65(1): 2–16. DOI: http://dx.doi.org/10.1016/j.isprsjprs.2009.06.004.

Bratsch S., Epstein H., Buchhorn M., Walker D. (2016) - *Differentiating among Four Arctic Tundra Plant Communities at Ivotuk, Alaska Using Field Spectroscopy*. Remote Sensing, 8(1): 51. DOI: http://dx.doi.org/10.3390/rs8010051.

Camps-Valls G., Gomez-Chova L., Calpe-Maravilla J., Martin-Guerrero J.D., Soria-Olivas E., Alonso-Chorda L., Moreno J. (2004) - *Robust support vector method for hyperspectral data classification and knowledge discovery*. IEEE Transactions on Geoscience and Remote Sensing, 42(7): 1530–1542. DOI: http://dx.doi.org/10.1109/TGRS.2004.827262.

Chytrý M., Kučera T., Kočí M. (eds.) (2001) - *Katalog biotopů České republiky*. Agentura ochrany přírody a krajiny ČR, Praha, pp. 307.

Duarte C.M., Middelburg J.J., Caraco N. (2005) - *Major role of marine vegetation on the oceanic carbon cycle*. Biogeoscience, 2(1): 1–8. DOI: http://dx.doi.org/10.5194/bg-2-1-2005.

European Space Agency (2015) - *SENTINEL-2 User Handbook*. Available from https://earth.esa.int/documents/247904/685211/Sentinel-2_User_Handbook.

Feilhauer H., Dahlke C., Doktor D., Lausch A., Schmidtlein S., Schulz G., Stenzel S. (2014) - *Mapping the local variability of Natura 2000 habitats with remote sensing.*

Applied Vegetation Science, 17(4): 765–779. DOI: http://dx.doi.org/10.1111/avsc.12115.

Felde V.A., Kapfer J., Grytnes J.-A. (2012) - *Upward shift in elevational plant species ranges in Sikkilsdalen, central Norway*. Ecography, 35(10): 922–932. DOI: http://dx.doi.org/10.1111/j.1600-0587.2011.07057.x.

Fernandez-Prieto D., Arino O., Borges T., Davidson N., Finlayson M., Grassl H., MacKay H., Prigent C., Pritchard D., Zalidis G. (2006) - *The Glob Wetland Symposium: Summary and way forward*. Proceedings of GlobWetland: Looking at Wetlands from Space, Frascati, Italy, 19-20 October 2006. 10p.

Frei E.R.; Hollister R.D.; Klanderud K.; Rixen, C. (eds) (2013) - *International Tundra Experiment ITEX - More than 20 years of tundra vegetation change research*. Abstracts. International conference, September 17 to 20, 2013 Bergün, Switzerland. Available from http://www.wsl.ch/epub/itex.

Halabuk A., Gerhatova K., Kohut F., Ponecova Z., Mojses M. (2013) - *Identification of season-dependent relationships between spectral vegetation indices and above-ground phytomass in alpine grassland by using field spectroscopy*. Ekologia, 32(2). DOI: http://dx.doi.org/10.2478/eko-2013-0016.

Haralick R. M., Shanmugam K., Dinstein, I. (1973) - *Textural Features for Image Classification*. IEEE Transactions on Systems, Man, and Cybernetics, SMC-3(6): 610–621. DOI: http://dx.doi.org/10.1109/TSMC.1973.4309314.

Harčarik J. (2007) - *Management výsadeb kleče na přírodovědně hodnotných lokalitách v Krkonoších*. Opera Corcontica, 36: 363–369.

Hejcman M., Klaudisová M., Hejcmanová P., Pavlů V., Jones M. (2009) - *Expansion of Calamagrostis villosa in sub-alpine Nardus stricta grassland: Cessation of cutting management or high nitrogen deposition?* Agriculture, Ecosystems & Environment, 129(1–3): 91–96. DOI: http://dx.doi.org/10.1016/j.agee.2008.07.007.

Jakešová L., Červená L., Kupková L., Suchá R., Andrštová M. (2014) - *Možnosti objektově-orientované klasifikace pro určování vybraných biotopů nad horní hranicí lesa v Krkonošském národním parku*. Sborník studentské vědecké konference Telč 2014. Telč.

Jarocińska, A.M., Kacprzyk, M., Marcinkowska-Ochtyra, A., Ochtyra, A., Zagajewski, B., & Meuleman, K. (2016) - the application of apex images in the assessment of the state of non-forest vegetation in the karkonosze mountains. *Miscellanea Geographica*, *20* (1). DOI: http://dx.doi.org/10.1515/mgrsd-2016-0009.

Jeník J., Štursa J. (2003) - Vegetation of the Giant Mountains, Central Europe. In: Nagy L., Grabherr G., Körner C., Thompson D.B.A. (2003) - *Alpine Biodiversity in Europe*. Springer, Berlin, Heidelberg, pp. 479.

Jones H.G., Vaughan R.A. (2010) - *Remote sensing of vegetation: principles, techniques, and applications*. Oxford University Press, New York, pp. 384.

Kapfer J., Birks H.J.B., Felde V.A., Klanderud K., Martinessen T., Ross L.C., Schei F.H., Virtanen R., Grytnes J.-A. (2013) - *Long-term vegetation stability in northern Europe as assessed by changes in species co-occurrences*. Plant Ecology & Diversity, 6(2): 289–302. DOI: http://dx.doi.org/10.1080/17550874.2013.782370.

Kapfer J., Virtanen R., Grytnes J.-A. (2012) - *Changes in arctic vegetation on Jan Mayen Island over 19 and 80 years*. Journal of Vegetation Science 23: 771–781. DOI: http://dx.doi.org/10.1111/j.1654-1103.2012.01395.x.

Kłos A., Bochenek Z., Bjerke J.W., Zagajewski B., Ziółkowski D., Ziembik Z., Rajfur M., Dołhańczuk-Śródka A., Tømmervik H., Krems P., Jerz D., Zielińska M. (2015) - *The Use Of Mosses In Biomonitoring Of Selected Areas In Poland And Spitsbergen In The Years From 1975 To 2014*. Ecological Chemistry and Engineering, S 22(2). DOI: http://dx.doi.org/10.1515/eces-2015-0011.

Král K. (2009) - *Classification of Current Vegetation Cover and Alpine Treeline Ecotone in the Praděd Reserve (Czech Republic), Using Remote Sensing*. Mountain Research and Development, 29(2): 177–183. DOI: http://dx.doi.org/10.1659/mrd.1077.

Lin D.H., Johnson D.R., Andresen C., Tweedie C.E. (2012) - *High spatial resolution decade-time scale land cover change at multiple locations in the Beringian Arctic (1948–2000s)*. Environmental Research Letters, 7(2): 25502. DOI: http://dx.doi.org/10.1088/1748-9326/7/2/025502.

Lokvenc, T. (1995) - *Analysis of anthropogenic changes of woody plant stands above the alpine timber line in the Krkonoše Mts*. Opera Corcontica, 32: 99–114.

Magiera A., Feilhauer H., Tephnadze N., Waldhardt R., Otte A. (2015) - *Separating reflectance signatures of shrub species - a case study in the Central Greater Caucasus*. Applied Vegetation Science, 19: 304–315. DOI: http://dx.doi.org/10.1111/avsc.12205

Marcinkowska A., Zagajewski B., Ochtyra A., Jarocińska A., Raczko E., Kupková L., Stych P., Meuleman K. (2014) - *Mapping vegetation communities of the Karkonosze National Park using APEX hyperspectral data and Support Vector Machines*. Miscellanea Geographica, 18(2). DOI: http://dx.doi.org/10.2478/mgrsd-2014-0007.

Margold M., Treml V., Petr L., Nyplová P. (2011) - *Snowpatch hollows and pronival ramparts in the Krkonoše Mountains, Czech Republic: Distribution, morphology and chronology of formation*. Geografiska Annaler: Series A, Physical Geography, 93(2): 137–150. DOI: http://dx.doi.org/10.1111/j.1468-0459.2011.00422.x.

Millennium Ecosystem Assessment (2005) - Ecosystems and Human Well-being: Biodiversity Synthesis. World Resources Institute, Washington, DC. Available from http://www.millenniumassessment.org/documents/document.354.aspx.pdf

Moody D.I., Brumby S.P., Rowland J.C., Altmann G.L. (2014) - *Land cover classification in multispectral imagery using clustering of sparse approximations over learned feature dictionaries*. Journal of Applied Remote Sensing, 8(1):84793. DOI: http://dx.doi.org/10.1117/1.JRS.8.084793.

Mountrakis G., Im J., Ogole C. (2011) - *Support vector machines in remote sensing: A review*. ISPRS Journal of Photogrammetry and Remote Sensing, 66(3): 247–259. DOI: http://dx.doi.org/10.1016/j.isprsjprs.2010.11.001.

Müllerová J. (2005) - *Use of digital aerial photography for sub-alpine vegetation mapping: A case study from the Krkonoše Mts., Czech Republic*. Plant Ecology, 175(2): 259–272. DOI: http://dx.doi.org/10.1007/s11258-005-0063-3.

Nagendra H., Mairota P., Marangi C., Lucas R., Dimopoulos P., Honrado J.P., Niphadkar M., Mücher C.A., Tomaselli V., Panitsa M., Tarantino C., Manakos I., Blonda P. (2015) - *Satellite Earth observation data to identify anthropogenic pressures in selected protected*

areas. International Journal of Applied Earth Observation and Geoinformation, 37: 124–132. DOI: http://dx.doi.org/10.1016/j.jag.2014.10.010.

Ndehedehe Ch., Ekpa A., Simeon O., Nse O. (2013) - *Understanding the Neural Network Technique for Classification of Remote Sensing Data Sets*. New York Science Journal, 6(8): 26–33. DOI: http://dx.doi.org/10.7537/marsnys060813.05.

Novák J., Petr L., Treml V. (2010) - *La-te-Holocene human-induced changes to the extent of alpine areas in the East Sudetes, Central Europe*. The Holocene, 20(6): 895–905. DOI: http://dx.doi.org/10.1177/0959683610365938.

Pal M., Mather P.M. (2005) - *Support vector machines for classification in remote sensing*. International Journal of Remote Sensing, 26(5): 1007– 1011.

Petropoulos G.P., Arvanitis K., Sigrimis N. (2012) - *Hyperion hyperspectral imagery analysis combined with machine learning classifiers for land use/cover mapping*. Expert Systems with Applications, 39(3): 3800–3809. DOI: http://dx.doi.org/10.1016/j.eswa.2011.09.083.

Reese H., Nyström M., Nordkvist K., Olsson H. (2014) - *Combining airborne laser scanning data and optical satellite data for classification of alpine vegetation*. International Journal of Applied Earth Observation and Geoinformation, 27: 81–90. DOI: http://dx.doi.org/10.1016/j.jag.2013.05.003.

Rundqvist S., Hedenås H., Sandström A., Emanuelsson U., Eriksson H., Jonasson C., Callaghan T.V. (2011) - *Tree and Shrub Expansion Over the Past 34 Years at the Tree-Line Near Abisko, Sweden*. AMBIO, 40(6): 683–692. DOI: http://dx.doi.org/10.1007/s13280-011-0174-0.

Schaepman M.E., Jehle M., Hueni A., D'Odorico P., Damm A., Weyermann J., Schneider F.D., Laurent V., Popp C., Seidel F.C., Lenhard K., Gege P., Küchler C., Brazile J., Kohler P., De Vos L., Meuleman K., Meynart R., Schläpfer D., Kneubühler M., Itten K.I. (2015) - *Advanced radiometry measurements and Earth science applications with the Airborne Prism Experiment (APEX)*. Remote Sensing of Environment, 158: 207–219. DOI: http://dx.doi.org/10.1016/j.rse.2014.11.014.

Song C., Woodcock C.E., Seto K.C., Lenney M.P., Macomber S.A. (2001) - *Classification and Change Detection Using Landsat TM Data*. Remote Sensing of Environment, 75(2): 230–244. DOI: http://dx.doi.org/10.1016/S0034-4257(00)00169-3.

Soukupová L., Kociánová M., Jeník J., Sekyra J. (1995) - *Arctic alpine tundra in the Krkonoše, the Sudetes*. Opera Corcontica, 32: 5–88.

Speranza A., Hanke J., van Geel B., Fanta J. (2000) - *Late-Holocene human impact and peat development in the Černá Hora bog, Krkonoše Mountains, Czech Republic*. The Holocene, 10(5): 575–585. DOI: http://dx.doi.org/10.1191/095968300668946885.

Sterckx S., Vreys K., Biesemans J., Iordache M.-D., Bertels L., Meuleman K. (2016) - *Atmospheric correction of APEX hyperspectral data*. Miscellanea Geographica, 20(1): 16–20. DOI: http://dx.doi.org/10.1515/mgrsd-2015-0022.

Suchá R., Jakešová L., Kupková L., Červená L. (2016) - *Classification of vegetation above the tree line in the Krkonoše Mts. National Park using remote sensing multispectral data*. AUC GEOGRAPHICA, 51(1): 113–129. DOI: http://dx.doi.org/10.14712/23361980.2016.10.

Treml V., Jankovská V., Petr L. (2008) - *Holocene dynamics of the alpine timberline in the High Sudetes*. Biologia, 63 (1): 73–80. DOI: http://dx.doi.org/10.2478/s11756-008-0021-3.

Treml V., Ponocná T., Büntgen U. (2012) - *Growth trends and temperature responses of treeline Norway spruce in the Czech-Polish Sudetes Mountains*. Climate Research, 55(2): 91–103. DOI: http://dx.doi.org/10.3354/cr01122.

Ullmann T., Schmitt A., Roth A., Duffe J, Dech S., Hubberten H.W., Baumhauer R. (2014) - Land Cover Characterization and Classification of Arctic Tundra Environments by Means of Polarized Synthetic Aperture X- and C-Band Radar (PolSAR) and Landsat 8 Multispectral Imagery — Richards Island, Canada. Remote Sensing, 6: 8565–8593; DOI: http://dx.doi.org/10.3390/rs6098565.

Virtanen T., Ek M. (2014) - *The fragmented nature of tundra landscape*. International Journal of Applied Earth Observation and Geoinformation, 27: 4–12. DOI: http://dx.doi.org/10.1016/j.jag.2013.05.010.

Vreys K., Iordache M.-D., Biesemans J., Meuleman K. (2016a) - *Geometric correction of APEX hyperspectral data*. Miscellanea Geographica, 20(1): 11–15. DOI: http://dx.doi.org/10.1515/mgrsd-2016-0006.

Vreys K., Iordache M.-D., Bomans B., Meuleman K. (2016b) - *Data acquisition with the APEX hyperspectral sensor*. Miscellanea Geographica, 20(1): 5–10. DOI: http://dx.doi.org/10.1515/mgrsd-2016-0001.

Wan-Kadir W.H., Latiff S.Z.A., Rasib A.W., Rahman M.Z. A., Ariffin A. (2013) - *Increasing accuracy of image classification using Artificial Neural Network*. 34th Asian Conference on Remote Sensing 2013, ACRS 2013, vol. 2. Bali. pp.1311–1316.

Waske, B., van der Linden, S., Benediktsson, J.A., Rabe, A., & Hostert, P. (2010) - sensitivity of support vector machines to random feature selection in classification of hyperspectral data. *Ieee Transactions On Geoscience And Remote Sensing*, *48*(7): 2880–2889. DOI: http://dx.doi.org/10.1109/TGRS.2010.2041784.

Zagajewski B. (2010) - *Ocena przydatności sieci neuronowych i danych hiperspektralnych do klasyfikacji roślinności Tatr Wysokich*. Klub Teledetekcji Środowiska Polskiego Towarzystwa Geograficznego, Warszawa, pp. 113.

Zhou L., Yang, X. (2008) - *Use of Neural Networks for Land Cover Classification from Remotely Sensed Imagery*. The International Archives of the Photogrammetry, Remote Sensing and Spatial Information Sciences, 37: 575–578.

Appendix – Error matrices for the best classifications of each data type

APEX SVM

	1.	2.	3.	4a.	4b.	5a.	5b.	5c.	6.	7.	8.	Total
1.	282	0	0	0	0	0	0	0	0	0	0	**282**
2.	3	708	7	0	0	0	0	0	0	29	0	**747**
3.	0	0	7	0	0	0	0	0	0	0	0	**7**
4a.	1	0	8	412	1	5	11	7	22	12	0	**479**
4b.	0	0	3	32	33	0	0	4	2	0	0	**74**
5a.	0	0	6	50	0	94	19	6	2	12	0	**189**
5b.	0	0	17	14	0	16	91	8	1	5	0	**152**
5c.	0	0	0	24	4	17	18	172	0	17	0	**252**
6.	0	1	33	21	0	0	0	0	253	0	0	**308**
7.	0	0	1	8	0	15	2	0	0	106	0	**132**
8.	0	0	0	0	0	0	0	0	0	0	43	**43**
Total	**286**	**709**	**82**	**561**	**38**	**147**	**141**	**197**	**280**	**181**	**43**	**2,665**

AISA SVM

	1.	2.	3.	4a.	4b.	5a.	5b.	5c.	6.	7.	8.	Total
1.	1,598	0	0	0	0	0	0	0	1	22	0	**1,621**
2.	9	5,193	27	0	0	0	0	0	6	39	1	**5,275**
3.	0	1	400	112	14	68	5	125	66	6	0	**797**
4a.	3	0	99	3,648	84	342	325	87	245	278	0	**5,111**
4b.	0	0	16	47	156	2	17	2	0	20	0	**260**
5a.	0	0	0	62	0	618	25	0	0	3	0	**708**
5b.	0	0	0	170	0	26	762	22	0	33	0	**1,013**
5c.	0	0	68	52	27	67	7	1,348	0	2	0	**1,571**
6.	0	1	0	217	0	0	0	0	1,712	113	0	**2,043**
7.	0	0	16	49	1	0	0	0	68	896	3	**1,033**
8.	0	0	0	0	0	0	0	0	0	0	328	**328**
Total	**1,610**	**5,195**	**626**	**4,357**	**282**	**1,123**	**1,141**	**1,584**	**2,098**	**1,412**	**332**	**19,760**

Sentinel-2A NN

	1.	2.	3.	4a.	4b.	5a.	5b.	5c.	6.	7.	Total
1.	38	0	0	0	0	0	0	0	2	0	**40**
2.	0	77	5	0	0	0	0	0	4	1	**87**
3.	0	0	17	2	0	0	11	2	0	5	**37**
4a.	2	0	0	52	5	1	8	12	14	2	**96**
4b.	1	0	0	7	6	0	0	3	0	0	**17**
5a.	0	0	0	4	1	7	2	0	2	0	**16**
5b.	0	0	0	3	0	1	6	0	0	0	**10**
5c.	0	0	0	29	0	13	13	23	4	5	**87**
6.	0	0	4	16	0	0	0	0	17	3	**40**
7.	0	0	0	0	0	0	0	0	2	21	**23**
Total	**41**	**77**	**26**	**113**	**12**	**22**	**40**	**40**	**45**	**37**	**453**

1. Block fields and anthropogenic areas
2. *Pinus mugo* scrub
3. Subalpine *Vaccinium* vegetation
4. Closed alpine grasslands
4a. *Nardus stricta* stands
4b. Species-rich vegetation with high cover of forbs
5. Subalpine tall grasslands
5a. *Calamagrostis villosa* stands
5b. *Molinia caeruela* stands
5c. *Deschampsia cespitosa* stands
6. Alpine heathlands
7. Wetlands and peat bogs
8. Water areas (not for Sentinel-2A)

Sentinel-2A MLC – Simplified legend

	1.	2.	3a.	3b.	4.	5.	6.	7.	Total
1.	282	1	0	0	7	18	12	1	**321**
2.	0	373	16	0	0	0	0	0	**389**
3a.	0	5	177	0	0	0	0	0	**182**
3b.	0	12	14	141	32	82	4	70	**355**
4.	0	0	0	0	169	21	6	4	**200**
5.	0	0	0	0	45	171	6	18	**240**
6.	0	0	0	0	0	2	151	2	**155**
7.	0	3	1	17	9	54	7	173	**264**
Total	**282**	**394**	**208**	**158**	**262**	**348**	**186**	**268**	**2,106**

1. Block fields and anthropogenic areas
2. *Picea abies* stands
3a. *Pinus mugo* scrub dense (more than 80% of total cover)
3b. *Pinus mugo* scrub sparse (30 – 80% of total cover)
4. Closed alpine grasslands dominated by *Nardus stricta*
5. Grasses (except *Nardus stricta*) and subalpine *Vaccinium* vegetation
6. Alpine heathlands
7. Wetlands and peat bogs

Paper 7: "FIELD SPECTROSCOPY FOR VEGETATION EVALUATION ALONG THE NUTRIENT AND ELEVATION GRADIENT ABOVE THE TREE LINE IN THE KRKONOŠE MOUNTAINS NATIONAL PARK"

Červená, Lucie, Lucie Kupková, a Renáta Suchá. 2016. „Field Spectroscopy for Vegetation Evaluation along the Nutrient and Elevation Gradient above the Tree Line in the Krkonoše Mountains National Park." ISPRS - *International Archives of the Photogrammetry, Remote Sensing and Spatial Information Sciences* XLI-B6 (červen): 211–14. https://doi.org/10.5194/isprs-archives-XLI-B6-211-2016.

Author Contributions:

LČ – 79%, LK – 12%, RS – 9%

The International Archives of the Photogrammetry, Remote Sensing and Spatial Information Sciences, Volume XLI-B6, 2016
XXIII ISPRS Congress, 12–19 July 2016, Prague, Czech Republic

FIELD SPECTROSCOPY FOR VEGETATION EVALUATION ALONG THE NUTRIENT AND ELEVATION GRADIENT ABOVE THE TREE LINE IN THE KRKONOŠE MOUNTAINS NATIONAL PARK

L. Červená *, L. Kupková, R. Suchá

Department of Applied Geoinformatics and Cartography, Faculty of Science, Charles University in Prague, Albertov 6, Prague 2, Czech Republic - (lucie.cervena, lucie.kupkova, renata.sucha)@natur.cuni.cz

Youth Forum

KEY WORDS: field spectroscopy, plant cover, fAPAR, nutrient and elevation gradient, tundra, The Krkonoše Mountains National Park

ABSTRACT:

This paper examines the relations between vegetation spectra measured in the field along the nutrient and elevation gradient in the most valuable parts of The Krkonoše Mountains tundra and selected parameters describing vegetation state and condition (fAPAR, plant cover and average vegetation height). The main goal was to find relations and indices based on spectral measurements that could be used for vegetation evaluation and classification in practice and management. The vegetation parameters and spectral properties were also compared for two datasets – one acquired in July and second in August 2015. The best correlations were obtained for plant cover (R^2 above 0.8 for July dataset and above 0.7 for August dataset) and two types of indices – using the wavelengths of red edge, e.g. OSAVI or mND705, and indices for vegetation water content estimates using the wavelengths in shortwave infrared region of the spectra in combination with wavelengths above 800 nm, e. g. NDII. The worst results were found for fAPAR with maximal values of R^2 just above 0.4 with the indices using the wavelengths around 700 nm. For vegetation height the results differ between July and August data – R^2 around 0.62 in July and only 0.47 in August for vegetation indices using the wavelengths of visible and red edge regions.

1. INTRODUCTION

The vegetation above the tree-line in the Krkonoše Mts., Czech Republic (50°N, 15°E, altitude above 1,350 m a. s. l.), is the unique ecosystem, southernmost relict area of the arctic-alpine tundra in Europe (Soukupová et al., 1995). Tundra belongs among the most valuable and also the most vulnerable ecosystem worldwide. Hence, sustainable management and preservation of tundra is important, but it requires comprehensive knowledge about vegetation cover and condition. And this knowledge can be provided by the remote sensing data and methods.

Two approaches to model the vegetation biophysical or biochemical parameters based on the spectral data exist: empirical (statistical methods) and physical (Radiative Transfer Models). Darvishzadeh et al. 2011 compared these two approaches for mapping the grassland leaf area index (LAI).

The empirical models for grass biomass estimation were tested by Mutanga and Skidmore (2004) using the band depth indices and stepwise regression under controlled laboratory conditions. Cho et al. (2007) compared the vegetation indices and partial least square regression (PLSR) for grass biomass estimations based on airborne hyperspectral images (HyMap). Biomass and groundcover were also estimated using the vegetation indices for winter crop fields by Prabhakara et al., 2015. Fensholt et al. (2004) evaluated the relations between MODIS fAPAR and NDVI for semi-arid environment. In Czech Republic the relationships between fAPAR resp. LAI of meadow vegetation and selected invasive species and their spectral properties (vegetation indices) were examined by Jelének et al. (2014).

Radiative Transfer Models for grassland parameters estimations were evaluated by e. g. Jarocinska et al. (2014) or Darvishzadeh (2008) for heterogeneous grasslands.

For arctic-alpine tundra vegetation parameters estimations no literature references were found. Thus, this paper aims to examine the statistical relations between tundra vegetation spectra measured in the field along the nutrient and elevation gradient in Krkonoše Mts. and selected parameters describing its state and condition (plant cover, average vegetation height and Fraction of Absorbed Photosynthetically Active Radiation – fAPAR). The main goal is to find indices and statistical models based on field spectral measurements that could be used for vegetation evaluation and classification in practice and management. Other aim of this study is to compare two field datasets acquired in different time horizons (July 2015 and August 2015) and relations based on them.

2. DATA AND METHODS

2.1 Field data

Parameters describing the vegetation state and condition (plant cover, average vegetation height and Fraction of Absorbed Photosynthetically Active Radiation – fAPAR) were measured along the nutrient and elevation gradient in the most valuable parts of The Krkonoše Mountains tundra. This gradient was established between Luční bouda hut in the altitude of 1,410 m

* Corresponding author

This contribution has been peer-reviewed.
doi:10.5194/isprsarchives-XLI-B6-211-2016

The International Archives of the Photogrammetry, Remote Sensing and Spatial Information Sciences, Volume XLI-B6, 2016
XXIII ISPRS Congress, 12–19 July 2016, Prague, Czech Republic

a. s. l., where also the mountain agriculture occurred till the first half of 20th century, and Luční Hora Mountain in the altitude of 1,550 m a. s. l. with no human impact. The nutrient and elevation gradient contains the following vegetation classes:
1) Herbaceous ruderal vegetation (near hut Luční bouda)
2) Species rich growths with high share of dicotyledonous (near the roads)
3) Grasslands with *Solidago virgaurea*
4) Connected alpine grasslands with dominant *Nardus stricta*
5) Nardus stricta stands
6) Alpine heathlands (growths of *Calluna vulgaris*)
7) Mosaic of *Calluna vulgaris*, lichens and bare land

All of the above mentioned parameters together with the reflectance spectra were determined in the field during two campaigns, in July and August 2015. Plots of 1 m x 1 m (Figure 1) were delimited for each vegetation class: 7x12=84 plots in July and 7x4=28 plots in August. The plant cover (in percents) was estimated by botanist. The vegetation height was measured in centimetres at five different places in the plot and afterwards averaged. Fraction of Absorbed Photosynthetically Active Radiation was measured by the instrument AccuPAR LP-80 at three different places in the plot and also averaged. In each plot at evenly distributed spots, five spectra were measured by ASD FieldSpec Wide-Res 4 (350 – 2,500 nm) with fibre optic cable. The radiance spectra were normalized against a 99% Spectralon white reference to produce relative reflectance spectra for each measurement. Afterwards one median spectrum for each plot was calculated.

Figure 1. Example of one plot (1 m x 1 m, class 2: species rich growths with high share of dicotyledonous) for which all the parameters were determined

2.2 Methods and software

At first, the differences between the classes in the parameters measured in the field were assessed using the Analysis of variance (ANOVA) and Tukey's Honest Significant Difference test (TukeyHSD) separately for July and August datasets. Also the averages and standard deviations were visualised for all classes and both time horizons – see the figure 2.

Secondly, fifty vegetation indices chosen based on the literature review (Thenkabail et al., 2012; Main et al., 2011; le Maire et al., 2004; Hernandez-Clemente et al., 2012; Yi at al., 2014, Zemek et al. 2014) were calculated using the field reflectance spectra. The models using the linear regression between each index and each parameter were built, again separately for July and August dataset. The models were evaluated using Coefficients of Determination (R^2) and p-value.

All the calculations were performed in R software with help of Microsoft Office Excel 2007.

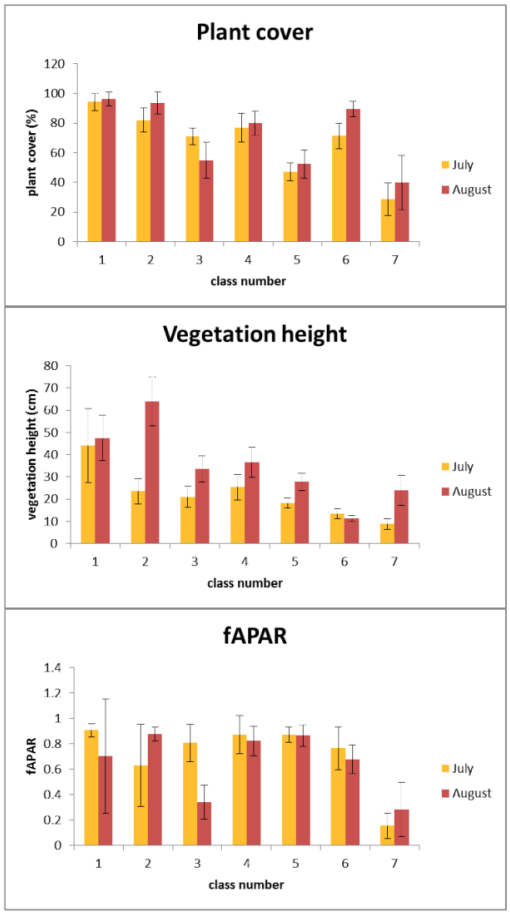

Figure 2. Means and standard deviations of the plant cover, vegetation height and fAPAR measured in July and August 2015 for seven vegetation classes

3. RESULTS

The aim of ANOVA method was to find out if there are significant differences in vegetation parameters (plant cover, average vegetation height and fAPAR) between seven observed vegetation classes. Significant differences between classes were proven for all the parameters in both time horizons. TukeyHSD test revealed that most differences are for plant cover and fAPAR caused by the class 7 which has the lower values of these parameters than most of other classes. This can be explained by the definition of the class 7 which includes bare land and lichens. On the contrary, for vegetation height the majority of differences can be seen between classes located near Luční bouda hut (class 1 in July and class 2 in August) and other classes. These classes are composed of different species of

This contribution has been peer-reviewed.
doi:10.5194/isprsarchives-XLI-B6-211-2016

The International Archives of the Photogrammetry, Remote Sensing and Spatial Information Sciences, Volume XLI-B6, 2016
XXIII ISPRS Congress, 12–19 July 2016, Prague, Czech Republic

plants which can grow higher during the vegetation season. The vegetation height is also the only studied parameter which values differ significantly between July and August. All of these results can be also found in figure 2.

Parameter	**Plant cover**	
month	July	August
R^2	0.70-0.88	0.60-0.73
indices with relevant R^2 in both time datasets	NDWI, SRWI, NDII, NMDI, OSAVI, mND705, Gitelson2, SR6, OSAVI2, Carter4, PSNDa, NDVI2, PSSRb, PSNDb, NDVI1	
indices with relevant R^2 just in one of the datasets	WI, MSI, DRI, NDWI2130, MSISR, Vogelmann, PSSRa, RNIRCRI550, PSSRc, PSNDc, PRICI.H, SIPI, PRIm1	TVI, DD, MCARI2, MCARI2OSAVI2
Parameter	**Vegetation height**	
month	July	August
R^2	0.45-0.62	0.30-0.47
indices with relevant R^2 in both time datasets	Gitelson2, Vogelmann, Vogelmann2, Datt2, SR6, Carter4, PSSRa, PSSRb	
indices with relevant R^2 just in one of the datasets	WI, NDWI, SRWI, NDII, OSAVI, MTCI, mND705, Maccioni, Datt, DD, OSAVI2, MCARI2, MCARI2OSAVI2, REP_LI, NDVI2, NPCI, SRPI, PRI	CRI550, RNIRCRI550, PSSRc, PSNDc, PRICI.Y, PRIm1
Parameter	**fAPAR**	
month	July	August
R^2	0.25-0.40	0.30-0.48
indices with relevant R^2 in both time datasets	MTCI, mND705, Maccioni, Vogelmann, Vogelmann2, Datt, Carter4, REP_LI	
indices with relevant R^2 just in one of the datasets	WI, NDWI, SRWI, NDII, MSI, DRI, NDWI2130, NMDI	SR6, DD

Table 1. The list of the indices for which the highest coefficients of determination (R^2) of linear regressions with the vegetation parameters were achieved. The best results are visualised in colour (yellow for July dataset, red for August dataset and green for both). For the indices formulas refer the literature: Thenkabail et al., 2012; Main et al., 2011; le Maire et al., 2004; Hernandez-Clemente et al., 2012; Yi at al., 2014, Zemek et al. 2014.

Table 1 summarizes the indices for which the coefficients of determination (R^2) of linear regressions with the vegetation parameters were the highest. The selection includes the indices which R^2 were no lower than $m - 0.2$, where m is the maximum value of R^2 obtained for the studied parameter.

The predictive equations modeled by the linear regressions show the similar values for both datasets (July and August) in case of plant cover and fAPAR and the corresponding indices. However, for the vegetation height the equations between the two datasets differ as the vegetation heights differ between the two field campaigns.

4. CONCLUSIONS

The best correlations were obtained for plant cover (R^2 above 0.8 for July dataset and above 0.7 for August dataset) and two basic types of indices – using the wavelengths of red edge, e.g. OSAVI or modified NDVI at 705 nm (mND705), and indices for vegetation water content estimates using the wavelengths in shortwave infrared region of the spectra (around 2,000 nm) in combination with wavelengths above 800 nm, e. g. NDII. For vegetation height the results differ between July and August datasets – R^2 around 0.62 in July and only 0.47 in August for vegetation indices using the wavelengths of visible and red edge regions, e. g. Vogelmann2 and Datt2 (names of the indices based on Main et al., 2011). The worst results were found for fAPAR. Coefficients of determination reached the maximal values of 0.4 for July dataset and 0.48 for August dataset for vegetation index proposed by Maccioni et al. (2001) using the wavelengths around 700 nm.

Comparison of the statistical prediction models for the datasets acquired in July and August confirmed that in the case of the similar values of the studied parameters (fAPAR, vegetation cover) it could be possible to use one model repetitively during the season. On the other hand, in case of even relatively small differences in parameters between the datasets (vegetation height) the prediction equations can be noticeably changed. Of course, these results can be also affected by the different number of plots in datasets (84 plots in July vs. 24 plots in August).

In conclusion, our results proved that all the examined parameters have an influence on the spectra. Various combinations of the parameters together with species composition, soil properties and other additional information obtained in the field will be further examined by multivariate statistical methods. Based on the results in the next step we will extract the information about the selected parameters for the whole tundra area of the Krkonoše Mts. National Park from aerial hyperspectral image data (AISA Dual, APEX).

ACKNOWLEDGEMENT

This research was made possible by the Charles University in Prague project GAUK No. 938214. Our thanks belong also to botanists Stanislav Březina and Jan Šturma for their help during the fieldwork.

REFERENCES

Darvishzadeh, R., Atzberger C., Skidmore, A., Schlerf, M., 2011. Mapping grassland leaf area index with airborne

This contribution has been peer-reviewed.
doi:10.5194/isprsarchives-XLI-B6-211-2016

The International Archives of the Photogrammetry, Remote Sensing and Spatial Information Sciences, Volume XLI-B6, 2016
XXIII ISPRS Congress, 12–19 July 2016, Prague, Czech Republic

hyperspectral imagery: A comparison study of statistical approaches and inversion of radiative transfer models. ISPRS *Journal of Photogrammetry and Remote Sensing*, 66(6): pp. 894-906.

Fensholt, R., Sandholt, I., Rasmussen, M. S., 2004. Evaluation of MODIS LAI, fAPAR and the relation between fAPAR and NDVI in a semi-arid environment using in situ measurements. *Remote Sensing of Environment*, 91 (3-4), pp. 490-507.

Hernández-Clemente, R., Navarro-Cerrillo, R. M., Zarco-Tejada, P. J., 2012. Carotenoid content estimation in a heterogeneous conifer forest using narrow-band indices and PROSPECT+DART simulations. *Remote Sensing of Environment*, 127, pp. 298-315.

Cho, M., A., Skidmore, A., K., Corsi, F., Sobhan, I., 2007. Estimation of green grass/herb biomass from airborne hyperspectral imagery using spectral indices and partial least squares regression. *International Journal of Applied Earth Observation and Geoinformation*, 9(4), pp. 414-424.

Jarocinska, A., Zagajewski, B., Ochtyra, A., Kupková, L., 2014. Prosail model for reflectance simulations of mountainous non-forest communities. *EARSeL eProceedings*, Special Issue: 34th EARSeL Symposium, pp. 18-23.

Jelének, J., Kupková, L., Zagajewski, B., Březina, S., Ochytra, A., Marcinkowska, A., 2014. Laboratory and image spectroscopy for evaluating the biophysical state of meadow vegetation in the Krkonoše National Park. *Miscellanea Geographica*, 18(2), pp. 15-22.

le Maire, G., François, C., Dufrêne, E., 2004. Towards universal broad leaf chlorophyll indices using PROSPECT simulated database and hyperspectral reflectance measurements. *Remote Sensing of Environment*, 89(1), pp. 1-28.

Maccioni, A., Agati, G., Mazzinghi, P., 2001. New vegetation indices for remote measurement of chlorophylls based on leaf directional reflectance spectra. *Journal of Photochemistry and Photobiology*, 61 (1–2), pp. 52–61.

Main, R., Cho, M. A., Mathieu, R., O'Kennedy, M. M., Ramoelo, A., Koch, S., 2011. An investigation into robust spectral indices for leaf chlorophyll estimation. *ISPRS Journal of Photogrammetry and Remote Sensing*, 66(6), pp. 751-761.

Mutanga, O., Skidmore, A., K., 2004. Hyperspectral band depth analysis for a better estimation of grass biomass (Cenchrus ciliaris) measured under controlled laboratory conditions. *International Journal of applied Earth Observation and Geoinformation*, 5 (2), pp. 87 - 96.

Prabhakara, K., Hively, W., D., McCarty, G., W., 2015. Evaluating the relationship between biomass, percent groundcover and remote sensing indices across six winter cover crop fields in Maryland, United States. *International Journal of Applied Earth Observation and Geoinformation*, 39, pp. 88-102.

Soukupová, L., Kociánová, M., Jeník, J., Sekyra, J., 1995. Arctic-alpina tundra in the Krkonoše, the Sudetes. *Opera Corcontica*, 32, pp. 5–88.

Thenkabail, P. S., Lyon, J., Huete, A., 2012. *Hyperspectral remote sensing of vegetation*. CRC Press, Boca Raton, FL, pp. 782.

Yi, Q., Jiapaer, G., Chen, J., Bao, A., Wang, F., 2014. Different units of measurement of carotenoids estimation in cotton using hyperspectral indices and partial least square regression. *ISPRS Journal of Photogrammetry and Remote Sensing*, 91, pp. 72-84.

Zemek, F. et al., 2014. *Letecký dálkový průzkum Země: teorie a příklady hodnocení terestrických ekosystémů*. Centrum výzkumu globální změny AV ČR, Brno, pp. 155.

This contribution has been peer-reviewed.
doi:10.5194/isprsarchives-XLI-B6-211-2016

6 Synthesis and discussion

6.1 Norway spruce forest ecosystem

The first part of the present thesis (Papers 1-4) analyzes the data measured for the Norway spruce stands in the Krušné hory Mountains in 2013. Besides the utilization of this data for solving the methodological issues associated with the research of the homogeneous spruce ecosystems using laboratory and image spectroscopy (Papers 2-4), the physiological status of the Norway spruce forest ecosystems in the Krušné hory Mountains was evaluated (Papers 1-2). Paper 1 shows the equalization of the Norway spruce physiological status between the central and western part of the Krušné hory Mountains in the period 1998 – 2013, which is given by the regeneration of the trees in the central part (area Kovářská) and slight worsening of the trees' physiological status in the western part (area Přebuz). This was proven based on the ratio between the total carotenoids and the total chlorophylls (*Car/Cab*), which significantly decreased in the area of Kovářská and increased in the area of Přebuz between 1998 and 2013. This result can be explained by the soil geochemical conditions, which are less favorable in the western part (prevailing poor soils on naturally acidic rocks with very low basic nutrient contents; Šrámek et al. 2015) and which are now, after elimination the air pollution, the main factor affecting the vegetation physiological status. From a methodological point of view, a similar conclusion about the physiological status of Norway spruce stands in the Krušné hory Mountains was investigated whether it can be derived from laboratory and image spectral data and what the relationships are between the spectral data and the biochemical and biophysical traits of the Norway spruce needles determined in the laboratory. The next methodological issues are associated with the measurements of the Norway spruce optical properties in the laboratory conditions and to what extent the spectra are influenced by the device used for the measurements. Three thematic groups of research questions joined with these topics were asked in Chapter 3. The answers are described in Papers 2-4 in detail. The most important findings and discussion of the results are presented in the following text.

Q1. Do the differences in the physiological status of the Norway spruce stands recorded during the 1990's between two differently polluted areas located in the western (Přebuz) and central (Kovářská) Krušné hory Mountains still exist? Is it possible to detect these differences based on the biochemical/biophysical retrievals of the pigments and water content, as well as from the laboratory and airborne image spectroscopic measurements? A different scale is also considered, i.e., the differences at the level of the areas, stands, position in the crown and the needle age classes. (Paper 2)

Significant differences ($p \leq 0.05$) between the western part (area Přebuz) and the central part (area Kovářská) of the Krušné hory Mountains were not detected by means of the analysis of variance based on the reflectance spectra measured with an ASD FieldSpec 4 Wide-Res spectroradiometer equipped with a plant contact probe on the shoot level or based on the reflectance spectra on the tree crown level obtained from airborne hyperspectral image acquired with the APEX sensor in 2013. However, the differences between the areas were proven based on the biochemically retrieved photosynthetic pigments and water content, though they were rather mild considering the absolute values of the derived compounds.

Using the biochemically retrieved photosynthetic pigments and water content and the reflectance spectra measured with the spectroradiometer and the plant contact probe, the differences were studied among various factors within the study areas – eleven stands consisting of five sampled trees, three vertical crown levels (the sunlit productive upper and lower parts, the shaded basal part) and the first three needle age classes. Significant differences were found in the case of the photosynthetic pigments (chlorophylls and carotenoids) in all the factors based on the laboratory biochemical data as well as based on the indices TCARI/OSAVI a CRI_{700}. In the case of water content, the differences were only proven for all the factors based on the laboratory biophysical data, based on the Water Index (WI), the differences were only significant when the needle age classes were considered. The most distinct groups for all the studied biochemical and biophysical traits are, according to Tukey's HSD test, the first needle age class from older needle age classes, the shaded basal part of the tree crown from the sunlit parts and some of the stands located in both areas, in Kovářská as well as Přebuz. The differences in the contents of the photosynthetic pigments and water and in the associated optical properties in different needle age classes were already described by the works of Soukupova, Rock, and Albrechtova (2001) or Lhotáková et al. (2007), the differences among the vertical positions in the tree crown are discussed in detail by Paper 4 (see research question Q3 in the following text).

The differences among the stands were also evaluated based on the aerial hyperspectral image data acquired with an APEX sensor. The tree crown is represented by four neighboring pixels in the aerial hyperspectral image. The averaged spectrum was calculated for every tree (in the event that the spectral reflectance of some pixels significantly differed from the others and from the expected vegetation spectrum, it was not included in the calculation of the mean). For a better comparison of the different scales of data (laboratory biochemical and biophysical data, laboratory spectroscopy and image spectroscopy data) for the purposes of assessing the areas or the stand differences, data measured in the laboratory (the contents of pigments and water, the laboratory spectra) was reduced by averaging the measured values also to the tree level, i.e., 55 samples from the original 495 samples. As expected, reducing the number of observations by averaging brought a higher similarity among all three types of measurements (laboratory biochemical and biophysical data, laboratory spectroscopy data and image spectroscopy data) and it caused smaller differences among the observations. No significant differences between the areas or among the stands were detected based on these 55 samples for the water content

retrieved in the laboratory or the water indices calculated from both types of spectral data. For the pigments and indices related to the pigments, the differences were significant for the stands based on the chlorophyll content, the TCARI/OSAVI and CRI_{700} calculated from both types of spectral data. The stands which are the most distinct from the others in the studied traits were detected by Tukey's HSD test and the Hot Spot Analysis (Getis-Ord Gi*). Bigger variability among the individual stands, than any significant differences between the Kovářská and Přebuz areas, were also reported in the soil properties (Kopačková, Mišurec, and Fárová 2017).

Q2. Are there differences between the spectra collected with a plant contact probe and an integrating sphere? Are the retrieved leaf biochemical properties obtained from the spectral measurements performed with a CP and an IS yielding comparable results? To what extent does the leaf morphological type (dorsiventral leaves vs. coniferous needles) affect the differences between the spectral leaf properties obtained with a CP and an IS? (Paper 3)

A review of in situ and laboratory measurements of conifers' spectral properties by Rautiainen et al. from 2018 reveals that *"the number of scientific studies especially on the spectral properties of coniferous needles has notably increased during the past decade - approximately 40% of the studies have been published after 2010, and 75% of the studies have been published after 2000"*. They also summarize all the strengths and weaknesses of the in situ and laboratory measurements of conifer spectral properties. One of the weaknesses is that the spectral measurements are not often well documented and not quantitatively comparable among campaigns due to the varying sampling schemes. This is in the agreement with *Paper 3* that compares spectra measured on identical samples (standard samples and vegetation specimens) using an ASD plant contact probe and two integrating spheres (ASD and Labsphere) and whose results are presented in the following text. *Paper 3* proved that, particularly in the case of Norway spruce needles spatially arranged on a shoot, the methodology of measurement matters remarkably and affects the values obtained by the different devices. However, the calibrated reflectance values of the 95% Zenith Lite® calibrated reference and the absolute reflectance measured with the ASD IS and ASD CP differed less than 0.5% (in relative units) in the best cases, which is on the level of the instrument performance. In the case of the colored papers, the discrepancies among the spectral reflectance values obtained from the different devices and the device settings were higher in comparison to that of the Spectralon. The best agreement was achieved between the measurements from the ASD IS and the Labsphere IS when the correction for the substitution error was applied. A linear transformation brought better agreement between the spectra of the same samples measured by different devices – good results were especially obtained for the colored papers, where after applying the transformation, significant differences between spectra were not observed. Concerning the vegetation samples, linear transformation worked better for broadleaved (dorsiventral) vegetation rather than for coniferous vegetation, but differences still existed. The Normalized Differential Index (NDI)

was calculated for all combinations of wavelength in the interval between 450 nm and 1800 nm, the devices, the device settings and all the measured samples. The correlation coefficients between the NDI values of the different devices generally confirms the increasing differences between the spectra obtained by the different instruments and their settings when moving from relatively homogeneous materials (i.e., colored papers and tobacco leaves) to more complicated measurements of Norway spruce needles. The majority of the fifty indices usually used for vegetation studies also differs significantly between the tested devices as proven by the t-test, however, the mean values of the indices among the devices differed within the standard deviation in the case of tobacco. Concerning the correlation coefficients between the leaf compounds and the NDI derived for the tobacco and Norway spruce samples, similar trends for all three devices can be observed in the case of tobacco, in spite of the differences in the correlation coefficient values. The correlation coefficient values were unfortunately low for both types of vegetation samples, especially for carotenoids and water content. The same low correlations were also obtained for fifty selected vegetation indices due to the low variability in the studied vegetation samples.

New studies dealing with a comparison of spectral devices emerged over the last two years. Leaf optical properties measurements using integrating spheres were also compared by Lukeš et al. (2017). They compared the reflectance and transmittance spectra of three Spectralon® panels, four artificial materials and leaves from six common broadleaf tree species measured in four integrating spheres (Dualsphere, Labsphere, ASD, and Li-cor). There was not one sphere that deviated significantly from the others across all the samples in the spectral region between 400 and 1600 nm, the only statistically significant differences were found between the Li-cor and Dualsphere measurements. The leaf reflectance and transmittance spectra of the white paper and tree leaves measured in two integrating spheres (the single ASD and small double OceanOptics) and by a leaf clip (PP systems) were compared by Hovi et al. (2017). The systematic difference in the mean reflectance spectra between the single and double integrating spheres was only minor, but the reflectance measured with the leaf clip was, on average, 14% higher compared to the single integrating sphere. The differences were also higher for the transmittance measurements. The authors confirm our findings that the different methods of spectra measurements also influence the vegetation indices computed from such spectra and that a comparison of the leaf spectra acquired by the different methods has to be performed with caution. The experiments with leaf stacking when measuring by a contact probe were made by Neuwirthová, Lhotáková, and Albrechtová (2017).

Q3. Are the prediction empirical models for the photosynthetic pigments and water content estimations based on laboratory spectroscopy on the leaf level of the Norway spruce comparable for the three vertical canopy levels? (Paper 4)

Significant differences were proven in three individual needle age classes and three vertical canopy levels by analysis of variance using the laboratory retrieved photosynthetic pigments and water content and the indices calculated from the reflectance spectra measured with an ASD FieldSpec 4 Wide-Res spectroradiometer equipped with the plant contact probe, as already described above, in the answers to the first group of research questions (Q1) and Paper 2. The influence of the position in the tree crown on the optical properties of the leaves/needles was also demonstrated for the Norway Spruce by Lukeš et al. (2013) and in deciduous forest canopies by Wang and Li (2013). Statistically based prediction models for the photosynthetic pigments and water content estimations were, thus, separately built in Paper 4 for all the three positions in the tree crown (the sunlit productive upper and lower parts, the shaded basal part). The modeling was performed using fifty vegetation indices computed from the laboratory measured reflectance spectra and the methods of continuum removal transformation, simple regression and partial least square regression (PLSR). The best correlation results between the vegetation indices and the photosynthetic pigments were achieved for the shaded basal part of the tree crown. On the contrary, the worst results were obtained for the sunlit upper part. This could be caused by the more complex shoot architecture in the sunlit part of the tree crown, where the needles are often very short and/or very tough, perpendicular to the shoot, which may affect the resulting spectra by additional scattering. In comparison, the needles in the shaded parts of the tree crown are flatter (Cescatti and Zorer 2003). The partial least square regression which uses the complete spectral curves gave better correlation results than simple regression using the vegetation indices, this is in accordance with the studies of Atzberger et al. (2010) for the chlorophylls and (Yi et al. 2014) for carotenoids.

6.2 Relict arctic-alpine tundra ecosystem

The second part of the thesis (Papers 5-7) investigated the heterogeneous natural ecosystem of relict arctic-alpine tundra located in the Krkonoše Mountains. Two research aims were defined for this montane ecosystem in Chapter 3. These two research aims are solved and described in detail in Papers 5-7. This chapter summarizes and discusses the most important results.

A1. To compare the selected multispectral and hyperspectral data with the various spatial and spectral resolutions for the tundra vegetation classification using two differently detailed legends and different classifiers including an object-based image analysis and a per-pixel approach. (Papers 5 and 6)

Two legends depending on the spatial resolution of the remote sensing image data were proposed for the relict arctic-alpine tundra ecosystem in the Krkonoše Mountains classifications. The detailed legend consisting of 13 classes was designed in cooperation with the botanist of the Krkonoše Mountains National Park. It also contains species which are expanding mostly at the expense of the original species *Nardus stricta* and need to be

monitored. These expansive species are *Calamagrostis villosa* (Hejcman et al. 2009), *Molinia caerulea* (Hejcman, Češková, and Pavlů 2010) and *Pinus mugo* scrub (Štursa and Wild 2014). However, not all the species can be distinguished using the data with the spatial resolutions of the freely available remote sensing data from Landsat or Sentinel-2 satellites, so a simplified legend consisting of 8 classes was also designed. All tall grass species and *Vaccinum* vegetation were joined into just one class while *Pinus mugo* scrub was divided into dense and sparse categories. Water bodies because of their small size were classified from the image data with very high spatial resolution only. This is in accordance with Virtanen and Ek (2014) who highlighted that *"Pixel sizes of 2.4 m or smaller are suitable for realistic classification of tundra land cover. Especially water bodies and fens occur in a narrow strips or small patches"*. Considering the mosaic structure of tundra in the Krkonoše Mountains, our research confirms that the spatial resolution is a key factor for obtaining high classification accuracies (a high overall accuracy of object-based image classification of orthoimages with only four spectral bands, but a spatial resolution of 12.5 cm is a proof). Besides Virtanen and Ek (2014), Angela Lausch et al. (2016) also emphasize the importance of spatial resolution for capturing the variability in heterogeneous ecosystems.

The best classification results for the detailed legend were reached for the AISA Dual data with a spatial resolution of 1 to 3 m and almost 500 spectral bands using a per-pixel support vector machine (SVM) classifier from 40 PCA bands with an overall accuracy (OA) of 84.3%. Very similar results were reached by the same classification method using a hyperspectral sensor APEX (OA=82.6%, 288 bands, 2 to 5 m spatial resolution). Good results for the detailed legend were also achieved by the object-based image classification (OBIA) of orthoimages with a spatial resolution of 12.5 cm and just four spectral bands (OA=72%). The results for the simplified legend show similar overall accuracies around 78% for the Landsat 8 and Sentinel-2A data (Maximum Likelihood classifier, MLC) and the best OA 84% for orthoimages (OBIA). These overall accuracies are comparable with the results of Marcinkowska-Ochtyra et al. (2018), who reached a median OA 84% for 22 high-mountain vegetation communities using an APEX hyperspectral data and an SVM classifier, and with Müllerová (2005), who reached OA 81.1% for 9 classes using aerial photographs and an MLC classifier. However, the lower overall accuracies in this study were achieved for the WorldView-2 data (OA=68.4% at best for simplified legend using OBIA).

The reasons why the WV-2 classifications exhibited the worst results could be in the date of the data acquisition in the middle of the season, when all the species are the greenest, and in the missing spectral bands in the shortwave infrared part of the spectrum, where the important wavelengths for distinguishing the studied categories are located. This was proven by linear discriminant analysis applied on the AISA Dual spectral bands in the diploma thesis of Miroslava Palúchová (2018) under my supervision. Other important bands are located in the red to near infrared region as can be seen in Figure 12. Nevertheless, this is valid for the species discrimination at the beginning of the vegetation season because the AISA Dual data was acquired on the 19th June, 2013. And the date of data acquisition, as mentioned above, also

plays an important role in the species discrimination – alpine heathlands have a typical pink color when blooming, as *Calamagrostis villosa* and *Juncus trifidus* (a typical species for wetlands) change their color to purple and red at the end of the season and, on the contrary, *Molinia caerulea* starts to grow later than other species at the beginning of the season, so its old dry biomass which appears very bright in the images can be recognized well (Figure 13). The phenology and multitemporal classifications of the area were studied in the bachelor thesis of Markéta Roubalová (2017), where I was a co-supervisor. The results were, however, poor due to a lack of data – there were basically no scenes of Sentinel-2A for 2015 and 2016 without any clouds and scenes for June and July were also missing. Also, the spatial resolution of the Sentinel-2 is not sufficient for such a detailed task as is needed. But the advantage of the late summer image data for the vegetation communities discrimination in the Krkonoše Mountains was proven by Marcinkowska-Ochtyra et al. (2018). The senescent phase was also the most discriminative phenophase for the identification of the majority of the low-Arctic tundra vegetation communities when using ground-based and simulated EnMAP reflectance spectra (Beamish et al. 2017).

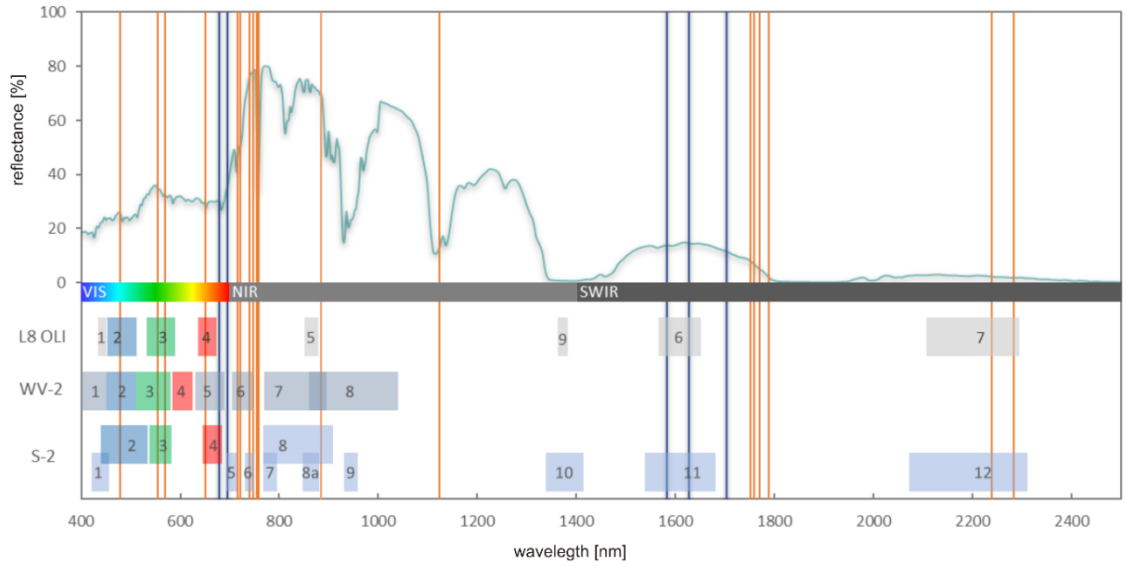

Figure 12: The significant bands for the detailed legend classes' discrimination (the blue lines represent the five most important bands, the orange lines represent the other significant bands) *(Source: Palúchová, 2018)*

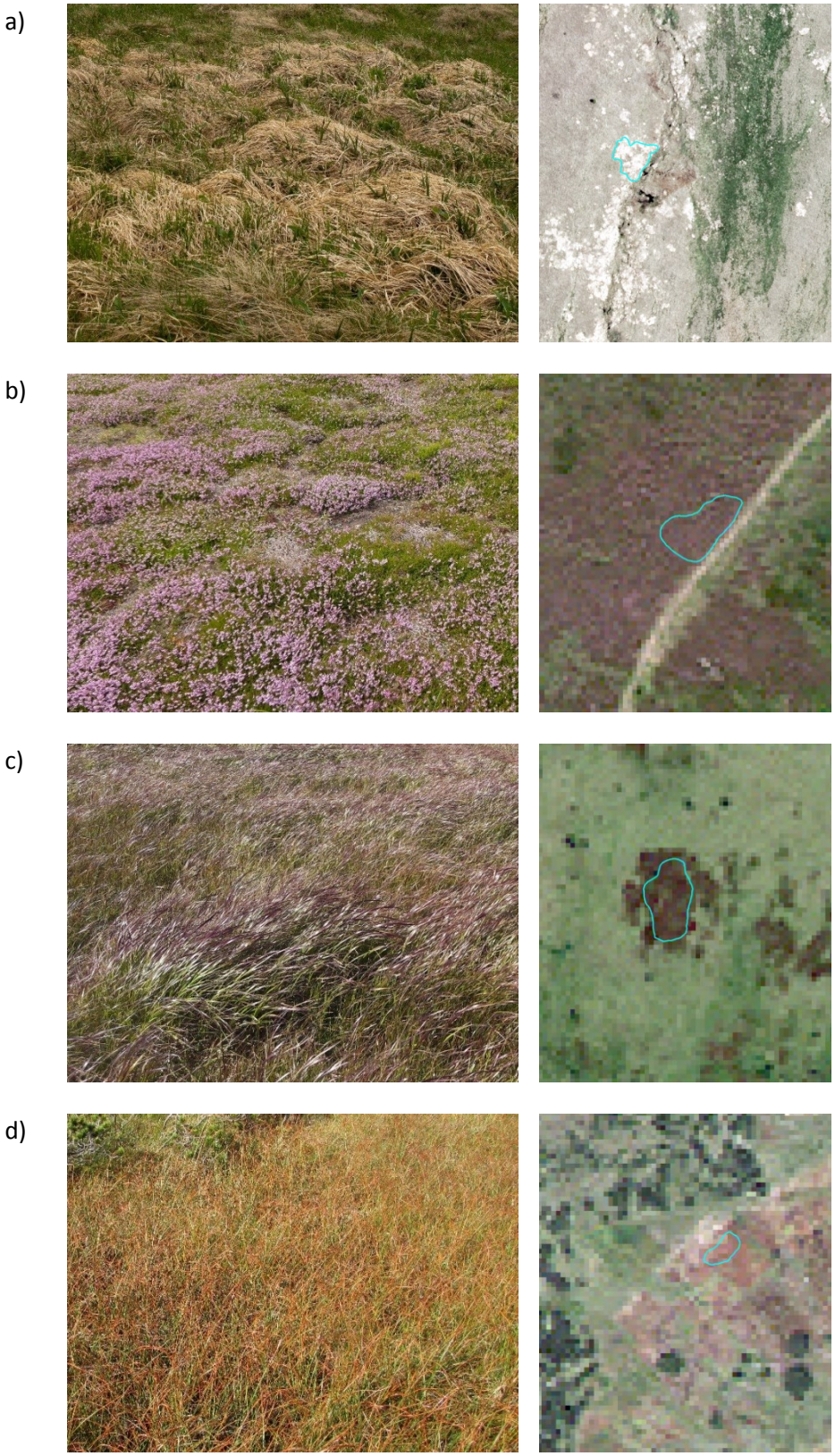

Figure 13: The most discriminative phenophases for the selected species: a) Molinia caerulea in the middle of June, b) Calluna vulgaris and c) Calamagrostis villosa in the middle of August, d) Juncus trifidus at the end of August. Left column: in situ pictures, right column: orthoimage, 2012-06-18, and WorldView-2 satellite images, 2014-08-10 and 2015-08-30.
(Source: author, WorldView-2 images and KRNAP orthoimages)

A2. To construct the prediction empirical models for the tundra vegetation height, cover and fAPAR based on the field spectral measurements and to compare how the models differ if the datasets are acquired in a different phenology phase (July 2015 and August 2015). (Paper 7)

The first case study dealing with the traits of the Krkonoše Mountains tundra vegetation was focused on the species which are continuously changing along the nutrient and vegetation gradient occurred between Luční bouda hut (1410 m a.s.l.) and Luční hora Mountain (1555 m a.s.l.). The plant cover, vegetation height and fAPAR (Fraction of photosynthetically active radiation absorbed by the vegetation canopy) were measured together with the field spectra in July and August 2015. Fifty vegetation indices were used to express the relationships between the vegetation traits and its reflectance. Better correlation results were achieved for the dataset from July than from August. The best results were achieved for the plant cover (R^2 = 0.8 for the July and 0.7 for the August datasets) and the worst results for fAPAR (R^2 = 0.48 for the August dataset, at maximum), which is in accordance with the study of Sakowska, Juszczak, and Gianelle (2016) who studied the fAPAR of alpine meadows. They had continuous measurements from two vegetation seasons, but were not able to establish any significant relationship between the vegetation indices and fAPAR. A similar coefficient of determination for fAPAR (R^2 = 0.37) to our results was presented for the mountain meadows in Krkonoše Mountains by Jarocińska et al. (2016). The vegetation height differs the most between July and August. In literature, the biomass is often evaluated instead of the height (e.g., Hope, Kimball, and Stow 1993; Bratsch et al. 2017).

7 Conclusions and future research

This thesis summarized the basics of the laboratory spectroscopy measurements and vegetation trait modeling and contributed to scientific issues in the use of laboratory/field spectroscopy and remote sensing image data for evaluation of vegetation traits in two structurally and functionally different montane ecosystems: (1) a homogeneous human-influenced evergreen coniferous forest represented by a Norway spruce forest in the Krušné hory Mountains and (2) a heterogeneous natural ecosystem of relict arctic-alpine tundra in the Krkonoše Muntains with predominance of grasses.

As one of the first studies, this thesis compared the laboratory spectra collected by a spectroradiometer ASD FieldSpec 4 Wide-Res coupled with different devices (a plant contact probe and two integrating spheres) for various heterogeneous materials. The results of Paper 3 confirmed the increasing inconsistency among the spectra obtained by different instruments when moving from relatively homogeneous materials to the more complex and unstable vegetation samples. The spectral reflectance curves of the 95% Zenith Lite® calibrated reference measured by different instruments show negligible differences. The differences between the spectral reflectance curves of the colored papers can be modeled well by linear transformation, but the spectral reflectance curves differed significantly in the case of the vegetation samples, although for tobacco dorsiventral leaves, the vegetation indices calculated from the reflectance data collected by the different devices mean values were in the range of the corresponding standard deviation. In the case of the Norway spruce needles, the methodology of the measurement matters remarkably and affects the values obtained by the different devices. More research on the comparability of the spectra acquired by the different devices is needed and the future studies should focus on the standardization of the measurements' procedures so that open access spectral libraries could serve as a reliable input for modeling the optical properties on a leaf level.

The thesis evaluated also data on different scales (biochemical/biophysical retrievals of pigments and water content, laboratory and airborne image spectroscopic measurements) for detection of differences in the physiological status of the Norway spruce stands. The results of Paper 2 showed significant differences between the model areas (located in the western and central parts of the Krušné hory Mountains) in the case of laboratory retrieved leaf pigments and water content dataset only. Differences among the stands on various levels of significance existed in all three datasets. Based on the laboratory datasets (leaf compounds and laboratory spectra), the differences among the needle age classes and among the positions in the tree crown were proven. Moreover, Paper 2 together with Paper 1, showed the leveling up of the Norway spruce physiological status between the central (area Kovářská) and western part (area Přebuz) of the Krušné hory Mountains in the period of 1998 – 2013, which was given by the

regeneration of the trees in the central part after air pollution sources restriction and the slight worsening of the trees' physiological status in the western part, where soil geochemical conditions are less favorable.

In the case of Norway spruce forest, the present thesis also contributed to the research on the canopy structure by comparing the prediction empirical models for the photosynthetic pigments and the water content estimations based on the laboratory spectroscopy for the three vertical canopy levels. The findings of Paper 4 were that the better correlation results between the vegetation indices and the photosynthetic pigments were achieved for the shaded basal part of the tree crown than for the sunlit upper part. The paper also confirmed the more accurate predictions of the biochemical and biophysical compound contents by models using the partial least square regression instead of the simple regressions using the vegetation indices. However, the results can be affected by the different architecture of the shoots within the tree crown, which may affect the resulting spectra measured by a plant contact probe by additional scattering. This should be tested in the future by another method of spectral measurements – e.g., acquiring the spectra of the individual needles in the integrating sphere.

Concerning the heterogeneous ecosystem of the relict arctic-alpine tundra in the Krkonoše Mountains, the species classifications were the main aim of this thesis (Papers 5 and 6). Two differently detailed legends were evaluated with use of remote sensing image data of different spatial and spectral resolutions. The best overall accuracy (84.3 %) of the classification for the detailed legend was reached by the airborne hyperspectral image data, AISA Dual with a high spatial resolution of 1 to 3 m spatial resolution. However, the object-based analysis of orthoimages with a spatial resolution of 12.5 cm and just four spectral bands also gave very promising results. The Landsat and Sentinel-2A data can be used for a general overview of the basic classes' distribution. Papers 5 and 6 with ongoing research in the area confirm the key role of the spatial resolution for capturing the variability in the heterogeneous ecosystems and suggest the importance of the date of remote sensing image data acquisition for the best species discrimination. Based on these results, the research of the Krkonoše Mountains tundra species phenology during vegetation season is our next goal for the future – the laboratory and field spectroscopies, as well as the high spatial and spectral resolutions image data acquired using hyperspectral camera carried on unmanned aerial vehicle (UAV) should be very helpful in the species monitoring and the differentiation based on the detailed spectral curves acquired during the season. Besides using the spectral data acquired during the season by field spectroscopy and hyperspectral camera carried on UAV for differentiation and mapping of the studied vegetation classes, the seasonal spectral data should be the basis for the research focused on the more detailed evaluation of the quantitative traits of the relict arctic-alpine tundra in the Krkonoše Mountains. The case study dealing with the Krkonoše Mountains tundra vegetation traits presented in this thesis (Paper 7) was focused on the empirical modeling of the vegetation height, plant cover and fAPAR in two terms of the vegetation season based on the field spectroscopy data using the vegetation indices and simple regression. The best results were achieved for the plant cover ($R^2 = 0.8$ for the July and 0.7 for the August datasets) and the worst

results for fAPAR (R^2 = 0.48 for the August dataset, at maximum). At present research focused on the vegetation parameters evaluation, the biomass (phytomass and necromass) and total canopy chlorophyll content are measured in the field and in the laboratory and the next research in the Krkonoše Mountains tundra will be focused on them. These traits will be further monitored for the selected homogeneous stands during the next seasons and their relationships to the field and the image spectral data will be evaluated.

References

Albrechtová, Jana, Lucie Kupková, and Petya K. E. Campbell. 2017. *Metody Hodnocení Fyziologického Stavu Smrkových Porostů: Případová Studie Sledování Vývoje Stavu Smrkových Porostů v Krušných Horách v Letech 1998-2013*. Geographica. Praha: Česká geografická společnost.

Ardö, Jonas, Nancy Lambert, Vladimir Henzlik, and Barry Rock. 1997. "Satellite Based Estimations of Coniferous Forest Cover Changes : Krusne Hory, Czech Republic." *Ambio* 26 (3): 158–66.

ARTMO. 2018. "Automated Radiative Transfer Models Operator (ARTMO)." 2018. http://ipl.uv.es/artmo/.

ASD Inc. 1999. *Technical Guide*. 3rd ed.

———. 2008. Integrating Sphere User Manual.

———. 2012. *FieldSpec 4 User Manual*. http://support.asdi.com/.

———. 2016. "FieldSpec 4 Wide-Res Field Spectroradiometer." 2016. http://www.asdi.com/products-and-services/fieldspec-spectroradiometers/fieldspec-4-wide-res.

Atzberger, Clement. 2000. "Development of an Invertible Forest Reflectance Model: The Infor-Model." In *Proceedings of the 20th EARSeL Symposium Dresden*, 39–44. Dresden.

Atzberger, Clement, Martine Guérif, Frédéric Baret, and Willy Werner. 2010. "Comparative Analysis of Three Chemometric Techniques for the Spectroradiometric Assessment of Canopy Chlorophyll Content in Winter Wheat." *Computers and Electronics in Agriculture* 73 (2): 165–73. https://doi.org/10.1016/j.compag.2010.05.006.

Beamish, Alison, Nicholas Coops, Sabine Chabrillat, and Birgit Heim. 2017. "A Phenological Approach to Spectral Differentiation of Low-Arctic Tundra Vegetation Communities, North Slope, Alaska." *Remote Sensing* 9 (11): 1200. https://doi.org/10.3390/rs9111200.

Bratsch, Sara, Howard Epstein, Marcel Buchhorn, and Donald Walker. 2016. "Differentiating among Four Arctic Tundra Plant Communities at Ivotuk, Alaska Using Field Spectroscopy." *Remote Sensing* 8 (1): 51. https://doi.org/10.3390/rs8010051.

Bratsch, Sara, Howard Epstein, Marcel Buchhorn, Donald Walker, and Heather Landes. 2017. "Relationships between Hyperspectral Data and Components of Vegetation Biomass in Low Arctic Tundra Communities at Ivotuk, Alaska." *Environmental Research Letters* 12 (2): 025003. https://doi.org/10.1088/1748-9326/aa572e.

Brovkina, O., E. Cienciala, F. Zemek, P. Lukeš, T. Fabianek, and R. Russ. 2017. "Composite Indicator for Monitoring of Norway Spruce Stand Decline." *European Journal of Remote Sensing* 50 (1): 550–63. https://doi.org/10.1080/22797254.2017.1372697.

Campbell, P. K. Entcheva, B. N. Rock, M. E. Martin, C. D. Neefus, J. R. Irons, E. M. Middleton, and J. Albrechtova. 2004. "Detection of Initial Damage in Norway Spruce Canopies Using Hyperspectral Airborne Data." *International Journal of Remote Sensing* 25 (24): 5557–84. https://doi.org/10.1080/01431160410001726058.

Červená, Lucie, Jan Mišurec, Lucie Kupková, and Markéta Potůčková. 2017. "Modely Přenosu Záření." In Metody Hodnocení Fyziologického Stavu Smrkových Porostů: Případová Studie Sledování Vývoje Stavu Smrkových Porostů v Krušných Horách v Letech 1998-2013., edited by Jana Albrechtová, Lucie Kupková, and Petya Entcheva Campbell, Geographica, 224–31. Praha: Česká geografická společnost.

Červená, Lucie, Markéta Potůčková, Lucie Kupková, Zuzana Lhotáková, and Jana Albrechtová. 2017a. "Laboratorní Spektroradiometrická Měření: Metodika." In *Metody Hodnocení Fyziologického Stavu Smrkových Porostů: Případová Studie Sledování Vývoje Stavu*

Smrkových Porostů v Krušných Horách v Letech 1998-2013., edited by Jana Albrechtová, Lucie Kupková, and Petya Entcheva Campbell, Geographica, 205–14. Praha: Česká geografická společnost.

———. 2017b. "Statistické Metody pro Vyhodnocení Spektrálních Dat a Jejich Vztahu Ke Stavovým Parametrům Vegetace." In Metody Hodnocení Fyziologického Stavu Smrkových Porostů: Případová Studie Sledování Vývoje Stavu Smrkových Porostů v Krušných Horách v Letech 1998-2013., edited by Jana Albrechtová, Lucie Kupková, and Petya Entcheva Campbell, Geographica, 215–23. Praha: Česká geografická společnost.

Cescatti, A., and R. Zorer. 2003. "Structural Acclimation and Radiation Regime of Silver Fir (Abies Alba Mill.) Shoots along a Light Gradient." *Plant, Cell and Environment* 26 (3): 429–42. https://doi.org/10.1046/j.1365-3040.2003.00974.x.

Chapin, F. Stuart, Gaius R. Shaver, Anne E. Giblin, Knute J. Nadelhoffer, and James A. Laundre. 1995. "Responses of Arctic Tundra to Experimental and Observed Changes in Climate." *Ecology* 76 (3): 694–711. https://doi.org/10.2307/1939337.

Crawley, Michael J. 2013. *The R Book*. Second edition. Chichester, West Sussex, United Kingdom: Wiley.

Darvishzadeh, Roshanak, Andrew Skidmore, Martin Schlerf, and Clement Atzberger. 2008. "Inversion of a Radiative Transfer Model for Estimating Vegetation LAI and Chlorophyll in a Heterogeneous Grassland." *Remote Sensing of Environment* 112 (5): 2592–2604. https://doi.org/10.1016/j.rse.2007.12.003.

Darvishzadeh, Roshanak, Andrew Skidmore, Martin Schlerf, Clement Atzberger, Fabio Corsi, and Moses Cho. 2008. "LAI and Chlorophyll Estimation for a Heterogeneous Grassland Using Hyperspectral Measurements." *ISPRS Journal of Photogrammetry and Remote Sensing* 63 (4): 409–26. https://doi.org/10.1016/j.isprsjprs.2008.01.001.

Daughtry, C.S.T., L.L. Biehl, and K.J. Ranson. 1989. "A New Technique to Measure the Spectral Properties of Conifer Needles." *Remote Sensing of Environment* 27 (1): 81–91. https://doi.org/10.1016/0034-4257(89)90039-4.

Davidson, Scott, Maria Santos, Victoria Sloan, Jennifer Watts, Gareth Phoenix, Walter Oechel, and Donatella Zona. 2016. "Mapping Arctic Tundra Vegetation Communities Using Field Spectroscopy and Multispectral Satellite Data in North Alaska, USA." *Remote Sensing* 8 (12): 978. https://doi.org/10.3390/rs8120978.

Dawson, T. P., and P. J. Curran. 1998. "Technical Note A New Technique for Interpolating the Reflectance Red Edge Position." *International Journal of Remote Sensing* 19 (11): 2133–39. https://doi.org/10.1080/014311698214910.

Dawson, Terence P., Paul J. Curran, and Stephen E. Plummer. 1998. "LIBERTY—Modeling the Effects of Leaf Biochemical Concentration on Reflectance Spectra." *Remote Sensing of Environment* 65 (1): 50–60. https://doi.org/10.1016/S0034-4257(98)00007-8.

Disney, M., P. Lewis, and P. Saich. 2006. "3D Modelling of Forest Canopy Structure for Remote Sensing Simulations in the Optical and Microwave Domains." *Remote Sensing of Environment* 100 (1): 114–32. https://doi.org/10.1016/j.rse.2005.10.003.

Disney, M.I., P. Lewis, and P.R.J. North. 2000. "Monte Carlo Ray Tracing in Optical Canopy Reflectance Modelling." *Remote Sensing Reviews* 18 (2–4): 163–96. https://doi.org/10.1080/02757250009532389.

Einzmann, Kathrin, Wai-Tim Ng, Markus Immitzer, Nicole Pinnel, and Clement Atzberger. 2014. "Method Analysis for Collecting and Processing In-Situ Hyperspectral Needle Reflectance Data for Monitoring Norway Spruce." *Photogrammetrie - Fernerkundung - Geoinformation* 2014 (5): 423–34. https://doi.org/10.1127/1432-8364/2014/0234.

Elmendorf, Sarah C., Gregory H. R. Henry, Robert D. Hollister, Robert G. Björk, Noémie Boulanger-Lapointe, Elisabeth J. Cooper, Johannes H. C. Cornelissen, et al. 2012. "Plot-Scale Evidence of Tundra Vegetation Change and Links to Recent Summer Warming." *Nature Climate Change* 2 (April): 453.

Fassnacht, Fabian Ewald, Hooman Latifi, Krzysztof Stereńczak, Aneta Modzelewska, Michael Lefsky, Lars T. Waser, Christoph Straub, and Aniruddha Ghosh. 2016. "Review of Studies on Tree Species Classification from Remotely Sensed Data." *Remote Sensing of Environment* 186 (December): 64–87. https://doi.org/10.1016/j.rse.2016.08.013.

Feng, Min, Joseph O. Sexton, Chengquan Huang, Anupam Anand, Saurabh Channan, Xiao-Peng Song, Dan-Xia Song, Do-Hyung Kim, Praveen Noojipady, and John R. Townshend. 2016. "Earth Science Data Records of Global Forest Cover and Change: Assessment of Accuracy in 1990, 2000, and 2005 Epochs." *Remote Sensing of Environment* 184 (October): 73–85. https://doi.org/10.1016/j.rse.2016.06.012.

Féret, J.-B., A.A. Gitelson, S.D. Noble, and S. Jacquemoud. 2017. "PROSPECT-D: Towards Modeling Leaf Optical Properties through a Complete Lifecycle." *Remote Sensing of Environment* 193 (May): 204–15. https://doi.org/10.1016/j.rse.2017.03.004.

Feret, Jean-Baptiste, Christophe François, Gregory P. Asner, Anatoly A. Gitelson, Roberta E. Martin, Luc P.R. Bidel, Susan L. Ustin, Guerric le Maire, and Stéphane Jacquemoud. 2008. "PROSPECT-4 and 5: Advances in the Leaf Optical Properties Model Separating Photosynthetic Pigments." *Remote Sensing of Environment* 112 (6): 3030–43. https://doi.org/10.1016/j.rse.2008.02.012.

Fourty, Th., F. Baret, S. Jacquemoud, G. Schmuck, and J. Verdebout. 1996. "Leaf Optical Properties with Explicit Description of Its Biochemical Composition: Direct and Inverse Problems." *Remote Sensing of Environment* 56 (2): 104–17. https://doi.org/10.1016/0034-4257(95)00234-0.

Gibbons, D. E., and R. R. Richard. 1979. "Determination of Noise Equivalent Reflectance for a Multispectral Scanner – A Scanner Sensitivity Study." NASA Technical Paper. http://ntrs.nasa.gov/archive/nasa/casi.ntrs.nasa.gov/19800004148.pdf.

Gitelson, Anatoly A., Galina P. Keydan, and Mark N. Merzlyak. 2006. "Three-Band Model for Noninvasive Estimation of Chlorophyll, Carotenoids, and Anthocyanin Contents in Higher Plant Leaves." *Geophysical Research Letters* 33 (11). https://doi.org/10.1029/2006GL026457.

Goel, Narendra S. 1988. "Models of Vegetation Canopy Reflectance and Their Use in Estimation of Biophysical Parameters from Reflectance Data." *Remote Sensing Reviews* 4 (1): 1–212. https://doi.org/10.1080/02757258809532105.

Green, R. O. 1992. "Determination of the In-Flight Spectral and Radiometric Characteristics of the Airborne Visible/Infrared Imaging Spectrometer (AVIRIS)." In *Imaging Spectroscopy: Fundamentals and Prospective Applications*, 103–23. Netherlands: Springer.

Hais, Martin, Jan Wild, Luděk Berec, Josef Brůna, Robert Kennedy, Justin Braaten, and Zdeněk Brož. 2016. "Landsat Imagery Spectral Trajectories—Important Variables for Spatially Predicting the Risks of Bark Beetle Disturbance." *Remote Sensing* 8 (8): 687. https://doi.org/10.3390/rs8080687.

Halabuk, Andrej, Katarina Gerhatova, Frantisek Kohut, Zuzana Ponecova, and Matej Mojses. 2013. "Identification of Season-Dependent Relationships between Spectral Vegetation Indices and Aboveground Phytomass in Alpine Grassland by Using Field Spectroscopy." *Ekologia* 32 (2). https://doi.org/10.2478/eko-2013-0016.

Hassol, Susan Joy. 2004. *Impacts of a Warming Arctic: Arctic Climate Impact Assessment*. Cambridge, U.K. ; New York, N.Y: Cambridge University Press.

Hejcman, Michal, Michaela Češková, and Vilém Pavlů. 2010. "Control of Molinia Caerulea by Cutting Management on Sub-Alpine Grassland." *Flora - Morphology, Distribution, Functional Ecology of Plants* 205 (9): 577–82. https://doi.org/10.1016/j.flora.2010.04.019.

Hejcman, Michal, Michaela Klaudisová, Pavla Hejcmanová, Vilém Pavlů, and Martina Jones. 2009. "Expansion of Calamagrostis Villosa in Sub-Alpine Nardus Stricta Grassland: Cessation of Cutting Management or High Nitrogen Deposition?" *Agriculture,*

Ecosystems & Environment 129 (1–3): 91–96. https://doi.org/10.1016/j.agee.2008.07.007.

Hernández-Clemente, Rocío, Rafael M. Navarro-Cerrillo, and Pablo J. Zarco-Tejada. 2012. "Carotenoid Content Estimation in a Heterogeneous Conifer Forest Using Narrow-Band Indices and PROSPECT+DART Simulations." *Remote Sensing of Environment* 127 (December): 298–315. https://doi.org/10.1016/j.rse.2012.09.014.

Homolová, Lucie, Růžena Janoutová, Petr Lukeš, Jan Hanuš, Jan Novotný, Olga Brovkina, and Rolling Richard Loayza Fernandez. 2017. "In Situ Data Supporting Remote Sensing Estimation of Spruce Forest Parameters at the Ecosystem Station Bílý Kříž." *Beskydy* 10 (1–2): 75–86. https://doi.org/10.11118/beskyd201710010075.

Homolová, Lucie, Petr Lukeš, Zbyněk Malenovský, Zuzana Lhotáková, Věroslav Kaplan, and Jan Hanuš. 2013. "Measurement Methods and Variability Assessment of the Norway Spruce Total Leaf Area: Implications for Remote Sensing." *Trees* 27 (1): 111–21. https://doi.org/10.1007/s00468-012-0774-8.

Homolová, Lucie, Zbyněk Malenovský, Jan G.P.W. Clevers, Glenda García-Santos, and Michael E. Schaepman. 2013. "Review of Optical-Based Remote Sensing for Plant Trait Mapping." *Ecological Complexity* 15 (September): 1–16. https://doi.org/10.1016/j.ecocom.2013.06.003.

Hope, A. S., J. S. Kimball, and D. A. Stow. 1993. "The Relationship between Tussock Tundra Spectral Reflectance Properties and Biomass and Vegetation Composition." *International Journal of Remote Sensing* 14 (10): 1861–74. https://doi.org/10.1080/01431169308954008.

Hovi, Aarne, Petri Forsström, Matti Mõttus, and Miina Rautiainen. 2017. "Evaluation of Accuracy and Practical Applicability of Methods for Measuring Leaf Reflectance and Transmittance Spectra." *Remote Sensing* 10 (2): 25. https://doi.org/10.3390/rs10010025.

Huang, Chengquan, Sunghee Kim, Kuan Song, John R.G. Townshend, Paul Davis, Alice Altstatt, Oscar Rodas, et al. 2009. "Assessment of Paraguay's Forest Cover Change Using Landsat Observations." *Global and Planetary Change* 67 (1–2): 1–12. https://doi.org/10.1016/j.gloplacha.2008.12.009.

Jacquemoud, S. 2000. "Comparison of Four Radiative Transfer Models to Simulate Plant Canopies Reflectance Direct and Inverse Mode." *Remote Sensing of Environment* 74 (3): 471–81. https://doi.org/10.1016/S0034-4257(00)00139-5.

Jacquemoud, S., and F. Baret. 1990. "PROSPECT: A Model of Leaf Optical Properties Spectra." *Remote Sensing of Environment* 34 (2): 75–91. https://doi.org/10.1016/0034-4257(90)90100-Z.

Jacquemoud, S., S.L. Ustin, J. Verdebout, G. Schmuck, G. Andreoli, and B. Hosgood. 1996. "Estimating Leaf Biochemistry Using the PROSPECT Leaf Optical Properties Model." *Remote Sensing of Environment* 56 (3): 194–202. https://doi.org/10.1016/0034-4257(95)00238-3.

Jacquemoud, Stéphane, Wout Verhoef, Frédéric Baret, Cédric Bacour, Pablo J. Zarco-Tejada, Gregory P. Asner, Christophe François, and Susan L. Ustin. 2009. "PROSPECT+SAIL Models: A Review of Use for Vegetation Characterization." *Remote Sensing of Environment* 113 (September): S56–66. https://doi.org/10.1016/j.rse.2008.01.026.

Jarocińska, Anna M. 2014. "Radiative Transfer Model Parametrization for Simulating the Reflectance of Meadow Vegetation." *Miscellanea Geographica* 18 (2). https://doi.org/10.2478/mgrsd-2014-0001.

Jarocińska, Anna M., Monika Kacprzyk, Adriana Marcinkowska-Ochtyra, Adrian Ochtyra, Bogdan Zagajewski, and Koen Meuleman. 2016. "The Application of APEX Images in the Assessment of the State of Non-Forest Vegetation in the Karkonosze Mountains." *Miscellanea Geographica* 20 (1). https://doi.org/10.1515/mgrsd-2016-0009.

Jarocinska, Anna, Bogdan Zagajewski, Adrian Ochtyra, Adriana Marcinkowska, and Lucie Kupkova. 2014. "PROSAIL Model for Reflectance Simulations of Mountainous Non-Forest Communities." EARSeL eProceedings.

Johansen, Bernt E., Stein Rune Karlsen, and Hans Tømmervik. 2012. "Vegetation Mapping of Svalbard Utilising Landsat TM/ETM+ Data." *Polar Record* 48 (01): 47–63. https://doi.org/10.1017/S0032247411000647.

Kociánová, Milena, Jan Štursa, and Jan Vaněk. 2015. *Krkonošská tundra*. Vrchlabí: Správa Krkonošského národního parku.

Kokaly, R, and R Clark. 1999. "Spectroscopic Determination of Leaf Biochemistry Using Band-Depth Analysis of Absorption Features and Stepwise Multiple Linear Regression." *Remote Sensing of Environment* 67 (3): 267–87. https://doi.org/10.1016/S0034-4257(98)00084-4.

Kopačková, Veronika, Jan Mišurec, and Kateřina Fárová. 2017. "Půdní Geochemická Analýza: Přebuz a Kovářská." In Metody Hodnocení Fyziologického Stavu Smrkových Porostů: Případová Studie Sledování Vývoje Stavu Smrkových Porostů v Krušných Horách v Letech 1998-2013., edited by Jana Albrechtová, Lucie Kupková, and Petya Entcheva Campbell, Geographica, 233–44. Praha: Česká geografická společnost.

Lambert, N. J., J. Ardo, B. N. Rock, and J. E. Vogelmann. 1995. "Spectral Characterization and Regression-Based Classification of Forest Damage in Norway Spruce Stands in the Czech Republic Using Landsat Thematic Mapper Data." *International Journal of Remote Sensing* 16 (7): 1261–87. https://doi.org/10.1080/01431169508954476.

Lausch, A., L. Bannehr, M. Beckmann, C. Boehm, H. Feilhauer, J.M. Hacker, M. Heurich, et al. 2016. "Linking Earth Observation and Taxonomic, Structural and Functional Biodiversity: Local to Ecosystem Perspectives." *Ecological Indicators* 70 (November): 317–39. https://doi.org/10.1016/j.ecolind.2016.06.022.

Lausch, Angela, Stefan Erasmi, Douglas King, Paul Magdon, and Marco Heurich. 2016. "Understanding Forest Health with Remote Sensing -Part I—A Review of Spectral Traits, Processes and Remote-Sensing Characteristics." *Remote Sensing* 8 (12): 1029. https://doi.org/10.3390/rs8121029.

———. 2017. "Understanding Forest Health with Remote Sensing-Part II—A Review of Approaches and Data Models." *Remote Sensing* 9 (2): 129. https://doi.org/10.3390/rs9020129.

Leeuwen, Martin van, and Maarten Nieuwenhuis. 2010. "Retrieval of Forest Structural Parameters Using LiDAR Remote Sensing." *European Journal of Forest Research* 129 (4): 749–70. https://doi.org/10.1007/s10342-010-0381-4.

Lhotáková, Zuzana, Jana Albrechtová, Zbyněk Malenovský, Barrett N. Rock, Tomáš Polák, and Pavel Cudlín. 2007. "Does the Azimuth Orientation of Norway Spruce (Picea Abies/L./Karst.) Branches within Sunlit Crown Part Influence the Heterogeneity of Biochemical, Structural and Spectral Characteristics of Needles?" *Environmental and Experimental Botany* 59 (3): 283–92. https://doi.org/10.1016/j.envexpbot.2006.02.003.

Lhotáková, Zuzana, Lukáš Brodský, Lucie Kupková, Veronika Kopačková, Markéta Potůčková, Jan Mišurec, Aleš Klement, Monika Kovářová, and Jana Albrechtová. 2013. "Detection of Multiple Stresses in Scots Pine Growing at Post-Mining Sites Using Visible to near-Infrared Spectroscopy." *Environmental Science: Processes & Impacts* 15 (11): 2004. https://doi.org/10.1039/c3em00388d.

Liang, Shunlin. 2004. *Quantitative Remote Sensing of Land Surfaces*. Wiley Series in Remote Sensing. Hoboken, N.J: Wiley-Interscience.

Liu, Nanfeng, Paul Budkewitsch, and Paul Treitz. 2017. "Examining Spectral Reflectance Features Related to Arctic Percent Vegetation Cover: Implications for Hyperspectral Remote Sensing of Arctic Tundra." *Remote Sensing of Environment* 192 (April): 58–72. https://doi.org/10.1016/j.rse.2017.02.002.

Lukeš, Petr, Lucie Homolová, Martin Navrátil, and Jan Hanuš. 2017. "Assessing the Consistency of Optical Properties Measured in Four Integrating Spheres." *International Journal of Remote Sensing* 38 (13): 3817–30. https://doi.org/10.1080/01431161.2017.1306144.

Lukeš, Petr, Pauline Stenberg, Miina Rautiainen, Matti Mõttus, and Kalle M. Vanhatalo. 2013. "Optical Properties of Leaves and Needles for Boreal Tree Species in Europe." *Remote Sensing Letters* 4 (7): 667–76. https://doi.org/10.1080/2150704X.2013.782112.

Mac Arthur, Alasdair. 2013. "The Design and Calibration of Spectrometers and Measurement Uncertainties." presented at the EuroSpec Summer School, Palermo. <http://cost-es0903.fem-environment.eu/training-schools/2013-palermo-summer-school/lecture-s-presentation/>.

Main, Russell, Moses Azong Cho, Renaud Mathieu, Martha M. O'Kennedy, Abel Ramoelo, and Susan Koch. 2011. "An Investigation into Robust Spectral Indices for Leaf Chlorophyll Estimation." *ISPRS Journal of Photogrammetry and Remote Sensing* 66 (6): 751–61. https://doi.org/10.1016/j.isprsjprs.2011.08.001.

Maire, G. le, C. François, and E. Dufrêne. 2004. "Towards Universal Broad Leaf Chlorophyll Indices Using PROSPECT Simulated Database and Hyperspectral Reflectance Measurements." *Remote Sensing of Environment* 89 (1): 1–28. https://doi.org/10.1016/j.rse.2003.09.004.

Malenovský, Z., C. Ufer, Z. Lhotáková, J. G. P. W. Clevers, M. E. Schaepman, J. Albrechtová, and P. Cudlín. 2006. "A New Hyperspectral Index for Chlorophyll Estimation of Forrest Canopy: Area under Curve Normalized to Maximal Band Depth between 650-725 Nm." *EARSeL E-Proceedings* 5 (2): 161–72.

Malenovský, Zbyněk, Lucie Homolová, Raúl Zurita-Milla, Petr Lukeš, Věroslav Kaplan, Jan Hanuš, Jean-Philippe Gastellu-Etchegorry, and Michael E. Schaepman. 2013. "Retrieval of Spruce Leaf Chlorophyll Content from Airborne Image Data Using Continuum Removal and Radiative Transfer." *Remote Sensing of Environment* 131 (April): 85–102. https://doi.org/10.1016/j.rse.2012.12.015.

Manion, Paul D. 1991. *Tree Disease Concepts*. 2nd ed. Englewood Cliffs, N.J: Prentice Hall.

Marcinkowska, Adriana, Bogdan Zagajewski, Adrian Ochtyra, Anna Jarocińska, Edwin Raczko, Lucie Kupková, Premysl Stych, and Koen Meuleman. 2014. "Mapping Vegetation Communities of the Karkonosze National Park Using APEX Hyperspectral Data and Support Vector Machines." *Miscellanea Geographica* 18 (2). https://doi.org/10.2478/mgrsd-2014-0007.

Marcinkowska-Ochtyra, Adriana, Bogdan Zagajewski, Adrian Ochtyra, Anna Jarocińska, Bronisław Wojtuń, Christian Rogass, Christian Mielke, and Samantha Lavender. 2017. "Subalpine and Alpine Vegetation Classification Based on Hyperspectral APEX and Simulated EnMAP Images." *International Journal of Remote Sensing* 38 (7): 1839–64. https://doi.org/10.1080/01431161.2016.1274447.

Marcinkowska-Ochtyra, Adriana, Bogdan Zagajewski, Edwin Raczko, Adrian Ochtyra, and Anna Jarocińska. 2018. "Classification of High-Mountain Vegetation Communities within a Diverse Giant Mountains Ecosystem Using Airborne APEX Hyperspectral Imagery." *Remote Sensing* 10 (4): 570. https://doi.org/10.3390/rs10040570.

Mesarch, Mark A., Elizabeth A. Walter-Shea, Gregory P. Asner, Elizabeth M. Middleton, and Stephen S. Chan. 1999. "A Revised Measurement Methodology for Conifer Needles Spectral Optical Properties." *Remote Sensing of Environment* 68 (2): 177–92. https://doi.org/10.1016/S0034-4257(98)00124-2.

Mevik, Bjørn-Helge, and Ron Wehrens. 2007. "The Pls Package: Principal Component and Partial Least Squares Regression in R." *Journal of Statistical Software* 18 (2). https://doi.org/10.18637/jss.v018.i02.

Ministerstvo zemědělství. 2017. *Zpráva o Stavu Lesa a Lesního Hospodářství České Republiky v Roce 2016*. Praha: Ministerstvo zemědělství. http://www.uhul.cz/ke-stazeni/informace-o-lese/zelene-zpravy-mze.

Mišurec, Jan, Veronika Kopačková, Zuzana Lhotáková, Petya Campbell, and Jana Albrechtová. 2016. "Detection of Spatio-Temporal Changes of Norway Spruce Forest Stands in Ore Mountains Using Landsat Time Series and Airborne Hyperspectral Imagery." *Remote Sensing* 8 (2): 92. https://doi.org/10.3390/rs8020092.

Morin, Xavier, Lorenz Fahse, Hervé Jactel, Michael Scherer-Lorenzen, Raúl García-Valdés, and Harald Bugmann. 2018. "Long-Term Response of Forest Productivity to Climate Change Is Mostly Driven by Change in Tree Species Composition." *Scientific Reports* 8 (1). https://doi.org/10.1038/s41598-018-23763-y.

Müllerová, Jana. 2005. "Use of Digital Aerial Photography for Sub-Alpine Vegetation Mapping: A Case Study from the Krkonoše Mts., Czech Republic." *Plant Ecology* 175 (2): 259–72. https://doi.org/10.1007/s11258-005-0063-3.

Nestola, E., A. Scartazza, D. Di Baccio, A. Castagna, A. Ranieri, M. Cammarano, F. Mazzenga, G. Matteucci, and C. Calfapietra. 2018. "Are Optical Indices Good Proxies of Seasonal Changes in Carbon Fluxes and Stress-Related Physiological Status in a Beech Forest?" *Science of The Total Environment* 612 (January): 1030–41. https://doi.org/10.1016/j.scitotenv.2017.08.167.

Neuwirthová, Eva, Zuzana Lhotáková, and Jana Albrechtová. 2017. "The Effect of Leaf Stacking on Leaf Reflectance and Vegetation Indices Measured by Contact Probe during the Season." *Sensors* 17 (6): 1202. https://doi.org/10.3390/s17061202.

North, P.R.J. 1996. "Three-Dimensional Forest Light Interaction Model Using a Monte Carlo Method." *IEEE Transactions on Geoscience and Remote Sensing* 34 (4): 946–56. https://doi.org/10.1109/36.508411.

Palúchová, Miroslava. 2018. "Vliv Spektrálního Rozlišení Na Klasifikaci Krajinného Pokryvu v Krkonošské Tundře." Diplomová práce. Praha. Univerzita Karlova, Přírodovědecká fakulta.

Patenaude, Genevieve, Ronald Milne, and Terence P. Dawson. 2005. "Synthesis of Remote Sensing Approaches for Forest Carbon Estimation: Reporting to the Kyoto Protocol." *Environmental Science & Policy* 8 (2): 161–78. https://doi.org/10.1016/j.envsci.2004.12.010.

Pause, Marion, Christian Schweitzer, Michael Rosenthal, Vanessa Keuck, Jan Bumberger, Peter Dietrich, Marco Heurich, András Jung, and Angela Lausch. 2016. "In Situ/Remote Sensing Integration to Assess Forest Health—A Review." *Remote Sensing* 8 (6): 471. https://doi.org/10.3390/rs8060471.

Pekár, Stanislav, and Marek Brabec. 2009. *Moderní analýza biologických dat. 1. díl, 1. díl,*. Praha: Scientia.

Pettorelli, Nathalie, Henrike Schulte to Bühne, Ayesha Tulloch, Grégoire Dubois, Cate Macinnis-Ng, Ana M. Queirós, David A. Keith, et al. 2018. "Satellite Remote Sensing of Ecosystem Functions: Opportunities, Challenges and Way Forward." Edited by Marcus Rowcliffe and Mat Disney. *Remote Sensing in Ecology and Conservation* 4 (2): 71–93. https://doi.org/10.1002/rse2.59.

Raczko, Edwin, and Bogdan Zagajewski. 2018. "Tree Species Classification of the UNESCO Man and the Biosphere Karkonoski National Park (Poland) Using Artificial Neural Networks and APEX Hyperspectral Images." *Remote Sensing* 10 (7): 1111. https://doi.org/10.3390/rs10071111.

Rautiainen, Miina, Petr Lukeš, Lucie Homolová, Aarne Hovi, Jan Pisek, and Matti Mõttus. 2018. "Spectral Properties of Coniferous Forests: A Review of In Situ and Laboratory Measurements." *Remote Sensing* 10 (2): 207. https://doi.org/10.3390/rs10020207.

Rautiainen, Miina, Pauline Stenberg, Tiit Nilson, and Andres Kuusk. 2004. "The Effect of Crown Shape on the Reflectance of Coniferous Stands." *Remote Sensing of Environment* 89 (1): 41–52. https://doi.org/10.1016/j.rse.2003.10.001.

Roubalová, Markéta. 2017. "Klasifikace Vybraných Vegetačních Kategorií Land Cover v Krkonošské Tundře z Dat Sentinel-2A s Využitím Časové Řady Dat." Bakalářská práce. Praha. Univerzita Karlova, Přírodovědecká fakulta.

Sakowska, Karolina, Radoslaw Juszczak, and Damiano Gianelle. 2016. "Remote Sensing of Grassland Biophysical Parameters in the Context of the Sentinel-2 Satellite Mission." *Journal of Sensors* 2016: 1–16. https://doi.org/10.1155/2016/4612809.

Savitzky, Abraham., and M. J. E. Golay. 1964. "Smoothing and Differentiation of Data by Simplified Least Squares Procedures." *Analytical Chemistry* 36 (8): 1627–39. https://doi.org/10.1021/ac60214a047.

Schlerf, Martin, and Clement Atzberger. 2006. "Inversion of a Forest Reflectance Model to Estimate Structural Canopy Variables from Hyperspectral Remote Sensing Data." *Remote Sensing of Environment* 100 (3): 281–94. https://doi.org/10.1016/j.rse.2005.10.006.

Schlerf, Martin, Clement Atzberger, and Joachim Hill. 2005. "Remote Sensing of Forest Biophysical Variables Using HyMap Imaging Spectrometer Data." *Remote Sensing of Environment* 95 (2): 177–94. https://doi.org/10.1016/j.rse.2004.12.016.

Schlerf, Martin, Clement Atzberger, Joachim Hill, Henning Buddenbaum, Willy Werner, and Gebhard Schüler. 2010. "Retrieval of Chlorophyll and Nitrogen in Norway Spruce (Picea Abies L. Karst.) Using Imaging Spectroscopy." *International Journal of Applied Earth Observation and Geoinformation* 12 (1): 17–26. https://doi.org/10.1016/j.jag.2009.08.006.

Senf, Cornelius, Rupert Seidl, and Patrick Hostert. 2017. "Remote Sensing of Forest Insect Disturbances: Current State and Future Directions." *International Journal of Applied Earth Observation and Geoinformation* 60 (August): 49–60. https://doi.org/10.1016/j.jag.2017.04.004.

Song, Xiao-Peng, Chengquan Huang, Joseph Sexton, Saurabh Channan, and John Townshend. 2014. "Annual Detection of Forest Cover Loss Using Time Series Satellite Measurements of Percent Tree Cover." *Remote Sensing* 6 (9): 8878–8903. https://doi.org/10.3390/rs6098878.

Soukupova, J., B. N. Rock, and J. Albrechtova. 2001. "Comparative Study of Two Spruce Species in a Polluted Mountainous Region." *New Phytologist* 150 (1): 133–45. https://doi.org/10.1046/j.1469-8137.2001.00066.x.

Soukupová, Lenka, Milena Kociánová, Jan Jeník, and Josef Sekyra. 1995. "Arctic Alpine Tundra in the Krkonoše, the Sudetes." *Opera Corcontica* 32: 5–88.

Šrámek, V., V. Balcar, V. Buriánek, F. Havránek, A. Jurásek, J. Liška, J. Novák, and M. Slodičák. 2015. "Aktualizace Studie Lesnické Hospodaření v Krušných Horách." Výzkumný ústav lesního hospodářství a myslivosti, v. v. i. http://www.vulhm.cz/sites/File/Informatika/studie_krusne_hory.pdf.

Stow, Douglas A, Allen Hope, David McGuire, David Verbyla, John Gamon, Fred Huemmrich, Stan Houston, et al. 2004. "Remote Sensing of Vegetation and Land-Cover Change in Arctic Tundra Ecosystems." *Remote Sensing of Environment* 89 (3): 281–308. https://doi.org/10.1016/j.rse.2003.10.018.

Stuckens, Jan, Willem W. Verstraeten, Stephanie Delalieux, Rony Swennen, and Pol Coppin. 2009. "A Dorsiventral Leaf Radiative Transfer Model: Development, Validation and Improved Model Inversion Techniques." *Remote Sensing of Environment* 113 (12): 2560–73. https://doi.org/10.1016/j.rse.2009.07.014.

Štursa, Jan, and Jan Wild. 2014. "Kleč a Smilka – Klíčoví Hráči Vývoje Alpínského Bezlesí Krkonoš (Vysoké Sudety, Česká Republika)." *Opera Corcontica* 51: 5–36.

Thenkabail, Prasad Srinivasa, J. G. Lyon, and Alfredo Huete, eds. 2012. *Hyperspectral Remote Sensing of Vegetation*. Boca Raton, FL: CRC Press.

Thulin, Susanne, Michael J. Hill, Alex Held, Simon Jones, and Peter Woodgate. 2012. "Hyperspectral Determination of Feed Quality Constituents in Temperate Pastures: Effect of Processing Methods on Predictive Relationships from Partial Least Squares Regression." *International Journal of Applied Earth Observation and Geoinformation* 19 (October): 322–34. https://doi.org/10.1016/j.jag.2012.06.006.

Tol, C. van der, W. Verhoef, J. Timmermans, A. Verhoef, and Z. Su. 2009. "An Integrated Model of Soil-Canopy Spectral Radiances, Photosynthesis, Fluorescence, Temperature and Energy Balance." *Biogeosciences* 6 (12): 3109–29. https://doi.org/10.5194/bg-6-3109-2009.

Tol, C. van der, J. A. Berry, P. K. E. Campbell, and U. Rascher. 2014. "Models of Fluorescence and Photosynthesis for Interpreting Measurements of Solar-Induced Chlorophyll Fluorescence: VAN DER TOL ET AL." *Journal of Geophysical Research: Biogeosciences* 119 (12): 2312–27. https://doi.org/10.1002/2014JG002713.

Townshend, John R., Jeffrey G. Masek, Chengquan Huang, Eric F. Vermote, Feng Gao, Saurabh Channan, Joseph O. Sexton, et al. 2012. "Global Characterization and Monitoring of Forest Cover Using Landsat Data: Opportunities and Challenges." *International Journal of Digital Earth* 5 (5): 373–97. https://doi.org/10.1080/17538947.2012.713190.

Treml, V, T Ponocná, and U Büntgen. 2012. "Growth Trends and Temperature Responses of Treeline Norway Spruce in the Czech-Polish Sudetes Mountains." *Climate Research* 55 (2): 91–103. https://doi.org/10.3354/cr01122.

Trumbore, S., P. Brando, and H. Hartmann. 2015. "Forest Health and Global Change." *Science* 349 (6250): 814–18. https://doi.org/10.1126/science.aac6759.

Tsai, Fuan, and William Philpot. 1998. "Derivative Analysis of Hyperspectral Data." *Remote Sensing of Environment* 66 (1): 41–51. https://doi.org/10.1016/S0034-4257(98)00032-7.

Turner, Woody, Sacha Spector, Ned Gardiner, Matthew Fladeland, Eleanor Sterling, and Marc Steininger. 2003. "Remote Sensing for Biodiversity Science and Conservation." *Trends in Ecology & Evolution* 18 (6): 306–14. https://doi.org/10.1016/S0169-5347(03)00070-3.

Valášek, Václav. 1998. "Alternativní Možnosti Optimalizace Těžby Hnědého Uhlí v České Republice." *Acta Montanistica Slovaca* 3 (3): 233–243.

Verhoef, W. 1984. "Light Scattering by Leaf Layers with Application to Canopy Reflectance Modeling: The SAIL Model." *Remote Sensing of Environment* 16 (2): 125–41. https://doi.org/10.1016/0034-4257(84)90057-9.

Verhoef, Wout, and Heike Bach. 2003. "Simulation of Hyperspectral and Directional Radiance Images Using Coupled Biophysical and Atmospheric Radiative Transfer Models." *Remote Sensing of Environment* 87 (1): 23–41. https://doi.org/10.1016/S0034-4257(03)00143-3.

Vermote, E.F., D. Tanre, J.L. Deuze, M. Herman, and J.-J. Morcette. 1997. "Second Simulation of the Satellite Signal in the Solar Spectrum, 6S: An Overview." *IEEE Transactions on Geoscience and Remote Sensing* 35 (3): 675–86. https://doi.org/10.1109/36.581987.

Verrelst, Jochem, Erika Romijn, and Lammert Kooistra. 2012. "Mapping Vegetation Density in a Heterogeneous River Floodplain Ecosystem Using Pointable CHRIS/PROBA Data." *Remote Sensing* 4 (9): 2866–89. https://doi.org/10.3390/rs4092866.

Vihervaara, Petteri, Ari-Pekka Auvinen, Laura Mononen, Markus Törmä, Petri Ahlroth, Saku Anttila, Kristin Böttcher, et al. 2017. "How Essential Biodiversity Variables and Remote Sensing Can Help National Biodiversity Monitoring." *Global Ecology and Conservation* 10 (April): 43–59. https://doi.org/10.1016/j.gecco.2017.01.007.

Vilfan, Nastassia, Christiaan van der Tol, Onno Muller, Uwe Rascher, and Wouter Verhoef. 2016. "Fluspect-B: A Model for Leaf Fluorescence, Reflectance and Transmittance Spectra." *Remote Sensing of Environment* 186 (December): 596–615. https://doi.org/10.1016/j.rse.2016.09.017.

Virtanen, Tarmo, and Malin Ek. 2014. "The Fragmented Nature of Tundra Landscape." *International Journal of Applied Earth Observation and Geoinformation* 27 (April): 4–12. https://doi.org/10.1016/j.jag.2013.05.010.

Vítek, Ondřej, Michaela Vítková, and Jana Müllerová. 2012. "Anthropogenic Changes of Vegetation above Timberline in the Krkonoše Mountains National Park Focusing on the Impact of Tourism." *Opera Corcontica* 49: 5–30.

Wang, Quan, and Pingheng Li. 2013. "Canopy Vertical Heterogeneity Plays a Critical Role in Reflectance Simulation." *Agricultural and Forest Meteorology* 169 (February): 111–21. https://doi.org/10.1016/j.agrformet.2012.10.004.

Yáñez, L, L Homolová, Z Malenovský, and Michael E Schaepman. 2008. "Geometrical and Structural Parametrization of Forest Canopy Radiative Transfer by LIDAR Measurements." https://doi.org/10.5167/uzh-20352.

Yanez-Rausell, Lucia, Zbynek Malenovsky, Jan G. P. W. Clevers, and Michael E. Schaepman. 2014. "Minimizing Measurement Uncertainties of Coniferous Needle-Leaf Optical Properties. Part II: Experimental Setup and Error Analysis." *IEEE Journal of Selected Topics in Applied Earth Observations and Remote Sensing* 7 (2): 406–20. https://doi.org/10.1109/JSTARS.2013.2292817.

Yanez-Rausell, Lucia, Michael E. Schaepman, Jan G. P. W. Clevers, and Zbynek Malenovsky. 2014. "Minimizing Measurement Uncertainties of Coniferous Needle-Leaf Optical Properties, Part I: Methodological Review." *IEEE Journal of Selected Topics in Applied Earth Observations and Remote Sensing* 7 (2): 399–405. https://doi.org/10.1109/JSTARS.2013.2272890.

Yi, Qiuxiang, Guli Jiapaer, Jingming Chen, Anming Bao, and Fumin Wang. 2014. "Different Units of Measurement of Carotenoids Estimation in Cotton Using Hyperspectral Indices and Partial Least Square Regression." *ISPRS Journal of Photogrammetry and Remote Sensing* 91 (May): 72–84. https://doi.org/10.1016/j.isprsjprs.2014.01.004.

Zemek, František. 2014a. Airborne Remote Sensing: Theory and Practice in Assessment of Terrestrial Ecosystems. Brno: Global Change Research Centre AS CR.

———. 2014b. Letecký dálkový průzkum Země: teorie a příklady hodnocení terestrických ekosystémů. Brno: Centrum výzkumu globální změny AV ČR.

Zvára, Karel. 2003. *Biostatistika*. Praha: Karolinum.

———. 2008. *Regrese*. Praha: Matfyzpress.

Curriculum Vitae

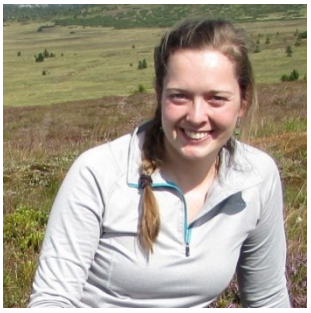

Personal Details

Name: Lucie Červená

Date of Birth: 29 February 1988

E-mail: lucie.cervena@natur.cuni.cz

Education

Since 2012	Ph. D. candidate – Faculty of Science, Charles University, Field of study: Cartography, Geoinformatics and Remote Sensing
2010 – 2012	Mgr. (M.Sc.) – Faculty of Science, Charles University in Prague, Field of study: Cartography and Geoinformatics
2007 – 2010	Bc. (B.Sc.) – Faculty of Science, Charles University in Prague, Field of study: Geography and Cartography

Courses

5. – 11. 7. 2016	ISPRS Summer School (Telč, Czech Republic)
28. 7. – 15. 8. 2014	GOFC-GOLD Data Initiative Training Sessions (USGS EROS Center in Sioux Falls, South Dakota, and Department of Earth and Environment, Boston University, Boston, Massachusetts, USA)
5. – 7. 6. 2014	Trans-Atlantic Training – Land Use/Land Cover Change and Ecosystem Processes (Institute of Geography and Spatial Management Krakow, Poland)
15. – 20. 7. 2013	EUROSPEC Summer School on field spectroscopy and ecological modeling (University of Palermo, Italy)
20. – 22. 6. 2013	Trans-Atlantic Training – Advanced Classification Methods in Land Use/Land Cover Change: Regional Applications (Faculty of Science, Charles University, Czech Republic)
21. – 23. 8. 2010	Quantitative research methods in Human Dimensions of Environmental Change within Eastern Europe (Vidzeme University of Applied Sciences, Valmiera, Latvia)

Employment

Since 2016	Researcher at the Department of Applied Geoinformatics and Cartography, Faculty of Science, Charles University

List of Publications

Impact factor publications

Blahut, Jan, Jan Klimeš, Jan Balek, Petr Hájek, **Lucie Červená**, and Jakub Lysák. 2017. „Snow Avalanche Hazard of the Krkonoše National Park, Czech Republic". *Journal of Maps* 13 (2): 86–90. https://doi.org/10.1080/17445647.2016.1262794.

* Kupková, Lucie, **Lucie Červená**, Renáta Suchá, Lucie Jakešová, Bogdan Zagajewski, Stanislav Březina, and Jana Albrechtová. 2017. „Classification of Tundra Vegetation in the Krkonoše Mts. National Park Using APEX, AISA Dual and Sentinel-2A Data". *European Journal of Remote Sensing* 50 (1): 29–46. https://doi.org/10.1080/22797254.2017.1274573.

* Potůčková, Markéta, **Lucie Červená**, Lucie Kupková, Zuzana Lhotáková, Petr Lukeš, Jan Hanuš, Jan Novotný, and Jana Albrechtová. 2016. „Comparison of Reflectance Measurements Acquired with a Contact Probe and an Integration Sphere: Implications for the Spectral Properties of Vegetation at a Leaf Level". *Sensors* 16 (12): 1801. https://doi.org/10.3390/s16111801.

Vilímek, Vít, Jan Klimeš, and **Lucie Červená**. 2016. „Glacier-Related Landforms and Glacial Lakes in Huascarán National Park, Peru". *Journal of Maps* 12 (1): 193–202. https://doi.org/10.1080/17445647.2014.1000985.

Peer-reviewed publications

Červená, Lucie, Lucie Kupková, Lucie Jakešová, and Renáta Suchá. 2016. „Terénní průzkum pro hodnocení vegetace pomocí dálkového průzkumu Země na příkladu tundry v Krkonošském národním parku". *Geografické rozhledy* 25 (3): 22–23.

* Potůčková, Markéta, **Lucie Červená**, Lucie Kupková, Zuzana Lhotáková, and Jana Albrechtová. 2016. „Statistical comparison of spectral and biochemical measurements on an example of Norway spruce stands in the Ore Mountains, Czech Republic". *Geoinformatics FCE CTU* 15 (1): 69–83. https://doi.org/10.14311/gi.15.1.6.

* Suchá, Renáta, Lucie Jakešová, Lucie Kupková, and **Lucie Červená**. 2016. „Classification of Vegetation above the Tree Line in the Krkonoše Mts. National Park Using Remote Sensing Multispectral Data". *AUC GEOGRAPHICA* 51 (1): 113–29. https://doi.org/10.14712/23361980.2016.10.

* **Červená, Lucie**, Zuzana Lhotáková, Veronika Kopačková, Lucie Kupková, Jan Mišurec, Markéta Potůčková, Pavel Cudlín, Petya Entcheva-Campbell, and Jana Albrechtová. 2014. „Temporal changes in Norway spruce physiological status using hyperspectral data: A case study of mountainous forests affected by long-term acidic depositions". *EARSeL eProceedings*. http://dx.doi.org/10.12760/02-2014-1-13.

Peer-reviewed book chapters

Albrechtová, Jana, Zuzana Lhotáková, Petya Entcheva Campbell, Zuzana Lhotáková, Jan Mišurec, Veronika Kopačková, **Lucie Červená**, and Pavel Cudlín. 2017. „Výběr, lokalizace a popis studovaných stanovišť v oblasti západního a středního Krušnohoří". In *Metody hodnocení fyziologického stavu smrkových porostů: případová studie sledování vývoje stavu smrkových porostů v Krušných horách v letech 1998-2013*, edited by Jana Albrechtová, Lucie Kupková, a Petya Entcheva Campbell, Geographica, 111–24. Praha: Česká geografická společnost.

Červená, Lucie, Zuzana Lhotáková, Markéta Potůčková, Lucie Kupková, and Jana Albrechtová. 2017. „Vegetační indexy ve vertikálním profilu koruny". In *Metody hodnocení fyziologického stavu smrkových porostů: případová studie sledování vývoje stavu smrkových porostů v Krušných horách v letech 1998-2013*, edited by Jana Albrechtová, Lucie Kupková, a Petya Entcheva Campbell, Geographica, 286–92. Praha: Česká geografická společnost.

* **Červená, Lucie**, Jan Mišurec, Lucie Kupková, and Markéta Potůčková. 2017. „Modely přenosu záření". In *Metody hodnocení fyziologického stavu smrkových porostů: případová studie sledování vývoje stavu smrkových porostů v Krušných horách v letech 1998-2013*, edited by Jana Albrechtová, Lucie Kupková, a Petya Entcheva Campbell, Geographica, 224–31. Praha: Česká geografická společnost.

* **Červená, Lucie**, Markéta Potůčková, Lucie Kupková, Zuzana Lhotáková, and Jana Albrechtová. 2017. „Laboratorní spektroradiometrická měření: metodika". In *Metody hodnocení fyziologického stavu smrkových porostů: případová studie sledování vývoje stavu smrkových porostů v Krušných horách v letech 1998-2013*, edited by Jana Albrechtová, Lucie Kupková, a Petya Entcheva Campbell, Geographica, 205–14. Praha: Česká geografická společnost.

* **Červená, Lucie**, Markéta Potůčková, Lucie Kupková, Zuzana Lhotáková, and Jana Albrechtová. 2017. „Statistické metody pro vyhodnocení spektrálních dat a jejich vztahu ke stavovým parametrům vegetace". In *Metody hodnocení fyziologického stavu smrkových porostů: případová studie sledování vývoje stavu smrkových porostů v Krušných horách v letech 1998-2013*, edited by Jana Albrechtová, Lucie Kupková, a Petya Entcheva Campbell, Geographica, 215–23. Praha: Česká geografická společnost.

Kupková, Lucie, Markéta Potůčková, **Lucie Červená**, and Jana Albrechtová. 2017. „Dlouhodobý vývoj využití půdy a jeho hybné síly v modelových územích Přebuz a Kovářská". In *Metody hodnocení fyziologického stavu smrkových porostů: případová studie sledování vývoje stavu smrkových porostů v Krušných horách v letech 1998-2013*, edited by Jana Albrechtová, Lucie Kupková, a Petya Entcheva Campbell, Geographica, 68–74. Praha: Česká geografická společnost.

Kupková, Lucie, Markéta Potůčková, **Lucie Červená**, Jan Mišurec, Zuzana Lhotáková, and Jana Albrechtová. 2017. „Laboratorní a obrazová spektroskopie a jejich využití pro pozorování vegetace". In *Metody hodnocení fyziologického stavu smrkových porostů: případová studie sledování vývoje stavu smrkových porostů v Krušných horách v letech 1998-2013*, edited by Jana Albrechtová, Lucie Kupková, a Petya Entcheva Campbell, Geographica, 193–202. Praha: Česká geografická společnost.

Conference publications

* **Červená, Lucie**, Lucie Kupková, and Renáta Suchá. 2016. „Field Spectroscopy for Vegetation Evaluation along the Nutrient and Elevation Gradient above the Tree Line in the Krkonoše Mountains National Park." *ISPRS - International Archives of the Photogrammetry, Remote Sensing and Spatial Information Sciences* XLI-B6 (červen): 211–14. https://doi.org/10.5194/isprs-archives-XLI-B6-211-2016.

* **Červená, Lucie**, Zuzana Lhotáková, Lucie Kupková, Monika Kovářová, and Jana Albrechtová. 2014. „Models for estimating leaf pigments and relative water content in three vertical canopy levels of Norway spruce based on laboratory spectroscopy". In *EARSeL 34th Symposium Proceedings*, edited by Bogdan Zagajewski, Marlena Kycko, a Rainer Reuter, 6.1-6.8. Warsaw, Poland: EARSeL and University of Warsaw. https://doi.org/0.12760/03-2014-11.

Suchá, Renáta, Martina Andrštová, Lucie Kupková, **Lucie Červená**, Bogdan Zagajewski, Adriana Marcinkowska, and Adrian Ochtyra. 2014. „Hyperspectral data for classification of selected vegetation species above tree-line in the Krkonoše Mts. National Park". In *EARSeL 34th Symposium Proceedings*, edited by Bogdan Zagajewski, Marlena Kycko, a Rainer Reuter, 5.1-5.9. Warsaw, Poland: EARSeL and University of Warsaw. http://dx.doi.org/10.12760/03-2014-10.

Lucie Jakešová, **Lucie Červená**, Lucie Kupková, Renáta Suchá, and Martina Andrštová. 2014. Možnosti objektově-orientované klasifikace pro určování vybraných biotopů nad horní hranicí

lesa v Krkonošském národním parku. *Sborník studentské vědecké konference Telč*, edited by Karel Pavelka. ČVUT v Praze.

Kupková, Lucie, Markéta Potůčková, Michaela Buřičová, Zuzana Lhotaková, Veronika Kopačková, **Lucie Červená**, and Jana Albrechtová. 2012. Determination of Soluble Phenolic Compounds in Norway Spruce Foliage Using Laboratory Spectroscopy. *4th International Conference on Cartography and GIS, proceedings vol 1*, edited by T. Bandrova, M. Konecny, a G. Zhelezov, p. 411 - 418. Sofia: Bulgarian Cartographic Assoc.

** Publications presented in this thesis.*